UNIVERSIDADE DE SÃO PAULO
FACULDADE DE MEDICINA DE RIBEIRÃO PRETO
PROGRAMA DE PÓS-GRADUAÇÃO EM FISIOLOGIA

BRUNA MAITAN SANTOS

Efeito do sulfeto de hidrogênio hipotalâmico modulando a tolerância ao LPS

Ribeirão Preto
2020

BRUNA MAITAN SANTOS

Efeito do sulfeto de hidrogênio hipotalâmico modulando a tolerância ao LPS

Tese de Doutorado apresentada à Faculdade de Medicina de Ribeirão Preto da Universidade de São Paulo para obtenção do título de Doutor em Ciências pelo Programa de Pós-graduação em Fisiologia.

Área de Concentração: Fisiologia

Orientador: Prof. Dr. Luiz Guilherme de Siqueira Branco

Ribeirão Preto
2020

FICHA CATALOGRÁFICA

Santos, Bruna Maitan

Efeito do sulfeto de hidrogênio hipotalâmico modulando a tolerância ao LPS / Bruna Maitan Santos; orientador Luiz Guilherme de Siqueira Branco – Ribeirão Preto, 2020.
100 p.

Tese (Doutorado) - Universidade de São Paulo, Faculdade de Medicina de Ribeirão Preto.

1.Gasotransmissores. 2.Lipopolissacarídeo. 3.Febre. 4. Inflamação sistêmica 5. Hipotálamo.

Tese de autoria de Bruna Maitan Santos, sob o título "**Efeito do sulfeto de hidrogênio hipotalâmico modulando a tolerância ao LPS**", apresentada à Faculdade de Medicina de Ribeirão Preto da Universidade de São Paulo, para obtenção do título de Doutor em Ciências pelo Programa de Pós-graduação em Fisiologia, na área de concentração Fisiologia, aprovada em _____ de _____ de 2020 pela comissão julgadora constituída pelos doutores:

_____

Prof. Dr. Luiz Guilherme de Siqueira Branco

Faculdade de Odontologia de Ribeirão Preto da Universidade de São Paulo

Presidente

_____

Prof. Dr. _____

(Instituição):

_____

Prof. Dr. _____

(Instituição):

_____

Prof. Dr. _____

(Instituição):

_____

Prof. Dr. _____

(Instituição):

Ribeirão Preto

2020

Á sabedoria do amor, da família, da amizade e dos professores.

Agradecimentos

Agradeço ao meu pai Beto por sua paciência e sabedoria. Agradeço à minha mãe Denilze por sua energia e disposição. Agradeço aos dois por me proverem a qualquer custo todo o suporte necessário para minha educação e crescimento profissional. Obrigada por me amarem. Amo vocês.

Agradeço a minha irmã amada por ser minha fiel confidente e pelo suporte para os momentos difíceis.

Agradeço às minhas amadas sobrinhas Lívia Maria e Marina por irradiarem luz e felicidade a qualquer momento do dia.

Agradeço ao meu vô Deuclides e minha vó Naninha por me abençoarem lá de cima.

Agradeço à minha vó Ana e meu vô Ernesto por sempre me abençoarem e cuidarem de mim.

Agradeço à minha família. Mesmo ausente, me sinto sempre abraçada por todos.

Agradeço ao professor Branco pelo aprendizado para toda vida. Serei sempre grata. Será meu exemplo de excelência como professor, pesquisador e como ser humano.

Agradeço aos técnicos Mauro, Nadir e Júnia por me ajudarem como doutoranda e como pessoa.

Agradeço ao cafezinho da Nadir por sempre me despertar nos momentos de sono e que foram essenciais para descansar e conversar com todos os meus amigos de laboratório.

Agradeço aos meus velhos amigos da minha querida Araraquara Mari Melo, Mari Lauar, Sivinha, Naira, Du, Guto e Werner pela amizade e por me apoiarem a seguir a carreira acadêmica.

Agradeço aos meus professores de Fisiologia de Araraquara. Sou grata pelo suporte oferecido para crescer no doutorado.

Agradeço a Flávia, João, Jonatas e Rodrigo. Vocês foram essenciais e amigos especiais para os meus primeiros passos no doutorado.

Agradeço aos meus amigos de Cursão. Terei sempre todos no meu coração.

Agradeço à Gabi, Maycon, Edu, Júnia e Mateus por todo apoio, carinho e amizade.

Agradeço à Glauce pela amizade e parceria. Meu exemplo de garra.

Agradeço aos meus amigos de Phoenix sendo eles Ana, Patrick, Robson, Ronnie, Grant, Nick, Ally e Giovana. Obrigada por fazerem parte de um momento tão especial para meu crescimento pessoal e profissional. Tenho todos guardados em meu coração. Agradeço aos meus amigos do laboratório da Prof. Elaine: João, Maurício, Dani, Airam e Celinha por fazerem meus dias mais felizes. Agradeço a Prof. Elaine por sempre me motivar na ciência.

Agradeço ao André pelo companheirismo durante meu mestrado e doutorado.

Agradeço ao meu amigo e professor Andrej. Serei sempre grata aos ensinamentos, carinho e atenção.

Agradeço aos meus mais novos amigos de laboratório Thaís, Pati, Hadder, Luís e Luana. Meu carinho por vocês já é imenso.

Agradeço a professora Evelin pelo carinho, atenção, e por abrir as portas para início de uma nova fase da minha vida profissional. Um exemplo de mulher na ciência.

Agradeço aos alunos do PAE que foram sensacionais comigo.

Agradeço às minhas amigas Camila, Graciane, Bruna Roder e Lissara. Mesmo ausente, guardo todas em meu coração.

Agradeço à vida. Brilhe sempre.

Agradeço à Deus e peço que me proteja por todos os caminhos de minha a vida.

Resumo

SANTOS, Bruna Maitan. **Efeito do sulfeto de hidrogênio endógeno hipotalâmico modulando a tolerância ao LPS**. 2020. 100 f. Tese (Doutorado em Ciências) – Faculdade de Medicina de Ribeirão Preto, Universidade de São Paulo, Ribeirão Preto, 2020.

A febre é por definição o aumento regulado da temperatura corporal produzido em defesa do organismo contra um patógeno. A interação do patógeno com o sistema imune gera a liberação de citocinas e PGs (mediadores da inflamação) que ativam regiões centrais envolvidas no controle da temperatura corporal (Tb), sendo a área pré-óptica anteroventral (AVPO) a região hierarquicamente mais importante na termorregulação. A administração sistêmica de lipopolissacarídeo (LPS - uma endotoxina extraída da parede celular de bactérias G^-) em ratos é o modelo mais utilizado para indução da febre. A administração repetida causa tolerância ao LPS que pode ser caracterizada pela resposta refratária do sistema imune à endotoxina, *i.e.*, ausência da resposta febril produzida no desafio imune à endotoxina. Nosso laboratório caracterizou o papel dos neuromoduladores gasosos óxido nítrico (NO) e monóxido de carbono (CO) na tolerância ao LPS, mas não há relatos sobre a eventual participação do sulfeto de hidrogênio (H_2S – outro neuromodulador gasoso produzido endogenamente). O presente projeto testa a hipótese que o H_2S, produzido endogenamente na AVPO, participa da tolerância ao LPS. Métodos: Ratos com cânulas centrais (para microinjeção de drogas) e datatalogger (para registro de temperatura corporal) receberam uma dose baixa de lipopolissacarídeo (LPS; 100 $\mu g.kg^{-1}$ intraperitonealmente) diariamente, por quatro dias consecutivos. A expressão de CBS e a taxa de produção de H_2S na AVPO foi avaliada juntamente com a análise da sinalização febrigênica. Ratos tolerantes receberam um inibidor da síntese de H_2S (AOA, 100 $pmol.\mu L^{-1}$ icv) ou seu veículo no último dia. Resultados: A taxa de produção de H_2S no hipotálamo (AVPO) e a expressão de CBS aumentaram em ratos tolerantes a endotoxina. Além disso, a inibição hipothalâmica do H_2S reverteu a tolerância à endotoxina, restabelecendo a febre, os níveis plasmáticos de PGE_2 e na AVPO sem alterar os surtos de citocinas plasmáticas ausentes. Conclusão: A tolerância à endotoxina não é apenas um reflexo da redução periférica para a liberação de citocinas, mas na verdade resulta de um conjunto complexo de mecanismos que atuam em vários níveis. A produção de H_2S hipotalâmico modula a maioria desses mecanismos.

Apoio financeiro: Fundação de Amparo à Pesquisa do Estado de São Paulo (FAPESP), #16/09364-3 e #16/17681-9; Conselho Nacional de Desenvolvimento Científico e Tecnológico, #142151/2016-5.

Palavras-chave: Gasotransmissores. Lipopolissacarídeo. Febre. Inflamação sistêmica. Hipotálamo.

Abstract

SANTOS, Bruna Maitan Santos.**The role of hypothalamic hydrogen sulphide modulating LPS tolerance**. 2020. 100 p. Thesis (Doctor of Science) – School of Medicine of Ribeirão Preto, University of São Paulo, São Paulo, 2020.

Fever is by definition a regulated increase in body temperature produced in defense of the organism against a pathogen. The interaction of the pathogen with the immune system generates the release of cytokines and prostaglandins (mediators of inflammation) that activate central regions involved in the control of body temperature (Tb), with the anteroventral preoptic area (AVPO) being the most important hierarchically region in thermoregulation. The systemic administration of lipopolysaccharide (LPS - an endotoxin extracted from the cell wall of G-bacteria) in rats is the most used model to induce fever. Repeated administration causes tolerance to LPS which can be characterized by the immune system's refractory response to the endotoxin, *i.e.*, absence of the febrile response produced in response to the endotoxin immune challenge. Our laboratory characterized the role of gas neuromodulators nitric oxide (NO) and carbon monoxide (CO) in tolerance to LPS, but there are no reports on the possible participation of hydrogen sulfide (H_2S - another endogenous gasotransmitter). The present project tests the hypothesis that H_2S, endogenously produced at AVPO, participates in LPS tolerance. Methods: Rats with central cannulas (drug microinjection) and datatalogger (body temperature recording) received a low dose of lipopolysaccharide (LPS; 100 $\mu g.kg^{-1}$ intraperitoneally) daily, for four consecutive days. CBS expression and H_2S production rate in AVPO were evaluated, along with the analysis of febrile signaling. Tolerant rats received an inhibitor of H_2S synthesis (AOA, 100 pmol 1 μL-1 icv) or its vehicle on the last day. Results: Antero-ventral preoptic area of the hypothalamus (AVPO) H_2S production rate and CBS expression were increased in endotoxin-tolerant rats. Additionally, hypothalamic H_2S inhibition reversed endotoxin tolerance reestablishing fever, AVPO and plasma PGE_2 levels without altering the absent plasma cytokines surges. Conclusion: Endotoxin tolerance is not simply a reflection of peripheral reduced cytokines release but actually results from a complex set of mechanisms acting at multiple levels. Hypothalamic H_2S production modulates most of these mechanisms. Funding information: Fundação de Amparo à Pesquisa do Estado de São Paulo (FAPESP), Grant/Award Number: 16/09364-3 and 16/17681-9; Conselho Nacional de Desenvolvimento Científico e Tecnológico, Grant/Award Number: 142151/2016-5.

Keywords: Gaseotransmiters. Lipopolysaccharide. Fever. Systemic inflammation. Hypothalamus.

Lista de figuras

Lista de abreviaturas e siglas

°C	Graus Celsius
α	Alfa
β	Beta
γ	Gama
µg	Micrograma
µm	Micrômetro
µM	Micromolar
ϰ	Kappa
3-MST	3-mercaptopiruvato súlfur-transferase
3V	Terceiro ventrículo
K^+_{ATP}	Canais de potássio sensíveis ao ATP
AOA	Amino-oxiacetato
ATP	Adenosina tri-fosfato
AVPO	Área ântero-ventral posterior do hipotálamo
CAT	Cisteina aminotransferase
CBS	Cistationina Beta-sintase
CSE	Cistationa y-liase
CO	Monóxido de carbono
CO_2	Dióxido de carbono
ELISA	Teste imunoenzimático por ensaio de imunoabsorção enzimáica
GABA	Ácido gama-aminobutírico
AMPc	Monofosfato cíclico de adenosina
h	Hora
HLI	Índice de perda de calor
H_2S	Sulfeto de hidrogênio
HPA	Hipotálamo-hipófise-glândulas adrenais
icv	Intracerebroventricular
IL	Interleucina
IML	Coluna intermediolateral da medula espinal
ip	Intraperitoneal
kg	Kilograma

L-NAME	N-Nitroarginina metil ester
LPB	Proteína ligadora de lipopolissacarídeo
LPS	Lipopolissacarídeo
min	Minutos
ml	Mililitro
mm	Milímetro
mM	Milimolar
mmHg	Milímetros de mercúrio
NFκB	Fator nuclear κB
NO	Óxido nítrico
NTS	Núcleo do trato solitário
O_2	Oxigênio
p/v	Peso/volume
PAMP	Moléculas associadas a patógenos
PGs	Prostaglandinas
PVN	Núcleo paraventricular do hipotálamo
R	Redutor
rpm	Rotações por minuto
SNC	Sistema nervoso central
Ta	Temperatura ambiente
TAM	Tecido adiposo marrom
Tb	Temperatura corporal
TNF	Fator de necrose tumoral
Tsk	Temperatura da pele da cauda
vs	Versus

Sumário

1 Introdução

Há 300 anos, o sulfeto de hidrogênio (H_2S) era considerado um gás tóxico e inflamável (SZABO, 2018). Atualmente, sabe-se que este mesmo gás é produzido endogenamente, tem função fisiológica e pode ter características terapêuticas ou patológicas dependendo de sua concentração e do tecido que é produzido (SZABÓ, 2007). Na primeira seção desta introdução será feito uma revisão sobre os efeitos deste gás produzido endogenamente.

Na sequência é abordado como tema a inflamação sistêmica induzida por LPS. Nesta seção, daremos ênfase a um dos sinais clínicos clássicos da inflamação, a resposta febril. Esta seção é importante para conhecimento básico de aspectos importantes para o tema analisado.

Depois desta análise, faremos uma breve revisão de um fenômeno conhecido como tolerância ao LPS. Antigamente, a tolerância a endotoxina, ou LPS (endotoxina encontrada na parede de bactérias Gram-negativas), era tratada somente como uma resposta imune atenuada observada pela re-exposição do organismo ao LPS (BEESON, 1946). Hoje, a tolerância ao LPS ganha notorieadade por ser um fenômeno de alta complexidade que envolve a reprogramação neuroimune e endócrina induzida pela re-exposição do organismo ao LPS (BISWAS; LOPEZ-COLLAZO, 2009).

Nas demais seções, foi feita uma revisão sobre o conhecimento já adquirido sobre papel dos gases [óxido nítrico (NO), monóxido de carbono (CO) e, o último descoberto, o H_2S] na tolerância ao LPS. Estes gases são referidos como gasotransmissores e recebem este nome por serem moléculas de sinalização produzidas endogenamente. Devido à baixa complexidade destes gases, eles podem atravessar as membranas biológicas de forma rápida (FAGONE et al., 2018). Além disso, estão presentes em todos os tecidos e células em quantidade significativa, o que marca também seus efeitos em várias respostas fisiológicas (LIAUDET; SORIANO; SZABÓ, 2000; SHEFA et al., 2017; FAGONE et al., 2018).

1.1 Sulfeto de hidrogênio (H_2S)

O H_2S no ambiente é um gás incolor, tóxico, inflamável e de odor forte característico de ovos podres (SZABO, 2018). Altamente permeável à membrana, o H_2S tem capacidade de agir por várias vias, através de canais, fatores de transcrição e receptores (BIBLI et al., 2015). Devido a esta capacidade, sabe-se que o H_2S é um gasotrasmissor que medeia muitos processos fisiológicos e/ou patológicos (SZABÓ, 2007). Vários trabalhos demonstraram diferentes

funções do H_2S na modulação de vias de sinalização em vários organismos, desde os mais simples como bactérias, aos mais complexos como em humanos (SHATALIN et al., 2011; BEŁTOWSKI, 2015). Essencialmente, quatro enzimas o produzem: a cistationa β-sintase (CBS); cistationa y-liase (CSE); cisteina aminotransferase (CAT), e a 3-mercaptopiruvato sulfur-transferase (3-MST) (KUMAR; SANDHIR, 2018). Os precursores da síntese endógena deste gás são a L-homocisteína, a L-cisteína e mais recentemente descoberta, a D-cisteína (KUMAR; SANDHIR, 2018; SEKI et al., 2018). Da dieta, é proveniente a metionina que pode ser convertida em homocisteína e, por sua clivagem causada por CBS e/ou CSE, podem gerar cisteína e, consequentemente, o H_2S. A CBS é capaz de gerar H_2S de forma eficiente a partir de uma combinação de cisteína e homocisteína, enquanto a CSE utiliza cisteína ou homocisteína para gerar H_2S. A 3-MST, após a clivagem de cisteína pela CAT em 3-mercaptopiruvato, cliva o 3-mercaptopiruvato para formar persulfeto (R-SH a R-SSH). O persulfeto libera H_2S na presença de um redutor (R′-SH) (KUMAR; SANDHIR, 2018). Com relação ao catabolismo de H_2S, ele ocorre principalmente na mitocôndria por meio de processos de oxidação com substrato final da reação o estável sulfato e a produção de ATP (HILDEBRANDT; GRIESHABER, 2008).

O H_2S é produzido em quantidades relativamente altas no sistema nervoso central (SNC) comparado a alguns tecidos periféricos, como no sangue (OLAS, 2015). Centralmente, há evidências de que a CBS é a isoforma que predomina, principalmente, em astrócitos (ISHIGAMI et al., 2009). Já a CSE é encontrada em neurônios, principalmente, sendo a 3-MST encontrada nas duas formas celulares (OLAS, 2015). De forma geral, a CSE está mais envolvida com as respostas periféricas em mamíferos (KIMURA, 2013). Além disso, o aumento de H_2S como produto final de CBS e CSE tem efeito regulador negativo na atividade destas enzimas (MOORE; BHATIA; MOOCHHALA, 2003).

Dos efeitos fisiopatológicos produzidos pelo H_2S, ainda há pouco conhecimento sobre seu mecanismo de ação. Entretanto, a formação de persulfetos de proteínas, ou sulfidratação de proteínas S, ou seja, a conversão de resíduos de cisteína -SH em persulfetos -S-SH é considerada um possível mecanismo responsável por estas alterações (PAUL; SNYDER, 2018).

Com o aumento dos estudos sobre os efeitos potenciais do H_2S em mamíferos, algumas ações já estão bem consolidadas na literatura como na resposta cardiovascular, na resposta nociceptiva, no processo de envelhecimento e, finalmente, na resposta inflamatória (LI et al., 2005; LEE et al., 2008; QABAZARD et al., 2014; PANTHI et al., 2016; KOROLEVA et al., 2017; WALLACE et al., 2018, 2019).

Em relação à função cardiovascular, o H_2S é relatado com um importante agente vasodilatador (BHATIA, 2005), capaz de induzir angiogênese (RAJENDRAN et al., 2019) e modular a pressão arterial (DAWE et al., 2008). Quanto ao seu efeito vasodilatador, o grupo de pesquisadores liderado por Rui Wang foi singular ao observar que o efeito vasodilatador do H_2S deve-se a hiperpolarização das células endoteliais e lisas por meio da ativação de canais de potássio sensíveis ao ATP(K^+_{ATP}) (WANG, 2011). Sabe-se, por exemplo, que o H_2S promove vascularização em tecidos isquêmicos (RAJENDRAN et al., 2019). Ainda, via ativação de K^+_{ATP} presentes no hipotálamo, há uma diminuição da pressão arterial, acompanhada pela diminuição na frequência cardíaca (DAWE et al., 2008).

Na resposta nociceptiva, Distrutti et al. (2006) mostraram que a administração sistêmica de diferentes doadores do H_2S inibe a nocicepção visceral, pela abertura de K^+_{ATP} (DISTRUTTI et al., 2006). Por outro lado, um estudo recente utilizando outro modelo de indução de dor demonstrou que o H_2S tem uma atividade pró-nociceptiva na periferia (KAWABATA et al., 2007). Esta conclusão é principalmente substanciada pela observação de que a administração intraplantar de um doador de H_2S induz uma hipernocicepção mecânica de início rápido (25 min) e que a inibição da formação de H_2S endógeno reduz a hipernocicepção inflamatória induzida por LPS (KAWABATA et al., 2007). Assim, esses estudos detectam papéis discrepantes nociceptivos para o mesmo mediador, com papéis pró-nociceptivos e anti-nociceptivos resultantes de vários mecanismos interconectados e dependentes da região da indução da resposta nociceptiva (MATSUNAMI et al., 2009; WALLACE; FERRAZ; MUSCARA, 2012). Dados prévios do nosso grupo de pesquisa (DONATTI et al., 2014) indicaram que na inflamação induzida pela administração de formalina na região orofacial, quando utilizado um inibidor da CSE localmente, induz uma redução proeminente no comportamento correspondente à dor orofacial, ou seja, o H_2S sintetizado durante a inflamação aguda atua como um agente pró-nociceptivo na região orofacial. No caso da dor crônica orofacial, foi observado que a expressão de CBS no gânglio trigeminal está aumentada, indicando seu papel pró-nociceptivo na dor orofacial crônica (MIAO et al., 2014). Dados de nosso laboratório ainda mostraram que o inibidor de H_2S na região orofacial atenua a resposta nociceptiva na dor persistente (SANTOS et al., 2018), sendo esta atenuação dependente da diminuída interação neuroimune facilitando a resposta dolorosa na região orofacial (GARATTINI et al., 2019).

Outro papel importante do H_2S é no processo de envelhecimento. Grande parte dos efeitos anti-envelhecimento descritos na literatura com este gás estão relacionados com o regime de restrição calórica ou de restrição intermitente calórica (KABIL et al., 2011; HINE et

al., 2015). Acredita-se que parte dos resultados positivos observados nestes protocolos para aumentar a expectativa de vida foi devido ao aumento na produção endógena de H_2S. Reforçando este efeito, a restrição do aminoácido essencial metionina, fornecido pela dieta alimentar e também um precursor na produção de cisteína, prolonga a expectativa de vida em roedores e em células humanas (HINE; MITCHELL, 2015). Outro estudos também descrevem o efeito anti-envelhecimento dos doadores de H_2S na vasculatura encefálica (DAS et al., 2018; MUN et al., 2019). No SNC, o envelhecimento da vasculatura encefálica pode resultar na perda da integridade da barreira hematoencefálica e consequente declínio cognitivo. É importante destacar que o efeito anti-envelhecimento do H_2S tem relação com seus próprios efeitos citoprotetivos como agente anti-oxidante e anti-inflamatório (MUN et al., 2019).

Outros trabalhos evidenciam que o H_2S é um importante anti-inflamatório e um possível e promissor agente na terapêutica medicamentosa (BEŁTOWSKI, 2015; FLANNIGAN; WALLACE, 2015). Atualmente, alguns anti-inflamatórios não esteroidais clássicos acoplados a doadores de H_2S estão na fase 2 dos ensaios clínicos, indicando seu potencial clínico como uma droga anti-inflamatória. No modelo de choque endotoxêmico em roedores, foi observado que o pré-tratamento com o doador de liberação lenta GYY4137 protege o animal contra o choque, diminuindo tanto a produção de citocinas inflamatórias séricas como os danos teciduais, indicando o efeito anti-inflamatório do H_2S no modelo (LI et al., 2009). In vitro, o H_2S em astrócitos reverte parcialmente a indução de NFκB e a liberação das citocinas TNF-α e IL-6 na inflamação, mostrando seu efeito anti-inflamatório central (LEE et al., 2009). Complementarmente, o H_2S também é capaz de modular a febre induzida por LPS (KWIATKOSKI et al., 2013). Entretanto, ainda é desconhecido se o H_2S está envolvido com outra importante resposta fisiológica que altera a resposta febril induzida por LPS: a tolerância ao LPS.

1.2 Inflamação sistêmica induzida por LPS

A febre é uma resposta fisiopatológica complexa conhecida como o marco da inflamação (“hallmark of inflammation”). Caracterizada como o aumento regulado da temperatura corporal (Tb), a febre favorece a atividade do sistema imune (KLUGER et al., 1998) aumentando a sobrevida do organismo inflamado ou infectado (KLUGER; RINGLER; ANVER, 1975). Em mamíferos, a instalação e manutenção da febre são dependentes da

ativação central e da sua integração com o sistema imune (ROMANOVSKY; STEINER; MATSUMURA, 2006).

O modelo experimental mais usado na literatura para indução e estudo da febre é a administração de lipopolissacarídeo (LPS), uma endotoxina extraída da parede celular de bactérias Gram-negativas. Sua resposta febrigênica é dependente tanto da dose de LPS, quanto da sua via de administração (ROTH; BLATTEIS, 2014). A resposta febril foi primeiramente explicada como uma resposta do hospedeiro dependente de sua exposição aos pirógenos exógenos, como bactérias ou vírus, que agindo em determinadas células produziriam determinadas proteínas que induziriam febre. Na época, estas ficaram conhecidas como pirógenos endógenos e foram primeiramente descritas em 1953 (BENNETT; BEESON, 1953). Hoje, sabe-se que o mecanismo de ação do LPS inicia-se por meio de sua ligação com a proteína ligadora de LPS, a LPB ("LPS protein biding"), proteína produzida por hepatócitos e liberada no plasma com papel chave na ativação das células mononucleares (SCHUMANN, 1992). Este complexo é detectado na periferia rapidamente por macrófagos e monócitos devido a grande quantidade de receptores TLR-4 na superfície celular desta linhagem (SABROE et al., 2002). A ligação com o TLR-4 ativa o NFκB, um fator de transcrição de citocinas (conhecidos também como pirógenos endógenos), sendo as principais citocinas induzidas na resposta febril a TNF-α, IL-6 e IL-1β (INUI, 2001). Estas citocinas coordenam a resposta pirética por três vias: (1) por meio da ligação e ativação de seus receptores, presentes nas células endoteliais da barreira hematoencefálica e perivasculares, desencadeando o aumento de mediadores inflamatórios, no SNC (CAO et al., 1996; SCHILTZ; SAWCHENKO, 2003); (2) por meio da ação direta em regiões centrais desprovidas de barreira hematoencefálica (NETEA; KULLBERG; VAN DER MEER, 2000); (3) ou por meio da estimulação vagal subdiafragmática (BLATTEIS, 2000; BLATTEIS; LI, 2000) que ativam projeções noradrenérgicas A_1 e A_2 provindas da primeira estação sináptica central, o núcleo do trato solitário (NTS), e que se projetam para a AVPO (BLATTEIS et al., 2005). Independentemente da via, os neurônios da AVPO são estimulados a produzir PGE_2 mediador proximal da febre (CAO et al., 1996; SCHILTZ; SAWCHENKO, 2003) que ligada ao seu receptor EP_3 acoplado a proteína Gi, inibe a atividade da adenilato ciclase diminuindo os níveis intracelulares de AMPc e, por conseguinte, a atividade dos neurônios sensíveis ao calor, resultando no aumento da Tb (STEINER; ANTUNES-RODRIGUES; BRANCO, 2002; STEINER; BRANCO, 2002; IVANOV; ROMANOVSKY, 2004).

Além da produção de citocinas, o LPS causa o aumento da atividade da fosfolipase A_2, degradando fosfolipídeos da membrana, gerando ácido araquidônico que é o substrato da

isoforma induzível da enzima ciclooxigenase (COX_2) que resulta na produção PGs, dentre elas a PGE_2 (MOHRI; SPRIGGS; KUFE, 1990; BARRIOS-RODILES; TIRALOCHE; CHADEE, 1999). Portanto, não causa surpresa que os níveis de PGE_2 plasmáticos estejam aumentados em animais tratados com LPS (UENO et al., 1982; KRALL et al., 2010). Ainda de acordo com esta noção, a administração de PGE_2 exógena induz febre (OOTSUKA et al., 2008). Entretanto, ainda há dúvidas sobre as vias pelas quais a PGE_2 periférica agiria no SNC. Uma possível via seria através de regiões desprovidas de barreira hematoencefálica ou através da ativação de seus receptores localizados em algumas aferências vagais (BLATTEIS; LI, 2000; PERLIK et al., 2005).

Outra importante prostaglandina produzida frente ao desafio induzido pelo LPS é a PGD_2. Mais abundante das PGs no SNC (UENO et al., 1982), a PGD_2 quando injetada no terceiro ventrículo (3V) ou na AVPO causa queda da Tb, em ratos. Durante o desafio imune, os níveis da PGD_2 plasmáticos e na AVPO estão aumentados, caracterizando um mecanismo contra-regulatório que limita o aumento da Tb durante a febre (UENO et al., 1982; GAO et al., 2009; KRALL et al., 2010).

As ações das citocinas e das PGE_2 e PGD_2, na resposta febril, podem ser moduladas por outras moléculas. Gasotransmissores como o NO, CO e o mais novo membro da família descrito na literatura, o H_2S possuem importante função modulatória da inflamação sistêmica induzida por LPS (STEINER; BRANCO, 2000; SORIANO et al., 2012; KWIATKOSKI et al., 2013).

Sabe-se, por exemplo, que na primeira fase da resposta febril induzida por LPS, a biodisponibilidade de NO na AVPO é reduzida (FELEDER; PERLIK; BLATTEIS, 2007). Ainda, é sabido que a biodisponibilidade de NO na AVPO afeta a produção de PGE_2 na mesma região, indicando seu papel antipirético. De modo contrário, estudos sobre o papel da do NO em um núcleo pontinho, o Locus Coreuleus (LC) (SORIANO et al., 2010), sugere que o NO tem papel propirético nesta região em vez de antipirético como observado na AVPO.

Quanto ao papel do NO sistêmico na resposta febril induzida por LPS, há correlação entre a produção de NO pelos macrófagos peritoneais e o aumento da temperatura corporal na resposta febril (PRITCHARD; LI; REPASKY, 2005). Ainda, a inibição do óxido nítrico sintase (NOS) com L-NAME sistemicamente atenuou a febre induzida por LPS. Porém esta resposta foi independente de alterações na produção de citocinas plasmáticas (ROTH et al., 1998). Mesmo sabendo que as citocinas são as principais moléculas envolvidas na sinalização febrigênica na periferia, ainda não podemos descartar o efeito do NO na periferia regulando positivamente a resposta febril.

Em outro trabalho de nosso laboratório, observou-se que o CO no SNC desempenha um papel importante na geração da febre. Também foi demonstrado que o efeito pirético do CO é independente da produção de PGs (STEINER; BRANCO, 2000). Não há relatos sobre o papel do CO periférico na reposta febril induzida por LPS. Contudo, o CO vem sendo considerado como ums ferramenta promissora no tratamento da sepse em humanos, uma resposta incontrolada do sistema imune a um agente infeccioso, por atenuar a produção de leucotrienos na sepse (FREDENBURGH et al., 2018). Além disso, a níveis fisiológicos, o CO atenua a produção de citocinas pró-inflamatórias induzidas por desafio imune por LPS em macrófagos, acompanhado pelo aumento na produção de uma importante citocina anti-inflamatória, a IL-10 (OTTERBEIN et al., 2000). *In vivo*, o mesmo efeito foi observado quando os animais sofreram desafio imune com LPS (OTTERBEIN et al., 2000).

Quanto ao H_2S, foi observado que este gás, na AVPO, tem papel importante na modulação da resposta febril induzida por LPS (KWIATKOSKI et al., 2013). Dados de nosso laboratório demostram que a injeção icv do inibidor da CBS, AOA atenua a produção de PGE_2 induzida por LPS, indicando que o H_2S tem papel antipirético (KWIATKOSKI et al., 2013). Em concordância com este dado, a microinjeção icv do doador de H_2S reduziu a produção de PGE_2 tal como a reposta febril. Curiosamente, neste mesmo trabalho foi observado que a taxa de produção de H_2S na AVPO diminui 2 horas após a injeção de LPS. Já na periferia, foi observado que os níveis de H_2S plasmáticos estão aumentados durante o desafio imune induzido por LPS (ANG; MOOCHHALA; BHATIA, 2010). Os resultados de nosso laboratório indicam que o inibidor da CSE foi capaz de atenuar a resposta febril induzida por LPS quando avaliado em temperatura ambiente relativamente baixa (16ºC) (SORIANO et al., 2018). Este dado indica que a produção de H_2S na periferia ativa o tecido adipos marrom nessas condições durante o desafio imune, facilitando a resposta febril.

1.3 Tolerância ao LPS

O fenômeno da tolerância a endotoxina foi inicialmente descrita por Beeson em 1946. Neste trabalho inaugural, coelhos que receberam repetidas injeções de certas bactérias tornaram-se resistentes ao sintoma clássico de febre, uma resposta que independia do tipo da cepa da bactéria injetada, mostrando seu aspecto inespecífico. Assim, foi observada a importância do tempo entre as exposições à bactéria na intensidade da resposta tolerante, onde maior o período entre as exposições, menor era a resposta de tolerância. Tão interessante

quanto, a atenuação da reposta febril utilizando drogas antipiréticas não atenuou a resposta de tolerância.

Como descrito anteriormente, quando há a invasão de bactérias, o sistema imunológico reage após exposição à endotoxina bacteriana (LPS). Se esta é a resposta natural do hospedeiro por qual razão há a atenuação da reposta imune quando expostos ao LPS de forma repetida? Tentando responder esta pergunta, Beeson e Roberts em 1947 sugeriram que a resposta de tolerância ocorre por aumento do clearance de LPS (BEESON; ROBERTS, 1947), o que explicaria até o momento o porquê do sintoma clássico de febre induzido por infecção estar atenuado nos coelhos de seus trabalhos seminais.Todavia, esta resposta não ficou presa a esta explicação quando outros pesquisadores observaram que macrófagos hepáticos, também conhecidos como células de Kupfer, produzem pirógenos endógenos quando expostos a um pirógeno exógeno, mas que animais tolerantes não tem esta capacidade (DINARELLO; BODEL; ATKINS, 1968).

Atualmente, após 70 anos destas descobertas, sabe-se que as moléculas no plasma que induzem febre são as citocinas e as PGs produzidas pelas células imunes, principalmente macrófagos, contra os agentes infecciosos ou inflamatórios, conhecidos como pirógenos exógenos. Quanto à tolerância, muitas descobertas foram feitas. Hoje, já se há conhecimento de que a tolerância é um fenômeno extremamente complexo que envolve uma míriade de respostas periféricas e centrais integradas (BISWAS; LOPEZ-COLLAZO, 2009). Além disso, a atenuação dos sintomas clínicos clássicos de infecção na tolerância não é consequência da atenuação da resposta imune, mas sim da reprogramação neuroimune e endócrina do hospedeiro (BISWAS; LOPEZ-COLLAZO, 2009; LÓPEZ-COLLAZO; DEL FRESNO, 2013). Sabe-se com convicção que a tolerância ao LPS desencadeia a atenuação de determinadas citocinas pró-inflamatórias como TNF-α, IL-1β e IL-6 (MUNOZ et al., 1991a, 1991b; DRAISMA et al., 2009), mas também o aumento de anti-inflamatórias como, por exemplo, IL-10 e TGF-β (MONNERET et al., 2004; DRAISMA et al., 2009) em macrófagos, uma resposta fenótipica muito parecida com a de macrófagos M2. Estas respostas estão relacionadas com a atividade diminuída e a plasticidade do fator de transcrição NFκB em macrófagos tolerantes (BISWAS; LOPEZ-COLLAZO, 2009).

No desafio imune, o NFκB tem papel fundamental na regulação da codificação de genes de citocinas pró-inflamatórias e enzimas induzidas por LPS como a ciclooxigenase 2 (COX_2) (ROMANOVSKY; STEINER; MATSUMURA, 2006). Na fase inicial do desafio imune ao LPS, há o aumento da expressão de COX_2 e seu substrato, a prostaglandina E_2 (PGE_2). Já durante a fase de resolução ou fase final da inflamação, observa-se um aumento adicional na

expressão de COX_2 (WEST; HEAGY, 2002), sem aumentar a produção de PGE_2, mas acompanhada do aumento da produção de PGD_2 (GILROY et al., 1999), outro substrato de COX_2. Na resposta do fator de transcrição NFκB é dependente da expressão de seus dímeros p50p50 e p65p50. Esta plasticidade de NFκB é bem descrita na sepse, uma condição letal induzida pela resposta imune incontrolada contra um agente infeccioso (RITTIRSCH; FLIERL; WARD, 2008). Sabe-se que na fase inicial da sepse há um aumento da expressão do heterodímero p65p50 e, consequentemente, um perfil de resposta mais pró-inflamatório. No entanto, na fase final da sepse há o aumento de homodímeros p50, os quais induzirão a expressão de moléculas mais anti-inflamatórias (ADIB-CONQUY et al., 2000). Este evento vai ao encontro com o observado em macrófagos nocaute para o homodímero p50, já que são incapazes de se tornarem tolerantes ao LPS (BOHUSLAV et al., 1998).

Estes últimos dados mostram que o aspecto translacional da tolerância ao LPS como modelo experimental para a fase final da resposta à sepse, a qual tem alto índice de mortalidade e, ainda, é pouco entendida (VERGADI; VAPORIDI; TSATSANIS, 2018). A maioria dos estudos sobre sepse foca na sua fase inicial, onde é observada uma produção incontrolada de citocinas inflamatórias e, portanto, de alta taxa de mortalidade. A fase seguinte da sepse está relacionada principalmente com a reprogramação da resposta imune ao agente infeccioso, sendo que esta reprogramação pode acarretar na inaptidão do sistema imune em combater infecções secundárias, o que explica a alta mortalidade de pacientes mesmo após a fase aguda da sepse. Vale ainda destacar que parte dos pacientes com sepse não apresentam resposta febril, o que pode ser explicado pelo fenômeno da tolerância (MARTINS et al., 2017).

De forma geral, o perfil inflamatório da periferia não é igual ao observado centralmente na tolerância ao LPS. Como descrito por alguns autores, a tolerância ao LPS atenua a produção de citocinas pró-inflamatórias na periferia, mas mantém a produção central aumentada (MONNERET et al., 2004; CHEN et al., 2005). Fica então a pergunta: como há o aumento na produção de citocinas pró-inflamatórias centralmente sem a produção de resposta febril? Infelizmente, não há resposta para esta pergunta. Entretanto, a reprogramação da resposta neuroimune e endócrina observada na tolerância e, provavelmente, uma reprogramação na produção de PGs centralmente são, de fato, possíveis explicações para este fenômeno.

Além das citocinas e PGs, é importante destacar o papel da produção dos glicocorticóides na tolerância. No caso, esta produção já foi descrita como atenuada (BUMILLER et al., 1999; BORGES et al., 2007) ou mantida aumentada (SZABÓ et al., 1994; CHEN et al., 2005; SORIANO et al., 2013). Entretanto, estas discordâncias nos achados podem

estar relacionadas ao protocolo utilizado para o desenvolvimento da tolerância, como a dose utilizada e o período entre os estímulos. Curiosamente, um dos trabalhos indicou que há um paralelo entre aumento na produção de corticosterona e aumento na produção de citocinas pró-inflamatórias centralmente, mas não na produção de citocinas na periferia em ratos tolerantes ao LPS (CHEN et al., 2005). Os autores sugerem que o aumento do "estresse central" induzido pelo aumento de citocinas induz a maior produção de corticosterona em animais tolerantes.

Quanto ao papel dos gasotransmissores na tolerância ao LPS, faremos uma breve revisão sobre o que foi encontrado na literatura para cada gasotransmissor. Para fins de padronização, esta revisão se baseou em estudos analisando a fase inicial da tolerância, i.e., a fase de reprogramação neuroimune e endócrina induzida pelo desafio com LPS.

1.3.1 Participação do óxido nítrico (NO) na tolerância ao LPS

Primeiro gás a ser descoberto endogenamente, o NO é produzido em grandes quantidades pela expressão da enzima óxido nítrico sintase induzível (iNOS) após exposição a endotoxina (HAUSER et al., 2005). Após uma revisão dos trabalhos descrevendo a produção de NO na tolerância ao LPS (Tabela 1), podemos sugerir que a produção de NO sistêmico é importante para o desenvolvimento da tolerância, mas não é para sua manutenção. Esta hipótese está fundamentada na maior produção de NO em desafios com somente uma reexposição ao LPS (FUJII et al., 2000; SPITZER; SPITZER, 2000; SPITZER et al., 2002; EBISAWA et al., 2004; KIM; JANG; PARK, 2010; HE et al., 2014), sendo que a produção de NO é atenuada em protocolos com várias exposições ao LPS em roedores (SOSZYNSKI, 2002; CEREZO et al., 2004; SORIANO et al., 2013; EFTEKHARI et al., 2014). Em discordância, outro trabalho observou que a atividade do óxido nítrico sintase (NOS) foi inibida em galinhas tolerantes reexpostas ao LPS uma única vez, indicando que a produção de NO está atenuada neste outro modelo animal logo na fase inicial da tolerância (CHANG et al., 1996). Quanto ao efeito do NO na ausência de resposta febril em animais tolerantes, foi observado que a inibição da iNOS tanto central quanto da periferia reverteu a resposta de tolerância febril, indicando seu efeito anti-pirético na tolerância (ALMEIDA et al., 1999; DIAS et al., 2005).

Outros trabalhos ainda analisaram o efeito central do NO na tolerância ao LPS. Foi observado que o NO produzido tanto perifericamente quanto centralmente tem efeito neuroprotetor na tolerância ao LPS (KAWANO et al., 2007; ORIO et al., 2007; LIN; WU; HUANG, 2010). A ação neuroprotetora de NO parece estar relacionada com o aumento da

atividade de iNOS na periferia e da óxido nítrico sintase endotelial (eNOS) central quando o insulto é realizado 24 h após uma única exposição ao LPS.

Tabela 1. Tolerância ao LPS e a produção de NO.

Dose LPS	Administração	Repetições LPS ou novo desafio	Intervalo	Modelo experimental	Tratamento	NO	Referências	DOI
50 $\mu g.kg^{-1}$	ip	Modelo de isquemia hipóxica (HI)	24 h	Ratas Sprague-Dawley filhotes		Ratos com pré-tratamento com LPS tiveram menor taxa de mortalidade e menor injúria encefálica. Ratos pré-tratados com LPS tiveram aumento na expressão de AKT- eNOS, mas não de nNOS ou iNOS no córtex cerebral.	Lin et al., 2010	10.1161/STROKEAHA.109.574004
50 $\mu g.kg^{-1}$	ip	Lesão do neocórtex com microinjeção de n-metil D-aspartato (NMDA)	30 min ou 24 h	Camundongo C57BL/6 e nocautes para iNOS e eNOS	7-NI (50 $mg.kg^{-1}$ ip; inibidor de nNOS); aminoguanidina (100 $mg.kg^{-1}$ ip; inibidor seletivo de iNOS).	Ratos com pré-tratamento com LPS tiveram a lesão no neocórtex diminuída. Tolerância antecipada é dependente de eNOS e nNOS. Tolerância tardia é dependente de iNOS.	Orio et al., 2007	10.1161/STROKEAHA.107.486837
500 $\mu g.kg^{-1}$	ip	Lesão do neocórtex com microinjeção de n-metil D-aspartato (NMDA)	24 h	Camondongos C57BL/6 e nocaute para iNOS; COX_2; NOX_2	Aminoguanidina (100 $mg.kg^{-1}$ i.p; inibidor seletivo de iNOS), (DPTA)-NONOate (1,36 µmol em 140 nl de solução salina tamponada com Na_2HPO_4/ fosfato; doador de NO).	O efeito neuroprotetor do pré-tratamento com LPS foi bloqueado pela inibição de iNOS e não é observada em camundongos nocaute para iNOS. O peroxinitrito, formado pelo superóxido derivado de NO e NADPH oxidase derivado de iNOS, é essencial para a tolerância às lesões NMDA.	Kawano et al., 2007	10.1038/sj.jcbfm.9600449
500 $\mu g.kg^{-1}$	iv	Infusão de etanol (3 h)	48 h	Ratas e ratos Sprague-Dawley		A tolerância ao LPS causou o aumento de NO produzido por hepatócitos e células de Kupffer.	Spitzer e Spitzer et al., 2002	10.1016/s0741-8329(99)00098-1
1 $mg.kg^{-1}$	ip	Modelo de isquemia e reperfusão (I/R) renal	5 ou 24 h ou 8 dias	Camundongos C57BL/6J e nocautes para eNOS e iNOS	Animais nocaute para iNOS não foram protegidos para o desafio de I/R.	A proteção renal conferida pelo pré-tratamento com LPS é mediada pelo aumento de iNOS.	Kim et al., 2010	10.5483/BMBRep.2010.43.9.629
3 $mg.kg^{-1}$	ip	Modelo de isquemia e reperfusão (I/R) renal	24 h	Camundongos C57BL/6 e nocautes para HIF-1α e HIF-2α	Aminoguanidina (inibidor seletivo de iNOS); L-NAME (inibidor não seletivo de NOS).	Camundongos pré-tratados com LPS tiveram aumento na produção de NO o que melhorou a recuperação da microcirculação afetada. O inibidor de iNOS inibiu o efeito protetor do pré-tratamento com LPS em camundongos C57BL/6. Não houve agravamento dos danos renais em camundongos nocaute para HIF-2α pré-tratados com LPS.	He et al., 2014	10.1038/ki.2013.342
150 $\mu g.kg^{-1}$ (1°) e 100–400 $\mu g.local^{-1}$ (2°)	ip (1°) sc (2°)	1	4 h	Cruzamento C57BL/6 com 129Sv e nocaute para iNOS		O vazamento de corante diminuiu localmente e a produção de NO aumentou em animais pré-tratados com LPS. O pré-tratamento com LPS não inibiu o extravazamento de corante induzido por LPS em nocautes para iNOS. A produção de corticosterona foi aumentada em animais tolerantes e tolerantes nocaute para iNOS.	Fujii et al., 2000	10.1038/sj.bjp.0703277
500 $mg.kg^{-1}$ (1°) e 2 $mg.kg^{-1}$ (2°)	iv (1°) e iv ou ip (2°)	1	12 h	Galinhas		A atividade de NOS foi inibida em galinhas tolerantes.	Chang et al., 1996	10.1152/ajpgi.1996.271.4.G539
500 $\mu g.kg^{-1}$ (1°) e 3 $mg.kg^{-1}$ (2°)	iv	1	48 h	Ratas e ratos Sprague-Dawley		Ratos tolerantes aumentaram a expressão de iNOS em células de Kupffer.	Spitzer et al., 2002	https://www.bioscience.org/2002/v7/af/A744/fulltext.htm
0.01-1000 $\mu g.kg^{-1}$ (1°) e 5 $mg.kg^{-1}$ (2°)	ip	1	4, 6, 8, 10, 12 e 16 h	Ratos Wistar	L-NAME (10 $mg.kg^{-1}$ ip; inibidor não seletivo de NOS).	O NO produzido pelo pré-tratamento com LPS tem efeito citoprotetor em hepatócitos na fase inicial da tolerância ao LPS.	Ebisawa et al., 2004	10.1016/S0022-4804(03)00348-2
1 $mg.kg^{-1}$	ip	1	24 h ou 7 dias	Ratos e ratas Sprague-Dawley filhotes	SB203580 (10 $\mu g.g^{-1}$, inibidor de p38).	A resposta de iNOS foi diminuída em ratos tolerantes. A inibição de p38 atenua a transcrição de NFκB aumentando a tolerância.	Cerezo et al., 2004	10.1097/00024382-200405000-00013
5 $mg.kg^{-1}$ (1°) e 60 ou 120 $mg.kg^{-1}$ (2°)	ip	1	96 h	Camundongo C57BL/6 e nocaute para iNOS		Animais nocaute para iNOS mantiveram o efeito protetor induzido pela tolerância mas não modificou a degradação de IκBα e a ativação de NFκB.	Zingarelli et al., 2002	10.1097/00024382-200206000-00007
50 $\mu g.kg^{-1}$	ip	2	24 h	Ratos Wistar	L-NAME (50 $mg.kg^{-1}$ ip, inibidor não seletivo de NOS).	A produção de NO foi atenuada após segunda injeção de LPS e quase abolida após a 3° dose de LPS. A inibição de NOS retardou a tolerância na hipofagia e retardou a tolerância na resposta febril induzida por LPS.	Soszynski et al., 2002	10.1016/s0031-9384(02)00693-5
50 $\mu g.kg^{-1}$	ip	2	48 h	Ratos Wistar	L-NAME (250 $g.mL^{-1}$ icv, inibidor não seletivo de NOS).	A inibição de NOS centralmente induziu resposta febril em ratos tolerantes.	Almeida et al., 1999	10.1097/00001756-199909290-00034
100 $\mu g.kg^{-1}$	ip	2	24 h	Ratos Wistar	Animais tolerances adrenalectomizados receberam por 7 dias dexametasona (0.6 $mg.kg.day^{-1}$, 1 $ml.kg^{-1}$, sc).	A produção de NO foi atenuada em animais tolerantes. A reposição de glicocorticóides suprimiu a atividade de NOS em animais tolerantes.	Soriano et al., 2013	https://doi.org/10.1139/cjpp-2013-0028
100 $\mu g.kg^{-1}$	ip	2	24 h	Camundongo C57BL/6 e nocaute para iNOS	L-NAME (40 $mg.kg^{-1}$ ip; inibidor não seletivo de NOS) e aminoguanidine (10 $mg.kg^{-1}$, i.p; inibidor seletivo de iNOS).	O tratamento com o inibidor da iNOS induziu resposta febril em camundongos tolerantes. Camundongos nocaute para iNOS não se tornaram tolerantes a resposta febrigênica induzida por LPS.	Dias et al., 2005	10.1152/japplphysiol.01243.2004
1 $mg.kg^{-1}$	ip	4	24 h	Ratos Sprague-Dawley	MCNA-343 (5 $ng.kg^{-1}$ icv; agonista muscarínico tipo 1).	Menor expressão de iNOS hepático em ratos tolerantes. O antagonista muscarínico reverteu a menor expressão de TNF-α hepático em ratos tolerantes.	Eftekhari et al., 2014	https://doi.org/10.1016/j.ejphar.2014.06.050

1.3.2 Participação do monóxido de carbono (CO) na tolerância ao LPS

Somente dois trabalhos descrevem a participação de CO na tolerância ao LPS. O primeiro trabalho foi publicado por nosso laboratório indicando o efeito de CO central na tolerância ao LPS (RAFFAINI; DIAS; BRANCO, 2006). Neste trabalho seminal, a ausência de resposta febril observada na tolerância ao LPS foi revertida por meio da injeção de heme-lisinato icv, uma droga indutora da via heme-oxigenase produzindo CO, sendo este efeito dependente de GMP cíclico. Estes dados sugerem que a produção de CO centralmente está diminuída na tolerância ao LPS. No outro trabalho (RIQUELME; BUENO; KALERGIS, 2015), foi observado que o pré-tratamento com CO antes do desafio imune com LPS diminui a expressão de TLR-4 em células mielóides. Este dado indica que o CO produz efeito parecido com o observado em animais pré-tratados ao LPS e reexpostos a endotoxina após um período de tempo, onde a expressão de TLR-4 é atenuada.

1.3.3 Participação do H_2S na tolerância ao LPS

Sabendo-se que a produção de H_2S via aumento da atividade de CSE está aumentada na periferia após desafio imune (LI et al., 2005), Rios et al., (2016) analisaram se a produção de H_2S induzido por CSE na periferia também estaria envolvida com a tolerância ao LPS. Intrigantemente, eles observaram que o H_2S não tem efeito no desenvolvimento da tolerância ao LPS. Vale lembrar que nosso laboratório demonstrou que, durante o desafio imune, a razão de produção de H_2S centralmente é atenuada (KWIATKOSKI et al., 2013), de forma contrária ao observado na periferia. Deste modo, sabendo-se da complexidade do fenômeno da tolerância ao LPS, nós avaliamos o papel do H_2S hipotalâmico na tolerância ao LPS.

2 Objetivos

2.1 Objetivo geral

Avaliar se a resposta imune reduzida durante a tolerância ao LPS relaciona-se à produção endógena aumentada de H_2S na AVPO.

2.2 Objetivos específicos

- Avaliar se a atividade dos termoefetores é desbloqueada por meio da inibição da produção de H_2S centralmente em animais tolerantes;
- Avaliar se a produção de PGs (PGE_2, PGD_2) na AVPO é modulada pelo bloqueio farmacológico da enzima produtora de H_2S, especificamente, a CBS centralmente na tolerância ao LPS;
- Avaliar se a produção sistêmica de citocinas (IL-1β, IL-6, TNF-α) é afetada pela inibição farmacológica da enzima CBS centralmente em animais tolerantes.
- Analisar a possível modulação do eixo hipotálamo-hipófise-adrenal (HPA) por meio da inibição farmacológica da enzima CBS central de animais tolerantes.
- Analisar a taxa de produção de H_2S e o perfil de expressão da enzima CBS na AVPO de animais tolerantes.

3 Material e métodos

3.1 Animais

Ratos Wistar adultos (290-300 g) foram individualmente separados e mantidos em temperatura controlada de 29°C com ciclo de 12h claro/escuro com comida e água ad libitum. Todos os experimentos foram aprovados pelo Comitê de Ética Animal, da Faculdade de Odontologia de Ribeirão Preto (2016.1.393.58.1). Além disso, todos os protocolos e procedimentos cumpriram as recomendações do Guia para o Cuidado e Uso de Animais de Laboratório do Conselho Nacional para o Controle da Experimentação Animal (CONCEA).

3.2 Drogas

O LPS extraído de Escherichia coli (sorotipo 0111:B4, lote #076K4020, Sigma-Aldrich, EUA) foi diluído em solução salina livre de pirógenos e injetado intraperitonealmente na dose de 100 $\mu g.kg^{-1}$. O desafio imunológico e a tolerância à endotoxina foram induzidos com a administração de LPS, o que foi suficiente para ativar a sinalização febrigênica e a vasoconstrição da cauda, um importante termoefetor em ratos mantidos dentro da zona termoneutra (29ºC) (ROMANOVSKY; IVANOV; SHIMANSKY, 2002; KRALL et al., 2010). O inibidor da CBS, AOA, foi administrado no terceiro ventrículo dos animais para verificar se a inibição de H_2S centralmente poderia abolir a tolerância à endotoxina. A droga foi dissolvida em solução salina livre de pirógenos até uma concentração final de 100 $pmol.\mu l^{-1}$. AOA foi administrado por via intracerebroventricular no volume de 1 µl, como relatado anteriormente (KWIATKOSKI et al., 2013).

3.3 Cirurgias

Sete dias antes do experimento, foram implantados uma cânula icv e um mini datalogger intra-abdominal (SubCue, AB, Canadá) nos animais. Todos os procedimentos cirúrgicos foram realizados sob anestesia utilizando uma mistura de 10% de ketamina e 2% de xilazina (1:1; $1ml.kg^{-1}$ de peso corporal) administrada por via intraperitoneal (ip). Proteção anti-inflamatória/antibiótica com flunixina meglumina (0,1 ml por via subcutânea) e pentabiótica

(1.200.000 UI; 0,1 ml por via intramuscular) foram fornecidas. Em um campo cirúrgico asséptico, a cavidade intraperitoneal foi exposta através de uma laparotomia mediana para inserção do datalogger. A cavidade intraperitoneal foi fechada por sutura da camada muscular e cutânea ao final da cirurgia. Os animais foram posteriormente fixados ao estereotáxico com a barra do incisivo ajustada em -3,3 mm. As seguintes coordenadas foram atribuídas com referência ao bregma: ântero-posterior: -0,4 mm, lateral: 0 mm e dorsoventral: - 4,5 mm. As coordenadas foram obtidas de estudos anteriores em laboratório (KWIATKOSKI et al., 2013). A eficácia da colocação da cânula guia (22 GG; comprimento de 16 mm) no terceiro ventrículo foi verificada pelo fato de que o líquido cefalorraquidiano fluiu para fora da cânula guia subsequente à sua inserção. A cânula icv foi fixada no crânio com um parafuso de aço inoxidável e resina odontológica. A microinjeção de AOA icv (inibidor de CBS) foi realizada com o uso de uma seringa Hamilton de 5 µl (Hamilton Bonaduz Ag, Suíça) acoplada a uma extensão de tubo de polietileno conectada à uma agulha de 20 mm de comprimento.

3.4 Grupos experimentais

Os grupos experimentais foram distribuídos aleatoriamente. O peso corporal foi medido diariamente (7-8 da manhã) antes das injeções. O grupo naïve foi dividido em quatro subgrupos que receberam injeções icv de AOA ou seu veículo (sal) seguido da injeção de LPS ip ou seu veículo (sal). O grupo tolerante recebeu LPS ip diariamente por três dias, até ao desenvolvimento da tolerância à endotoxina verificada por meio da atenuação da febre (Fig. 2). No quarto dia, os animais tolerantes receberam AOA ou seu veículo (sal) icv antes da quarta injeção de LPS. Os ratos não tolerantes (grupos controle) receberam sal ip por quatro dias e no quarto dia receberam AOA ou sal icv antes da quarta injeção de sal ip. As amostras de plasma foram coletadas 2h após a última injeção de LPS durante o período efervescente de febre (KWIATKOSKI et al., 2013).

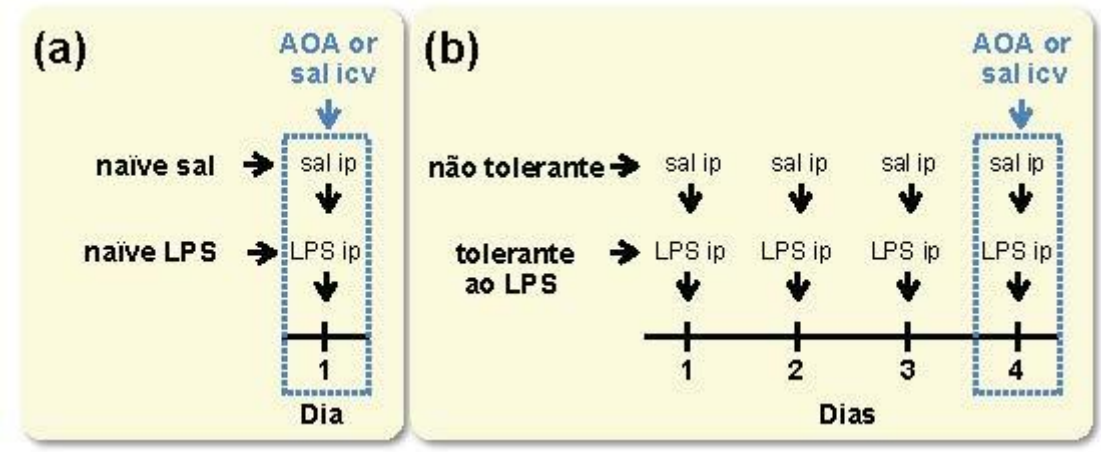

Fig. 1 Desenho experimental. Os animais foram separados em quatro grupos naïve sal, naïve lipopolissacarídeo (LPS), não tolerante e ratos tolerantes ao LPS no dia do experimento (indicado pela caixa azul). (A) Desenho experimental de ratos naïve. Ratos naïve não receberam injeções antes do dia experimental, ou seja, dia 1 (indicado pela caixa azul). Ratos naïve receberam ácido amino-oxiacético (AOA), inibidor da enzima cistationina β-sintase (CBS) ou seu veículo (sal) icv seguido pela injeção de sal ou LPS ip. (B) Desenho experimental de ratos não tolerantes e tolerantes. Ratos não tolerantes receberam veículo de LPS (sal) ip por três dias consecutivos antes do dia do experimento, ou seja, dia 4 (indicado pela caixa azul). Ratos tolerantes receberam LPS ip por três dias consecutivos antes do dia do experimento. Ratos não tolerantes e tolerantes receberam AOA ou seu veículo (sal) icv seguido pela injeção de sal ip (ratos não tolerantes) ou LPS (ratos tolerantes) ip no dia experimental, respectivamente.

3.5 Medida indireta de termogênese sem tremor

O consumo de oxigênio foi determinado em ratos conscientes e sem restrição, no estado alimentado e alojados em uma câmara selada individual. Os ratos foram adaptados ao aparato um dia antes e no dia do experimento por 20 minutos antes da medida do volume de O_2 (VO_2). As amostras de ar passaram por um analisador de oxigênio (OA 272; Saylor Servomex, Reino Unido). Para o cálculo do consumo de O_2 (VO_2), os dados de: FO_{2IN}; fração de O_2 na saída da câmara (FO_{2OUT}), fluxo de ar em mililitros por minuto (AirFlow) e peso do animal em kg (PC) foram plotados para o cálculo. Foi utilizada a fórmula : VO_2 = Fluxo de Ar (FO_{2IN} - FO_{2OUT}) $.PC^{-1}$.

3.6 Medida do índice de perda de calor (HLI, iniciais da sigla em inglês "heat loss index")

Tb, temperatura da pele da cauda (Tsk), e temperatura ambiente (Ta) foram adquiridas para o cálculo do HLI. A Tb foi adquirida pelo datalogger programado para o período do

experimento (dados de registro a cada 5 minutos) e extraído usando o software SubCue. A alta precisão dos dados de Tb foi alcançada usando os valores de calibração de cada datalogger fornecidos pela empresa. Uma câmera de sensibilidade termográfica (sensibilidade de 0,1°C; FLIR ONE; FLIR Systems Inc.) foi usada para medir o terço médio do comprimento da cauda como referência para a medida da temperatura cutânea (Tsk). A Ta foi mantida a 29°C e verificada a cada 30 min (min) usando um termômetro fixo à caixa. O HLI foi utilizado para avaliar as respostas termoefetoras da vasculatura da pele da cauda e calculado com base na fórmula: HLI = (Tsk-Ta).$(Tb-Ta)^{-1}$. Os limites do HLI são 0 (vasoconstrição máxima da pele) e 1 (vasodilatação máxima) (ROMANOVSKY; IVANOV; SHIMANSKY, 2002).

3.7 Aquisição da AVPO e plasma

Os animais foram decapitados e o sangue do tronco foi coletado em tubos revestidos com anti-coagulante e imediatamente centrifugados (2000 g por 20 minutos a 4°C) 2h após a injeção de LPS/sal ip no período efervescente da febre, como relatado anteriormente (BLATTEIS; SEHIC, 1998). O cérebro foi removido e congelado instantaneamente (40 s) com isopentano resfriado com gelo seco. Cortes coronais do cérebro foram feitos com um micrótomo (Microm HM 505 E, Thermo Scientific, EUA). Três cortes coronais de 500 μm de espessura foram cortados na área anterior do hipotálamo, a AVPO bilateral foi perfurada com uma agulha de 16 GG, homogeneizada e centrifugada no tampão de lise apropriado. A concentração total de proteínas no homogenato foi medida com um kit de ensaio Bradford (Bio-Rad Laboratories, Munique, Alemanha).

3.8 Dosagem de PGE_2 e PGD_2

Amostras da AVPO foram homogeneizadas em tampão fosfato salino (PBS), pH 7,4, contendo EDTA (1 mM) e indometacina (10 μg/ml) e centrifugadas (18000 g por 10 min a 4 ºC) para a coleta do sobrenadante. A dosagem de PGD_2 e PGE_2 foi determinada por kits ELISA e realizada de acordo com as instruções do fabricante (#514010 and #512011 Cayman Chemical). A concentração das proteínas no sobrenadante foi analisada pelo método de Bradford modificado (Bio-Rad Laboratories, EUA) e utilizada para a normalização dos resultados.

3.9 Dosagem de citocinas

As citocinas plasmáticas TNF-α, IL-1β, IL-6 foram analisadas por kits ELISA de acordo com as instruções dos fabricantes (rat DuoSet, R&D Systems, EUA).

3.10 Dosagem de corticosterona

A corticosterona foi extraída de 25 µl de plasma sanguíneo através da adição de 1 ml de etanol 100%. A solução foi agitada e centrifugada (1200 rpm por 15 min à 4 °C). O sobrenadante foi coletado e liofilizado. Os níveis de corticosterona foram analisados por radioimunoensaio utilizando-se de um anticorpo anti-corticosterona (SigmaAldrich, St. Louis, MO, EUA). Os limites de detecção foram de 0,12 à 2000 $\mu g.dL^{-1}$.

3.11 Western Blot

A expressão da proteína CBS relacionada com a síntese de H_2S no AVPO foi medida usando o ensaio de imunotransferência. O tecido analisado foi removido do AVPO bilateralmente e homogeneizado a 4°C em tampão de lise (Tris – HCl 50 mM, pH 7,4, NaCl 150 mM, Triton X-100 à 1%, Triton X-100 à 1%, SDS à 0,1%, 1 $\mu g.mL^{-1}$ de aprotinina, 1 $\mu g.mL^{-1}$ de leupeptina, fluoreto de fenilmetilsulfonil 1 mM, ortovanadato de sódio 1 mM, pH 10, pirofosfato de sódio 1 mM, pirofosfato de sódio 1 mM, fluoreto de sódio 25 mM e EDTA 0,001 M - pH 8). O sobrenadante (40000 rpm por 10 min a 4°C) dos homogenatos de tecido foi coletado. Um total de 30 µg de proteína em alíquotas foi dissolvido em tampão de carga e as proteínas foram separadas por eletroforese em gel de poliacrilamida com dodecilsulfato de sódio à 10%. As bandas de proteína foram então transferidas para membranas de nitrocelulose e incubadas em 50 mL de tampão de bloqueio (PBS, leite desnatado a 2,5%) por 1 h e lavadas em tampão (PBS, 0,1% Tween 20, pH 7,6). Após, as membranas foram incubadas com o anticorpo primário correspondente em albumina de soro bovino a 5% (BSA) e deixadas durante a noite a 4°C. O anticorpo primário CBS anti-camundongo monoclonal de coelho foi incluído (1:1000; Cell Signaling Technology, Beverly, MA). Depois disso, as membranas foram lavadas e incubadas com o anticorpo secundário anti-coelho conjugado com peroxidase de rábano silvestre (CBS) (1:5000; Dako, Glostrup, Dinamarca) por 1h em temperatura ambiente. As proteínas marcadas foram reveladas usando substrato quimioluminescente Supersignal West

Pico (Pierce, Rockford, IL, EUA). Utilizando um tampão de remoção (100 mM de 20-mercaptoetanol, dodecilsulfato de sódio a 2%, Tris-HCl 62,5 mM, pH 6,8), as membranas foram recuperadas (30 min a 50°C) para remoção e nova sondagem. Para regular a equivalência da carga ou transferência de proteínas, as membranas foram embebidas com TBS-T antes do bloqueio e incubadas com anticorpo primário monoclonal contra anti-GAPDH (1:5000, Sigma-Aldrich, em 5% de BSA) e deixadas durante a noite à 4°C.

3.12 Taxa de produção de H_2S na AVPO

Os níveis de H_2S na AVPO foram determinados conforme descrito anteriormente em nosso laboratório (56,57). As amostras de AVPO foram homogeneizadas em tampão fosfato de potássio (100 mM; pH 7,4) usando o microprocessador de laboratório (VirTis, Gardiner, NY, EUA). Cada amostra (50% p/v; 100 µl) continha L-cisteína (10 mM; 20 µl), 5'-fosfato de piridoxal (2 mM; 20 µl) e PBS (30 µl). A reação foi realizada em tubos eppendorf selados com parafina e transferidos para um banho à 37° C para incubação (2 h). Foi adicionado acetato de zinco (1% p/v; 100 µl) para capturar H_2S produzido, seguido por ácido tricloroacético (10% p/v; 100 µl) para precipitar as proteínas e subsequentemente bloquear a reação. Sulfato de N, N-dimetil-p-fenilenodiamina (20 mM; 50 µl) em HCl 7,2 M, seguido de FeCl3 (30 mM; 50 µl) em HCl 1,2 M foram adicionados a 50 µl do sobrenadante após a centrifugação e a densidade óptica foi medido a 670 nm. A curva de calibração da absorvância foi alcançada usando soluções de NaHS (#161527, Sigma-Aldrich, EUA; 0,1–100 $\mu g.ml^{-1}$). As amostras foram testadas usando um reagente de corante protéico (Bio-Rad Laboratories; Hercules, CA, EUA) para determinar o teor de proteína.

3.13 Estatísticas

As análises estatísticas utilizadas para cada teste estão completamente descritas na tabela suplementar. A distribuição normal foi analisada para todos os dados e testes não paramétricos foram realizados quando necessário. As figuras e estatísticas foram preparadas usando o software Prism (versão 8.0; GraphPad Software Inc.). Os experimentos e cirurgias foram realizados pelo autor mais especializado de cada técnica para diminuir as variabilidades. Um cálculo de potência foi utilizado ($\alpha = 0,05$ e $\beta = 0,8$) para estimar o número do grupo. Um

estudo piloto (Dados Suplementares) foi utilizado para verificar a indução de tolerância e antecipar os valores para o cálculo da potência. As PGs plasmáticas são expressas com o log de seus níveis. A análise densitométrica dos Western blots foi realizada usando ImageJ. Os dados de western blot foram normalizados usando GAPDH e os dados representados como expressão relativa ($CBS.GAPDH^{-1}$). Todos os outros dados foram expressos com a média ± SEM.

4 Resultados

4.1 Desenvolvimento da tolerância ao LPS

Para análise do desenvolvimento da tolerância ao LPS foi feito a medida das alterações na Tb de animais tratados sistemicamente com LPS na dose de 100 $\mu g.kg^{-1}$ (ip) ou seu veículo, salina (sal) ip (Fig. 2). Primeiramente, os animais foram aclimatados a 29°C uma temperatura relativamente alta dentro da zona termoneutra de ratos Wistar. No primeiro dia do tratamento, os animais que receberam LPS desenvolveram febre característica de animais desafiados imunologicamente com uma dose baixa de LPS aclimatados a uma temperatura alta dentro da zona termoneutra. Como podemos observar, a injeção do veículo de LPS não alterou a temperatura corporal comparada a temperatura antes de sua injeção. Ao segundo dia do tratamento com LPS, a reposta febril dos animais foi atenuada comparada com a resposta observada ao primeiro dia. Ao terceiro dia, animais que receberam pela terceira vez LPS sistemicamente tiveram sua resposta térmica similar ao observado em animais que receberam seu veículo por 3 dias, i.e. a resposta febril foi suprimida e, portanto, a tolerância foi induzida.

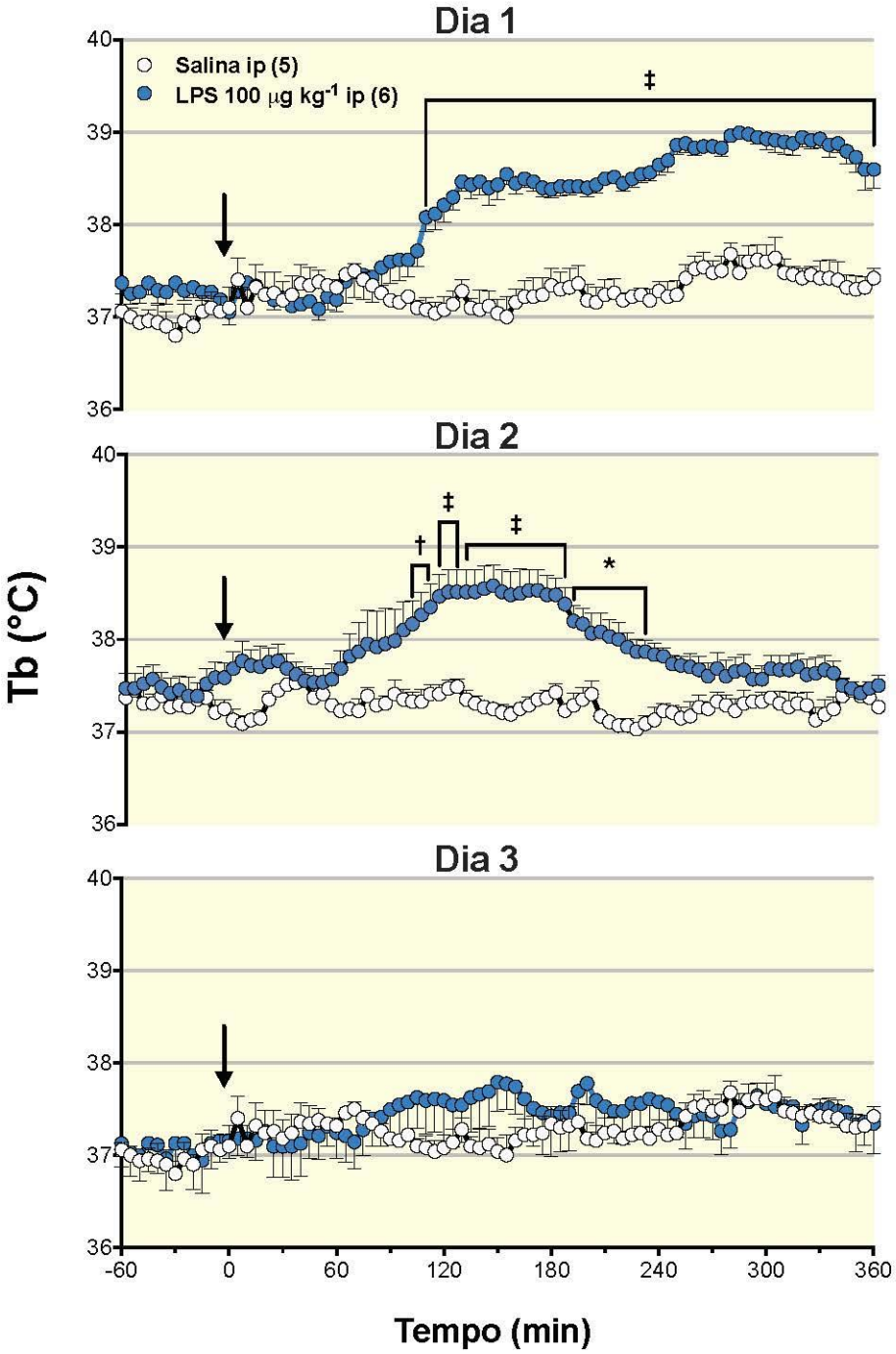

Fig. 2 Desenvolvimento da tolerância ao lipopolissacarídeo (LPS). Os animais foram separados em grupos que receberam salina ou LPS ip por três dias consecutivos numa dose capaz de produzir resposta febril ao primeiro desafio imunológico (100 $\mu g.kg^{-1}$). Durante este período foi analisada a resposta térmica após as injeções. A tolerância ao LPS foi confirmada após a observação de ausência de resposta febril em animais expostos repetidamente ao LPS (dia 3).

4.2 Efeito da inibição de CBS hipotalâmico na temperatura corporal (Tb), no consumo de O_2 e no HLI de animais naïve LPS e tolerantes ao LPS

Inicialmente, foi feita a avaliação se a inibição do H_2S hipotalâmico alteraria a Tb de ratos eutérmicos com a injeção de AOA (inibidor de CBS) icv. Como podemos observar nas Fig. 3A, gráfico superior, animais que receberam AOA icv não tiveram alterações na temperatura corporal. Além disso, nós também avaliamos especificamente qual termoefetor estaria sendo ativado para indução do aumento da temperatura corpórea por meio da medida indireta de termogênese sem tremor (estimado pelo consumo de O_2) ou aumento do tônus vasomotor cutâneo analisado pela diminuição do HLI (usando termografia de cauda, Tb e temperatura ambiente). No caso destes animais, como não houve alteração na temperatura corporal, nenhuma resposta termoefetora foi alterada como pode ser observado na Fig. 3B e C, gráficos superiores. Seguindo o mesmo raciocínio, animais naïve que receberam injeções de sal ip e sal icv não apresentaram diferenças na temperatura corporal (Fig. 3A, gráfico superior) e, portanto, nenhum termoefetor foi positivamente regulado, i.e. não houve ativação de termogênese sem tremor (Fig. 3B, gráfico superior) ou diminuição do HLI induzido por aumento do tônus vasomotor cutâneo (Fig. 3C, gráfico superior).

Para ratos naïve LPS, uma resposta febril típica foi desenvolvida após administração de uma dose relativamente baixa de LPS (100 $\mu g.kg^{-1}$ ip) em comparação com ratos naïve que receberam salina (Fig. 3A). A resposta febril induzida por LPS em ratos naïve resultou de um HLI reduzido (Fig. 3C, gráfico inferior), sem contribuição da termogênese sem tremor (Fig. 3B, gráfico inferior). Ratos naïve LPS com injeção de AOA icv tiveram um ligeiro aumento na Tb em comparação com ratos naïve LPS tratados com sal icv 165 minutos após LPS injeção (Fig. 3A, gráfico inferior). Após esta análise, a seguinte pergunta foi levantada: H_2S central modularia a tolerância à febre induzida por LPS *per se*? Para verificar esta possibilidade, a tolerância ao LPS foi desenvolvida após injeções repetidas de LPS (4 × LPS). A tolerância foi confirmada pela ausência de febre em animais tolerantes tratado com sal icv (Fig. 3D). Além disso, AOA foi administrado antes do LPS em ratos tolerantes e um aumento na Tb foi observada em comparação aos ratos tolerantes ao LPS que receberam sal icv (Fig. 3D, gráfico inferior). A resposta febril ao LPS em ratos tolerantes tratados com AOA foi resultante do aumento da termogênese sem tremor (Fig. 3E, gráfico inferior) e HLI diminuído (Fig. 3F, gráfico inferior), indicando que H_2S central modula ambos termoefetores na tolerância ao LPS em ratos. Não foram observadas diferenças entre os grupos que receberam injeções repetidas de sal, independentemente do tratamento icv, na Tb (Fig. 3D, gráfico superior), na termogênese sem tremor (Fig. 3E, gráfico superior) e no HLI (Fig. 3F).

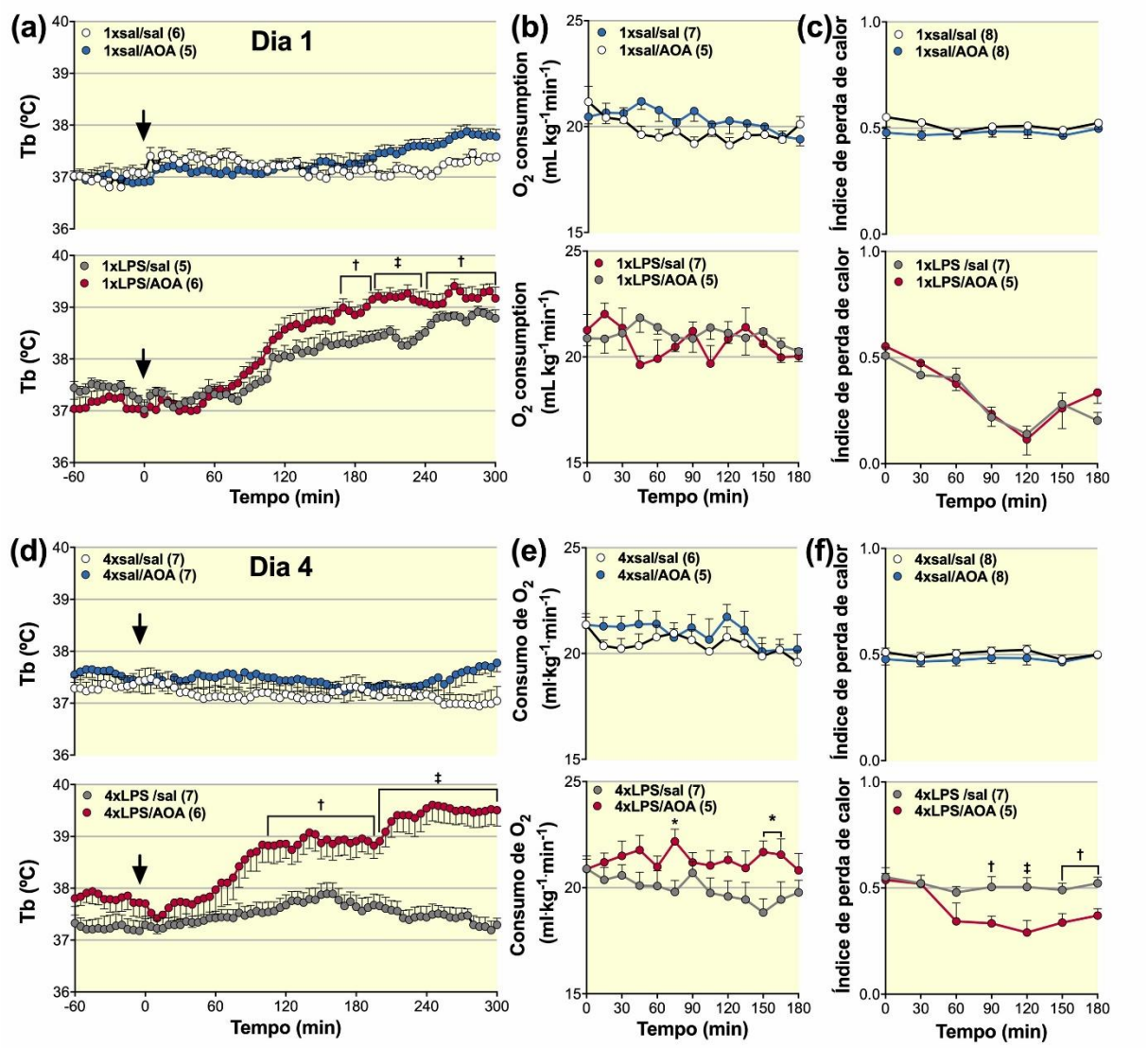

Fig. 3 Efeito da microinjeção do inibidor da enzima cistationina β-sintase, ácido aminooxiacético (AOA) intracerebroventricularmente (icv) na temperatura corporal (Tb; Fig. 3A e D); no consumo de O2 (Fig. 3B e E) e no índice de perda de calor (HLI; Fig. 3C e F) em animais naïve injetados lipopolissacarídeo (LPS) (1 × LPS) ou seu veículo (1xsal) e tolerantes ao LPS (4 × LPS) ou com a injeção repetida de seu veículo (4xsal). LPS (100 µg.kg −1 ip) ou seu veículo (solução salina ip) foi injetado no tempo zero (indicado pelas setas nas Figuras 3A e E). A microinjeção da AOA (inibidor da cistationina Y-liase) ou seu veículo (sal) icv foi realizada imediatamente antes do LPS ou do seu veículo (sal) ip. N = 5-8. Dados representados pela média ± SEM. * P < 0,05, † P <0,01 e ‡ P < 0,001 vs. grupo controle, mesmo gráfico.

4.3 Efeito da inibição de H_2S hipotalâmico nos níveis de PGs na AVPO e plasmáticos em animais naïve LPS e tolerantes ao LPS

Para investigarmos os mecanismos da resposta febril induzida em animais tolerantes ao LPS quando tratados com AOA icv, os níveis de PGs na AVPO também foram medidos, uma

vez que a AVPO tem papel fundamental na modulação da ativação dos termoefetores. Além disso, examinamos os níveis plasmáticos das PGs, uma vez que são fundamentais para as respostas termorregulatórias induzidas por LPS. Ao contrário da PGE_2, a PGD_2 é reconhecida por seu papel criogênico e também foi analisada (KRALL et al., 2010).

A microinjeção de AOA icv não causou efeito na produção de de PGE_2 na AVPO e no plasma (Fig. 4a) ou mesmo na produção de PGD_2 (Fig. 4c) em comparação aos animais naïve salina que receberam sal icv. Não foram observadas diferenças entre tratamento com AOA ou sal icv na produção de PGE_2 (Fig. 4b) e PGD_2 (Fig. 4d) na AVPO ou no plasma de ratos não tolerantes. Estes dados indicam que a inibição hipotalâmica do H_2S não causa efeitos na produção de PGs em ratos naïve ou não tolerantes.

Conforme descrito na literatura, ratos naïve LPS tratados com sal icv tiveram aumento nos níveis de PGE_2 (Fig. 4a) e PGD_2 (Fig. 4c) na AVPO e no plasma. O tratamento com AOA icv em ratos naïve LPS causou um ligeiro aumento nos níveis de PGE_2 na AVPO (Fig. 3a) e uma diminuição nos níveis de PGD_2 na AVPO (Fig. 4c) sem alterar os níveis plasmáticos de PGE_2 (Fig. 4A) e PGD_2 (Fig. 4c) em comparação aos ratos naïve LPS tratados com sal icv.

Animais tolerantes ao LPS tratados com sal icv apresentaram baixos níveis de PGE_2 na AVPO e no plasma, resultados semelhantes aos observados em ratos tratados repetidamente com sal ip (Fig. 4b). Entretanto, foi observado um aumento nos níveis de PGE_2 na AVPO e plasmáticos quando o LPS foi combinado com a administração de AOA icv em ratos tolerantes (Fig. 4b). Além disso, os ratos tolerantes ao LPS tiveram um aumento nos níveis de PGD_2 na AVPO e no plasma que foram diminuídos pela administração de AOA icv (Fig. 3d). Estes dados indicam que o H_2S centralmente desempenha um papel fundamental na modulação da resposta imune em ratos tolerantes ao LPS, regulando positivamente a principal molécula pirética (PGE_2) e, simultaneamente, regulando negativamente uma molécula criogênica (PGD_2).

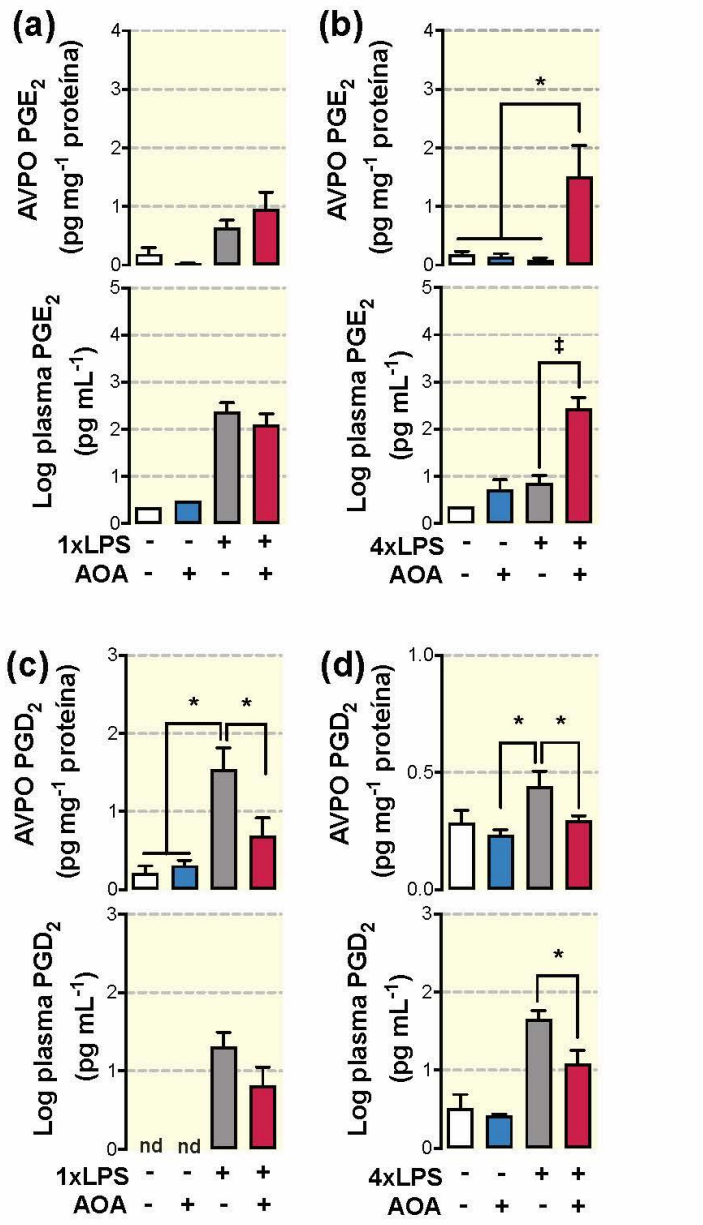

Fig. 4 Níveis de PGs na área pré-ótica ântero-ventral do hipotálamo (AVPO) e no plasma de animais que receberam lipopolissacarídeo (LPS) naïve (1×LPS) ou de animais tolerantes ao LPS (4×LPS) e o efeito da microinjeção central do inibidor da enzima cistationina β-sintase, ácido amino-oxacético (AOA). Os níveis de PGE2 e PGD2 na AVPO e no plasma foram analisados 2 h pós-injeção de solução salina ou LPS na dose de 100 µg.kg−1 ip. (A) Níveis de PGE2 na AVPO e no plasma (na forma logarítmica) em ratos naïve que receberam lipopolissacarídeo (LPS) (1×LPS) ou seu veículo (1xsal) com microinjeção de AOA ou seu veículo (sal) icv. (B) Níveis de PGE2 na AVPO e no plasma (na forma logarítmica) em ratos tolerantes ao lipopolissacarídeo (4×LPS) ou seu veículo (4xsal) com microinjeção de AOA ou seu veículo (sal) icv. (C) Níveis de PGD2 na AVPO e no plasma (na forma logarítmica) em ratos naïve que receberam lipopolissacarídeo (LPS) (1×LPS) ou seu veículo (1xsal) com microinjeção de AOA ou seu veículo (sal) icv.(D) Níveis de PGD2 na AVPO e no plasma (na forma logarítmica) em ratos tolerantes ao lipopolissacarídeo (4×LPS) ou seu veículo (4xsal) com microinjeção de AOA ou seu veículo (sal) icv. As barras representam a média ±SEM de cada grupo. Grupos com dados não detectáveis (nd) não foram incluídos nas estatísticas. N = 5-8. * $P < 0,05$ e ‡ $P < 0,0001$.

4.4 Efeitos da inibição central de H_2S nos níveis plasmáticos de citocinas em animais naïve LPS e tolerantes ao LPS

Como relatado anteriormente, (KRALL et al., 2010; NOGUEIRA et al., 2017) ratos naïve sal e não tolerantes apresentaram níveis plasmáticos indetectáveis de TNF-α (Fig. 5a e b). Por outro lado, foi observado um aumento nos níveis plasmáticos de TNF-α em ratos naïve LPS (Fig. 5a). Este aumento induzido por LPS nos níveis de TNF-α plasmáticos foi reduzido em ratos naïve LPS tratados com AOA icv (Fig. 4a), indicando que o H_2S regula positivamente os níveis plasmáticos de TNF-α em animais naïve LPS. Por outro lado, os aumentos induzidos por LPS nos níveis de IL-6 e IL-1β no plasma não foram afetados pela administração de AOA icv, indicando que o H_2S não desempenha nenhum papel na modulação hipotalâmica nos níveis de IL-6 e IL-1β no plasma em animais naïve LPS (Fig. 5c, d , e e f).

Essencialmente, ratos tolerantes ao LPS e ratos não tolerantes ao sal (Fig. 5b, d e f) apresentaram níveis indetectáveis de citocinas no plasma e o tratamento com AOA icv em ratos tolerantes ao LPS não reverteu a imunossupressão observada em ratos tolerantes ao LPS tratados com sal icv.

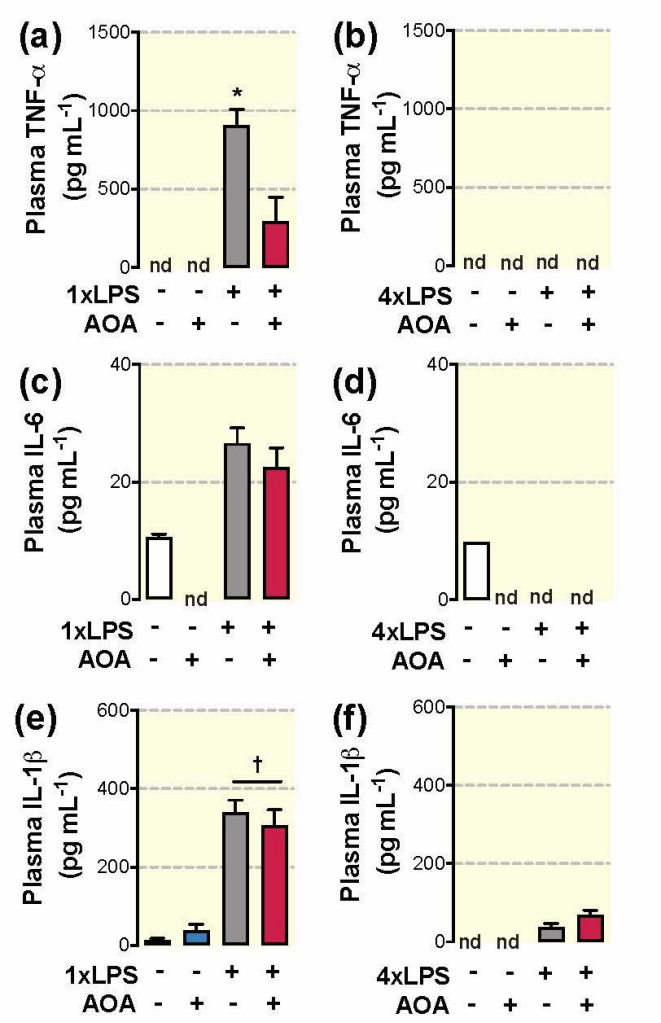

Fig. 5 Níveis plasmáticos de citocinas em animais naïve que receberam lipopolissacarídeo (1×LPS) e animais tolerantes ao LPS (4×LPS) e o efeito da inibição da cistationina β-sintase centralmente usando ácido aminooxiacético (AOA). Os níveis de citocinas plasmáticas foram verificados 2 h após a injeção de salina ou LPS na dose de 100 μg.kg^{-1} ip subesequente a microinjeção central de AOA ou solução salina. Níveis plasmáticos de TNF-α em ratos com uma injeção de LPS (A) ou tolerantes ao LPS (B). Níveis plasmáticos de IL-6 em ratos com uma injeção de LPS (C) ou tolerantes ao LPS (D). Níveis plasmáticos de IL - 1β em em ratos com uma injeção de LPS (E) ou tolerantes ao LPS (F). As barras de erro exibem a média ±SEM. Grupos com dados não detectáveis (nd) não foram incluídos nas estatísticas. N = 5-8. * P < 0,05 e † P < 0,01.

4.5 Efeitos da inibição central da CBS nos níveis plasmáticos de corticosterona em animais naïve LPS e tolerantes ao LPS

A corticosterona plasmática desempenha um papel criogênico durante a inflamação sistêmica (COELHO; SOUZA; PELÁ, 1992). Medimos os níveis plasmáticos de corticosterona relativamente reduzidos em ratos sal naïve, independentemente do tratamento icv (Fig. 6). Por

outro lado, os ratos naïve LPS apresentaram níveis aumentados de corticosterona plasmático em comparação com ratos naïve sal (Fig. 6).

Ratos tolerantes ao LPS que receberam sal icv também apresentaram níveis aumentados de corticosterona no plasma em comparação com os ratos não tolerantes que receberam sal icv (Fig. 6). Não foram observadas diferenças nos níveis plasmáticos de corticosterona entre os animais naïve LPS e tolerantes ao LPS. Além disso, a injeção de AOA icv causou um aumento adicional nos níveis plasmáticos de corticosterona tanto em ratos naïve LPS quanto em tolerantes ao LPS (Fig. 6).

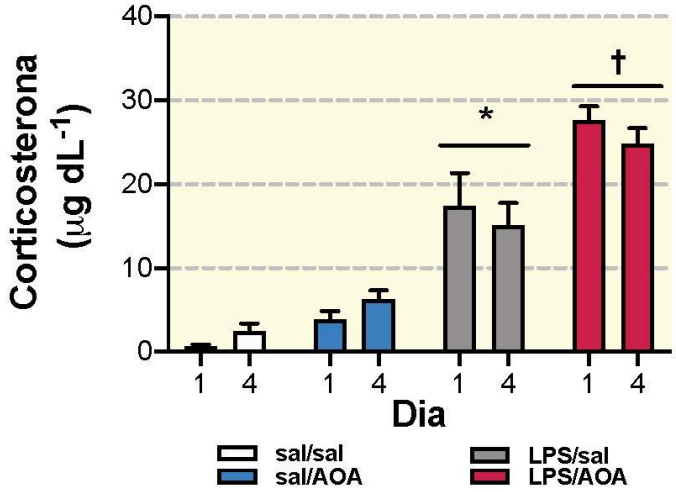

Fig. 6 Níveis plasmáticos de corticosterona em animais naïve injetados lipopolissacarídeo (1xLPS) e tolerantes ao LPS (4x LPS) e o efeito da microinjeção central do inibidor da cistationina β-sintase (CBS), ácido aminooxiacético (AOA). Níveis plasmáticos de corticosterona 2 h pós-salina ou injeção de LPS na dose de 100 μg.kg− 1 ip com inibição central de CBS com AOA ou solução salina. As barras exibem a média ± SEM. N = 5-8. * P < 0,05 e ‡ P < 0,001.

4.6 Expressão da proteína CBS na AVPO e taxa de produção de H_2S em animais naïve LPS e tolerantes ao LPS

Kwiatkoski et al. (2013) observaram uma diminuição na taxa de produção de H_2S na AVPO 2h após a injeção de LPS em ratos naïve LPS usando a mesma dose de LPS deste trabalho. Aqui, observamos que a expressão da proteína CBS na AVPO de animais naïve LPS não aumentou significativamente 2 h após a injeção de LPS, de acordo com a observação de nossos dados. Vinte e quatro horas após a injeção de LPS em ratos naïve, os níveis de H_2S na AVPO estavam aumentados nos animais naïve LPS (Fig. 7e), seguidos por um ligeiro aumento na expressão da proteína AVPO CBS (Fig. 7c). Esses dados indicam que a diminuição da produção de H_2S hipotalâmico ocorre apenas nas primeiras horas após a injeção de LPS sem

alterar a expressão de CBS (Fig. 7c), mas há um aumento na produção de H_2S 24 h mais tarde (Fig.6f), provavelmente pela liberação de H_2S de algumas proteínas. Posteriormente, após injeções repetidas de LPS, é observada uma expressão aumentada de CBS 2 e 24 h após a última injeção de LPS (Fig. 7c). Aliás, a taxa de produção de AVPO H_2S permanece alta 24 horas após a última injeção de LPS em ratos tolerantes ao LPS (Fig. 7d). A expressão aumentada de CBS na AVPO não depende do tempo, conforme indicado pela ANOVA (por mais detalhes, consulte a tabela complementar). A expressão de CBS na AVPO aumentou quase 50% em animais tolerantes ao LPS em comparação com os ratos naïve, independentemente do tempo de injeção de LPS ou sal (Fig. 7e).

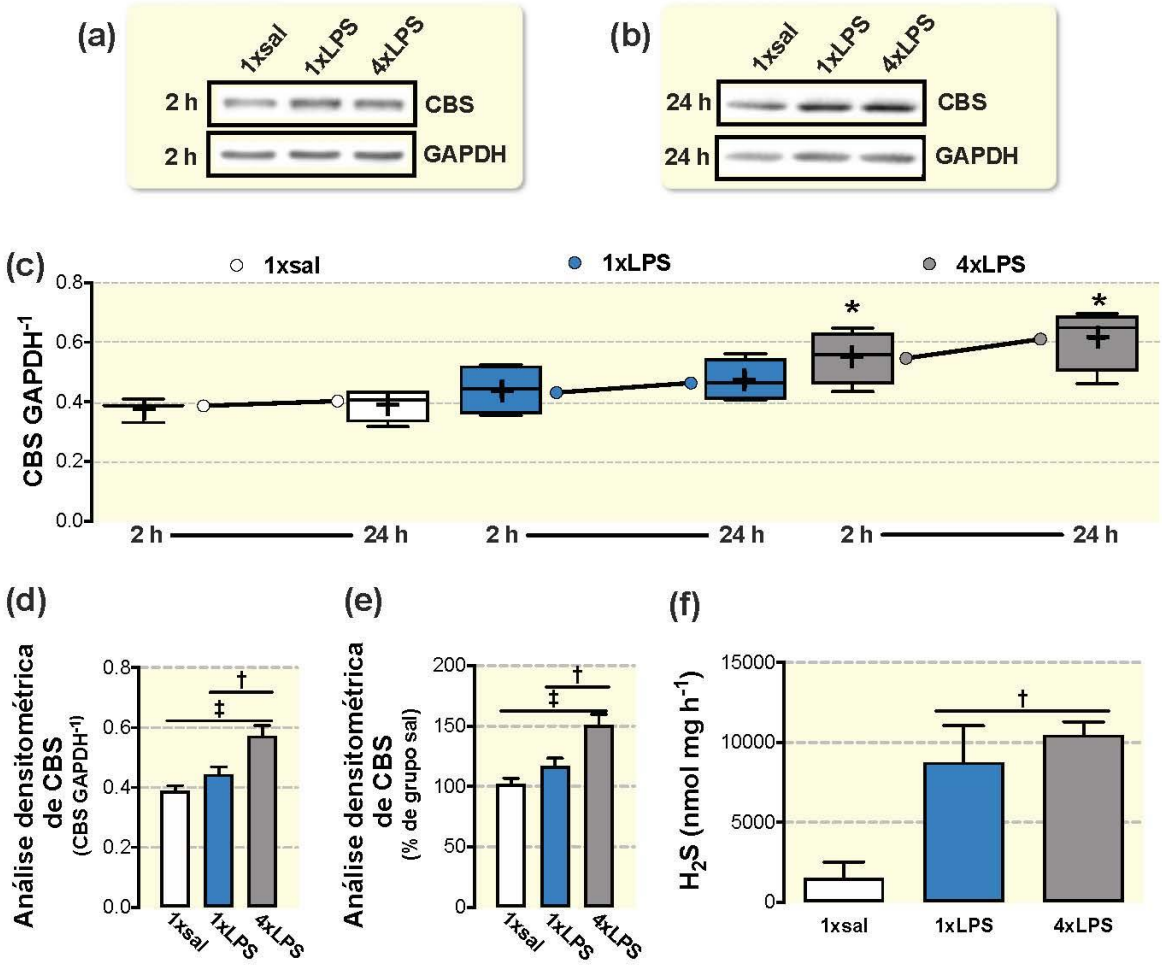

Fig. 7 Perfil de expressão de cistationina β-sintase (CBS) na área pré-ótica ântero-ventral do hipotálamo (AVPO) e razão de produção de sulfeto de hidrogênio (H_2S) na AVPO em animais naïve injetados LPS (1xLPS) ou tolerantes ao LPS (4xLPS). Expressão de CBS na AVPO 2 ou 24h após injeção de solução salina ou LPS em ratos LPS naïve (1xLPS) ou tolerantes ao LPS (4xLPS). (A) Bandas representativas de western blot mostrando qualitativamente a expressão de CBS na AVPO 2 h após a injeção de LPS ou seu veículo (sal). (B) bandas representativas de western blot mostrando qualitativamente a expressão de CBS na AVPO 24h após a injeção de LPS ou seu veículo. (C) A expressão de CBS no AVPO em animais LPS naïve (1×LPS) e tolerantes ao LPS (4xLPS) foram analisadas usando western (N = 3-5). A média está representada pelo sinal de mais (+). (D) análise

densitométrica da expressão de CBS na AVPO normalizada pela proteína constitutiva GAPDH. (E) análise densitométrica da expressão de CBS na AVPO normalizada pela proteína constitutiva GAPDH e ilustrada pela porcentagem de expressão comparada ao grupo salina. (f) Razão de produção de H2S em animais com uma injeção de LPS (1xLPS) ip ou tolerantes ao LPS (4xLPS). As barras de erro exibem SEM. N = 4-7. * P < 0,05 e † P < 0,01 vs grupo salina.

5 Discussão

Os presentes dados são consistentes com a noção de que a tolerância à endotoxina é resultante, dentre outros mecanismos, do aumento do H_2S produzido endogenamente na AVPO, pois demonstramos que: (a) a expressão de CBS e a taxa de produção de H_2S na AVPO aumentam em animais tolerantes ao LPS, (b) a inibição farmacológica da CBS hipotalâmica em ratos tolerantes ao LPS é capaz de montar uma resposta febril normal; (c) a febre foi acompanhada pela redução do índice de perda de calor e (d) aumento NST, indicando que esses termoefetores estão silentes, mas não prejudicados durante a tolerância à endotoxina. Curiosamente, esse conjunto consistente de descobertas foi observado como independente de algumas citocinas febrigênicas periféricas importantes, uma vez que a injeção de LPS não induziu aumento nas citocinas plasmáticas (TNF-α, IL-6 e IL-1β) após a inibição hipotalâmica da CBS em animais tolerantes ao LPS. Por outro lado, outro conjunto de resultados indica que os níveis de PGE_2 e PGD_2 na AVPO e no plasma foram de fato consistentemente afetados pela inibição hipotalâmica da CBS (Fig. 3) e medeia o efeito da inibição hipotalâmica da CBS na tolerância, ou seja, não apenas a produção aumentada de PGE_2 plasmática observada em ratos naïve LPS foi restabelecida em ratos tolerantes ao LPS tratados com AOA icv, mas também o aumento de PGD_2 em ratos tolerantes ao LPS foi revertido pelo mesmo tratamento.

Especulamos que a inibição de mecanismos centrais que envolvem a sinalização neuronal pelos astrócitos geradores de H_2S (TAN; WONG; BIAN, 2010) é de fato um mecanismo poderoso e eficaz para reverter a tolerância à endotoxina regulando positivamente a produção de PGE_2 e negativamente a de PGD_2 (Fig. 3). Além disso, conjecturamos que essas descobertas interessantes com o inibidor da CBS fornecem evidências sólidas que nos permitem sugerir que o H_2S é uma molécula antipirética endógena muito poderosa que atua a nível central durante a tolerância à endotoxina.

No encéfalo, o H_2S é produzido principalmente pela enzima CBS, que está expressa principalmente em astrócitos (TAN; WONG; BIAN, 2010). Essas células interagem de forma recíproca com os neurônios (CARMIGNOTO, 2000; KIMURA; SHIBUYA; KIMURA, 2012),

ou seja, astrócitos da vizinhança podem ser ativados por aumento da atividade neuronal e que, por sua vez, podem controlar a atividade sináptica neuronal. Tais interações recíprocas também podem ocorrer entre astrócitos e neurônios da AVPO, determinando a geração e modulação da febre (FELEDER; PERLIK; BLATTEIS, 2004; BLATTEIS, 2006).

A interação da periferia com mecanismos centrais mediadores da resposta imune é bidirecional (ORDOVAS-MONTANES et al., 2015). Para investigar a ação periférica do H_2S hipotalâmico na tolerância à endotoxina, determinamos os níveis plasmáticos de PGE_2, PGD_2, TNF-α, IL-1β, IL-6 e corticosterona (Fig. 4, 5, 6). Verificou-se que a inibição do H_2S hipotalâmico não alterou os níveis diminuídos dessas citocinas em animais tolerantes (Fig. 5), enquanto que foi capaz de modular os níveis de PGE_2, PGD_2 (Fig. 4) em animais tolerantes ao LPS. Curiosamente, parece que animais tolerantes ao LPS têm os níveis plasmáticos de PGE_2 reduzidos e os níveis de PGD_2 mantidos relativamente altos em comparação com ratos naïve LPS no plasma (Fig. 4).

Kwiatkoski et al. (2013) observaram que o H_2S desempenha um papel inibitório na produção de PGE_2 no hipotálamo. Além do mais, existem evidências indicando que a PGE_2 centralmente desempenha um papel importante na ativação simpática esplâncnica induzida por LPS e, simultaneamente, na atividade simpática esplênica (KENNEY; GANTA, 2014), que causa menor produção de TNF-α através da ativação de células T colinérgicas no baço e, consequentemente, a inibição de macrófagos pela ativação de receptores α 7nAchR (TRACEY, 2002; MARTELLI et al., 2014). Portanto, esse é um mecanismo plausível para explicar como a inibição hipotalâmica da produção de H_2S pode regular os níveis circulantes de TNF-α.

Em conformidade com o estudo anterior (KWIATKOSKI et al., 2013), observamos que a inibição de CBS na região hipotalâmica estava associada ao aumento dos níveis hipotalâmicos de PGE_2 em ratos tolerantes ao LPS (Fig. 4B), que é conhecido por causar uma estimulação simpática (KENNEY; GANTA, 2014) e uma subseqüente regulação positiva da produção periférica de PGE_2 (VIKSE et al., 1985; NAGARAJA et al., 2016). Especulamos que esse mecanismo explique como a inibição hipotalâmica da produção de H_2S regula os níveis circulantes de PGE_2.

Observou-se que os níveis plasmáticos de corticosterona são altos em ratos naïve LPS e tolerantes ao LPS (Fig. 6). Foi documentado que o H_2S central causa despolarização dos neurônios paraventriculares e, consequentemente, uma liberação crescente de corticosterona (DELLO RUSSO et al., 2000; DAWE et al., 2008), indicando que a taxa de produção aumentada de H_2S pode desempenhar uma ação excitatória no eixo HPA durante a endotoxemia (Fig. 6). Vale ressaltar que a corticosterona é um hormônio que desempenha um papel anti-

inflamatório importante, incluindo um efeito antipirético durante a inflamação sistêmica (COELHO; SOUZA; PELÁ, 1992). Por outro lado, também observamos que a inibição da CBS hipotalâmica está associada ao aumento nos níveis plasmáticos de corticosterona (Fig. 6). Esta resposta pode ser explicada pela interação neuroimune de PGE_2 ativando eixo hipotálamo-hipófise (SAPER; ROMANOVSKY; SCAMMELL, 2012). Especulamos que o aumento da produção de PGE_2 após a inibição da CBS tenha um efeito preponderante, modulando o eixo HPA em relação ao próprio gasotransmissor em ratos tolerantes ao LPS. Além disso, os níveis de corticosterona ainda eram altos em ratos tolerantes ao LPS (Fig. 6) e a inibição hipotalâmica do H_2S aumentaram ainda mais a produção de corticosterona em ratos tolerantes ao LPS, indicando seu papel no controle dos níveis de corticosterona durante o desafio imune com LPS.

Além de atuar inibindo a enzima CBS, o AOA inibe parcialmente a CSE e o ácido γ-aminobutírico (GABA) (LÖSCHER, 1981), o que não exclui o papel da CBS centralmente na tolerância à endotoxina. Um estudo anterior do nosso grupo (KWIATKOSKI et al., 2013) documentou que a inibição hipotalâmica de CBS com AOA causou uma diminuição na taxa de produção de AVPO H_2S, enquanto o doador H_2S causou uma resposta oposta em ratos que receberam LPS, indicando que o efeito de AOA é realmente mediado pela síntese de H_2S. Além disto, foi relatado que a inibição gabaérgica central leva ao aumento nos níveis plasmáticos de corticosterona (ROLAND; SAWCHENKO, 1993), o que não foi observado no presente estudo (Fig. 6). Portanto, é muito improvável que os efeitos observados da AOA no presente estudo tenham sido mediados por GABA.

Atuando sistemicamente, o H_2S tem desempenhado um papel neuroprotetor em ratos e camundongos em modelo de lesão cerebral por trauma (ZHANG et al., 2014; KARIMI et al., 2017). Este efeito pode resultar de uma ação anti-inflamatória do gás, uma vez que o tratamento com H_2S induzindo hipotermia atenua a expressão da NFκB no modelo de oclusão duradoura da artéria cerebral média (FLORIAN et al., 2008). Kwiatkosky et al. (2013) documentaram que o H_2S é uma molécula antipirética endógena poderosa que pode atuar através da supressão da síntese de PGE_2 e/ou estimulação da produção de AMPc no hipotálamo, com base em dados obtidos usando o modelo de desafio imune induzido por LPS, fortalecendo o efeito antipirético e sugerindo seu efeito neuroprotetor. Vale destacar que, como observado por outros autores, a tolerância induz neuroinflamação além da resposta inflamatória de baixo grau na periferia (MONNERET et al., 2004; CHEN et al., 2005). Assim, podemos especular que o H_2S seja responsável não só por bloquear a resposta febril, mas também por reprimir uma resposta neuroinflamatória ainda maior induzida pelo desafio imunológico crônico.

Os mecanismos moleculares de tolerância à endotoxina na periferia foram bem caracterizados (WEST; HEAGY, 2002; BISWAS; LOPEZ-COLLAZO, 2009; LÓPEZ-COLLAZO; DEL FRESNO, 2013). Existem poucos relatos em relação aos mecanismos centrais de tolerância à endotoxina, embora esse tópico tenha sido adequadamente abordado em importantes estudos recentes na literatura (BEUREL; JOPE, 2010; NORDEN et al., 2016). Além do mais, em um experimento elegante, enquanto os neurônios e a astroglia são afetados pela neuroinflamação crônica, a microglia falha no desenvolvimento da tolerância à endotoxina (CHU et al., 2016). Os autores concluíram que a ausência de tolerância microglial pode ser importante para os mecanismos patogenéticos envolvidos no dano neuronal associado à inflamação. Contudo, estes experimentos foram conduzidos com abordagem *in vitro* e, portanto, pode não refletir as observações de um experimento in vivo o desafio ao LPS. Especulamos que a tolerância à endotoxina pode ativar os astrócitos, aumentando a produção de H_2S centralmente. Em níveis elevados, esta molécula pode modular negativamente a produção de mediadores inflamatórios por micróglias e neurônios, principalmente PGE_2, e anular a resposta febril, como conseqüência.

6 Conclusão

Em resumo, o presente estudo conclui que: (a) durante a tolerância ao LPS, é observada atividade termoefetora silente, mas não prejudicada, incluindo a atividade simpática que inerva o tecido adiposo marrom responsável para termogênese sem tremor e o tecido cutâneo da cauda responsável pela perda de calor (Fig. 3); (b) os níveis plasmáticos de PGs são drasticamente alteradas durante a tolerância à endotoxina, ou seja, foi reduzida a produção de PGE_2 induzida por LPS e aumentada a de PGD_2 (Fig. 4); (c) as citocinas plasmáticas estão em seus níveis nadir (Fig. 5); e, (d) os níveis plasmáticos de corticosterona estão mantidos alto (Fig. 6). Reconciliando estes dados, sugerimos que tolerância febril não é simplesmente um reflexo da ausência as citocinas plasmáticas aumentadas, mas um fenômeno de múltiplos níveis e de mecanismos distintos. A maioria dessas mudanças observadas em ratos tolerantes parece depender do aumento da produção de H_2S hipotalâmico (Fig. 7), uma vez que a inibição da CBS restaurou as respostas dos termoefetores ao LPS (Fig. 3); causou o aumento nos níveis de PGE_2 plasmáticos e diminuição dos níveis plasmáticos de PGD_2 (Figura 3); e causou aumento dos níveis plasmáticos de corticosterona (Fig. 6), no entanto, os níveis de citocinas plasmáticas não foram afetados (Fig. 5).

A melhor compreensão dos mecanismos envolvidos na tolerância à endotoxina pode fornecer uma estratégia terapêutica baseada na produção de H_2S hipotalâmico para prevenir os danos teciduais causados pelo desafio imunológico crônico.

Referências

ADIB-CONQUY, M. et al. NF- κ B Expression in Mononuclear Cells of Patients with Sepsis Resembles That Observed in Lipopolysaccharide Tolerance. **American Journal of Respiratory and Critical Care Medicine**, v. 162, n. 5, p. 1877–1883, 2000.

ALMEIDA, M. C. et al. Tolerance to lipopolysaccharide is related to the nitric oxide pathway. **Neuroreport**, v. 10, n. 14, p. 3061–5,. 1999.

ANG, S.-F.; MOOCHHALA, S. M.; BHATIA, M. Hydrogen sulfide promotes transient receptor potential vanilloid 1-mediated neurogenic inflammation in polymicrobial sepsis*. **Critical Care Medicine**, v. 38, n. 2, p. 619–628, 2010.

BARRIOS-RODILES, M.; TIRALOCHE, G.; CHADEE, K. Lipopolysaccharide modulates cyclooxygenase-2 transcriptionally and posttranscriptionally in human macrophages independently from endogenous IL-1 beta and TNF-alpha. **Journal of immunology**, v. 163, n. 2, p. 963–9, 1999.

BEESON, P. B. Development of tolerance to typhoid bacterial pyrogen and its abolition by reticulo-endothelial blockade. **Proceedings of the Society for Experimental Biology and Medicine. Society for Experimental Biology and Medicine**, v. 61, p. 248–50, 1946.

BEESON, P. B.; ROBERTS, E. Tolerance to bacterial pyrogens: II. role of the reticulo-endothelial system. **Journal of Experimental Medicine**, v. 86, n. 1, p. 39–44, 1947.

BEŁTOWSKI, J. Hydrogen sulfide in pharmacology and medicine--An update. **Pharmacological reports : PR**, v. 67, n. 3, p. 647–58, 2015.

BENNETT, I. L.; BEESON, P. B. Studies on the pathogenesis of fever. I. The effect of injection of extracts and suspensions of uninfected rabbit tissues upon the body temperature of normal rabbits. **The Journal of experimental medicine**, v. 98, n. 5, p. 477–492, 1953.

BEUREL, E.; JOPE, R. S. Glycogen synthase kinase-3 regulates inflammatory tolerance in astrocytes. **Neuroscience**, v. 169, n. 3, p. 1063–1070, 2010.

BHATIA, M. Hydrogen sulfide as a vasodilator. **IUBMB life**, v. 57, n. 9, p. 603–6, 2005.

BIBLI, S.-I. et al. Role of cGMP in hydrogen sulfide signaling. **Nitric oxide : biology and chemistry / official journal of the Nitric Oxide Society**, v. 46, p. 7–13, 2015.

BISWAS, S. K.; LOPEZ-COLLAZO, E. Endotoxin Tolerance: New Mechanisms, Molecules and Clinical Significance. **Trends in immunology**, v. 30, n. 10, p. 475–487, 2009.

BLATTEIS, C. M. The afferent signalling of fever. **The Journal of physiology**, v. 526 Pt 3, p. 470, 2000.

BLATTEIS, C. M. et al. Cytokines, PGE2 and endotoxic fever: a re-assessment. **Prostaglandins & other lipid mediators**, v. 76, n. 1–4, p. 1–18, 2005.

BLATTEIS, C. M. Endotoxic fever: New concepts of its regulation suggest new approaches to its management. **Pharmacology & Therapeutics**, v. 111, n. 1, p. 194–223, 2006.

BLATTEIS, C. M.; LI, S. Pyrogenic signaling via vagal afferents: what stimulates their receptors? **Autonomic neuroscience : basic & clinical**, v. 85, n. 1–3, p. 66–71, 2000.

BLATTEIS, C. M.; SEHIC, E. Cytokines and Fever [a]. **Annals of the New York Academy of Sciences**, v. 840, n. 1, p. 608–618, 1998.

BOHUSLAV, J. et al. Regulation of an essential innate immune response by the p50 subunit of NF-κB. **Journal of Clinical Investigation**, v. 102, n. 9, p. 1645–1652, 1998.

BORGES, B. et al. Expression of hypothalamic neuropeptides and the desensitization of pituitary–adrenal axis and hypophagia in the endotoxin tolerance. **Hormones and Behavior**, v. 52, n. 4, p. 508–519, 2007.

BUMILLER, A. et al. Effects of repeated injections of interleukin 1β or lipopolysaccharide on the HPA axis in the newborn rat. **Cytokine**, v. 11, n. 3, p. 225–230, 1999.

CAO, C. et al. Endothelial cells of the rat brain vasculature express cyclooxygenase-2 mRNA in response to systemic interleukin-1 beta: a possible site of prostaglandin synthesis responsible for fever. **Brain research**, v. 733, n. 2, p. 263–72, 1996.

CARMIGNOTO, G. Reciprocal communication systems between astrocytes and neurones. **Progress in neurobiology**, v. 62, n. 6, p. 561–81, 2000.

CEREZO, C. S. et al. REGULATION OF ADOLESCENT RAT INTESTINAL EPITHELIAL INDUCIBLE NITRIC OXIDE SYNTHASE EXPRESSION IN ENDOTOXIN TOLERANCE: MODULATION OF SIGNAL TRANSDUCTION. **Shock**, v. 21, n. 5, p. 476–483, 2004.

CHANG, C. C. et al. Inhibition of nitric oxide synthase gene expression in vivo and in vitro by repeated doses of endotoxin. **American Journal of Physiology - Gastrointestinal and Liver Physiology**, v. 271, n. 4 34-4, 1996.

CHEN, R. et al. Differential expression of cytokines in the brain and serum during endotoxin tolerance. **Journal of Neuroimmunology**, v. 163, n. 1–2, p. 53–72, 2005.

CHU, C.-H. et al. Neurons and astroglia govern microglial endotoxin tolerance through macrophage colony-stimulating factor receptor-mediated ERK1/2 signals. **Brain, Behavior, and Immunity**, v. 55, p. 260–272, 2016.

COELHO, M. M.; SOUZA, G. E.; PELÁ, I. R. Endotoxin-induced fever is modulated by endogenous glucocorticoids in rats. **The American journal of physiology**, v. 263, n. 2 Pt 2, p. R423-7, 1992.

DAS, A. et al. Impairment of an Endothelial NAD+-H2S Signaling Network Is a Reversible Cause of Vascular Aging. **Cell**, v. 173, n. 1, p. 74- 89.e20, 2018.

DAWE, G. S. et al. Hydrogen sulphide in the hypothalamus causes an ATP-sensitive K+ channel-dependent decrease in blood pressure in freely moving rats. **Neuroscience**, v. 152, n. 1, p. 169–77, 2008.

DELLO RUSSO, C. et al. Evidence that hydrogen sulphide can modulate hypothalamo-pituitary-adrenal axis function: in vitro and in vivo studies in the rat. **Journal of neuroendocrinology**, v. 12, n. 3, p. 225–33, 2000.

DIAS, M. B. et al. Role of nitric oxide in tolerance to lipopolysaccharide in mice. **Journal of applied physiology**, v. 98, n. 4, p. 1322–7, abr. 2005.

DINARELLO, C. A.; BODEL, P. T.; ATKINS, E. The role of the liver in the production of fever and in pyrogenic tolerance. **Transactions of the Association of American Physicians**, v. 81, p. 334–344, 1968.

DISTRUTTI, E. et al. Evidence that hydrogen sulfide exerts antinociceptive effects in the gastrointestinal tract by activating KATP channels. **The Journal of pharmacology and experimental therapeutics**, v. 316, n. 1, p. 325–35, 2006.

DONATTI, A. F. et al. Role of hydrogen sulfide in the formalin-induced orofacial pain in rats. **European journal of pharmacology**, v. 738, p. 49–56, 2014.

DRAISMA, A. et al. Development of endotoxin tolerance in humans in vivo. **Critical Care Medicine**, v. 37, n. 4, p. 1261–1267, 2009.

EBISAWA, Y. et al. Direct evidence that induced nitric oxide production in hepatocytes prevents liver damage during lipopolysaccharide tolerance in rats. **Journal of Surgical Research**, v. 118, n. 2, p. 183–189, 2004.

EFTEKHARI, G. et al. Activation of central muscarinic receptor type 1 prevents development of endotoxin tolerance in rat liver. **European Journal of Pharmacology**, v. 740, p. 436–441, 2014.

FAGONE, P. et al. Gasotransmitters and the immune system: Mode of action and novel therapeutic targets. **European Journal of Pharmacology**, v. 834, p. 92–102, 2018.

FELEDER, C.; PERLIK, V.; BLATTEIS, C. M. Preoptic alpha 1- and alpha 2-noradrenergic agonists induce, respectively, PGE2-independent and PGE2-dependent hyperthermic responses in guinea pigs. **American journal of physiology. Regulatory, integrative and comparative physiology**, v. 286, n. 6, p. R1156-66, 2004.

FELEDER, C.; PERLIK, V.; BLATTEIS, C. M. Preoptic nitric oxide attenuates endotoxic fever in guinea pigs by inhibiting the POA release of norepinephrine. **American Journal of Physiology - Regulatory Integrative and Comparative Physiology**, v. 293, n. 3, set. 2007.

FLANNIGAN, K. L.; WALLACE, J. L. Hydrogen sulfide-based anti-inflammatory and chemopreventive therapies: an experimental approach. **Current pharmaceutical design**, v. 21, n. 21, p. 3012–22, 2015.

FLORIAN, B. et al. Long-term hypothermia reduces infarct volume in aged rats after focal ischemia. **Neuroscience Letters**, v. 438, n. 2, p. 180–185, 2008.

FREDENBURGH, L. E. et al. A phase I trial of low-dose inhaled carbon monoxide in sepsis-induced ARDS. **JCI insight**, v. 3, n. 23, 2018.

FUJII, E. et al. Evaluation of iNOS-dependent and independent mechanisms of the microvascular permeability change induced by lipopolysaccharide. **British Journal of Pharmacology**, v. 130, n. 1, p. 90–94, 2000.

GAO, W. et al. Prostaglandin D2 produced by hematopoietic prostaglandin D synthase contributes to LPS-induced fever. **Journal of physiology and pharmacology : an official journal of the Polish Physiological Society**, v. 60, n. 2, p. 145–50, 2009.

GARATTINI, E. G. et al. Propargylglycine decreases neuro-immune interaction inducing pain response in temporomandibular joint inflammation model. **Nitric Oxide**, v. 93, p. 90–101, 2019.

GILROY, D. W. et al. Inducible cyclooxygenase may have anti-inflammatory properties. **Nature Medicine**, v. 5, n. 6, p. 698–701, 1999.

HAUSER, B. et al. Nitric oxide synthase inhibition in sepsis? Lessons learned from large-animal studies. **Anesthesia and Analgesia**, v. 101, n. 2, p. 488–498, 2005.

HE, K. et al. Lipopolysaccharide-induced cross-tolerance against renal ischemia-reperfusion injury is mediated by hypoxia-inducible factor-2α-regulated nitric oxide production. **Kidney International**, v. 85, n. 2, p. 276–288, 2014.

HILDEBRANDT, T. M.; GRIESHABER, M. K. Three enzymatic activities catalyze the oxidation of sulfide to thiosulfate in mammalian and invertebrate mitochondria. **The FEBS journal**, v. 275, n. 13, p. 3352–61, 2008.

HINE, C. et al. Endogenous Hydrogen Sulfide Production Is Essential for Dietary Restriction Benefits. **Cell**, v. 160, n. 1–2, p. 132–144, 2015.

HINE, C.; MITCHELL, J. R. Calorie restriction and methionine restriction in control of endogenous hydrogen sulfide production by the transsulfuration pathway. **Experimental Gerontology**, v. 68, p. 26–32, 2015.

INUI, A. Cytokines and sickness behavior: implications from knockout animal models. **Trends in Immunology**, v. 22, n. 9, p. 469–473, 2001.

ISHIGAMI, M. et al. A Source of Hydrogen Sulfide and a Mechanism of Its Release in the Brain. **Antioxidants & Redox Signaling**, v. 11, n. 2, p. 205–214, 2009.

IVANOV, A. I.; ROMANOVSKY, A. A. Prostaglandin E2 as a mediator of fever: synthesis and catabolism. **Frontiers in bioscience : a journal and virtual library**, v. 9, p. 1977–93, 2004.

KABIL, H. et al. Increased transsulfuration mediates longevity and dietary restriction in Drosophila. **Proceedings of the National Academy of Sciences of the United States of America**, v. 108, n. 40, p. 16831–16836, 2011.

KARIMI, S. A. et al. The protective effect of hydrogen sulfide (H 2 S) on traumatic brain injury (TBI) induced memory deficits in rats. **Brain Research Bulletin**, v. 134, p. 177–182, 2017.

KAWABATA, A. et al. Hydrogen sulfide as a novel nociceptive messenger. **Pain**, v. 132, n. 1–2, p. 74–81, 2007.

KAWANO, T. et al. iNOS-derived NO and nox2-derived superoxide confer tolerance to excitotoxic brain injury through peroxynitrite. **Journal of cerebral blood flow and metabolism : official journal of the International Society of Cerebral Blood Flow and Metabolism**, v. 27, n. 8, p. 1453–62, 2007.

KENNEY, M. J.; GANTA, C. K. Autonomic nervous system and immune system interactions. **Comprehensive Physiology**, v. 4, n. 3, p. 1177–200, 2014.

KIM, J.-I.; JANG, H.-S.; PARK, K.-M. Endotoxin-induced renal tolerance against ischemia and reperfusion injury is removed by iNOS, but not eNOS, gene-deletion. **BMB Reports**, v. 43, n. 9, p. 629–634, 2010.

KIMURA, H. Physiological role of hydrogen sulfide and polysulfide in the central nervous system. **Neurochemistry international**, v. 63, n. 5, p. 492–7,. 2013.

KIMURA, H.; SHIBUYA, N.; KIMURA, Y. Hydrogen Sulfide Is a Signaling Molecule and a Cytoprotectant. **Antioxidants & Redox Signaling**, v. 17, n. 1, p. 45–57, 2012.

KLUGER, M. J. et al. Role of fever in disease. **Annals of the New York Academy of Sciences**, v. 856, p. 224–233, 1998.

KLUGER, M. J.; RINGLER, D. H.; ANVER, M. R. Fever and survival. **Science (New York, N.Y.)**, v. 188, n. 4184, p. 166–8, 1975.

KOROLEVA, K. et al. Receptor Mechanisms Mediating the Pro-Nociceptive Action of Hydrogen Sulfide in Rat Trigeminal Neurons and Meningeal Afferents. **Frontiers in Cellular Neuroscience**, v. 11, p. 226, 2017.

KRALL, C. M. et al. Food deprivation alters thermoregulatory responses to lipopolysaccharide by enhancing cryogenic inflammatory signaling via prostaglandin D2. **AJP: Regulatory, Integrative and Comparative Physiology**, v. 298, n. 6, p. R1512–R1521, 2010.

KUMAR, M.; SANDHIR, R. Hydrogen Sulfide in Physiological and Pathological Mechanisms in Brain. **CNS & Neurological Disorders - Drug Targets**, v. 17, n. 9, p. 654–670, 2018.

KWIATKOSKI, M. et al. Hydrogen sulfide inhibits preoptic prostaglandin E2 production during endotoxemia. **Experimental neurology**, v. 240, p. 88–95, 2013.

LEE, A. T.-H. et al. A nociceptive-intensity-dependent role for hydrogen sulphide in the formalin model of persistent inflammatory pain. **Neuroscience**, v. 152, n. 1, p. 89–96, 2008.

LEE, M. et al. Astrocytes produce the antiinflammatory and neuroprotective agent hydrogen sulfide. **Neurobiology of aging**, v. 30, n. 10, p. 1523–34, 2009.

LI, L. et al. Hydrogen sulfide is a novel mediator of lipopolysaccharide-induced inflammation in the mouse. **The**

FASEB Journal, v. 19, n. 9, p. 1196–1198, 2005.

LI, L. et al. GYY4137, a novel hydrogen sulfide-releasing molecule, protects against endotoxic shock in the rat. **Free radical biology & medicine**, v. 47, n. 1, p. 103–13, 2009.

LIAUDET, L.; SORIANO, F. G.; SZABÓ, C. Biology of nitric oxide signaling. **Critical care medicine**, v. 28, n. 4 Suppl, p. N37-52, 2000.

LIN, H.-Y.; WU, C.-L.; HUANG, C.-C. The Akt-endothelial nitric oxide synthase pathway in lipopolysaccharide preconditioning-induced hypoxic-ischemic tolerance in the neonatal rat brain. **Stroke**, v. 41, n. 7, p. 1543–51, 2010.

LÓPEZ-COLLAZO, E.; DEL FRESNO, C. Pathophysiology of endotoxin tolerance: mechanisms and clinical consequences. **Critical care (London, England)**, v. 17, n. 6, p. 242, 2013.

LÖSCHER, W. Effect of Inhibitors of GABA Aminotransferase on the Metabolism of GABA in Brain Tissue and Synaptosomal Fractions. **Journal of Neurochemistry**, v. 36, n. 4, p. 1521–1527, 1981.

MARTELLI, D. et al. Reflex control of inflammation by sympathetic nerves, not the vagus. **The Journal of Physiology**, v. 592, n. 7, p. 1677–1686, 2014.

MARTINS, F. de S. et al. Suspected infection in afebrile patients: Are they septic? **Medicine**, v. 96, n. 10, p. e6299, 2017.

MATSUNAMI, M. et al. Luminal hydrogen sulfide plays a pronociceptive role in mouse colon. **Gut**, v. 58, n. 6, p. 751–61, 2009.

MIAO, X. et al. Upregulation of cystathionine-β-synthetase expression contributes to inflammatory pain in rat temporomandibular joint. **Molecular Pain**, v. 10, n. 1, 2014.

MOHRI, M.; SPRIGGS, D. R.; KUFE, D. Effects of lipopolysaccharide on phospholipase A2 activity and tumor necrosis factor expression in HL-60 cells. **Journal of immunology (Baltimore, Md. : 1950)**, v. 144, n. 7, p. 2678–82, 1990.

MONNERET, G. et al. The anti-inflammatory response dominates after septic shock: Association of low monocyte HLA-DR expression and high interleukin-10 concentration. **Immunology Letters**, v. 95, n. 2, p. 193–198, 2004.

MOORE, P. K.; BHATIA, M.; MOOCHHALA, S. Hydrogen sulfide: from the smell of the past to the mediator of the future? **Trends in pharmacological sciences**, v. 24, n. 12, p. 609–11, 2003.

MUN, J. et al. **Role of hydrogen sulfide in cerebrovascular alteration during agingArchives of Pharmacal Research**Pharmaceutical Society of Korea, 2019.

MUNOZ, C. et al. Dysregulation of in vitro cytokine production by monocytes during sepsis. **Journal of Clinical Investigation**, v. 88, n. 5, p. 1747–1754, 1991a.

MUNOZ, C. et al. Dissociation between plasma and monocyte-associated cytokines during sepsis. **European Journal of Immunology**, v. 21, n. 9, p. 2177–2184, 1991b.

NAGARAJA, A. S. et al. Sustained adrenergic signaling leads to increased metastasis in ovarian cancer via increased PGE2 synthesis. **Oncogene**, v. 35, n. 18, p. 2390–2397, 2016.

NETEA, M. G.; KULLBERG, B. J.; VAN DER MEER, J. W. Circulating cytokines as mediators of fever. **Clinical infectious diseases : an official publication of the Infectious Diseases Society of America**, v. 31 Suppl 5, p. S178-84, 2000.

NOGUEIRA, J. E. et al. Effect of Physical Exercise on the Febrigenic Signaling is Modulated by Preoptic Hydrogen Sulfide Production. **PLOS ONE**, v. 12, n. 1, p. e0170468,. 2017.

NORDEN, D. M. et al. Sequential activation of microglia and astrocyte cytokine expression precedes increased Iba-1 or GFAP immunoreactivity following systemic immune challenge. **Glia**, v. 64, n. 2, p. 300–16, 2016.

OLAS, B. **Hydrogen sulfide in signaling pathwaysClinica Chimica Acta** Elsevier, , 2015.

OOTSUKA, Y. et al. Fever response to intravenous prostaglandin E2 is mediated by the brain but does not require afferent vagal signaling. **American journal of physiology. Regulatory, integrative and comparative physiology**, v. 294, n. 4, p. R1294-303, 2008.

ORDOVAS-MONTANES, J. et al. The Regulation of Immunological Processes by Peripheral Neurons in Homeostasis and Disease. **Trends in Immunology**, v. 36, n. 10, p. 578–604, 2015.

ORIO, M. et al. Lipopolysaccharide induces early tolerance to excitotoxicity via nitric oxide and cGMP. **Stroke**, v. 38, n. 10, p. 2812–7, 2007.

OTTERBEIN, L. E. et al. Carbon monoxide has anti-inflammatory effects involving the mitogen- activated protein kinase pathway. **Nature Medicine**, v. 6, n. 4, p. 422–428, 2000.

PANTHI, S. et al. Physiological Importance of Hydrogen Sulfide: Emerging Potent Neuroprotector and Neuromodulator. **Oxidative Medicine and Cellular Longevity**, v. 2016, p. 1–11, 2016.

PAUL, B. D.; SNYDER, S. H. **Gasotransmitter hydrogen sulfide signaling in neuronal health and diseaseBiochemical Pharmacology**Elsevier Inc., , 2018. .

PERLIK, V. et al. LPS-activated complement, not LPS per se, triggers the early release of PGE2 by Kupffer cells. **American journal of physiology. Regulatory, integrative and comparative physiology**, v. 289, n. 2, p. R332–R339, ago. 2005.

PRITCHARD, M. T.; LI, Z.; REPASKY, E. A. Nitric oxide production is regulated by fever-range thermal stimulation of murine macrophages. **Journal of Leukocyte Biology**, v. 78, n. 3, p. 630–638, 2005.

QABAZARD, B. et al. Hydrogen Sulfide Is an Endogenous Regulator of Aging in *Caenorhabditis elegans*. **Antioxidants & Redox Signaling**, v. 20, n. 16, p. 2621–2630, 2014.

RAFFAINI, M. S.; DIAS, M. B.; BRANCO, L. G. S. S. Central heme oxygenase-carbon monoxide pathway participates in the lipopolysaccharide-induced tolerance in rats. **Brain research**, v. 1111, n. 1, p. 83–9, 21 set. 2006.

RAJENDRAN, S. et al. Nitric oxide and hydrogen sulfide regulation of ischemic vascular growth and remodeling. **Comprehensive Physiology**, v. 9, n. 3, p. 1213–1247, 2019.

RIQUELME, S. A.; BUENO, S. M.; KALERGIS, A. M. Carbon monoxide down-modulates Toll-like receptor 4/MD2 expression on innate immune cells and reduces endotoxic shock susceptibility. **Immunology**, v. 144, n. 2, p. 321–332, 2015.

RITTIRSCH, D.; FLIERL, M. A.; WARD, P. A. Harmful molecular mechanisms in sepsis. **Nature reviews. Immunology**, v. 8, n. 10, p. 776–87, 2008.

ROLAND, B. L.; SAWCHENKO, P. E. Local origins of some GABAergic projections to the paraventricular and supraoptic nuclei of the hypothalamus in the rat. **The Journal of Comparative Neurology**, v. 332, n. 1, p. 123–143, 1993.

ROMANOVSKY, A. A.; IVANOV, A. I.; SHIMANSKY, Y. P. Selected Contribution: Ambient temperature for experiments in rats: a new method for determining the zone of thermal neutrality. **Journal of Applied Physiology**,

v. 92, n. 6, p. 2667–2679, 2002.

ROMANOVSKY, A. A.; STEINER, A. A.; MATSUMURA, K. Cells that trigger fever. **Cell cycle (Georgetown, Tex.)**, v. 5, n. 19, p. 2195–7, 2006.

ROTH, J. et al. Inhibition of nitric oxide synthase attenuates lipopolysaccharide- induced fever without reduction of circulating cytokines in guinea-pigs. **Pflugers Archiv European Journal of Physiology**, v. 436, n. 6, p. 858–862, 1998.

ROTH, J.; BLATTEIS, C. M. Mechanisms of fever production and lysis: lessons from experimental LPS fever. **Comprehensive Physiology**, v. 4, n. 4, p. 1563–604, 2014.

SABROE, I. et al. Toll-like receptor (TLR)2 and TLR4 in human peripheral blood granulocytes: a critical role for monocytes in leukocyte lipopolysaccharide responses. **Journal of immunology (Baltimore, Md. : 1950)**, v. 168, n. 9, p. 4701–10, 2002.

SANTOS, B. M. et al. The therapeutic potential of cystathionine gamma-lyase in temporomandibular inflammation-induced orofacial hypernociception. **Physiology & Behavior**, v. 188, n. November 2017, p. 128–133, 2018.

SAPER, C. B.; ROMANOVSKY, A. A.; SCAMMELL, T. E. Neural circuitry engaged by prostaglandins during the sickness syndrome. **Nature neuroscience**, v. 15, n. 8, p. 1088–95, 2012.

SCHILTZ, J. C.; SAWCHENKO, P. E. Signaling the brain in systemic inflammation: the role of perivascular cells. **Frontiers in bioscience : a journal and virtual library**, v. 8, p. s1321-9, 2003.

SCHUMANN, R. R. Function of lipopolysaccharide (LPS)-binding protein (LBP) and CD14, the receptor for LPS/LBP complexes: a short review. **Research in immunology**, v. 143, n. 1, p. 11–5, 1992.

SEKI, T. et al. D-Cysteine promotes dendritic development in primary cultured cerebellar Purkinje cells via hydrogen sulfide production. **Molecular and Cellular Neuroscience**, v. 93, p. 36–47, 2018.

SHATALIN, K. et al. H2S: A universal defense against antibiotics in bacteria. **Science**, v. 334, n. 6058, p. 986–990, 2011.

SHEFA, U. et al. Role of Gasotransmitters in Oxidative Stresses, Neuroinflammation, and Neuronal Repair. **BioMed Research International**, v. 2017, p. 1–15, 2017.

SORIANO, R. N. et al. Propyretic role of the locus coeruleus nitric oxide pathway. **Experimental Physiology**, v. 95, n. 6, p. 669–677, 2010.

SORIANO, R. N. et al. Interaction between the carbon monoxide and nitric oxide pathways in the locus coeruleus during fever. **Neuroscience**, v. 206, p. 69–80, 2012.

SORIANO, R. N. et al. Glucocorticoids downregulate systemic nitric oxide synthesis and counteract overexpression of hepatic heme oxygenase-1 during endotoxin tolerance. **Canadian Journal of Physiology and Pharmacology**, v. 91, n. 10, p. 861–865, 2013.

SORIANO, R. N. et al. Endogenous peripheral hydrogen sulfide is propyretic: its permissive role in brown adipose tissue thermogenesis in rats. **Experimental Physiology**, v. 103, n. 3, p. 397–407, 2018.

SOSZYNSKI, D. Inhibition of nitric oxide synthase delays the development of tolerance to LPS in rats. **Physiology and Behavior**, v. 76, n. 1, p. 159–169, 2002.

SPITZER, J. A. et al. Ethanol and LPS modulate NF-kappaB activation, inducible NO synthase and COX-2 gene expression in rat liver cells in vivo. **Frontiers in bioscience : a journal and virtual library**, v. 7, p. a99-108, 2002.

SPITZER, J. A.; SPITZER, J. J. Lipopolysaccharide tolerance and ethanol modulate hepatic nitric oxide production in a gender-dependent manner. **Alcohol**, v. 21, n. 1, p. 27–35, 2000.

STEINER, A. A.; ANTUNES-RODRIGUES, J.; BRANCO, L. G. . Role of preoptic second messenger systems (cAMP and cGMP) in the febrile response. **Brain Research**, v. 944, n. 1–2, p. 135–145, 2002.

STEINER, A. A.; BRANCO, L. G. Central CO-heme oxygenase pathway raises body temperature by a prostaglandin-independent way. **Journal of applied physiology (Bethesda, Md. : 1985)**, v. 88, n. 5, p. 1607–13, 2000.

STEINER, A. A.; BRANCO, L. G. S. Role of the preoptic carbon monoxide pathway in endotoxin fever in rats. **Brain research**, v. 927, n. 1, p. 27–34, 2002.

SZABO, C. **A timeline of hydrogen sulfide (H2S) research: From environmental toxin to biological mediatorBiochemical Pharmacology**Elsevier Inc., 2018. .

SZABÓ, C. et al. Attenuation of the induction of nitric oxide synthase by endogenous glucocorticoids accounts for endotoxin tolerance in vivo. **Proceedings of the National Academy of Sciences of the United States of America**, v. 91, n. 1, p. 271–5, 4 jan. 1994.

SZABÓ, C. Hydrogen sulphide and its therapeutic potential. **Nature reviews. Drug discovery**, v. 6, n. 11, p. 917–35, nov. 2007.

TAN, B. H.; WONG, P. T.-H.; BIAN, J.-S. Hydrogen sulfide: A novel signaling molecule in the central nervous system. **Neurochemistry International**, v. 56, n. 1, p. 3–10, 2010.

TRACEY, K. J. The inflammatory reflex. **Nature**, v. 420, n. 6917, p. 853–859, 2002.

UENO, R. et al. Role of prostaglandin D2 in the hypothermia of rats caused by bacterial lipopolysaccharide. **Proceedings of the National Academy of Sciences of the United States of America**, v. 79, n. 19, p. 6093–7, 1982.

VERGADI, E.; VAPORIDI, K.; TSATSANIS, C. Regulation of Endotoxin Tolerance and Compensatory Anti-inflammatory Response Syndrome by Non-coding RNAs. **Frontiers in Immunology**, v. 9, p. 2705, 2018.

VIKSE, A. et al. Haemodynamic conditions for renal PGE_2 and renin release during α- and β-adrenergic stimulation in dogs. **Acta Physiologica Scandinavica**, v. 124, n. 2, p. 163–172, 1985.

WALLACE, J. L. et al. **Hydrogen Sulfide-Releasing Therapeutics: Translation to the ClinicAntioxidants and Redox Signaling**Mary Ann Liebert Inc., 2018. .

WALLACE, J. L. et al. A proof-of-concept, Phase 2 clinical trial of the gastrointestinal safety of a hydrogen sulfide-releasing anti-inflammatory drug. **British Journal of Pharmacology**, 2019.

WALLACE, J. L.; FERRAZ, J. G. P.; MUSCARA, M. N. Hydrogen sulfide: an endogenous mediator of resolution of inflammation and injury. **Antioxidants & redox signaling**, v. 17, n. 1, p. 58–67, 2012.

WANG, R. Signaling pathways for the vascular effects of hydrogen sulfide. **Current Opinion in Nephrology and Hypertension**, v. 20, n. 2, p. 107–112, 2011.

WEST, M. A.; HEAGY, W. Endotoxin tolerance: A review. **Critical care medicine**, v. 30, n. 1 Supp, p. S64–S73, 2002.

ZHANG, M. et al. Hydrogen sulfide offers neuroprotection on traumatic brain injury in parallel with reduced apoptosis and autophagy in mice. **PloS one**, v. 9, n. 1, p. e87241, 2014.

Tabelas suplementares

Tabela 1. Análise estatística dependendo da medida e do grupo analisado.

	Grupos*	Análise	F or t	P
Temperatura corporal (Tb)	1xsal/sal; 1xsal/AOA; 1xLPS/sal; 1xLPS/AOA	ANOVA de 2 vias ordinária (Tukey pós-teste recomendado)	$F_{tratamento}$ (3,1241) = 728.5	P<0.001
			F_{tempo} (72,1241) = 32.5	P<0.001
			$F_{interação}$ (216,1241) = 7.7	P<0.001
	4xsal/sal; 4xsal/AOA; 4xLPS/sal; 4xLPS/AOA	ANOVA de 2 vias ordinária (Tukey pós-teste recomendado)	$F_{tratamento}$ (3,1241) = 409.4	P<0.0001
			F_{tempo} (72,1241) = 1.8	P<0.0001
			$F_{interação}$ (216,1241) = 1.9	P<0.0001
Consumo de oxigênio	1xsal/sal; 1xsal/AOA; 1xLPS/sal; 1xLPS/AOA	ANOVA de 2 vias ordinária (Tukey pós-teste recomendado)	$F_{tratamento}$ (3, 260) = 9.932	P<0.0001
			F_{tempo} (12, 260) = 1.338	P=0.1971
			$F_{interação}$ (36, 260) = 0.7941	P=0.7951
	4xsal/sal; 4xsal/AOA; 4xLPS/sal; 4xLPS/AOA	ANOVA de 2 vias ordinária (Tukey pós-teste recomendado)	$F_{tratamento}$ (3, 273) = 13.65	P<0.0001
			F_{tempo} (12, 273) = 1.213	P=0.2735
			$F_{interação}$ (36, 273) = 0.5229	P=0.9896
Índice de perda de calor (HLI)	1xsal/sal; 1xsal/AOA; 1xLPS/sal; 1xLPS/AOA	ANOVA de 2 vias ordinária (Tukey pós-teste recomendado)	$F_{tratamento}$ (3, 175) = 46.04	P<0.0001
			F_{tempo} (6, 175) = 11.54	P<0.0001
			$F_{interação}$ (18, 175) = 3.987	P<0.0001
	4xsal/sal; 4xsal/AOA; 4xLPS/sal; 4xLPS/AOA	ANOVA de 2 vias ordinária (Tukey pós-teste recomendado)	$F_{tratamento}$ (3, 189) = 20.16	P<0.0001
			F_{tempo} (6, 189) = 2.180	P=0.0467
			$F_{interação}$ (18, 189) = 2.111	P=0.0070
Níveis de PGE_2 na AVPO	1xsal/sal; 1xsal/AOA; 1xLPS/sal; 1xLPS/AOA	ANOVA de 2 vias ordinária (Tukey pós-teste recomendado)	F_{LPS} (1, 19) = 16.20	P=0.0007
			F_{AOA} (1, 19) = 0.08341	P=0.7759
			$F_{interação}$ (1, 19) = 1.413	P=0.1491
	4xsal/sal; 4xsal/AOA; 4xLPS/sal; 4xLPS/AOA	ANOVA de 2 vias ordinária (Tukey pós-teste recomendado)	F_{LPS} (1, 19) = 5.116	P=0.0356
			F_{AOA} (1, 19) = 6.045	P=0.0237
			$F_{interação}$ (1, 19) = 6.792	P=0.0174
Níveis de PGD_2 na AVPO	1xsal/sal; 1xsal/AOA; 1xLPS/sal; 1xLPS/AOA	ANOVA de 2 vias ordinária (Tukey pós-teste recomendado)	F_{LPS} (1, 19) = 16.26	P<0.001
			F_{AOA} (1, 19) = 3.139	P=0.0925
			$F_{interação}$ (1, 19) = 5.164	P<0.05
	4xsal/sal; 4xsal/AOA; 4xLPS/sal; 4xLPS/AOA	ANOVA de 2 vias ordinária (Tukey pós-teste recomendado)	F_{LPS} (1, 23) = 4.229	P=0.0413
			F_{AOA} (1, 23) = 4.741	P=0.0400
			$F_{interação}$ (1, 23) = 0.4289	P=0.5190
TNF-α plasmático	1xLPS/sal; 1xLPS/AOA	T-test não pareado	t=3.433, df=12	P=0.0025

	Grupos*	Análise	F or t	P
IL-6 plasmático	1xLPS/sal; 1xLPS/AOA	T-test não pareado	t=0.9740, df=12	P=0.3493
IL-1β plasmático	1xsal/AOA; 1xLPS/sal; 1xLPS/AOA	ANOVA de 1 via (Comparações múltiplas de Dunnett; pós-teste recomendado)	$F_{tratamento}$ (2, 20) = 24.52	P<0.0001
Log de PGE_2 no plasma	1xLPS/sal; 1xLPS/AOA	Teste de Mann Whitney	-	P=0.2684
	4xLPS/sal; 4xLPS/AOA	Teste de Mann Whitney	-	P<0.0001
Log de PGD_2 no plasma	1xsal/AOA; 1xLPS/sal; 1xLPS/AOA	Teste de Kruskal-Wallis (Comparações múltiplas de Dunn, recomendado)	-	P=0.1153
	4xsal/AOA; 4xLPS/sal; 4xLPS/AOA	Teste de Kruskal-Wallis (Comparações múltiplas de Dunn, recomendado)	-	P=0.0033
Expressão de CBS na AVPO	1xsal (2h and 24h post-LPS);1xLPS (2h and 24h post-LPS); 4xLPS(2h and 24h post-LPS)	ANOVA de 2 vias ordinária (Tukey pós-teste recomendado)	F_{LPS} (2, 18) = 9.886	P=0.001
			F_{tempo} (1, 18) = 0.002644	P=1.298
			$F_{interação}$ (2, 18) = 2.424	P=0.8383
H_2S na AVPO	1xsal (24h post-LPS);1xLPS (24h post-LPS); 4xLPS(24h post-LPS)	ANOVA de 1 via (Comparações múltiplas de Dunnett; pós-teste recomendado)	F_{LPS} (2, 15) = 9.764	P>0.001
Corticosterona plasmatic	1xsal/sal; 1xsal/AOA; 1xLPS/sal; 1xLPS/AOA; 4xsal/sal; 4xsal/AOA; 4xLPS/sal; 4xLPS/AOA	ANOVA de 2 vias ordinária (Tukey pós-teste recomendado)	F_{LPS} (3, 44) = 49.63	P<0.0001
			F_{AOA} (1, 44) = 20.77	P<0.0001
			$F_{interação}$ (3, 44) = 1.631	P=0.1959

* Grupos com valores não detectáveis foram excluídos da estatística.

Artigo publicado na Acta Physiologica

Received: 14 May 2019 | Revised: 13 August 2019 | Accepted: 28 August 2019

DOI: 10.1111/apha.13373

REGULAR PAPER

ACTA PHYSIOLOGICA

Increased hypothalamic hydrogen sulphide contributes to endotoxin tolerance by down-modulating PGE_2 production

Bruna M. Santos[1] | **Heloísa D. C. Francescato**[1] | **Flávia C. Turcato**[1] | **José Antunes-Rodrigues**[1] | **Terezila M. Coimbra**[1] | **Luiz G. S. Branco**[2]

[1]Department of Physiology, Medical School of Ribeirão Preto, University of São Paulo, Ribeirão Preto, Brazil

[2]Department of Basic and Oral Biology, Dental School of Ribeirão Preto, University of São Paulo, Ribeirão Preto, Brazil

Correspondence
Luiz G. S. Branco, Department of Basic and Oral Biology, Dental School of Ribeirão Preto, University of São Paulo, 14049-904 Ribeirão Preto, São Paulo, Brazil.
Email: branco@forp.usp.br

Funding information
Fundação de Amparo à Pesquisa do Estado de São Paulo, Grant/Award Number: 16/09364-3 and 16/17681-9; Conselho Nacional de Desenvolvimento Científico e Tecnológico, Grant/Award Number: 142151/2016-5

Abstract

Aim: Whereas some patients have important changes in body core temperature (Tb) during systemic inflammation, others maintain a normal Tb, which is intrinsically associated to immune paralysis. One classical model to study immune paralysis is the use of repeated administration of lipopolysaccharide (LPS), the so-called endotoxin tolerance. However, the neuroimmune mechanisms of endotoxin tolerance remain poorly understood. Hydrogen sulphide (H_2S) is a gaseous neuromodulator produced in the brain by the enzyme cystathionine β-synthase (CBS). The present study assessed whether endotoxin tolerance is modulated by hypothalamic H_2S.

Methods: Rats with central cannulas (drug microinjection) and intraperitoneal datalogger (temperature record) received a low-dose of lipopolysaccharide (LPS; 100 μg kg^{-1}) daily for four consecutive days. Hypothalamic CBS expression and H_2S production rate were assessed, together with febrigenic signalling. Tolerant rats received an inhibitor of H_2S synthesis (AOA, 100 pmol 1 μL^{-1} icv) or its vehicle in the last day.

Results: Antero-ventral preoptic area of the hypothalamus (AVPO) H_2S production rate and CBS expression were increased in endotoxin-tolerant rats. Additionally, hypothalamic H_2S inhibition reversed endotoxin tolerance reestablishing fever, AVPO and plasma PGE_2 levels without altering the absent plasma cytokines surges.

Conclusion: Endotoxin tolerance is not simply a reflection of peripheral reduced cytokines release but actually results from a complex set of mechanisms acting at multiple levels. Hypothalamic H_2S production modulates most of these mechanisms.

KEYWORDS
corticosterone, cytokines, fever, gasotransmitters, inflammation, lipopolysaccharide

1 | INTRODUCTION

Systemic inflammation is observed during sepsis, a well-known phenomenon characterized by its acute immune hyperactivity followed by a long-term immunosuppressive state. Independently of the state, the risk of mortality remains unacceptably high.[1] Among the sepsis mechanisms, it is now clear that an increased endogenous production of hydrogen sulphide (H_2S)[2] and activation of the hypothalamic-pituitary-adrenal (HPA) axis take place.[3]

Endotoxin (lipopolysaccharide-LPS) administration induces non-infectious systemic inflammation and its repeated administration causes endotoxin tolerance,[4] which has been used as a model of immune paralysis since it preserves host

homeostasis without affecting the hosted pathogen.[5] There are remarkable efforts in understanding the mechanisms of immune paralysis, because they have been reported to be important for mitigating all the harmful consequences of sustained inflammation and/or sepsis.[6] More recently, this endotoxin tolerance model has gained even more attention because of the vulnerability of patients in the late stage of sepsis toward secondary infections.[7,8]

Likewise, a number of studies report the mechanisms underlying endotoxin tolerance (for review[5,9,10]) and among them, the gaseous neurotransmitters (nitric oxide[11-13] and carbon monoxide[12,14,15]) have been reported to play key roles during endotoxin tolerance. Recently, a third gas has been described. H_2S has been recently reported to be endogenously produced arising from L-cysteine.[16] The physiological action of this gas is facilitated by its characteristic to pass through the plasma membrane in all mammalian cells including neurons.[17,18] H_2S plays crucial roles in a number of physiological and pathophysiological conditions.[19,20] In the brain, H_2S is mainly synthesized by the enzyme cystathionine-β-synthase (CBS) and exerts important anti-inflammatory effects.[21,22]

H_2S acts through several interconnected mechanisms,[16,17] modulating neuronal activity,[23,24] inhibiting NFkappaB activity,[9] and affecting prostaglandin E_2 (PGE_2) production.[21] Considering that PGE_2 is a proximal mediator of systemic inflammation, it seems plausible that central H_2S may exert a considerable impact on endotoxin tolerance. Thus, in this study, we assessed the antero-ventral preoptic area of the hypothalamus (AVPO) H_2S production rate and CBS expression in tolerant rats, and pharmacologically inhibited H_2S production in the hypothalamus to evaluate whether LPS-induced tolerance is affected by inhibition of the enzyme CBS. We then assessed putative mechanisms of the pharmacological effects found, examining AVPO PGE_2 and prostaglandin D_2 (PGD_2) production, plasma febrigenic (cytokines and PGE_2) and cryogenic (corticosterone and PGD_2) signalling and thermoeffectors (heat loss index [HLI] and non-shivering thermogenesis [NST]).

2 | RESULTS

To facilitate the understanding of the protocols used, we design an experimental timeline in Figure 1. Briefly, the animals were divided into three groups before the day of the experiment: naive rats, non-tolerant and tolerant rats. Naive rats had no injections before the experiment day. Non-tolerant rats received saline (sal) ip for three consecutive days before the experiment day to be the control of the tolerant rats, which received LPS ip injection for three consecutive days before the experiment day. On the day of the experiment, naive rats received aminooxyacetic acid (AOA) or its vehicle (sal) icv followed by injection of sal or LPS ip. For the case of the non-tolerant rats, AOA or its vehicle (sal) were injected icv followed by sal ip injection and, for the tolerant rats, AOA or its vehicle (sal) were injected followed by LPS ip injection on the experiment day.

2.1 | Effects of central H_2S on body core temperature (Tb), O_2 consumption and HLI in LPS naive rats and LPS-tolerant rats

We evaluated whether the inhibition of H_2S hypothalamic production alters Tb of euthermic rats maintained at 29°C using AOA (CBS inhibitor) as a pharmacological tool. We also evaluated specifically which thermoeffector is activated,

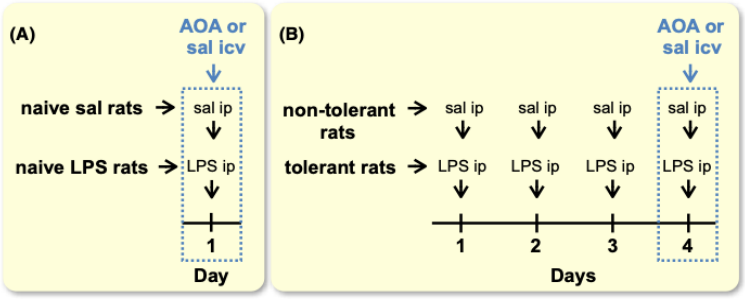

FIGURE 1 Experimental timeline. The animals were separated in four groups naive sal, naive lipopolysaccharide (LPS), non-tolerant, and tolerant rats on the day of the experiment (indicated by the blue box). A, Experimental timeline of naïve rats. Naïve rats had no injections before the experiment day, that is, day 1 (indicated by the blue box). Naive rats received aminooxyacetic acid (AOA) cystathionine β-synthase (CBS) inhibitor or its vehicle (sal) icv followed by injection of sal or LPS ip. B, Experimental timeline of non-tolerant and tolerant rats. Non-tolerant rats received saline (sal) ip for three consecutive days before the experiment day, that is, day 4 (indicated by the blue box). Tolerant rats received LPS ip injection for three consecutive days before the experiment day. Non-tolerant and tolerant rats received AOA or its vehicle (sal) icv followed by sal (non-tolerant rats) or LPS (tolerant rats) ip on the experiment day respectively

measuring NST (estimated by O_2 consumption) and HLI (using tail thermography and Tb—see details in Methods section). Naive animals that received sal ip and sal icv injections had no differences in NST (Figure 2B, upper graph) or in HLI (Figure 2C, upper graph) and consequently no differences in Tb (Figure 2A, upper graph) were observed. Injection of AOA immediately after sal ip injection in naive rats caused no significant change in Tb (Figure 2A, upper graph). Consistent with this observation, no significant changes were observed in their NST (Figure 2B, upper graph) and HLI (Figure 2C, upper graph) indicating that AOA has no effect on thermoregulation during euthermia.

In LPS naive rats, a typical febrile response was developed after administration of a relatively low dose of LPS

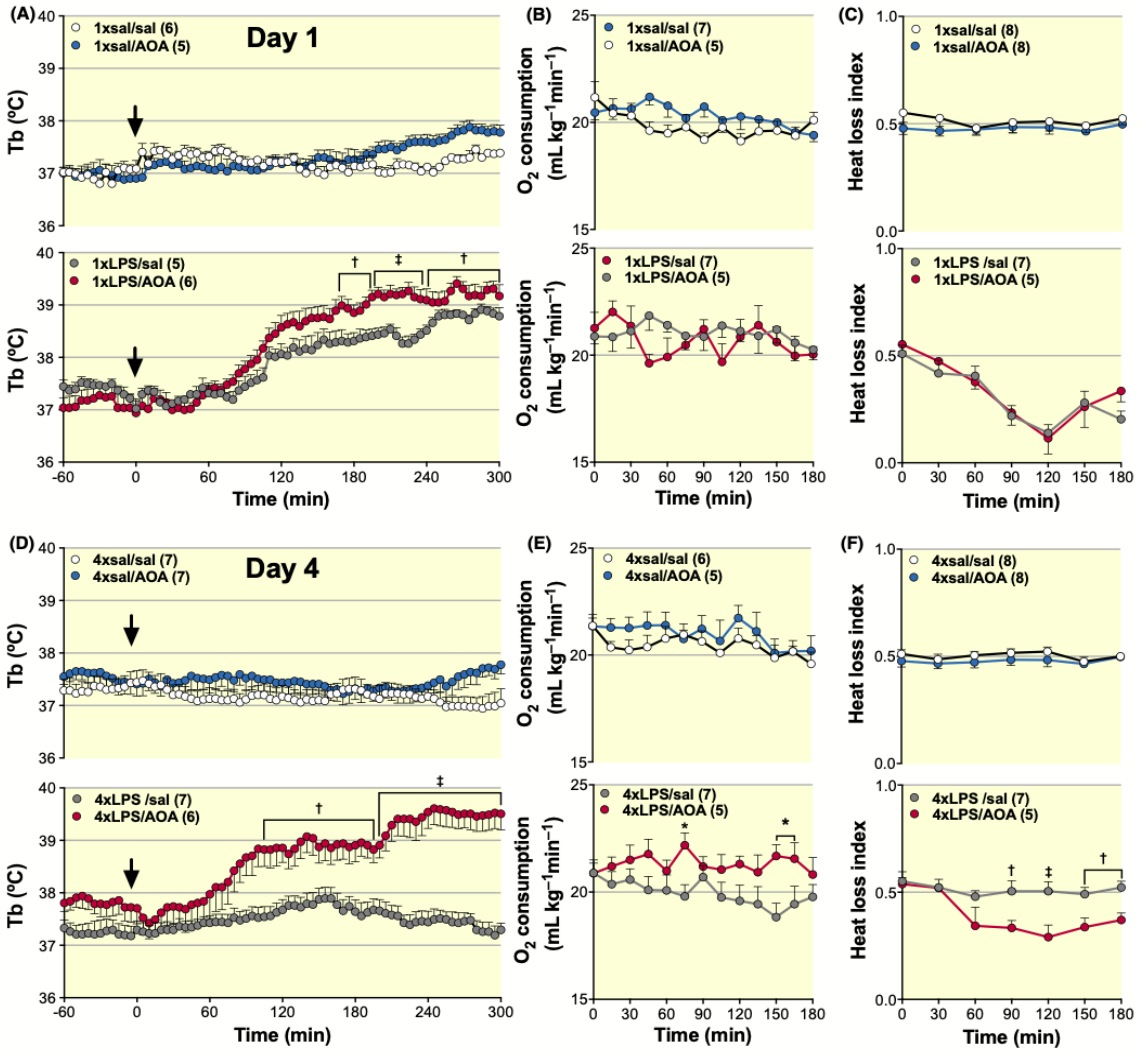

FIGURE 2 Effect of a cystathionine β-synthase inhibitor aminooxyacetic acid (AOA) microinjection on T_b, O_2 consumption and heat loss index (HLI) of lipopolysaccharide (LPS) naive (1× LPS) and LPS-tolerant (4× LPS) animals. LPS (100 μg kg^{-1} ip) or its vehicle (saline ip) was injected once (LPS naive, graphics on the top) or four times daily (endotoxin tolerance, bottom graphics) in time zero (indicated by the arrows in Figure 2A,E). AOA (cystathionine Y-lyase inhibitor) icv microinjection was performed immediately before LPS or saline ip in LPS naive. A, Body core temperature (Tb). B, O_2 consumption. C, HLI in immune challenged rats with or without AOA icv injection. D, Body core temperature (Tb). E, O_2 consumption. F, HLI in LPS-tolerant rats with or without AOA icv injection. N = 5-8. Error display SEM. $^*P < .05$, $^\dagger P < .01$ and $^\ddagger P < .001$ vs control group, same graph

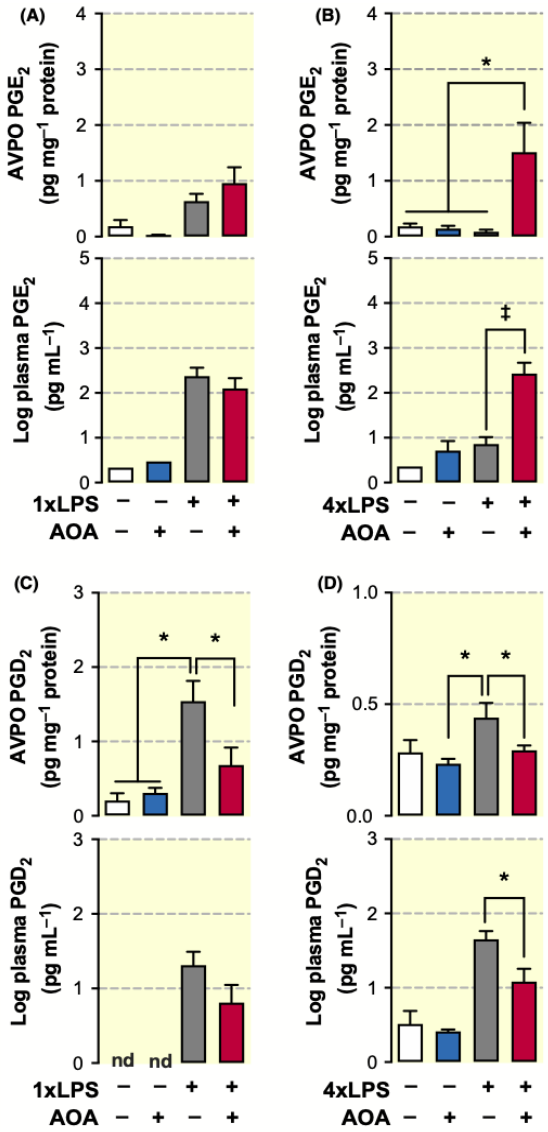

FIGURE 3 Antero-ventral preoptic area of the hypothalamus (AVPO) and plasma levels of prostaglandins in lipopolysaccharide (LPS) naive (1× LPS) and LPS-tolerant (4× LPS) animals and the effect of central microinjection of a cystathionine β-synthase inhibitor aminooxyacetic acid (AOA). AVPO and plasma PGE_2 and PGD_2 levels 2 h post-saline or LPS 100 μg kg^{-1} ip injection with central microinjection of AOA or saline in LPS naive (1× LPS) or LPS-tolerant (4× LPS) rats. A, AVPO and log of plasma PGE_2 levels in LPS naive rats. B, AVPO and log of plasma PGE_2 levels in LPS-tolerant rats. Error bars display SEM. C, AVPO and log of plasma PGE_2 levels in LPS naive rats. D, AVPO and log of plasma PGE_2 levels in LPS-tolerant rats. Error bars display SEM. Groups with some or all non-detectable data (nd) were not included in the statistics. N = 5-8. $^*P < .05$ and $^‡P < .0001$

(100 μg kg^{-1} ip) compared with sal naive rats (Figure 2A, bottom graph). Febrile response to LPS in naive rats resulted from a reduced HLI (Figure 2C, bottom graph), with no contribution of NST (Figure 2B, bottom graph). LPS naive rats injected AOA icv had a slight increase in Tb compared with LPS naive rats treated with sal icv 165 minutes after LPS injection (Figure 2A, bottom graph).

The following question was then taken into consideration: Would central H_2S modulate endotoxin fever tolerance per se? To address this possibility, LPS tolerance was developed after repeated LPS injections (4× LPS) which can be verified by the absence of fever in tolerant animals treated with sal icv (Figure 2D). Additionally, AOA was administered before LPS in tolerant rats and an increase in Tb was observed compared with LPS-tolerant rats that received sal icv (Figure 2D, bottom graph). The febrile response to LPS in tolerant rats treated with AOA resulted from an increased NST (Figure 2E, bottom graph) and decreased HLI (Figure 2F, bottom graph), indicating that central H_2S modulates both thermoeffectors in LPS-tolerant rats. No differences were observed between groups that received repeated sal injection regardless of the icv treatment, on Tb (Figure 2D, upper graph), NST (Figure 2E, upper graph) and HLI (Figure 2F).

2.2 | Effects of central H_2S inhibition on plasma prostaglandins levels in LPS naive and LPS-tolerant animals

To investigate the mechanisms of the febrile response of LPS-tolerant animals treated with AOA icv, we examined the plasma levels of prostaglandins since they are fundamental to the LPS-induced thermoregulatory responses. Moreover, the AVPO prostaglandins levels were also measured since AVPO has a key role in controlling the thermoeffectors. In contrast to PGE_2, PGD_2 is recognized by its cryogenic role.[25]

AOA icv microinjection caused no effect in AVPO and plasma PGE_2 production (Figure 3A) or even in AVPO and plasma PGD_2 production (Figure 3C) compared with sal in naive rats treated with sal icv. No differences were observed between AOA and sal icv treatment in AVPO or plasma PGE_2 (Figure 3B) and PGD_2 (Figure 3D) production in sal non-tolerant rats. These data indicate that hypothalamic inhibition of H_2S causes no effects in prostaglandins production in sal naive or sal non-tolerant rats.

As described in the literature, LPS naive rats with sal icv treatment had surges in their AVPO and plasma PGE_2 (Figure 3A) and PGD_2 (Figure 3C) levels. AOA icv treatment in LPS naive rats caused a slight increase in AVPO PGE_2 levels

(Figure 3A) and a decrease in AVPO PGD_2 (Figure 3C) levels without altering plasma PGE_2 (Figure 2A) and PGD_2 (Figure 3C) levels compared with LPS naive rats treated with sal icv.

LPS in tolerant animals treated with sal icv had low AVPO and plasma PGE_2 levels similar to that observed in rats treated repeatedly with sal ip (Figure 3B), but a full surge in AVPO and plasma PGE_2 were measured when LPS was combined with AOA administration in LPS-tolerant rats (Figure 3B). Moreover, LPS in tolerant rats showed an increase in AVPO and plasma PGD_2 levels that were diminished by AOA (Figure 3D). These data indicate that central H_2S plays a key role modulating the immune response of LPS-tolerant rats, by up-regulating a major pyretic molecule (PGE_2) and simultaneously down-regulating a major cryogenic molecule (PGD_2).

2.3 | Effects of central H_2S inhibition on plasma cytokines levels in LPS naive and LPS-tolerant animals

As previously reported,[25,26] sal naive and sal non-tolerant rats had undetectable plasma TNFα levels (Figure 4A,B). A surge in plasma TNFα was observed in LPS naive rats (Figure 4A). This LPS-induced surge in plasma TNFα was reduced in AOA treated LPS naive rats (Figure 4A), indicating that H_2S up-regulates TNFα plasma levels in LPS naive animals. Conversely, the LPS-induced surges in plasma IL-6 and IL-1β were not affected by AOA, indicating that H_2S plays no role in hypothalamic modulation of plasma IL-6 and IL-1β in LPS naive animals (Figure 4C-F).

Essentially, LPS-tolerant rats and sal non-tolerant rats (Figure 4B,D,F) had undetectable cytokine levels in plasma and the treatment with AOA icv in LPS-tolerant rats did not revert the immunosuppression observed in LPS-tolerant rats treated with sal icv.

2.4 | Effects of central CBS inhibition on plasma corticosterone levels in LPS naive and LPS-tolerant animals

Plasma corticosterone plays a cryogenic role during systemic inflammation.[27] We measured relatively reduced plasma corticosterone levels in the sal naive rats independently of the icv treatment (Figure 5). Conversely, LPS naive rats showed enhanced plasma corticosterone levels compared with sal naive rats (Figure 5).

The LPS-tolerant rats also showed increased plasma corticosterone levels compared with sal non-tolerant rats (Figure 5). No differences were observed in plasma corticosterone levels between LPS naive and LPS-tolerant animals. Additionally, AOA caused a further increase in plasma corticosterone levels in both LPS naive and LPS-tolerant rats (Figure 5).

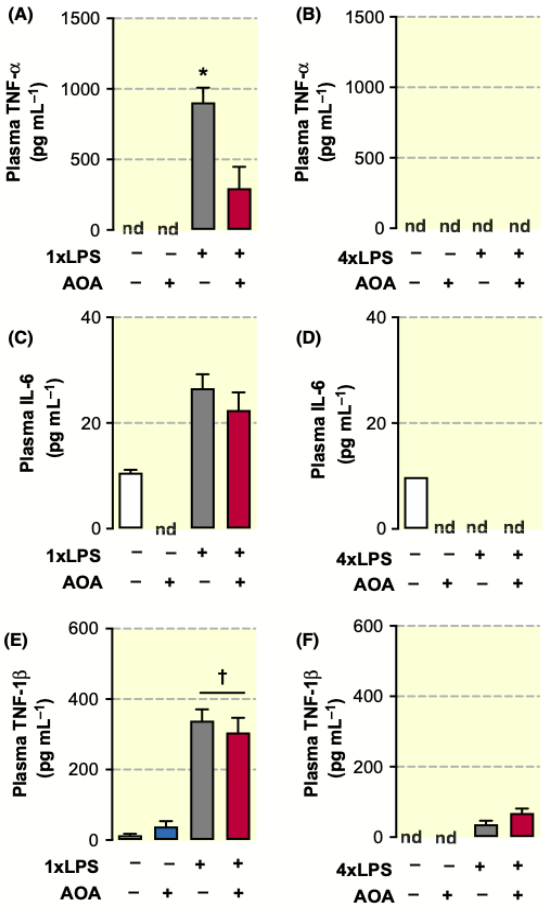

FIGURE 4 Plasma levels of cytokines in lipopolysaccharide (LPS) naive (1× LPS) and LPS-tolerant (4× LPS) animals and the effect of central cystathionine β-synthase inhibition using aminooxyacetic acid (AOA). Plasmatic cytokines levels 2 h post-saline or LPS 100 μg kg^{-1} ip injection with central microinjection of AOA or saline in LPS naive or LPS-tolerant rats. Plasma TNF-α levels in LPS naive (A) or LPS-tolerant (B) rats. Plasma IL-6 levels in LPS naive (C) or LPS-tolerant (D) rats. Plasma IL-1β levels in LPS naive (E) or LPS-tolerant (F) rats. Error bars display SEM. Groups with some or all non-detectable data (nd) were not included in the statistics. N = 5-8. $^*P < .05$ and $^\dagger P < .01$

2.5 | AVPO CBS protein expression and H_2S production rate in LPS naive and LPS-tolerant animals

Kwiatkoski et al[21] observed a decrease in AVPO H_2S levels 2 hours after LPS injection in LPS naive rats using the same dose of LPS. Here, we observed that AVPO CBS protein expression in LPS naive animals was not significantly increased 2 hours after LPS injection, in agreement with the observation

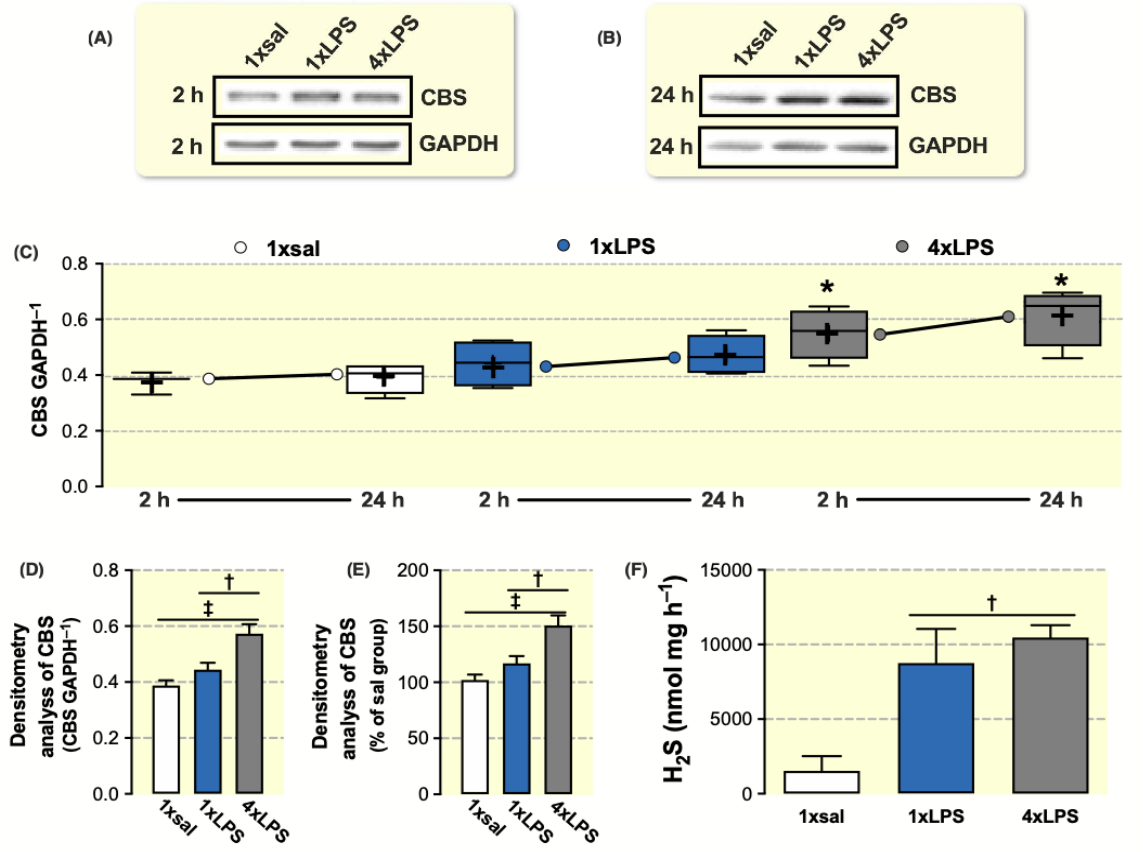

FIGURE 5 Plasma levels of corticosterone in lipopolysaccharide (LPS) naive (1× LPS) and LPS-tolerant (4× LPS) animals and the effect of central microinjection of a cystathionine β-synthase (CBS) inhibitor aminooxyacetic acid (AOA). Plasmatic corticosterone levels 2 h post-saline or LPS 100 μg kg^{-1} ip injection with central inhibition of CBS with AOA or saline in LPS naive or LPS-tolerant rats. Error bars display SEM. N = 5-8. $^{*}P < .05$ and $^{‡}P < .001$

by those authors. Twenty-four hours after LPS injection in naive rats, AVPO H_2S levels increased in the LPS naive animals (Figure 6E) followed by a slight increase in AVPO CBS protein expression (Figure 6C). These data indicate that the decreased production of hypothalamic H_2S happens only in the first hours after LPS injection without altering CBS expression (Figure 6C), but there is an increase in H_2S production 24 hours later (Figure 6F) probably by unbounding the sulphate sulphur from some proteins. Subsequently, after repeated injections of LPS, an increased expression of CBS is observed 2 and 24 hours after the last LPS injection (Figure 6C). Furthermore, the production rate of AVPO H_2S remains high 24 hours after the last LPS injection in LPS-tolerant rats (Figure 6D). The increased AVPO CBS expression was not dependent upon the time, as indicated by ANOVA (for further details see Table S1). AVPO CBS expression increased almost 50% in LPS-tolerant animals compared with the naive sal rats, independently of the time of LPS or sal injection (Figure 6E).

3 | DISCUSSION

The present data are consistent with the notion that endotoxin tolerance results among other mechanisms from increased endogenous produced H_2S in the AVPO, since we demonstrated that: (a) the AVPO CBS expression and H_2S production rate are increased in LPS-tolerant animals, (b) pharmacological inhibition of hypothalamic CBS in LPS-tolerant rats are able to mount a normal febrile response, (c) fever was accompanied by reduced HLI, and (d) increased NST, indicating that these thermoeffectors are silent but not impaired during endotoxin tolerance. Interestingly, this consistent set of findings was observed to be independent

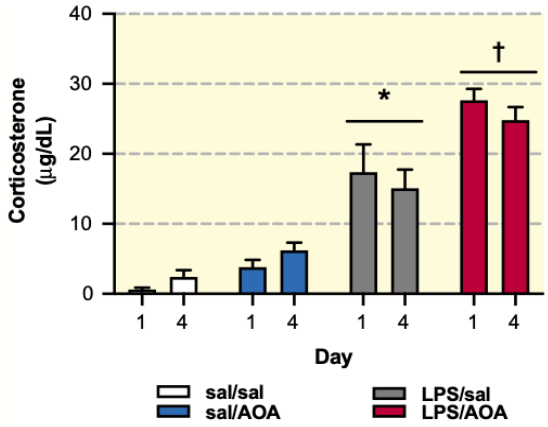

FIGURE 6 Antero-ventral preoptic area of the hypothalamus (AVPO) cystathionine β-synthase (CBS) expression and AVPO H_2S levels in LPS naive (1× LPS) or LPS-tolerant (4× LPS) animals. AVPO CBS expression 2 or 24 h after saline injection or LPS injection in LPS naive (1× LPS) or LPS-tolerant (4× LPS) rats. A, Representative bands of western blot showing the AVPO protein levels of CBS 2 h after LPS or its vehicle. B, Representative bands of western blot showing the AVPO protein levels of CBS 24h after LPS or its vehicle. C, CBS expression in the AVPO in LPS naive (1× LPS) and LPS-tolerant (4× LPS) rats was studied using western blotting dependent upon the time of LPS administration (N = 3-5). Mean is represented by a red plus (+). D, Densitometry analysis of AVPO CBS expression normalized by the constitutive protein GAPDH. E, Densitometry analysis of AVPO CBS expression normalized by the constitutive protein GAPDH and illustrated by the percentage of expression compared to the saline group. F, H_2S levels in LPS naive (1× LPS) and LPS-tolerant (4× LPS) rats. Error bars display SEM. N = 4-7. $^*P < .05$ and $^\dagger P < .01$ vs saline group

of some key peripheral febrigenic cytokines, since LPS did not induce increases in plasma cytokines (TNF-α, IL-6 and IL-1β) after hypothalamic CBS inhibition in LPS-tolerant animals. Conversely, another set of results indicate that AVPO and plasma PGE_2 and PGD_2 levels were indeed consistently affected by hypothalamic CBS inhibition (Figure 3) and are very likely to mediate the hypothalamic CBS inhibition effect on tolerance, that is, not only the abolished LPS-induced plasma PGE_2 observed in tolerant rats was re-established in rats treated with AOA icv, but also the LPS-induced PGD_2 surge observed in LPS-tolerant rats was reverted by the same treatment.

We speculate that central mechanisms involving neuronal signalling by astrocytes generated H_2S[28] is indeed a powerful and effective mechanism to revert endotoxin tolerance that acts by down-regulating PGE_2 and up-regulating PGD_2 (Figure 3). Moreover, we conjecture that these exciting findings with the CBS inhibitor provide solid evidence that allow us to suggest that H_2S is a very powerful endogenous antipyretic molecule acting in the brain during endotoxin tolerance.

In the brain, H_2S is mainly produced by the enzyme CBS which has been demonstrated to be expressed mainly in astrocytes.[29] These cells show reciprocal interaction with neurons,[19,30] that is, nearby astrocytes can be activated by neuronal activity that in turn control their synaptic activity. Such reciprocal interactions may also occur between astrocytes and neurons in the AVPO, determining generation and modulation of fever.[31,32]

The interaction of the periphery with central mechanisms mediating immune response is bidirectional.[33] To investigate the peripheral action of hypothalamic H_2S in endotoxin tolerance, we determined the plasma levels of PGE_2, PGD_2, TNF-α, IL-1β, IL-6 and corticosterone (Figures 3, 4, and 5). It was found that hypothalamic H_2S inhibition does not alter the diminished levels of these cytokines in tolerant animals (Figure 4) while H_2S modulates the levels of PGE_2, PGD_2 in LPS-tolerant animals. Interestingly, it seems that LPS-tolerant animals show reduced plasma PGE_2 levels and maintained relatively high plasma PGD_2 compared with LPS naive rats (Figure 3).

Kwiatkoski et al observed that H_2S plays an inhibitory role on hypothalamic PGE_2.[21] Additionally, there is evidence indicating that central PGE_2 plays an important role in LPS-induced splanchnic sympathetic activation and, concurrently, splenic sympathetic activity,[34] which cause lower TNF-α production through the activation of cholinergic T cells in the spleen, and consequently, the inhibition of macrophages by activation of α 7nAchR receptors.[35,36] Thus, this is a plausible mechanism through which hypothalamic inhibition of H_2S production can regulate circulating levels of TNF-α.

In agreement with a previous study,[21] in the present study we observed that CBS inhibition was associated with increased hypothalamic PGE_2 levels in LPS-tolerant rats (Figure 3B), which is known to cause a sympathetic stimulation[34] and a subsequent up-regulation of peripheral PGE_2 production.[37-39] We speculate that this mechanism explains how hypothalamic inhibition of H_2S production regulates circulating levels of PGE_2.

Plasma corticosterone levels were observed to be high in both LPS naive and LPS-tolerant rats (Figure 5). It has been documented that central H_2S causes depolarization of paraventricular neurons and consequently an increasing release of corticosterone,[40,41] thus indicating that the enhanced H_2S production rate may play an excitatory action on the HPA axis during endotoxemia (Figure 5). It may be worth mentioning that corticosterone is a hormone that plays an important anti-inflammatory role, including displaying an antipyretic effect during systemic inflammation.[27] We also observed that hypothalamic CBS inhibition was associated with increases in the corticosterone plasma levels (Figure 6). This response might be explained by the neuroimmune

interaction of PGE_2 to activate the hypothalamic-pituitary axis. We speculate that increased PGE_2 production after CBS inhibition has a preponderant effect, modulating the HPA axis in relation to the gasotransmitter itself in LPS-tolerant rats. Also, corticosterone levels were still high in LPS-tolerant rats (Figure 6) and hypothalamic H_2S inhibition enhanced the augmented corticosterone production in LPS-tolerant rats, indicating its role in the control of the corticosterone levels in LPS.

Besides acting on CBS, AOA partially inhibits cystathionine-γ-lyase (CSE) and γ-aminobutyric acid (GABA) transaminase,[42] which does not exclude the role of central CBS in endotoxin tolerance. A previous study by our group[21] documented that hypothalamic CBS inhibition with AOA causes a decrease in the AVPO H_2S production rate whereas H_2S donor causes an opposite response in rats, indicating that the effect of AOA is indeed mediated through H_2S synthesis. Moreover, it has been reported that central gabaergic inhibition leads to an enhancement of plasma corticosterone levels,[43] which was not observed in the present study (Figure 5). Thus it is very unlikely that the observed effects of AOA in the present study were mediated by GABA.

Acting systemically, H_2S has been observed to play a neuroprotective role in rats and mice in a traumatic brain injury model.[24,44] This effect may result from an anti-inflammatory action of the gas, since H_2S seems to down-regulate the expression of NFkappaB in a model of long-lasting occlusion of the middle cerebral artery.[45] Kwiatkosky et al[21] documented that H_2S is a powerful endogenous antipyretic molecule that may act through suppression of PGE_2 synthesis and/or stimulation of cAMP production in the hypothalamus, based on data obtained using a model of LPS-induced immune challenge.

The molecular mechanisms of endotoxin tolerance in the periphery have been well-characterized.[6,9,46] Fewer reports exist in relation to the central mechanisms of endotoxin tolerance, even though this topic has been aptly addressed in important recent studies in the literature.[47,48] Besides, in an elegant experiment described by Chu et al[49] while neurons and astroglia are affected by chronic neuroinflammation, microglia fails to develop endotoxin tolerance. The authors concluded that the absence of microglial endotoxin tolerance could be important for the pathogenetic mechanisms involved in inflammation-associated neuronal damage. We speculate that endotoxin tolerance can activate astrocytes enhancing the production of H_2S centrally. In high levels this signalling molecule can modulate microglia and neuron inflammatory mediator production, mainly PGE_2, and fever abrogation, as a consequence.

In summary, the present study provides evidence that: (a) during LPS tolerance, thermoeffector activity is observed to be silent but it is not impaired, including the sympathetic activity which innervate brown adipose tissue responsible for NST, and cutaneous tissue of the tail responsible for heat loss (Figure 2); (b) the plasma prostaglandins levels are drastically altered during endotoxin tolerance, that is, reduced LPS-induced PGE_2 and increased PGD_2 levels (Figure 3); (c) plasma cytokines are at their nadir levels (Figure 4); and (d) plasma corticosterone levels are kept high (Figure 5). Reconciling these data, we suggest that febrile tolerance is not simply a reflection of the absent plasma cytokines surges, but it is rather a phenomenon that results from multiple levels and through distinct mechanisms. Most of these observed changes in tolerant rats seem to be dependent on increased hypothalamic H_2S production (Figure 6), since CBS inhibition restored thermoeffectors responses to LPS (Figure 2); caused increased plasma PGE_2 levels and decreased plasma PGD_2 levels (Figure 3); and caused increased plasma corticosterone levels (Figure 5), however, plasma cytokines levels were not affected (Figure 4).

A better understanding of the mechanisms involved in endotoxin tolerance might provide a hypothalamic H_2S-based therapeutic strategy to prevent systemic tissue damage in cases of chronic immune challenge.

4 | METHODS

4.1 | Animals

Adult male Wistar rats (290-300 g) were individually caged and maintained at a controlled temperature of 29°C with a 12 hours light/dark cycle with food and water ad libitum. All experiments were approved by the Animal Ethical Committee of the Dental School of Ribeirão Preto (2016.1.393.58.1). All protocols and procedures complied with the recommendations of the Guide for the Care and Use of Laboratory Animals of the National Council for the Control of Animal Experimentation (CONCEA).

4.2 | Drugs

LPS extracted from Escherichia coli (serotype 0111: B4, lot #076K4020, Sigma-Aldrich, USA) was diluted in pyrogen-free saline and injected ip at a dose of 100 μg kg^{-1}. Immune challenge and endotoxin tolerance were induced with LPS administration which was sufficient to activate febrigenic signalling and tail vasoconstriction, an important thermoeffector of rats kept in the themoneutral zone (29°C).[25,50] AOA, an inhibitor of CBS was administered in the third ventricle to verify if the inhibition of central H_2S could abolish endotoxin tolerance. The drug was dissolved in pyrogen-free saline to a final concentration of 100 pmol μL^{-1}. A volume of 1 μL of AOA was administered intracerebroventricularly, as previously reported.[21]

4.3 | Surgery

Seven days before the experiment, the rats were implanted with an icv cannula and an intra-abdominal mini datalogger (SubCue). All surgery procedures were performed under anaesthesia using a mixture of 10% ketamine and 2% xylazine (1:1; 1mL kg^{-1} of body weight) administered intraperitoneally (ip). Anti-inflammatory/antibiotic protection with flunixin meglumine (0.1 mL subcutaneously) and pentabiotic (1 200 000 IU; 0.1 mL intramuscular) were provided. In a surgical aseptic field, the intraperitoneal cavity was exposed through a median laparotomy for insertion of the datalogger. The intraperitoneal cavity was closed by muscular and cutaneous layers at the end of this surgery. The animals were subsequently fixed to a stereotaxic apparatus with the incisor bar set at −3.3 mm. The following coordinates were assigned with a reference from the bregma: anterior-posterior: −0.4 mm, lateral: 0 mm and dorsoventral: −4.5 mm. The coordinates were obtained from previous studies in the laboratory.[21] The effectiveness of the guide cannula (22-gauge; 16-mm of length) placement into the third ventricle was verified by the fact that the cerebrospinal fluid flows out of the guide cannula subsequent to its insertion. The icv cannula was fixed to the skull with a stainless-steel screw and dental cement. Icv microinjection of AOA (CBS inhibitor) was performed with the use of a 5-μL Hamilton syringe (Hamilton Bonaduz Ag) coupled to a polyethylene tube extension connected to a 20-mm length needle.

4.4 | Groups

Experimental groups were randomly assigned. Body weight was measured daily (7-8 AM) before injections. The naive group was divided into four subgroups which received icv injections of AOA or its vehicle (sal) followed by LPS ip injection or its vehicle (sal). The tolerant group received LPS ip daily for three days until endotoxin tolerance by fever attenuation was verified (Data S1). At day 4, the tolerant animals received AOA or its vehicle (sal) icv before the fourth LPS injection. The non-tolerant rats (control groups) received sal ip for four days and on the 4th day they received either icv AOA or icv sal before the 4th ip sal injection. Plasma samples were collected 2 hours after the last LPS injection of each protocol in the effervescent period of fever.[51]

4.5 | Non-shivering thermogenesis measurements

Oxygen consumption was determined in conscious non-restrained rats, in a fed state, and housed in an individual sealed chamber. The rats were allowed to adapt to the sealed chamber one day before, and on the day of the experiment for 20 minutes before VO_2 was measured. The air samples passed through an oxygen analyser (OA 272; Saylor Servomex). For the calculation of O_2 consumption (VO_2), the data from: FO_{2IN}; fraction of O_2 at the exit of the chamber (FO_{2OUT}), air flow in millilitres per minute (AirFlow), and animal weight in kg (BW) were plotted for the calculation. The formula used was: $VO_2 = \text{Airflow}\,(FO_{2IN} - FO_{2OUT})\,BW^{-1}$.

4.6 | Heat loss index measurements

Tb, tail skin temperature (Tsk) and ambient temperature (Ta) were acquired to calculate HLI. Tb was acquired by the programmed datalogger (5-min record data) and extracted using SubCue software. The high accuracy of Tb data was achieved using the calibration values of each datalogger provided by the company. A thermographic sensitivity camera (sensitivity of 0.1°C; FLIR ONE; FLIR Systems Inc) was used to measure the middle third of the tail length as a reference for cutaneous temperature measurement (Tsk). Ta was maintained at 29°C and verified every 30 minutes (min) using a fixed thermometer. The HLI was used to assess thermoeffector responses of the tail skin vasculature and calculated based on the formula: $HLI = (Tsk - Ta)\,(Tb - Ta)^{-1}$. The limits of HLI were 0 (maximal skin vasoconstriction) and 1 (maximal vasodilatation).[52]

4.7 | AVPO and plasma acquisition

The animals were decapitated and trunk blood was collected in anti-coagulant coated tubes and immediately centrifuged (2000 g for 20 minutes at 4°C) 2 hours after LPS/sal ip injection in the effervescent period of fever, as previously reported.[51] The brain was removed and flash-frozen (40 seconds) with dry-ice cold isopentane. Coronal sections of the brain were made with a cryostat microtome (Microm HM 505 E, Thermo Scientific). Three 500-μm-thick coronal sections were cut through the anterior area of the hypothalamus, the bilateral AVPO was then punched out with a 16-gauge needle, homogenized and centrifuged in the appropriated lysis buffer. Total protein concentration in the homogenate was measured with a Bradford assay kit (Bio-Rad Laboratories).

4.8 | Prostaglandins, cytokines and corticosterone measurements

Measurements were performed by the Enzyme-linked immunosorbent assay technique (ELISA) following the manufacturer's instructions for PGE_2, PGD_2 (#514010 and #512011 Cayman Chemical) and TNF-α, IL-1β and IL-6 (#DY510, #DY501, and #DY506 - R&D Systems) respectively. Additionally, plasma corticosterone levels by radioimmunoassay were determined as previously described.[53]

4.9 | Western blot

H_2S-related synthase CBS protein expression in the AVPO was measured using immunoblotting assay. The tissue analysed was removed from bilateral AVPO and homogenized at 4°C in lysis buffer (50 mM Tris–HCl, pH 7.4, 150 mM NaCl, 1% Triton X-100, 0.1% SDS, 1 μg mL^{-1} aprotinin, 1 μg/mL leupeptin, 1 mM phenylmethylsulphonyl fluoride, 1 mM sodium orthovanadate, pH 10, 1 mM sodium pyrophosphate, 25 mM sodium fluoride and 0.001 M EDTA - pH 8). The supernatant (40 000 rpm for 10 minutes at 4°C) of the tissue homogenates was collected. A total of 30 μg of protein in aliquots were dissolved in loading buffer and the proteins were separated by 10% sodium dodecyl sulphate polyacrylamide gel electrophoresis. The protein bands were then transferred to nitrocellulose membranes and incubated in 50 mL of blocking buffer (PBS, 2.5% skim milk) for 1 hour and washed in buffer (PBS, 0.1% Tween 20, pH 7.6). The membranes were then incubated with the corresponding primary antibody in 5% bovine serum albumin (BSA), and left overnight at 4°C. The primary antibody included monoclonal rabbit anti-mouse CBS (1:1000; Cell Signaling Technology). Thereafter, the membranes were washed and incubated with secondary antibody horseradish peroxidase-conjugated anti-rabbit (CBS) (1:5000; Dako) for 1 hour at Ta. Labelled proteins were revealed using Supersignal West Pico Chemiluminescent substrate (Pierce). Using a stripping buffer (100 mM 20-mercaptoethanol, 2% sodium dodecyl sulphate, 62.5 mM Tris-HCl, pH 6.8), the membranes were recovered (30 minutes at 50°C) for stripping and re-probing. To regulate the equivalence of protein loading or transfer, the membranes were soaked with TBS-T before blocking and incubated with monoclonal primary antibody against anti-GAPDH (1:5000, Sigma-Aldrich, in 5% BSA) and left overnight at 4°C.

4.10 | AVPO H_2S production rate

AVPO H_2S levels were determined as previously described by our laboratory.[54,55] AVPO bilateral samples were homogenized in potassium phosphate buffer (100 mM; pH 7.4) using the lab microprocessor (VirTis). Each sample (50% w v^{-1}; 100 μL) contained L-cysteine (10 mM; 20 μL), pyridoxal 5′-phosphate (2 mM; 20 μL), and PBS (30 μL). The reaction was executed in eppendorf tubes sealed with paraffin and transferred to a bath at 37°C for incubation (2 hours). Zinc acetate (1% w/v; 100 μL) was then added to trap evolved H_2S followed by tricloroacetic acid (10% w v^{-1}; 100 μL) to precipitate proteins and subsequently block the reaction. N,N-dimethyl-p-phenylenediamine sulphate (20 mM; 50 μL) in HCl 7.2 M followed by FeCl3 (30 mM; 50 μL) in HCl 1.2 M were added to 50 μL of the supernatant after centrifugation, and optical density was measured at 670 nm. The calibration curve of absorbance was achieved using NaHS solutions (#161527, Sigma-Aldrich; 0.1-100 μg mL^{-1}). The samples were assayed using a protein dye reagent (Bio-Rad Laboratories) to determine protein content.

4.11 | Statistics

The statistical methods used for each test are fully described in the Table S1. Normal distribution was analysed for all data and non-parametric tests were performed when necessary. Figures and statistics were prepared using Prism software (version 8.0; GraphPad Software Inc). The experiments and surgeries were performed by the most specialized author of each technique to decrease variabilities. A power calculation was used ($\alpha = 0.05$ and $\beta = 0.8$) to estimate group number. A pilot study (Data S1) was used to verify tolerance induction and to anticipate the values for power calculation. Plasma prostaglandins are expressed as the log of their levels. Densitometry analysis of western blots was performed using ImageJ. The western blot data were normalized using GAPDH and data represented as relative expression (enzyme of interest $GAPDH^{-1}$). All other data were expressed as mean ± SEM.

CONFLICT OF INTEREST

The authors disclose no conflicts of interests.

ORCID

Luiz G. S. Branco https://orcid.org/0000-0003-0292-4947

REFERENCES

1. Rittirsch D, Flierl MA, Ward PA. Harmful molecular mechanisms in sepsis. *Nat Rev Immunol*. 2008;8:776-787.
2. Ang S-F, Moochhala SM, Bhatia M. Hydrogen sulfide promotes transient receptor potential vanilloid 1-mediated neurogenic inflammation in polymicrobial sepsis. *Crit Care Med*. 2010;38:619-628.
3. Schroeder S, Wichers M, Lehmann LE, Putensen C, Hoeft A, Stuber F. The hypothalamic-pituitary-adrenal axis of patients with severe sepsis: altered response to corticotropin-releasing hormone. *Crit Care Med*. 2001;29:310-316.
4. Beeson PB. Development of tolerance to typhoid bacterial pyrogen and its abolition by reticulo-endothelial blockade. *Proc.Soc Exp Biol Med*. 1946;61:248-250.
5. Soares MP, Teixeira L, Moita LF. Disease tolerance and immunity in host protection against infection. *Nat Rev Immunol*. 2017;17:83-96.
6. West MA, Heagy W. Endotoxin tolerance: a review. *Crit Care Med*. 2002;30:S64-S73.
7. Arnold C. News feature: the quest to solve sepsis. *Proc Natl Acad Sci USA*. 2018;115:3988-3991.

8. Vergadi E, Vaporidi K, Tsatsanis C. Regulation of endotoxin tolerance and compensatory anti-inflammatory response syndrome by non-coding RNAs. *Front Immunol*. 2018;9:2705.
9. Biswas SK, Lopez-Collazo E. Endotoxin tolerance: new mechanisms, molecules and clinical significance. *Trends Immunol*. 2009;30:475-487.
10. Qin L, Wu X, Block ML, et al. Systemic LPS causes chronic neuroinflammation and progressive neurodegeneration. *Glia*. 2007;55:453-462.
11. Almeida MC, Trevisan FN, Barros RC, Carnio EC, Branco LG. Tolerance to lipopolysaccharide is related to the nitric oxide pathway. *NeuroReport*. 1999;10:3061-3065.
12. Raffaini MS, Dias MB, Branco L. Central heme oxygenase-carbon monoxide pathway participates in the lipopolysaccharide-induced tolerance in rats. *Brain Res*. 2006;1111:83-89.
13. Szabó C, Thiemermann C, Wu CC, Perretti M, Vane JR. Attenuation of the induction of nitric oxide synthase by endogenous glucocorticoids accounts for endotoxin tolerance in vivo. *Proc Natl Acad Sci USA*. 1994;91:271-275.
14. Kapturczak MH, Atkinson MA, Brusko TM, Wasserfall CH, Agarwal A. Regulatory T cells + CD25 + tolerance by CD4 carbon monoxide in maintaining peripheral an integral role for heme oxygenase-1 and an integral role for heme oxygenase-1 and carbon monoxide in maintaining peripheral tolerance by CD4 + CD25 + Regulatory T Cells. *J Immunol*. 2005;174:5181-5186.
15. Jeney V, Ramos S, Bergman M-L, et al. Control of disease tolerance to malaria by nitric oxide and carbon monoxide. *Cell Rep*. 2014;8:126-136.
16. Abe K, Kimura H. The possible role of hydrogen sulfide as an endogenous neuromodulator. *Off J Soc Neurosci*. 1996;16:1066-1071.
17. Ishigami M, Hiraki K, Umemura K, Ogasawara Y, Ishii K, Kimura H. A Source of hydrogen sulfide and a mechanism of its release in the brain. *Antioxid Redox Signal*. 2009;11:205-214.
18. Kimura H. Physiological role of hydrogen sulfide and polysulfide in the central nervous system. *Neurochem Int*. 2013;63:492-497.
19. Kimura H, Shibuya N, Kimura Y. Hydrogen sulfide is a signaling molecule and a cytoprotectant. *Antioxid Redox Signal*. 2012;17:45-57.
20. Szabó C. Hydrogen sulphide and its therapeutic potential. *Nat Rev Drug Discov*. 2007;6:917-935.
21. Kwiatkoski M, Soriano RN, Araujo RM, et al. Hydrogen sulfide inhibits preoptic prostaglandin E2 production during endotoxemia. *Exp Neurol*. 2013;240:88-95.
22. Lee M, Schwab C, Yu S, McGeer E, McGeer PL. Astrocytes produce the antiinflammatory and neuroprotective agent hydrogen sulfide. *Neurobiol Aging*. 2009;30:1523-1534.
23. Li Y-L, Zhou J, Zhang H, et al. Hydrogen sulfide promotes surface insertion of hippocampal AMPA receptor GluR1 subunit via phosphorylating at Serine-831/Serine-845 sites through a sulfhydration-dependent mechanism. *CNS Neurosci Ther*. 2016;22:789-798.
24. Zhang M, Shan H, Chang P, et al. Hydrogen sulfide offers neuroprotection on traumatic brain injury in parallel with reduced apoptosis and autophagy in mice. *PLoS ONE*. 2014;9:e87241.
25. Krall CM, Yao X, Hass MA, Feleder C, Steiner AA. Food deprivation alters thermoregulatory responses to lipopolysaccharide by enhancing cryogenic inflammatory signaling via prostaglandin D2. *Am J Physiol Regul Integr Comp Physiol*. 2010;298:R1512-R1521.
26. Nogueira JE, Soriano RN, Fernandez R, et al. Effect of physical exercise on the febrigenic signaling is modulated by preoptic hydrogen sulfide production. *PLoS ONE*. 2017;12:e0170468.
27. Coelho MM, Souza GE, Pelá IR. Endotoxin-induced fever is modulated by endogenous glucocorticoids in rats. *Am J Physiol*. 1992;263:R423-R427.
28. Tan BH, Wong PT-H, Bian J-S. Hydrogen sulfide: A novel signaling molecule in the central nervous system. *Neurochem Int*. 2010;56:3-10.
29. Wang Z, Liu D-X, Wang F-W, et al. L-Cysteine promotes the proliferation and differentiation of neural stem cells via the CBS/H_2S pathway. *Neuroscience*. 2013;237:106-117.
30. Carmignoto G. Reciprocal communication systems between astrocytes and neurones. *Prog Neurogibol*. 2000;62:561-581.
31. Blatteis CM. Endotoxic fever: New concepts of its regulation suggest new approaches to its management. *Pharmacol Ther*. 2006;111:194-223.
32. Feleder C, Perlik V, Blatteis CM. Preoptic alpha 1- and alpha 2-noradrenergic agonists induce, respectively, PGE_2-independent and PGE_2-dependent hyperthermic responses in guinea pigs. *Am J Physiol Regul Integr Comp Physiol*. 2004;286:R1156-R1166.
33. Ordovas-Montanes J, Rakoff-Nahoum S, Huang S, Riol-Blanco L, Barreiro O, von Andrian UH. The regulation of immunological processes by peripheral neurons in homeostasis and disease. *Trends Immunol*. 2015;36:578-604.
34. Kenney MJ, Ganta CK. Autonomic nervous system and immune system interactions. *Compr Physiol*. 2014;4:1177-1200.
35. Tracey KJ. The inflammatory reflex. *Nature*. 2002;420:853-859.
36. Martelli D, Yao ST, McKinley MJ, McAllen RM. Reflex control of inflammation by sympathetic nerves, not the vagus. *J. Physiol*. 2014;592:1677-1686.
37. Quaas L, Zahradnik HP. The effects of alpha- and beta-adrenergic stimulation on contractility and prostaglandin (prostaglandins E2 and F2 alpha and 6-keto-prostaglandin F1 alpha) production of pregnant human myometrial strips. *Am J Obstet Gynecol*. 1985;152:852-856.
38. Vikse A, Holdaas H, Sejersted OM, Kill F. Haemodynamic conditions for renal PGE_2 and renin release during α- and β-adrenergic stimulation in dogs. *Acta Physiol Scand*. 1985;124:163-172.
39. Nagaraja AS, Dorniak PL, Sadaoui NC, et al. Sustained adrenergic signaling leads to increased metastasis in ovarian cancer via increased PGE_2 synthesis. *Oncogene*. 2016;35:2390-2397.
40. Dello Russo C, Tringali G, Ragazzoni E, et al. Evidence that hydrogen sulphide can modulate hypothalamo-pituitary-adrenal axis function: in vitro and in vivo studies in the rat. *J Neuroendocrinol*. 2000;12:225-233.
41. Dawe GS, Han SP, Bian JS, Moore PK. Hydrogen sulphide in the hypothalamus causes an ATP-sensitive K+ channel-dependent decrease in blood pressure in freely moving rats. *Neuroscience*. 2008;152:169-177.
42. Löscher W. Effect of Inhibitors of GABA Aminotransferase on the Metabolism of GABA in brain tissue and synaptosomal fractions. *J Neurochem*. 1981;36:1521-1527.
43. Roland BL, Sawchenko PE. Local origins of some GABAergic projections to the paraventricular and supraoptic nuclei of the hypothalamus in the rat. *J Comp Neurol*. 1993;332:123-143.
44. Karimi SA, Hosseinmardi N, Janahmadi M, Sayyah M, Hajisoltani R. The protective effect of hydrogen sulfide (H 2 S) on traumatic

brain injury (TBI) induced memory deficits in rats. *Brain Res Bull*. 2017;134:177-182.
45. Florian B, Vintilescu R, Balseanu AT, et al. Long-term hypothermia reduces infarct volume in aged rats after focal ischemia. *Neurosci Lett*. 2008;438:180-185.
46. López-Collazo E, del Fresno C. Pathophysiology of endotoxin tolerance: mechanisms and clinical consequences. *Crit Care*. 2013;17:242.
47. Beurel E, Jope RS. Glycogen synthase kinase-3 regulates inflammatory tolerance in astrocytes. *Neuroscience*. 2010;169:1063-1070.
48. Norden DM, Trojanowski PJ, Villanueva E, Navarro E, Godbout JP. Sequential activation of microglia and astrocyte cytokine expression precedes increased Iba-1 or GFAP immunoreactivity following systemic immune challenge. *Glia*. 2016;64:300-316.
49. Chu C-H, Wang S, Li C-L, et al. Neurons and astroglia govern microglial endotoxin tolerance through macrophage colony-stimulating factor receptor-mediated ERK1/2 signals. *Brain Behav Immun*. 2016;55:260-272.
50. Romanovsky AA. Skin temperature: its role in thermoregulation. *Acta Physiol*. 2014;210:498-507.
51. Blatteis CM, Sehic E. Cytokines and fever. *Ann N Y Acad Sci*. 1998;840:608-618.
52. Romanovsky AA, Ivanov AI, Shimansky YP. Selected Contribution: Ambient temperature for experiments in rats: a new method for determining the zone of thermal neutrality. *J Appl Physiol*. 2002;92:2667-2679.
53. Haack D, Vecsei P, Lichtwald K, Vielhauer W. Corticosteroid and corticosteroid metabolite levels in animals immunized against corticosteroids. *J Steroid Biochem*. 1979;11:971–980.
54. Kwiatkoski M, Soriano RN, da Silva G, et al. Endogenous preoptic hydrogen sulphide attenuates hypoxia-induced hyperventilation. *Acta Physiol (Oxf)*. 2014;210:913-927.
55. da Silva G, Soriano RN, Kwiatkoski M, Giusti H, Glass ML, Branco LG. Central hydrogen sulphide mediates ventilatory responses to hypercapnia in adult conscious rats. *Acta Physiol*. 2014;212:239-247.

SUPPORTING INFORMATION

Additional supporting information may be found online in the Supporting Information section at the end of the article.

How to cite this article: Santos BM, Francescato HDC, Turcato FC, Antunes-Rodrigues J, Coimbra TM, Branco LGS. Increased hypothalamic hydrogen sulphide contributes to endotoxin tolerance by down-modulating PGE_2 production. *Acta Physiol*. 2019;e13373. https://doi.org/10.1111/apha.13373

Artigo publicado na Journal of Thermal Biology

Journal of Thermal Biology 84 (2019) 245–249

Contents lists available at ScienceDirect

Journal of Thermal Biology

journal homepage: www.elsevier.com/locate/jtherbio

Central leukotrienes modulate fever tolerance to LPS in rats

Bruna M. Santos[a,**], Luis H.A. Costa[b], Maria J. Rocha[b,c], Luiz G.S. Branco[a,c,*]

[a] Department of Physiology, Medical School of Ribeirão Preto, University of São Paulo, Ribeirão Preto, SP, Brazil
[b] Department of Neurosciences and Behavioral Sciences, Medical School of Ribeirão Preto, University of São Paulo, Ribeirão Preto, SP, Brazil
[c] Department of Basic and Oral Biology, Dental School of Ribeirão Preto, University of São Paulo, Ribeirão Preto, SP, Brazil

ARTICLE INFO

Keywords:
MK-886
Fever
Prostaglandins
Hypothalamus

ABSTRACT

Leukotrienes mediate several inflammatory events such as neutrophil chemoattraction, leukocyte adhesion, and central-release of cytokines and fever. However, there is no information available about their putative role in lipopolysaccharide (LPS) tolerance. The rational of the present study was to find out if central leukotrienes are involved in the development of LPS tolerance. Thus, we inhibited central leukotriene synthesis in tolerant rats using a pharmacological tool, *i.e.*, a selective inhibitor of leukotriene synthesis MK-886 injected into the third ventricle (3V) of rats. Body core temperature (Tb) was measured using a datalogger placed inside the abdominal cavity. A low-dose of LPS (100 μg/kg ip) was given for 4 consecutive days to induce LPS tolerance. At day 4, rats received a microinjection of MK-886 into the 3V immediately before LPS, whereas control groups were treated with vehicle (saline). We observed that LPS failed to induce plasma cytokines surges, increased hypothalamic PGE_2 levels and fever 3 days post LPS treatment, aptly characterizing the tolerance. When MK-886 was given to control rats treated with saline, no significant change in Tb was observed. However, a full LPS-induced fever was observed in tolerant rats pretreated with MK-886, which was associated with an enhancement in the hypothalamic PGE_2 levels, that were not accompanied by plasma cytokines (IL-1β, and IL-6) and PGE_2 surges. These data are consistent with the notion that central leukotrienes play a role in fever tolerance to LPS.

1. Introduction

Sepsis is a life-threatening organ dysfunction induced by an inappropriate host response against pathogens. In the early phase of sepsis, a hyper-inflammatory response to infection is observed, followed by tissue damage and organ failure. At the late phase of sepsis, there is a reprogramming in the immune response causing immunoparalysis and increasing the vulnerability of the patient to other infections (Boomer et al., 2011). Despite recent progress in the knowledge of sepsis, septic patients still have high mortality rates due to the uncontrolled inflammation at the early stage or by long-term lethal secondary infections caused by the immunosuppressive state (Hotchkiss et al., 2013; Stevenson et al., 2014).

One of the ongoing methods used to study the pathophysiology of immunoparalysis to find effective therapies to restore host defense in the septic patient is lipopolysaccharide (LPS; bacterial outer membrane component) tolerance (Andrade et al., 2019; Jędrzejewski et al., 2019). LPS tolerance can be experimentally induced by repeated injections of LPS, which virtually abrogate fever (BEESON, 1946) and other pattern signals of sickness syndrome including achiness, loss of appetite, and sleepiness.

Sickness syndrome is mediated by a classical set of brain immune responses during illnesses in which prostaglandins are the main brain mediators (Saper et al., 2012). There is no doubt that the inhibition of COX, an enzyme that converts arachidonic acid (AA) into prostaglandin H_2, alleviates the symptoms of sickness. Specifically, PGE_2 produced in the preoptic area (POA) of anterior hypothalamus has been thought to play a role as the proximal, putative mediator of fever (Schiltz and Sawchenko, 2003).

There is substantial evidence that other eicosanoids, such as leukotrienes, have their synthesis significantly increased in the hypothalamus during endotoxemia (Azab and Kaplanski, 2004; Goulet et al., 1994; Kozak and Fraifeld, 2004a; Lopes et al., 2017; Paul et al., 1999). 5-lipoxygenase (5-LO) is a key enzyme in the biosynthesis of this mediator, acting directly on AA and other intermediates, that results in the synthesis of leukotrienes B4 (LTB4) and Cys-LTs (LTC4, LTD4, and LTE4) (Funk, 2001). Unlike prostaglandins, leukotrienes seem to play a cryogenic role in LPS-induced fever (Kozak and Fraifeld, 2004b; Paul et al., 1999). However, their central role in temperature control during LPS tolerance has not been investigated.

* Corresponding author. Department of Basic and Oral Biology, Dental School of Ribeirão Preto, University of São Paulo, 14040-904, Ribeirão Preto, SP, Brazil.
** Corresponding author.
E-mail addresses: brunamaitan@usp.br (B.M. Santos), branco@forp.usp.br (L.G.S. Branco).

https://doi.org/10.1016/j.jtherbio.2019.07.015
Received 24 May 2019; Received in revised form 4 July 2019; Accepted 7 July 2019
Available online 08 July 2019

In the present study, we investigate the central role of hypothalamic leukotrienes, specifically in LPS tolerance by analyzing body core temperature (Tb) and the hypothalamic PGE_2 levels in rats. We also investigate the role of hypothalamic leukotrienes in peripheral pyrogens production, *i.e.*, plasma PGE_2, IL-1β, and IL-6 of tolerant rats.

2. Methods

2.1. Animals

Adult male Wistar rats (290–300 g) were individually caged and maintained at a controlled temperature of 29 °C on a 12-h light/dark cycle (lights on at 6 a.m.). Regular food and water were provided ad libitum. All experiments were approved by the Animal Care and Use Committee of the University of São Paulo/Brazil at the Ribeirão Preto campus (Protocol number 2016.1.393.58.1). The present study was performed in accordance with the Guide for the Care and Use of Laboratory Animals of the National Council for the Control of Animal Experimentation (CONCEA).

2.2. Drugs

LPS tolerance was induced using a low dose of LPS (Sigma, MO, USA; serotype 0111: B4; dose: 100 μg/kg ip) administration. The dose of LPS administered was sufficient to activate febrigenic signaling in a slightly high temperature inside the thermoneutral zone (29 °C) (23). LPS was diluted in pyrogen-free saline. The dose was based on body mass measured immediately before LPS administration of each rat, since LPS induces important body weight changes. MK-886 (3-[1-(p-chlorobenzyl)-5- (isopropyl)-3-tert-butylthioindol-2-yl]-2, 2-dimethylpropanoic acid; Sigma, MO, USA) was used as an inhibitor of leukotrienes biosynthesis. This drug selectively inhibits FLAP (5-lipoxygenase-activating protein), a protein required for leukotrienes formation. It was dissolved in pyrogen-free saline at a final concentration of 4 μg/kg and administered into the third ventricle (3V) (dos Santos et al., 2012; Martins et al., 2011).

2.3. Surgeries

Five days before the experiment, an intracerebroventricular (3V) cannula (for MK-886/vehicle administration) was implanted, and an intra-abdominal temperature datalogger (for T_b recording; SubCue, Alberta, Canada) was inserted in the peritoneum of all animals. All surgery procedures were performed under anesthesia with a mixture of 10% ketamine and 2% xylazine (1:1; 1 ml/kg of body weight) ip and anti-inflammatory flunixin meglumine (0.1 ml subcutaneously) and antibiotic pentabiotic (1.200.000 IU; 0.1 ml intramuscular) were injected subcutaneously and intramuscularly, respectively. In a surgical aseptic field, the intraperitoneal cavity was exposed for the datalogger insertion and closed at the end of this surgery. After that, the animals were fixed to a stereotaxic apparatus with the incisor bar set at −3.3 mm. The following coordinates were assigned with a reference from bregma (Paxinos and Watson, 2007): anterior-posterior: −0.4 mm; lateral: 0 mm and dorsoventral: −4.5 mm. The intracerebroventricular cannula (22-gauge; 16-mm of length) was fixed to the skull with a stainless-steel screw and dental cement.

2.4. LPS tolerance induction

The LPS tolerance protocol started by food intake and body weight measurement (7–8 am) followed by injection of LPS ip or its vehicle (saline). This procedure was conducted daily until day 3 to verify LPS tolerance by fever and anorexia attenuation (Figs. 1 and 2, respectively). At day 4, the animals received MK-886 or its vehicle (saline) icv 60 min before LPS/saline ip injection and after 5 h the animals were decapitated and brain and plasma samples were quickly collected for posterior analysis.

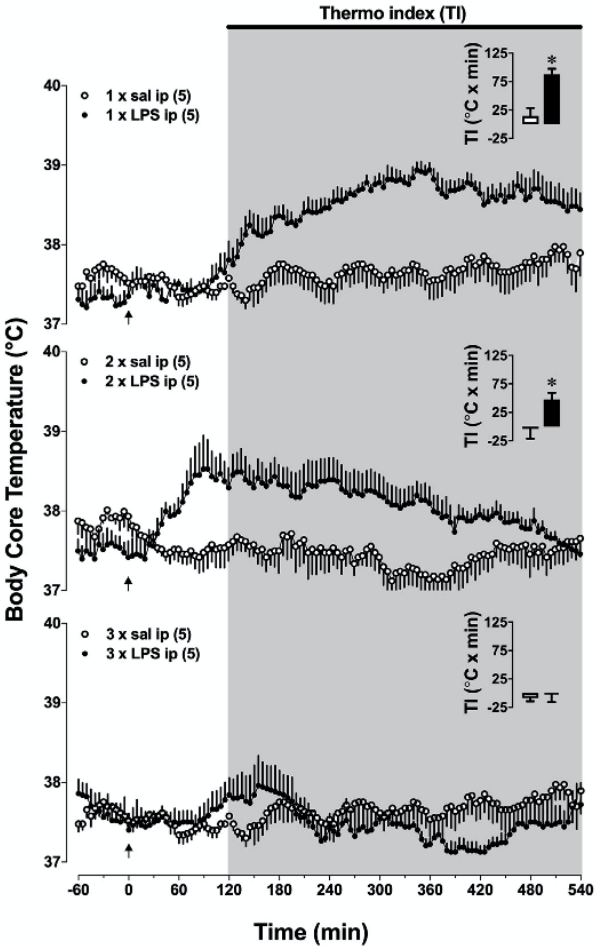

Fig. 1. Development of LPS tolerance by daily deep body temperature (Tb) measurement. Time courses of Tb of saline (sal) and LPS groups on day 1 (Fig. 1 upper graph), 2 (Fig. 1 middle graph), and 3 (Fig. 1 bottom graph). Arrow indicate the time of injection of saline or LPS intraperitoneally daily. The gray area indicates the febrile period analyzed by thermal indexes. Thermal indexes of the febrile periods between saline and LPS-treated groups are represented on the upper right corner of the time-course graph in each day. Values are means ± SEM. n = 6–8. *P < 0.05, LPS group vs. SAL group.

2.5. PGE_2 and cytokines measurements

Plasma collection was performed using EDTA as an anticoagulant, and indomethacin (at a final concentration of 10 μM) to prevent ex-vivo eicosanoids production. Samples were centrifuged (at 2,000 g/10 min/4°C), and stored for posterior analysis at - 80°C. To understand if central inhibition of leukotriene synthesis could alter the immune non-responsiveness state of LPS tolerant animals, we measured the plasma IL-1β and IL-6 levels. Additionally, we hypothesized that LPS tolerance is accompanied by changes in hypothalamic PGE_2 levels. Hypothalamus was dissected, homogenized in lysis buffer (RIPA) with a protease inhibitor cocktail, centrifuged (2,000 g/20 min/4°C) and the supernatant was separated for PGE_2 measurement. It was used the enzyme-linked immunosorbent assay technique (ELISA) following manufacturer's instructions for PGE_2, IL-1β, and IL-6 measurements.

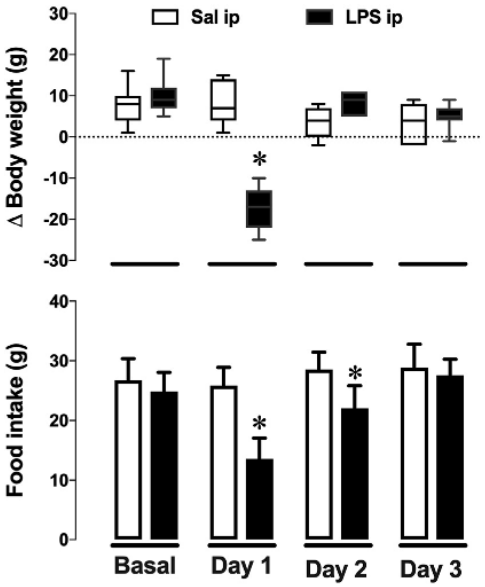

Fig. 2. Development of LPS tolerance by body weight deviation (Δ) and food intake measurements. Body weight deviation (A) and food intake (B) of saline (sal) and LPS groups on day 1, 2, and 3. Values are means ± SEM. n = 6–8. *P < 0.05, LPS group vs. SAL group.

2.6. Statistical analyzes

Thermal index (TI) from the area under the curve (AUC) of values of Tb during the febrile period (120–300 min post-LPS injection) was analyzed by one-way ANOVA test followed by the post hoc Student-Newman Keuls. Baseline was fixed in 37.2 °C. One-way ANOVA test was used to analyze hypothalamic and plasma PGE_2 levels followed by the post hoc Student-Newman Keuls. Data were expressed by means ± SEM. P < 0.05 was considered statistically significant.

3. Results

3.1. LPS-induced tolerance in rats

As shown in Fig. 1, LPS tolerance was induced by three daily consecutive injections of low doses of LPS (100 μg/kg ip) in rats. The effectiveness of the LPS tolerance was evaluated by the undetectable plasma cytokines (IL-6 and IL-1β) levels and the attenuation of two pattern symptoms of the sickness syndrome [5]: (1) fever, determined by the thermal indexes comparing Tb of LPS and saline-treated animals in the febrile phase (area under curve; indicated by the top right corner graphs in Fig. 1); and (2) anorexia, determined by the evaluation of daily body weight deviation and food intake of the groups (Fig. 2).

On the first day of LPS-injection, fever was observed (Fig. 1) as well as a decrease in body weight and food intake (Fig. 2) of LPS-treated rats compared to their control (P < 0.05). On the second day of LPS injection, an altered course-time of Tb was observed (Fig. 1, *middle graph*) along with an increase in body weight (Fig. 2) in LPS-treated animals, indicating the development of LPS tolerance. On the third day of LPS-injection, LPS tolerance was completed since we observed the absence of differences in Tb (Fig. 1, *bottom graph*), body weight deviation, and food intake (Fig. 2) between LPS-treated animals and their control (P > 0.05).

3.2. Effect of central leukotrienes inhibition on fever tolerance to LPS in rats

Pretreatment with MK-886 at a dose of 4 μg/kg icv restored the febrile response in LPS tolerant animals (Fig. 3), evidenced by the enhancement of Tb compared with LPS-tolerant animals treated with saline icv (P < 0.05). These data support the idea that the leukotrienes play a role in LPS tolerance in rats.

3.3. Central leukotrienes inhibition and hypothalamic PGE_2 production in LPS tolerant rats

To investigate the central role of leukotrienes in fever abrogation in LPS tolerant rats, we measured the hypothalamic PGE_2 levels, the proximal mediator of fever [6]. As shown in Fig. 4, LPS tolerant animals had a similar hypothalamic PGE_2 production compared to saline treated rats that was reverted by the inhibition of central leukotrienes in LPS tolerant animals (P < 0.05).

3.4. Central leukotrienes inhibition and plasma PGE_2, IL-6, and IL-1β production in LPS tolerant rats

To investigate whether central leukotrienes act only in the central development of LPS tolerance, we examined plasma production of PGE_2, IL-6, and IL-1β. We did not observe any differences in plasma PGE_2 levels between groups (Fig. 4). All the groups had undetectable plasma cytokine levels (data not shown). These data indicate that leukotrienes act only in central areas reverting fever tolerance without altering peripheral febrigenic signaling.

4. Discussion

In the present study, we investigated the potential role of central leukotrienes in fever tolerance to LPS. To address the cryogenic potential of leukotrienes in LPS tolerance, we had to validate the LPS tolerance protocol. The efficacy of the protocol was proved by the

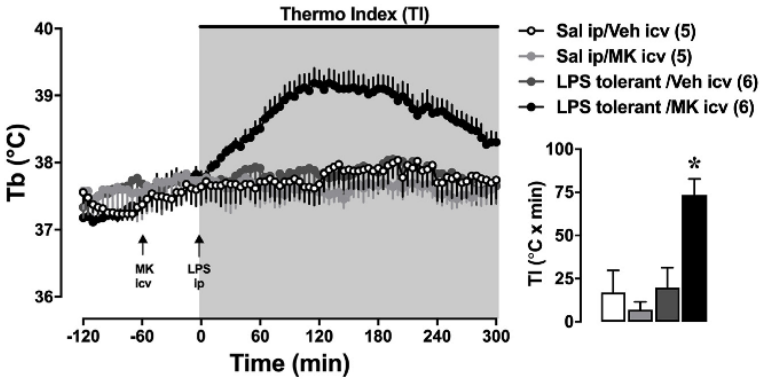

Fig. 3. Role of central leukotrienes in LPS tolerance. Time course of Tb of animals treated for 4 days with saline (sal group) or LPS (LPS tolerant group) and pre-treated with MK-886 (leukotrienes synthesis inhibitor) or its vehicle (veh) at the fourth day of saline or LPS injections. Arrow indicate the time of injection of MK-886 intracerebroventricularlly, and saline or LPS intraperitoneally. Gray areas indicate the febrile period analyzed by thermal indexes. Thermal index of the febrile periods is represented on the side of its time-course graph. Values are means ± SEM. n = 6–8. *P < 0.05, LPS group vs. SAL group.

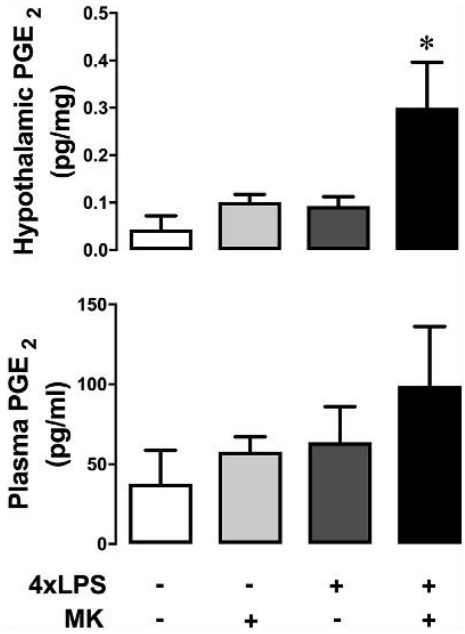

Fig. 4. Role of central leukotrienes in hypothalamic and plasma PGE_2 production in fever tolerance to LPS. Hypothalamic and plasma levels of PGE_2 at 300 min after LPS or saline administration in saline of LPS tolerant rats pretreated with MK-886 (leukotrienes synthesis inhibitor) or its vehicle (veh) at the last day of injections (day 4). Values are means ± SEM. n = 6. *P < 0.05, LPS group vs. SAL group.

absence of two indicators of sickness syndrome: fever and anorexia. The LPS tolerance protocol was performed by daily injection of a low dose of LPS (100 μg/kg ip) in rats for 3 days. The dose selected was the same utilized by another study (Kwiatkoski et al., 2013) that evokes the rise in body core temperature at the first immune challenge. As expected, first LPS-injection induced not only an increase in Tb but also a decrease in daily body weight deviation and food intake. After the third injection, we detected an abrogation of the signals analyzed, legitimizing the protocol used.

Fever is a classical signal of immune challenge. The activation of peripheral immune cells by the infectious agent increases the production of a number of inflammatory mediators. The first induced mediator by the immune challenge is TNF-α, followed by other cytokines such as IL-1β and IL-6 (Kluger et al., 1995), eicosanoids such as prostaglandins and leukotrienes (Blatteis, 2006; Ivanov and Romanovsky, 2004; Kozak and Fraifeld, 2004b), and gasotransmitters such as nitric oxide and hydrogen sulfide (Branco et al., 2014). These mediators act direct or indirectly and culminate in an increase of hypothalamic PGE_2, inducing fever. In humans, some studies have described that febrile patients had a better outcome compared to patients who did not display fever (Ahkee et al., 1997; Bryant et al., 1971). In a model of septic shock in rats, the control of Tb was correlated with a poor outcome (Su et al., 2005). Here, central inhibition of leukotrienes reverted fever tolerance by increasing PGE_2. In the literature, an increased synthesis of PGE_2 was observed in 5-LO–deficient mice after arachidonic acid inflammation in ear tissue (Goulet et al., 1994), and the pharmacological inhibition of 5-LO enhanced the production of PGE_2 in mice after LPS injection (Azab and Kaplanski, 2004; Fraifeld et al., 2000; Paul et al., 1999). The mechanisms involved in this response still need to be investigated. We speculate a possible shift induced by the higher production of leukotrienes, decreasing the availability of arachidonic acid to produce PGE_2 in the hypothalamus of tolerant animals. However, we still do not know the responsible for the shift in the production of these hypothalamic eicosanoids in LPS tolerance.

It is also important to mention that the production of hypothalamic PGE_2 in LPS tolerant rats may differ among conditions such as the dose of LPS, the rat strain, the time-course after LPS injection and the ambient temperature. Chemo et al. (1997) observed that a second exposure (48 h after the first injection) to a relatively high dose of LPS (250 μg/kg ip) caused a decrease in hypothermia and fever induced by LPS in Sprague-Dawley rats in a low ambient temperature. This response was reported to be followed by a decrease in hypothalamic PGE_2 levels 2 h after LPS re-exposure and an increase 24 h later compared to animals that received a single LPS injection. In essence, their results seem to contrast with the present study, since we observed that a fourth exposure to a low dose of LPS (100 μg/kg ip) leads to no significant changes in Tb of Wistar rats. These data are associated with decreased hypothalamic PGE_2 levels, 2 h after the fourth LPS exposure. Reconciling these data, it seems reasonable to state that LPS tolerance is a complex immune response, associated with intricate changes in hypothalamic PGE_2 production that depends upon the factors aforementioned.

Fever tolerance takes place by decreasing the production of the endogenous pyrogens. Interestingly, central leukotrienes seem to downregulate central PGE_2 (Fig. 4), without affecting peripheral pyrogens in LPS tolerance. This response might be related to the differences between peripheral and central immune activation in tolerance. For example, splenic cytokines expression is different from that observed in the central nervous system in LPS-immune challenge re-exposure (del Rey et al., 2009). Additionally, it was observed that microglial cells are dependent upon neurons and astroglia to induce tolerance (Chu et al., 2016), indicating the exceptionality of the CNS. Faggioni et al. (1995) observed that the LPS pretreatment (3 daily LPS injections given ip) does not blunt brain TNF-α production when LPS was administered centrally. These data indicate that peripheral LPS tolerance does not cause central LPS tolerance, if we consider TNF-α only as a marker of LPS tolerance. However, these results do not imply that peripheral LPS tolerance occurs independently of the CNS. Moreover, previous studies have already documented that the CNS plays a key role in peripheral LPS tolerance (Almeida et al., 1999; Navarro et al., 2007; Raffaini et al., 2006) which are in agreement with the present study. Here, we suggest that central leukotrienes are one of the central mechanisms participating in fever tolerance to LPS.

5. Conclusion

Our results indicate that central leukotrienes play a key role in fever tolerance by decreasing hypothalamic PGE_2 production without altering peripheral pyrogens.

Conflicts of interest

We have no conflict of interest to declare.

Financial support

This work was supported by Grants #16/17681-9, #16/09364-3, São Paulo Research Foundation (FAPESP), and Grants #404927/2018-1, #301040/2018-4, The Brazilian National Council for Scientific and Technological Development (CNPq).

Acknowledgments

The authors wish to acknowledge Mauro F. Silva and Nadir Fernandes' technical support. We also thank Grant Harris, Phoenix, AZ, for the English revision.

Appendix A. Supplementary data

Supplementary data to this article can be found online at https://doi.org/10.1016/j.jtherbio.2019.07.015.

References

Ahkee, S., Srinath, L., Ramirez, J., 1997. Community-acquired pneumonia in the elderly: Association of mortality with lack of fever and leukocytosis. South. Med. J. 90, 296–298.

Almeida, M.C., Trevisan, F.N., Barros, R.C., Carnio, E.C., Branco, L.G., 1999. Tolerance to lipopolysaccharide is related to the nitric oxide pathway. Neuroreport 10, 3061–3065.

Andrade, M.M.C., Ariga, S.S.K., Barbeiro, D.F., Barbeiro, H.V., Pimentel, R.N., Petroni, R.C., Soriano, F.G., 2019. Endotoxin tolerance modulates TREG and TH17 lymphocytes protecting septic mice. Oncotarget 10, 3451–3461. https://doi.org/10.18632/oncotarget.26919.

Azab, A.N., Kaplanski, J., 2004. Involvement of eicosanoids in the hypothermic response to lipopolysaccharide during endotoxemia in rats. Prostaglandins Leukot. Essent. Fatty Acids 70, 67–75.

BEESON, P.B., 1946. Development of tolerance to typhoid bacterial pyrogen and its abolition by reticulo-endothelial blockade. Proc. Soc. Exp. Biol. Med. 61, 248–250.

Blatteis, C.M., 2006. Endotoxic fever: New concepts of its regulation suggest new approaches to its management. Pharmacol. Ther. 111, 194–223. https://doi.org/10.1016/J.PHARMTHERA.2005.10.013.

Boomer, J.S., To, K., Chang, K.C., Takasu, O., Osborne, D.F., Walton, A.H., Bricker, T.L., Jarman, S.D., Kreisel, D., Krupnick, A.S., Srivastava, A., Swanson, P.E., Green, J.M., Hotchkiss, R.S., 2011. Immunosuppression in patients who die of sepsis and multiple organ failure. J. Am. Med. Assoc. 306, 2594. https://doi.org/10.1001/jama.2011.1829.

Branco, L.G.S., Soriano, R.N., Steiner, A.A., 2014. Gaseous mediators in temperature regulation. Comp. Physiol. 4, 1301–1338. https://doi.org/10.1002/cphy.c130053.

Bryant, R.E., Hood, A.F., Hood, C.E., Koenig, M.G., 1971. Factors affecting mortality of gram-negative rod bacteremia. Arch. Intern. Med. 127, 120–128.

Chemo, A., Fraifeld, V., Adramovich, L., Sod-Moriah, U.A., Kaplanski, J., 1997. Tolerance to lipopolysaccharide is not related to the ability of the hypothalamus to produce prostaglandin E2. Life Sci. 61, 813–818.

Chu, C.-H., Wang, S., Li, C.-L., Chen, S.-H.S.-L., Hu, C.-F., Chung, Y.-L., Chen, S.-H.S.-L., Wang, Q., Lu, R.-B., Gao, H.-M., Hong, J.-S., 2016. Neurons and astroglia govern microglial endotoxin tolerance through macrophage colony-stimulating factor receptor-mediated ERK1/2 signals. Brain Behav. Immun. 55, 260–272. https://doi.org/10.1016/j.bbi.2016.04.015.

del Rey, A., Randolf, A., Wildmann, J., Besedovsky, H.O., Jessop, D.S., 2009. Re-exposure to endotoxin induces differential cytokine gene expression in the rat hypothalamus and spleen. Brain Behav. Immun. 23, 776–783. https://doi.org/10.1016/j.bbi.2009.02.009.

dos Santos, J.F., de Oliveira-Pelegrin, G.R., Athayde, L.A., da Rocha, M.J.A., 2012. An inhibitor of leukotriene synthesis affects vasopressin secretion following osmotic stimulus in rats. Regul. Pept. 179, 6–9. https://doi.org/10.1016/j.regpep.2012.08.012.

Faggioni, R., Fantuzzi, G., Villa, P., Buurman, W., van Tits, L.J., Ghezzi, P., 1995. Independent down-regulation of central and peripheral tumor necrosis factor production as a result of lipopolysaccharide tolerance in mice. Infect. Immun. 63, 1473–1477.

Fraifeld, V., Paul, L., Kaplanski, J., 2000. The relationship between hypothalamic prostaglandin E2 or leukotrienes and the body temperature response to lipopolysaccharide in different murine strains. J. Therm. Biol. 25, 17–20. https://doi.org/10.1016/S0306-4565(99)00047-9.

Funk, C.D., 2001. Prostaglandins and leukotrienes: Advances in eicosanoid biology. Science 294, 1871–1875. https://doi.org/10.1126/science.294.5548.1871.

Goulet, J.L., Snouwaert, J.N., Latour, A.M., Coffman, T.M., Koller, B.H., 1994. Altered inflammatory responses in leukotriene-deficient mice. Proc. Natl. Acad. Sci. U.S.A. 91, 12852–12856.

Hotchkiss, R.S., Monneret, G., Payen, D., 2013. Sepsis-induced immunosuppression: From cellular dysfunctions to immunotherapy. Nat. Rev. Immunol. 13, 862–874. https://doi.org/10.1038/nri3552.

Ivanov, A.I., Romanovsky, A.A., 2004. Prostaglandin E2 as a mediator of fever: Synthesis and catabolism. Front. Biosci. 9, 1977–1993.

Jędrzejewski, T., Piotrowski, J., Pawlikowska, M., Wrotek, S., Kozak, W., 2019. Extract from Coriolus versicolor fungus partially prevents endotoxin tolerance development by maintaining febrile response and increasing IL-6 generation. J. Therm. Biol. 83, 69–79. https://doi.org/10.1016/J.JTHERBIO.2019.05.005.

Kluger, M.J., Kozak, W., Leon, L.R., Soszynski, D., Conn, C.A., 1995. Cytokines and fever. Neuroimmunomodulation 2, 216–223. https://doi.org/10.1159/000097199.

Kozak, W., Fraifeld, V., 2004a. Non-prostaglandin eicosanoids in fever and anapyrexia. Front. Biosci. 9, 3339–3355.

Kozak, W., Fraifeld, V., 2004b. Non-prostaglandin eicosanoids in fever and anapyrexia. Front. Biosci. 9, 3339–3355.

Kwiatkoski, M., Soriano, R.N., Araujo, R.M., Azevedo, L.U., Batalhao, M.E., Francescato, H.D.C., Coimbra, T.M., Carnio, E.C., Branco, L.G.S., 2013. Hydrogen sulfide inhibits preoptic prostaglandin E2 production during endotoxemia. Exp. Neurol. 240, 88–95. https://doi.org/10.1016/j.expneurol.2012.11.008.

Lopes, D.E.M., Jabr, C.L., Dejani, N.N., Saraiva, A.C., de Aquino, S.G., Medeiros, A.I., Junior, C.R., 2017. Inhibition of 5-lipoxygenase (5-Lo) attenuates inflammation and bone resorption in lipopolysaccharide (Lps)-Induced periodontal disease. J. Periodontol. 1–18. https://doi.org/10.1902/jop.2017.170210.

Martins, T.F., Sorgi, C.A., Faccioli, L.H., Rocha, M.J.A., 2011. Leukotriene synthesis inhibitor decreases vasopressin release in the early phase of sepsis. J. Neuroimmunol. 238, 52–57. https://doi.org/10.1016/j.jneuroim.2011.08.001.

Navarro, V.P., Rocha, M.J.A., Branco, L.G.S., 2007. Reduced central c-fos expression and febrile response to repeated LPS injection into periodontal tissue of rats. Brain Res. 1152, 57–63. https://doi.org/10.1016/J.BRAINRES.2007.03.045.

Paul, L., Fraifeld, V., Kaplanski, J., 1999. Evidence supporting involvement of leukotrienes in LPS-induced hypothermia in mice. Am. J. Physiol. Integr. Comp. Physiol. 276, R52–R58. https://doi.org/10.1152/ajpregu.1999.276.1.R52.

Paxinos, G., Watson, C., 2007. The Rat Brain in Stereotaxic Coordinates. Elsevier.

Raffaini, M.S., Dias, M.B., Branco, L.G.S.S., 2006. Central heme oxygenase-carbon monoxide pathway participates in the lipopolysaccharide-induced tolerance in rats. Brain Res. 1111, 83–89. https://doi.org/10.1016/j.brainres.2006.06.102.

Saper, C.B., Romanovsky, A.A., Scammell, T.E., 2012. Neural circuitry engaged by prostaglandins during the sickness syndrome. Nat. Neurosci. 15, 1088–1095. https://doi.org/10.1038/nn.3159.

Schiltz, J.C., Sawchenko, P.E., 2003. Signaling the brain in systemic inflammation: The role of perivascular cells. Front. Biosci. 8, s1321–s1329.

Stevenson, E.K., Rubenstein, A.R., Radin, G.T., Wiener, R.S., Walkey, A.J., 2014. Two decades of mortality trends among patients with severe sepsis. Crit. Care Med. 42, 625–631. https://doi.org/10.1097/CCM.0000000000000026.

Su, F., Nguyen, N.D., Wang, Z., Cai, Y., Rogiers, P., Vincent, J.-L., 2005. Fever control in septic shock: Beneficial or harmful? Shock 23, 516–520.

Artigo publicado na American Journal of Comparative, Integrative Physiology

Am J Physiol Regul Integr Comp Physiol 317: R223–R231, 2019.
First published May 15, 2019; doi:10.1152/ajpregu.00390.2018.

RESEARCH ARTICLE | *Cardiovascular and Renal Integration*

Sex differences and the role of ovarian hormones in site-specific nociception of SHR

Bruna M. Santos,[1]* Glauce C. Nascimento,[2]* Camila P. Capel,[2] Gabriela S. Borges,[1] Thales Rosolen,[2] João P. J. Sabino,[3] Christie R. A. Leite-Panissi,[4] and Luiz G. S. Branco[2]

[1]*Department of Physiology, Medical School of Ribeirão Preto, University of São Paulo, Ribeirão Preto, São Paulo, Brazil;* [2]*Department of Morphology, Physiology and Basic Pathology, Ribeirão Preto Dentistry Faculty, University of São Paulo, Ribeirão Preto, São Paulo, Brazil;* [3]*Department of Biophysics and Physiology, Federal University of Piauí, Teresina, Piauí, Brazil; and* [4]*Psychobiology Graduate Program, School of Philosophy, Science and Literature of Ribeirão Preto, University of São Paulo, Ribeirão Preto, São Paulo, Brazil*

Submitted 17 December 2018; accepted in final form 6 May 2019

Santos BM, Nascimento GC, Capel CP, Borges GS, Rosolen T, Sabino JP, Leite-Panissi CR, Branco LG. Sex differences and the role of ovarian hormones in site-specific nociception of SHR. *Am J Physiol Regul Integr Comp Physiol* 317: R223–R231, 2019. First published May 15, 2019; doi:10.1152/ajpregu.00390.2018.—Accurate diagnosis and treatment of pain is dependent on knowledge of the variables that might alter this response. Some of these variables are the locality of the noxious stimulus, the sex of the individual, and the presence of chronic diseases. Among these chronic diseases, hypertension is considered a serious and silent disease that has been associated with hypoalgesia. The main goal of this study was to evaluate the potential nociceptive differences in spontaneously hypertensive rats (SHR) regarding the locality of the stimulus, i.e., the temporomandibular joint or paw, the sex, and the role of ovarian hormones in a model of mechanical nociception (Von Frey test) or formalin-induced inflammatory nociception. Our results indicate that SHR had lower orofacial mechanical nociception beyond the lower mechanical nociception in the paw compared with WKY rats. In a model of formalin-induced inflammatory nociception, SHR also had decreased nociception compared with normotensive rats. We also sought to evaluate the influence of sex and ovarian hormones on orofacial mechanical nociception in SHR. We observed that female SHR had higher mechanical nociception than male SHR only in the paw, but it had higher formalin-induced orofacial nociception than male SHR. Moreover, the absence of ovarian hormones caused an increase in mean arterial pressure and a decrease in paw nociception in female SHR.

formalin; hypertension; hypoalgesia; orofacial pain

INTRODUCTION

Hypertension is a medical condition that triggers organ damage and dysfunction (3, 23), representing a risk factor for several other cardiovascular diseases such as heart attack, cardiac arrest, and stroke. Curiously, one of the symptoms of hypertension is hypoalgesia (18, 19, 47). In most of the experimental models of hypertension in rats, excluding the Dahl salt-sensitive model (49), a decrease in acute nociception was observed in models of acute nociception along with an increase in persistent nociception induced by inflammation (48, 49). The decreased ability to detect and react to a noxious stimulus is harmful to the patient (19) and can also hide warning symptoms of acute myocardial infarction (29). Until now, the pain mechanisms studied in models using spontaneous hypertensive rats (SHRs) specifically focused on noxious stimuli that activate the dorsal root ganglia, a relay for information going to the central nervous system. However, no study has addressed the orofacial mechanical nociception and formalin-induced nociception in SHRs or the differences between paw and orofacial mechanical nociception in normotensive rats and SHRs.

The peculiarity of the trigeminocervical system in its anatomic, neural, and molecular composition indicates a different pain mechanism from that innervated by the dorsal ganglion of the spinal cord (33). Orofacial pain, guided by the complex neural arrangement of the trigeminal nerve, has gained considerable scientific interest because of its high prevalence in the population, such as the commitment to understand its physiology for correct diagnosis and treatment (22). Undeniably, sex differences seem to exert a considerable influence on the modulation of this sensory stimulus. In this sense, it is well established in the literature that women have a decreased pain threshold compared with men (4, 12, 13, 21) but are more susceptible to having chronic pain (12, 37).We therefore hypothesized that orofacial nociception in SHRs is sex-dependent. Indeed, women are most likely to have chronic orofacial pain than men (24) and are more prone to having jaw pain as a warning sign of acute myocardial infarction, increasing the risk of making the wrong diagnosis (20).

Briefly, the goals of this study were *1*) to analyze sex differences in paw and orofacial mechanical nociception and in formalin-induced orofacial nociception in SHRs and *2*) to evaluate the role of ovarian hormones in paw and orofacial mechanical nociception and analyze formalin-induced orofacial nociception in SHRs.

METHODS

Ethical Approval

All animal procedures were approved by the local Animal Care and Use Committee of the University of São Paulo/Brazil at the Ribeirão

* B. M. Santos and G. C. Nascimento contributed equally to the work.

Address for reprint requests and other correspondence: L. G. S. Branco, Dept. of Morphology, Physiology and Basic Pathology, Dental School of Ribeirão Preto, Univ. of São Paulo, 14040-904 Ribeirão Preto, SP, Brazil (e-mail: branco@forp.usp.br).

Preto campus (Protocol No. 2017.1.123.58.5) and are in accordance with the *Guide for the Care and Use of Laboratory Animals* of the National Council for the Control of Animal Experimentation.

Animals

Wistar-Kyoto rats (WKY; 37 rats) and SHRs (36 rats) were kept in individual cages in a quiet room with controlled temperature (23 ± 1°C) and on a 12:12-h light-dark cycle (light cycle starting at 7:00 AM) with water and food ad libitum. All experiments were carried out in a quiet room during the morning to minimize variations. Animal care, including manual recording of body weight, food, water intake, and cage changes, occurred daily at 8:00 AM during the light cycle. Rats were left undisturbed during the entirety of the dark cycle. As described in a consensus report (21), we first carried out the experiments to study nociception with naïve male and female rats of the same age (15–16 wk old) followed by a study in same-age (10 wk old) rats of the role of ovarian hormone in nociception.

Study Design

The Von Frey test was used to evaluate sex differences in site-specific mechanical nociception of naïve male ($n = 6$) and female ($n = 5$) normotensive (WKY) rats and naïve male ($n = 6$) and female ($n = 6$) SHRs (Fig. 1). The same test was used to evaluate the role of ovarian hormones in site-specific mechanical nociception of sham-operated (SHAM; $n = 8$) and ovariectomized (OVX; $n = 8$) normotensive (WKY) rats or SHAM ($n = 8$) and OVX ($n = 6$) SHRs (see Fig. 3).

The formalin test was performed to evaluate the sex differences in orofacial nociceptive responses induced by an inflammatory stimulus in naïve male ($n = 5$) and female ($n = 5$) WKY rats and naïve male ($n = 5$) and female ($n = 5$) SHRs (Fig. 2). The same test was used to evaluate the role of ovarian hormones in orofacial nociceptive response using SHAM ($n = 8$) and OVX ($n = 8$) WKY rats or SHAM ($n = 8$) and OVX ($n = 6$) SHRs (see Fig. 4). A saline group was not used in this experiment, since it is common sense that saline does not have any nociceptive behavior (4).

Finally, mean arterial pressure (MAP) was recorded in the same experimental groups, since ovarian hormones play an important role in blood pressure control, and this analysis will improve our understanding of the influence of blood pressure levels in the absence of ovarian hormone influence. Regression analyses were made between paw mechanical threshold (Von Frey test) with orofacial mechanical threshold and each one with MAP.

Experimental Procedures

All tests were performed on rats during the light phase, in the morning period (8:00–12:00 AM) and at the same place (in the same laboratory). Moreover, the same person performed the nociception tests who had received training for one month before the experiments started.

Mechanical nociception test (Von Frey test). To evaluate paw and orofacial mechanical sensitivity, the Von Frey test was performed. The animals were placed individually in small cages [for temporomandibular joint (TMJ) mechanical nociception measurements] or on an elevated mesh platform (hindpaw mechanical nociception measurements) 1 h before start of the experiment. Then, progressive forces from the filament (nonharmful mechanical stimulus) of an electronic Von Frey anesthesiometer (Insight Instruments, Ribeirão Preto, SP, Brazil) were applied to the hindpaws (plantar region) or temporomandibular region (2 mm below the posterior border of the zygomatic arch) bilaterally. The paw (for paw mechanical threshold evaluation) or head (for orofacial mechanical threshold evaluation) removal was evaluated after this application. The force applied was measured in grams. Three threshold measurements were performed on each animal on each side with 10-min intervals between each session, with the mean of these three values defined as the withdrawal threshold (39). The mechanical nociception in the hindpaw and TMJ was conducted on different days with at least 3 days between experiments.

Formalin-induced inflammatory nociception test (formalin test). The formalin test can be used to evaluate orofacial hyperalgesia by measuring the time spent performing the nociceptive behavior, i.e., exhibiting face rubbing responses. The animals were habituated individually in an observation chamber (30 × 30 × 30 cm in transparent acrylic) for 20 min with no water or food available. Subsequently, the animals were briefly anesthetized with halothane (4%). When there was a momentary loss of spontaneous movement with preservation of deep spontaneous respiration, blink, and pinnae reflexes, the animals received an injection of 50 μl of formalin diluted in 0.9% saline in a concentration of 2.5% (8) with a 27-gauge needle in the right vibrissae area (for orofacial mechanical threshold evaluation). The right side was selected arbitrarily, since there are no differences between sides. After injection, the animals were immediately reallocated to the observation chamber, and behavior analyses were initiated.

A timeline of the time spent performing orofacial nociceptive behavior was done starting at *time 0* (formalin injection time) and finishing 45 min later (Figs. 2 and 4 *top*). Each point represents the mean of each group of the time spent performing orofacial nociceptive behavior during 3 min without interruption. *Phase 1* (0–3 min postformalin injection) and *phase 2* (15–39 min postformalin injection) are represented by the gray areas in the graphic timeline.

Vaginal smears. Estrous cycle was determined and classified daily (7:00–8:00 AM) (15) by microscope examination of vaginal smears and confirmed by at least two regular cycles. Proestrus phase was distinguished by the almost total predominance of nucleated epithelial cells and was chosen due to its high ovarian hormone levels (7). This phase was used to compare the pain responses with the OVX rats due to the absence of ovarian hormones (Figs. 3, 4, and 5). Additionally, we examined acute and persistent nociception of naïve females with no estrous cycle determination (Figs. 1 and 2).We did this because

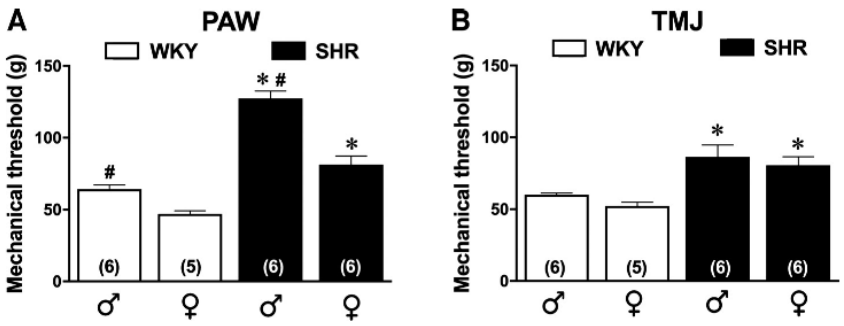

Fig. 1. Mechanical threshold (force measured in grams) of paw withdrawal (*A*) and head-withdrawal (*B*) of male or female (respective bars labeled below of the *x*-axis in symbols ♂ and ♀, respectively) Wistar-Kyoto (WKY; open bars) rats and spontaneously hypertensive rats (SHR; filled bars), using the Von Frey test. Mechanical stimulus was applied in the plantar area of the hindpaw (*A*, entitled "Paw") or in the temporomandibular joint (*B*, entitled "TMJ"), respectively. Data are presented as means ± SE and analyzed using two-way ANOVA followed by recommended post hoc analysis; $n = 5–6$. $P < 0.05$: *vs. ♂ and ♀WKY rats; #vs. ♀ rats, same strain.

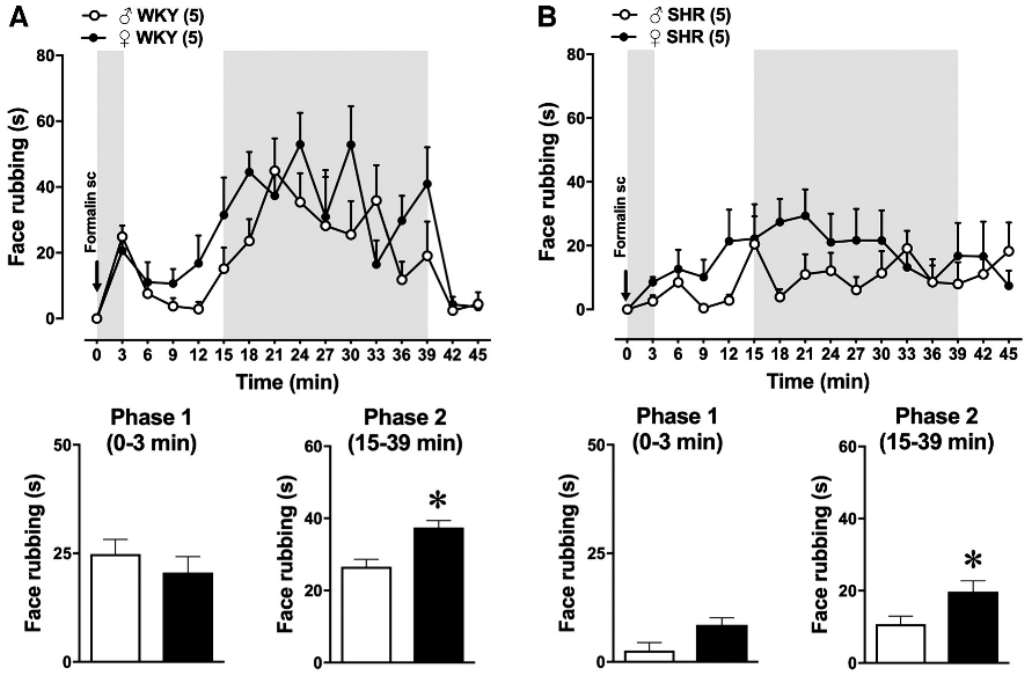

Fig. 2. Measurement of time spent producing nociceptive behaviors postformalin 2.5% injection in the upper lip (unilateral) of males (♂; open bars) and females (♀; filled bars) Wistar-Kyoto (WKY; *A*) and spontaneously hypertensive rats (SHR; *B*) in *phase 1* (0–3 min postformalin injection) and in *phase 2* (15–39 min postformalin-injection) of a model of formalin-induced orofacial nociception. Nociceptive behavior was measured by time (in seconds) spent rubbing the orofacial area and separated in 3-min blocks without interruption. An illustrative timeline (*A* and *B, top*) exhibits the expression of the nociceptive responses along the time. Arrow in the timeline indicates formalin injection (*time 0*); gray areas indicate *phase 1* and *phase 2* of the formalin test. The average of the sum of *phase 1* (*A* and *B, bottom* graphs in *left* corner) and phase 2 (*A* and *B, bottom* graphs in *right* corner) of each group was used to illustrate the data and perform the statistics. Data are presented as means ± SE and analyzed by two-way ANOVA followed by recommended post hoc test; $n = 6–8$. $P < 0.05$: *vs. ♂ rats, same graph.

repeated vaginal smears have a chance to alter nociceptive thresholds (30) but not MAP (9).

Ovariectomy. Ovariectomy was performed (female WKY/SHRs; 10 wk old) under anesthesia with a mixture of 10% ketamine and 2% xylazine (1:1; 1 ml/kg body wt) intraperitoneally followed by an anti-inflammatory (flunixinmeglumine; 0.1 ml subcutaneously) and antibiotic (pentabiotic; 1,200,000 IU; 0.1 ml intramuscular) protection, respectively. In a surgical aseptic field, the intraperitoneal cavity was exposed through bilateral upper flank incisions, and the ovaries were exposed by pulling the ovary out through the muscle incision by grasping the periovarian fat. The ovaries were removed by cutting off the junction between the fallopian tube and the uterine horn, and the remaining tissue was returned to the intraperitoneal cavity. The intraperitoneal cavity was closed by layers at the end of the ovariectomy. After that, health status was checked by every hour for the first 4 h postsurgery and daily until the experiment. The effectiveness of the surgery was checked by the absence of estrous cycles by 5 consecutive days. Sham surgery followed almost all the steps above, except that the ovaries were not cut off. We also evaluated ovariectomy effectiveness by measuring the decrease in uterus weight of OVX rats compared with SHAM rats (0.09 ± 0.01 vs. 0.35 ± 0.09 g, respectively), confirming the absence of the ovarian hormones.

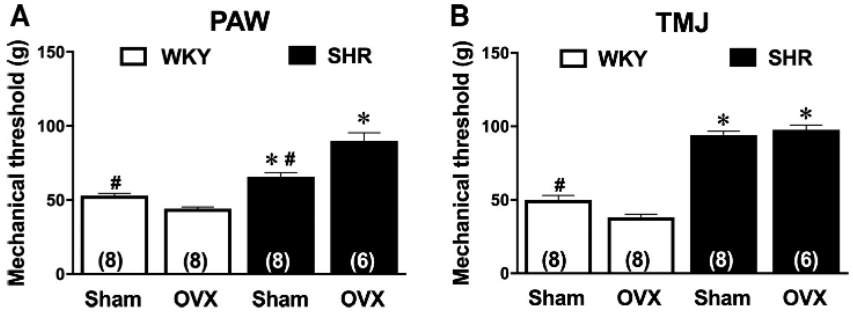

Fig. 3. Mechanical threshold (force applied measured in grams) of hindpaw withdrawal (*A*) and head-withdrawal (*B*) in SHAM (female rats in proestrus with SHAM surgery; bars labeled below as SHAM) and ovariectomized (OVX; bars labeled below as OVX) Wistar-Kyoto (WKY; open bars) rats and spontaneously hypertensive rats (SHR; filled bars), using the Von Frey test. Mechanical stimulus was applied in the plantar area of the hindpaw (*A*, entitled "Paw") or in the temporomandibular joint (TMJ; *B*, entitled "TMJ"), respectively. Data are presented as means ± SE and evaluated statistically by two-way ANOVA followed by recommended post hoc test; $n = 6–8$. $P < 0.05$: *vs. SHAM and OVX WKY rats; #vs. OVX rats, same strain.

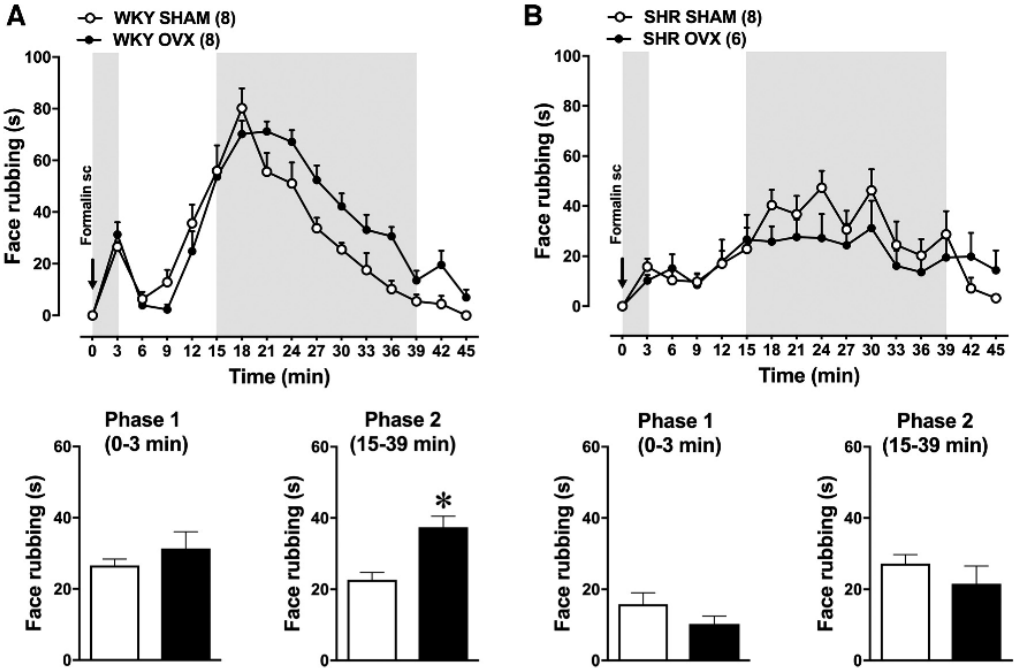

Fig. 4. Measurement of time spent producing nociceptive behaviors after unilateral chemical stimulation with formalin 2.5% in the upper lip of SHAM (female rats in proestrus with sham surgery; open bars) and ovariectomized (OVX; filled bars) Wistar-Kyoto (WKY; *A*) or spontaneously hypertensive rats (SHR; *B*) in a model of formalin-induced orofacial nociception. Nociceptive behavior was measured by time spent rubbing the orofacial area and separated in 3-min blocks without interruption (time measured in seconds). Representative timeline (*A* and *B*, *top* graph) shows expression of nociceptive responses along the time (each point represented by the mean ± SE). Timeline also indicates time of the formalin injection (*time 0*) by an arrow and *phase 1* (0–3 min postformalin injection) and *phase 2* (15–39 min postformalin injection) of the formalin test by gray squares. Average of the sum of *phase 1* (*A* and *B*, *bottom* graphs in *left* corner) and phase 2 (*A* and *B*, *bottom* graphs in *right* corner) of each group was used to illustrate data and perform statistics. Data presented as means ± SE and interpreted using two-way ANOVA followed by recommended post hoc test; $n = 6–8$. $P < 0.05$: *vs. SHAM rats, same graph.

MAP recording. MAP was recorded in anesthetized SHAM or OVX rats in the postexperimental period. The animals were anesthetized with the same dose previously described above in *Ovariectomy*. Polyethylene tubing (PE-10) was connected to a PE-50 (Intramedic, Clay Adams, Parsippany, NJ). A catheter was filled with sterile saline (0.9% heparin) and inserted into the abdominal aorta through the femoral artery and fixed by suture. Arterial catheters were tunneled subcutaneously and exposed onto the back of the rat to allow free access in unrestrained rats. Twenty-four hours postrecovery, the extremity of the system was connected to a pressure transducer (MLT 0699; ADInstruments, Bella Vista, Australia), an amplifier-coupler (Bridge Amp, FE2211861, ADInstruments), and connected to a pulsatile arterial pressure (PAP) recording system (Powerlab 8/35, PL35080562, ADInstruments). Data acquisition was obtained with the corresponding software (Laboratory Chart Pro v. 7.3.1, ADInstruments). MAP was calculated by means of real-time PAP signal, and the data were collected after stability of the recording.

Data Analysis

Data are expressed as means ± SE. Statistical analysis for mechanical nociception evaluation was performed using a two-way ANOVA with sex and strain (Fig. 1) or with ovarian hormones and strain (Fig. 3) as factors. We also evaluated the site-specific differences in mechanical nociception in each group by using an independent *t*-test (Figs. 1 and 3). Statistical analysis for orofacial hyperalgesia evaluation in *phase 1* (0–3 min postformalin injection) and in *phase 2* (15–39 min postformalin injection) was conducted using the sum of the means of the time spent performing nociceptive behaviors of each animal in the group, as described by Donatti et al. (10). The average of the sums of the time performing nociceptive responses was used to perform a two-way ANOVA with sex and strain (Fig. 2), formalin phase and sex (Fig. 2), ovarian hormones and strain (Fig. 4), or strain and time (Fig. 4) as factors. To evaluate the interaction between MAP and the presence of ovarian hormones in female SHRs (Fig. 5*A*), we used the two-way ANOVA. All the ANOVAs were followed by proper post hoc tests. Correlations between orofacial or paw mechanical nociception and MAP parameters evaluated in female rats were analyzed by mean Pearson correlation coefficients (two-tailed; Fig. 5, *B–E*). $P < 0.05$ was set as statistically significant. Figures and statistics were prepared using Prism software (version 8.0, GraphPad Software). Experiments and surgeries were performed by the most experienced personnel of each technique in order to decrease the chances of experimental variability. Besides, Dayton et al. (9) described the nonnecessity to have a greater number of female rats than male rats, since there are no differences in coefficient of variation between the sexes. Finally, using all precautions available to decrease the standard deviation as aforementioned and using a pilot study to anticipate values for the power calculation (traditionally using α or $P = 0.05$ and β or power level = 0.8), an estimated number of animals was found for each experiment ($n = 5–8$ each group).

RESULTS

Site-Specific Differences in Mechanical Threshold (Von Frey Test)

To test the hypothesis that acute nociception is dependent on the site of the stimulus, we compared the nociceptive response

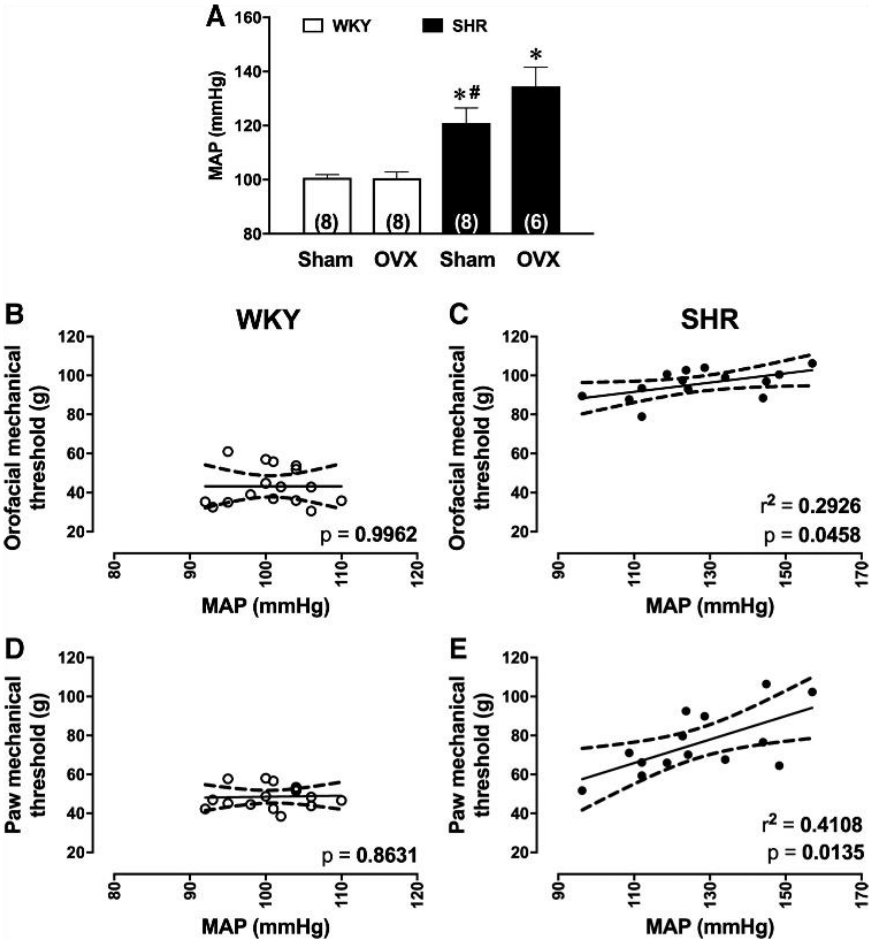

Fig. 5. *A*: measurement of mean arterial pressure (MAP) in unrestrained SHAM (female rats at proestrus with sham surgery) and ovariectomized (OVX) Wistar-Kyoto (WKY; open bars) or spontaneously hypertensive rats (SHR; filled bars). Data are presented as means ± SE and analyzed by two-way ANOVA followed by recommended post hoc test. *vs. SHAM and OVX female WKY rats; #vs. OVX SHR; $n = 6–8$. *B*: linear regression analysis of MAP with orofacial mechanical threshold of pain in female WKY rats. *C*: linear regression analysis of MAP with orofacial mechanical threshold of pain in female SHR. *D*: linear regression analysis of MAP with paw mechanical threshold of pain in female WKY rats. *E*: linear regression analysis of MAP with paw mechanical threshold of pain in female SHRs.

between the paw and TMJ in each group (Fig. 1, *A* and *B*). Only male SHRs had significant differences in mechanical nociception dependent on the site of the stimulus. Greater nociception was observed in the paw of male SHRs compared with the values found in TMJ (127.4 ± 5.2 vs. 86.3 ± 8.3 g, respectively).

Sex Differences In Mechanical Threshold (Von Frey Test)

Regarding nociception in the paw (Fig. 1*A*), it was observed that both SHR sexes had a greater mechanical threshold than the same-sex WKY rats (male: 127.4 ± 5.2 vs. 64.3 ± 3.0 g; female: 81.2 ± 6.0 vs. 47.1 ± 2.1 g, respectively; Fig. 1*A*), indicating that SHRs had a diminished nociception compared with WKY rats. The significant effect of strain [$F(1,19) = 114.7$, $P < 0.0001$] was confirmed by two-way ANOVA.

In addition, the mechanical threshold in the paw of male SHRs was higher than in female SHRs (127.4 ± 5.2 vs. 81.2 ± 6.0 g, respectively; Fig. 1*A*, *left bars*), and male WKY rats had their mechanical threshold in the paw greater than that of female WKY rats (64.3 ± 3.0 vs. 47.1 ± 2.1 g, respectively; Fig. 1*A*, *right bars*), as expected (44). The data indicate that female rats had a significantly lower mechanical threshold than male rats independently of the strain. The effect of strain [$F(1,19) = 48.8$, $P < 0.0001$] in mechanical nociception was confirmed by two-way ANOVA.

Significant changes in orofacial mechanical threshold could be considered an indicator of hypertension in female patients and may suggest an alternative pharmacology for the therapeutic approach to treatment. In this study, the orofacial mechanical threshold measured in the TMJ (Fig. 1*B*) was greater in the TMJ of SHRs than in WKY rats of the same sex (male: 86.3 ± 8.3 vs. 57.3 ± 2.3 g; female: 80.4 ± 5.9 vs. 52.1 ± 3.4 g, respectively; Fig. 1*B*). Two-way ANOVA revealed a significant effect of strain in the analysis [$F(1,19) = 24.12$, $P < 0.0001$].

Nevertheless, no differences were observed between the sexes in both strains. These data support the idea that *1*) SHRs had diminished orofacial nociception compared with WKY rats, and *2*) there were no differences in orofacial nociception between the sexes of the normotensive and hypertensive rats.

Sex Differences in Formalin-Induced Orofacial Nociception (Formalin Test)

Formalin was injected in the upper lip to induce an increase in orofacial nociceptive response. This chemical stimulus induces a fast and short-term nociceptive response (0–3 min postformalin injection), called *phase 1*. An intervening phase

(10–15 min) separates *phase 1* from *phase 2*, which it consists of a long period of nociceptive responses (10–39 min postformalin injection) (10, 49). Orofacial nociception was evaluated by the time spent rubbing the formalin-injected area. The time course of orofacial nociceptive behavior induced by a chemical stimulus was represented in Fig. 2*A*, *top* for WKY rats and Fig. 2*B*, *top* for SHRs. The total sum of the time spent performing nociceptive behavior ± SE in *phase 1* of WKY rats is represented in Fig. 2*A*, *bottom left*, and *phase 2* is represented in Fig. 2*A*, *bottom right*. The same graphic design is maintained for SHRs in Fig. 2*B*.

As shown in Fig. 2*A*, the time performing nociceptive behavior by WKY rats was not different between sexes in *phase 1* of the formalin test (Fig. 2*A*, *bottom left*), but the male WKY rats spent less time performing nociceptive behavior compared with the females in *phase 2* (26.6 ± 2 vs. 37.4 ± 1.9 s; Fig. 2*A*, *bottom right*). As described elsewhere (14), we confirm that normotensive female (WKY) rats had greater orofacial nociception than male WKY rats.

As shown in Fig. 2*B*, the time spent performing nociceptive behavior by SHRs was not different between the sexes in *phase 1* of the formalin test (Fig. 2*B*, *bottom left*), but male SHRs spent less time performing nociceptive behavior than female SHRs in *phase 2* of the formalin test (10.8 ± 2.2 vs. 19.8 ± 2.9 s, respectively; Fig. 2*B*, *bottom right*). These data indicate that not only female WKY rats but also female SHRs had greater orofacial nociception than males of respective strain. ANOVA of the orofacial nociceptive behavior performed in *phase 2* revealed a significant effect of sex [$F(1,16) = 18.20$, $P < 0.0001$].

Concerning the strain differences (see Supplementary Figure at https://doi.org/10.6084/m9.figshare.8072327.v1 for further details), WKY rats spent more time rubbing compared with SHRs in a sex-independent manner in *phase 1* (male: 24.8 ± 3.8 vs. 2.6 ± 1.8 s; female: 20.6 ± 3.8 vs. 8.5 ± 1.6 s, respectively; Fig. 2, *A* and *B*) and in *phase 2* of the formalin test. (male: 26.7 ± 2 vs. 10.7 ± 2.2 s; female:37.5 ± 1.9 vs. 19.8 ± 2.9 s, respectively; Fig. 2, *A* and *B*). ANOVA comparing sex and formalin phases revealed a significant effect of male and female sex that was independent of the formalin phase [$F(1,16) = 61,16$, $P < 0.0001$; $F(1,16) = 30,91$, $P < 0.0001$, respectively]

Role of Ovarian Hormones in Site-Specific Differences in Mechanical Threshold (Von Frey Test)

To test the hypothesis that site-specific differences in mechanical threshold is dependent on the presence of the ovarian hormones, we compared the nociceptive response between paw and TMJ in each group (Fig. 3, *A,*and *B*). Only SHAM SHRs showed a significant difference in mechanical nociception dependent on the site of the stimulus, as an increase in nociception was observed in the paw compared with the TMJ nociception (64.6 ± 2.8 vs. 94.1 ± 2.2 g, respectively). Surprisingly, this difference was abolished in OVX SHRs (89.8 ± 5.6 vs. 97.7 ± 3.3 g, respectively).

Role of Ovarian Hormones in Mechanical Threshold (Von Frey Test)

As shown in Fig. 3*A*, OVX normotensive (WKY) rats exhibited a diminished mechanical threshold in the paw, compared with SHAM normotensive rats in proestrus (44.24 ± 3.2 vs. 52.88 ± 4.6 g, respectively), as also described by Fisher et al. (14). In contrast, it was observed that OVX SHRs had a greater paw mechanical threshold than SHAM SHRs in proestrus (89.78 ± 5.6 vs. 65.7 ± 2.8 g, respectively). Two-way ANOVA revealed a significant effect of ovarian hormones [$F(1,26) = 7$, $P < 0.01$].

Concerning the mechanical threshold in the paw between strains, female WKY rats had a diminished threshold compared with female SHRs regardless of the absence or presence of ovarian hormones. Two-way ANOVA indicated a significant effect of strain [$F(1,26) = 699.3$, $P < 0.0001$] in the analysis of the mechanical nociception in the paw.

As shown in Fig. 3*B*, OVX normotensive (WKY) rats exhibited a diminished mechanical threshold in the TMJ compared with SHAM normotensive rats in proestrus (38.2 ± 2.2 vs. 49.9 ± 3.2 g, respectively), as also described elsewhere (24). Nevertheless, it was observed that OVX SHRs had no differences in orofacial mechanical threshold compared with sham SHRs in proestrus (97.7 ± 3.3 vs. 94.1 ± 2.6 g, respectively).

Concerning the differences in the orofacial mechanical threshold between strains, female WKY rats had a diminished mechanical threshold compared with the female SHRs independently of the presence or absence of ovarian hormones. Two-way ANOVA revealed a significant effect of strain [$F(1,26) = 699.3$, $P < 0.0001$] in the analysis of TMJ nociception in mechanical nociception, but no significant effect was observed for the ovarian hormones. However, the interaction between strain and ovarian hormone factors was revealed by ANOVA [$F(1,26) = 9.9$; $P < 0.05$].

Role of Ovarian Hormones in a Model of Orofacial Nociception (Formalin Test)

As shown in Fig. 4*A*, the time performing nociceptive behavior of WKY rats was not different between groups (SHAM/OVX) in *phase 1* of the formalin test (Fig. 4*A*, *left*), but SHAM WKY rats spent less time performing nociceptive behavior compared with OVX WKY in *phase 2* (22.6 ± 2.1 vs. 37.4 ± 3.1 s, Fig. 4*A*, *right*).

As shown in Fig. 4*B*, no differences were observed between SHAM SHRs and OVX SHRs in both phases (*phase 1*: 15.8 ± 3.2 vs. 10.3 ± 2.2 s; *phase 2*: 27.2 ± 2.5 vs. 21.5 ± 5 s, respectively) of the formalin test.

Regarding the orofacial nociceptive responses between strains, we observed that female WKY rats spent more time performing nociceptive responses than female SHRs in *phase 1* of the formalin test. ANOVA detected a significant effect of strain [$F(1,26) = 9.9$, $P < 0.05$] in this analysis. Two-way ANOVA detected a significant effect only from strain [$F(1,26) = 22.8$, $P < 0.0001$] in the analysis of *phase 1*. Regarding *phase 2*, a significant effect was observed from strain and interaction between ovarian hormones and strain [$F(1,26) = 3.2$, $P < 0.05$ and $F(1,26) = 10.6$, $P < 0.0001$, respectively].

Interestingly, WKY rats and SHRs in proestrus had no differences in the time spent performing nociceptive responses in *phase 2*, using the sum of the times spent performing nociceptive behavior. To analyze the possible effect of time in this variable, we ran a two-way ANOVA between SHAM animals, using time and strain as factors. We observed an effect

in strain and interaction between strain and time factors [$F(8,234) = 15.75$, $P < 0.0001$ and $F(8,26) = 3.2$, $P < 0.0001$, respectively]. A significant difference between these groups was observed 15, 18, and 21 min postformalin injection.

Correlation Between MAP and Mechanical Threshold in Female Rats

Because ovarian hormones (mainly 17β-estradiol) play an important role in blood pressure control (25), we also assessed blood pressure levels in the absence of ovarian hormones. First, we confirmed hypertension by the increased MAP of female SHAM SHRs compared with SHAM WKY rats (121.0 ± 5.5 vs. 100.8 ± 1.1 mmHg, respectively; Fig. 5*A*). Concerning the effect of the absence of ovarian hormone, we observed an enhancement in MAP in OVX SHRs compared with the SHAM SHRs (134.5 ± 7.1 vs. 121.0 ± 5.5 mmHg, respectively; Fig. 5*A*) but not in WKY strain (100.6.0 ± 2.4 vs. 100.8 ± 1.1 mmHg, respectively; Fig. 5*A*). ANOVA detected a significant effect of strain [$F(1,26) = 38.9$, $P < 0.0001$].

To ascertain whether the acute nociception was dependent on blood pressure in female rats, we analyzed the correlation of the orofacial and paw nociceptive responses with the MAP. We observed a positive correlation between MAP in both orofacial (Fig. 5*C*) and paw (Fig. 5*E*) nociception in SHRs. As expected, no correlation was observed in MAP and orofacial (Fig. 5*B*) or paw (Fig. 5*D*) nociception in female WKY rats, since no significant deviation was observed in MAP of this strain with or without intact ovaries.

DISCUSSION

Mechanical Hyponociception in SHRs: Sex and Site-Specific Differences

Mechanical nociception has received little attention in the literature so far compared with chronic nociception. In healthy volunteers, women exhibit greater mechanical nociception than men (6, 12, 42), but this difference is significantly correlated with anxiety (11). Guione et al. (18) observed no differences in acute orofacial nociception between hypertensive women and men. In rats, no differences in mechanical nociception in the tail (tail flick) was shown between sexes (40).

In this study, our results indicate that the paw (but not orofacial) mechanical nociception is sex dependent; i.e., male normotensive and hypertensive rats have higher mechanical threshold than female normotensive and hypertensive rats, respectively. Several sources in the literature suggest the antinociceptive role of some blood pressure modulators, such as the baroreflex system and the opioidergic system (9a, 34, 36, 43, 45, 47, 50). In the present study, male SHRs have higher mechanical threshold in the paw than in the TMJ (Fig. 1*B*). It is common sense that male SHRs have higher MAP than female SHRs of the same age (21, 41). We hypothesize that some of these blood pressure modulators contribute to nociceptive signaling in the orofacial area, having a more pronounced effect on dorsal root ganglia nociceptive signaling. Since endogenous opioids are present along neural pain circuitry (35) modulating nociceptive information (5, 28), we suggest that this blood pressure modulator has a role in nociception of SHRs. In agreement with this notion, the activation of μ- or κ-opioid receptors induces analgesia in a sex-dependent manner; μ-opioid receptor activation seems to elicit a greater antinociception in males than in females (2, 26), whereas κ-opioid receptors a greater increase in analgesia in women than in men (17). Moreover, major upregulation of the κ-opioidergic system in rat myocardium has been reported in SHRs compared with WKY rats (51). Thus, we speculate that there is not only a cardiac but also a trigeminal and spinal ganglia opioidergic reprogramming in SHRs, contributing to the sex differences in acute hyponociception observed in SHRs.

Sex Differences in Formalin-Induced (But Not Mechanical) Orofacial Nociception in SHRs

Our study indicates that there are no sex differences in mechanical orofacial nociception, but they do exist in formalin-induced orofacial nociception in both strains. This difference in nociception response dependent on the test might be explained by the different genetic mechanisms observed in these models of nociception (38).

Interestingly, the difference in orofacial nociceptive responses between strains in naïve female rats (Fig. 2) disappeared between SHAM WKY rats and SHAM SHRs in Fig. 4. This absence of difference might be due to the antinociceptive role of ovarian hormones that decreased the orofacial nociception of SHAM WKY compared with naïve female WKY rats in *phase 2* of the formalin test (model of acute inflammation).

Role of Ovarian Hormones in Mechanical Threshold

The ovaries secrete two important hormones: estrogen and progesterone. These two hormones have a role in pain modulation. Concerning the paw mechanical threshold, previous studies show that ovariectomy decreases mechanical threshold in the Von Frey test, which was reversed by estrogen replacement (32, 46). The ovariectomy also increased paw nociception responses in both phases of the formalin test (1, 16) which was prevented by progesterone and estrogen replacement (31). A few studies show the role of ovarian hormones in TMJ nociception in the models used in this study. Estrogen and progesterone replacement therapy decrease nociception in the TMJ of OVX normotensive rats in the formalin test (14). They also found that female rats in proestrus had no differences in the nociceptive responses compared with male rats in *phase 2* of the formalin test.

We also used the bilateral ovary removal (OVX) surgery to mimic menopause in women and to analyze the role of ovarian hormones in nociception in both strains. In our experiment, we observed that OVX WKY rats had an increase in orofacial nociception with the use of both models of nociception (Figs. 3*B* and 4*A*). We also observed an increase in mechanical paw nociception in OVX WKY rats. Taking all these data together, we conclude that the absence of ovarian hormones has a hypernociceptive role not only in a model of orofacial nociception induced by inflammation (formalin) but also in mechanical orofacial nociception (Von Frey test) in normotensive rats.

Regarding nociception in female SHRs, it was observed that SHRs in proestrus had a hypernociceptive response in the paw compared with the TMJ in the Von Frey test. This site-specific difference in nociception was not observed in OVX SHRs. Since ovarian hormones increase nociception in normotensive animals, the present data indicate that ovarian hormones might

modulate mechanical nociception by indirect means in SHRs. The lack of estrogen in OVX SHRs induces an increase in sympathetic activity followed by an increase in MAP (25). We suggest that the increased sympathetic activity or other blood-pressure mediators induced by the lack of estrogen causes not only an increase in MAP but also a decrease in mechanical paw nociception, but not mechanical orofacial nociception in OVX SHRs. We still do not know how these blood-pressure mediators can differently modulate orofacial and paw nociception, but we speculate that differences in trigeminocervical and dorsal root ganglia pain signaling (33) might be responsible for this contrasting modulation compared with normotensive rats. We cannot rule out the possibility that the enhanced stress response induced by ovariectomy in OVX SHRs could facilitate the decrease in paw nociception. However, if this assumption is true, the stress response does not interfere in mechanical orofacial nociception in OVX SHRs.

Interestingly, we observed that mechanical orofacial and paw nociception are dependent on the MAP in female SHRs, as illustrated in Fig. 5, *E* and *G*. However, the slope of the linear relationship between the MAP and orofacial mechanical threshold variables (slope = 0.05) is much lower than the slope between the MAP and paw mechanical threshold (slope = 1.25) of female SHRs. We conclude that the increases in MAP have a lower capacity to decrease orofacial mechanical threshold but have a higher capacity to decrease paw mechanical threshold. We cannot rule out that the non-difference in orofacial mechanical threshold between SHAM and OVX SHRs, shown in Fig. 3, might be due to the number of days (20 days) chosen to start the experiment. Perhaps this length of time was not enough to find a difference in TMJ nociception of OVX SHRs.

Our results indicate that SHRs have reduced orofacial nociception and that the observed sex differences depend on *1*) the type of the noxious stimulus, *2*) the site of the stimulus (paw or TMJ), and *3*) the relative magnitude of the elevated blood pressure.

Perspectives and Significance

Our data support the conclusion that SHRs have lower orofacial nociception and that ovarian hormones play different roles in the strains studied. This finding is increasingly relevant as substantial increases in the hypertensive population takes place. Hypertensive patients have a high rate of unrecognized myocardial infarction, which has an increased probability of occurrence in middle-aged women (29). One of the main features of myocardial infarction is pain. The loss of trigeminocervical pain may mask the pain related to cardiovascular events in male and mainly in female (menopausal or not) hypertensive patients.

ACKNOWLEDGMENTS

We gratefully acknowledge Dr. Jose Vanderlei Menani for helpful discussion on the data analysis. We are grateful Mauro F. Silva and Nadir Fernandes for technical support. We also thank Grant Harris for the careful English corrections.

GRANTS

This study was supported by Grant Nos. 16/17681-9, 17/03645-3, and 16/09364-3, São Paulo Research Foundation (FAPESP) and No. 301040/2018-4, Conselho Nacional de Desenvolvimento Científico e Tecnológico (CNPq).

DISCLOSURES

No conflicts of interest, financial or otherwise, are declared by the authors.

AUTHOR CONTRIBUTIONS

B.M.S., G.C.N., and L.G.S.B. conceived and designed research; B.M.S., G.C.N., C.P.C., G.S.B., T.R., and J.P.J.S. performed experiments; B.M.S., G.C.N., G.S.B., and J.P.J.S. analyzed data; B.M.S., G.C.N., G.S.B., J.P.J.S., and L.G.S.B. interpreted results of experiments; B.M.S., G.C.N., and C.P.C. prepared figures; B.M.S. and G.C.N. drafted manuscript; B.M.S., G.C.N., J.P.J.S., C.R.A.L.-P., and L.G.S.B. edited and revised manuscript; C.R.A.L.-P. and L.G.S.B. approved final version of manuscript.

REFERENCES

1. **Aloisi AM, Albonetti ME, Carli G.** Sex differences in the behavioural response to persistent pain in rats. *Neurosci Lett* 179: 79–82, 1994. doi:10.1016/0304-3940(94)90939-3.
2. **Bai X, Zhang X, Li Y, Lu L, Li B, He X.** Sex differences in peripheral mu-opioid receptor mediated analgesia in rat orofacial persistent pain model. *PLoS One* 10: e0122924, 2015. doi:10.1371/journal.pone.0122924.
3. **Bankir L, Bichet DG, Bouby N.** Vasopressin V2 receptors, ENaC, and sodium reabsorption: a risk factor for hypertension? *Am J Physiol Renal Physiol* 299: F917–F928, 2010. doi:10.1152/ajprenal.00413.2010.
4. **Bartley EJ, Fillingim RB.** Sex differences in pain: a brief review of clinical and experimental findings. *Br J Anaesth* 111: 52–58, 2013. doi:10.1093/bja/aet127.
5. **Basbaum AI, Fields HL.** Endogenous pain control systems: brainstem spinal pathways and endorphin circuitry. *Annu Rev Neurosci* 7: 309–338, 1984. doi:10.1146/annurev.ne.07.030184.001521.
6. **Berkley KJ.** Sex differences in pain. *Behav Brain Sci* 20: 371–380, 1997. doi:10.1017/S0140525X97221485.
7. **Butcher RL, Collins WE, Fugo NW.** Plasma concentration of LH, FSH, prolactin, progesterone and estradiol-17β throughout the 4-day estrous cycle of the rat. *Endocrinology* 94: 1704–1708, 1974. doi:10.1210/endo-94-6-1704.
8. **Clavelou P, Pajot J, Dallel R, Raboisson P.** Application of the formalin test to the study of orofacial pain in the rat. *Neurosci Lett* 103: 349–353, 1989. doi:10.1016/0304-3940(89)90125-0.
9. **Dayton A, Exner EC, Bukowy JD, Stodola TJ, Kurth T, Skelton M, Greene AS, Cowley AW Jr.** Breaking the cycle: estrous variation does not require increased sample size in the study of female rats. *Hypertension* 68: 1139–1144, 2016. doi:10.1161/HYPERTENSIONAHA.116.08207.

9a. **de Jong W, Cox van Put J, Sándor P.** Influence of opiate peptides on blood pressure regulation and on hypothalamic blood flow. In: *Opioid Peptides and Blood Pressure Control*, edited by Stumpe KO, Kraft K, Faden AI. Berlin, Heidelberg: Springer, 1988, p. 98–102.

10. **Donatti AF, Araujo RM, Soriano RN, Azevedo LU, Leite-Panissi CA, Branco LGSS.** Role of hydrogen sulfide in the formalin-induced orofacial pain in rats. *Eur J Pharmacol* 738: 49–56, 2014. doi:10.1016/j.ejphar.2014.05.023.
11. **Eli I, Bar-Tal Y, Fuss Z, Korff E.** Effect of biological sex differences on the perception of acute pain stimulation in the dental setting. *Pain Res Manag* 1: 201–206, 1996. doi:10.1155/1996/149823.
12. **Fillingim RB.** Sex, gender, and pain: women and men really are different. *Curr Rev Pain* 4: 24–30, 2000. doi:10.1007/s11916-000-0006-6.
13. **Fillingim RB, King CD, Ribeiro-Dasilva MC, Rahim-Williams B, Riley JL III.** Sex, gender, and pain: a review of recent clinical and experimental findings. *J Pain* 10: 447–485, 2009. doi:10.1016/j.jpain.2008.12.001.
14. **Fischer L, Torres-Chávez KE, Clemente-Napimoga JT, Jorge D, Arsati F, de Arruda Veiga MCF, Tambeli CH.** The influence of sex and ovarian hormones on temporomandibular joint nociception in rats. *J Pain* 9: 630–638, 2008. doi:10.1016/j.jpain.2008.02.006.
15. **Freeman M.** Neuroendocrine control of the ovarian cycle of the rat. In: *Knobil and Neill's Physiology of Reproduction*, edited by Neill JD, Plant TM, Pfaff DW, Challis JRG, de Krester DM, Richards JS, and Wassarman PM. Amsterdam: Elsevier, 2006, p. 2327–2388.
16. **Gaumond I, Arsenault P, Marchand S.** The role of sex hormones on formalin-induced nociceptive responses. *Brain Res* 958: 139–145, 2002. doi:10.1016/S0006-8993(02)03661-2.
17. **Gear RW, Miaskowski C, Gordon NC, Paul SM, Heller PH, Levine JD.** The kappa opioid nalbuphine produces gender- and dose-dependent analgesia and antianalgesia in patients with postoperative pain. *Pain* 83: 339–345, 1999. doi:10.1016/S0304-3959(99)00119-0.

18. **Ghione S.** Hypertension-associated hypalgesia. Evidence in experimental animals and humans, pathophysiological mechanisms, and potential clinical consequences. *Hypertension* 28: 494–504, 1996. doi:10.1161/01.HYP.28.3.494.
19. **Ghione S, Rosa C, Mezzasalma L, Panattoni E.** Arterial hypertension is associated with hypalgesia in humans. *Hypertension* 12: 491–497, 1988. doi:10.1161/01.HYP.12.5.491.
20. **Goldberg RJ, O'Donnell C, Yarzebski J, Bigelow C, Savageau J, Gore JM.** Sex differences in symptom presentation associated with acute myocardial infarction: a population-based perspective. *Am Heart J* 136: 189–195, 1998. doi:10.1053/hj.1998.v136.88874.
21. **Greenspan JD, Craft RM, LeResche L, Arendt-Nielsen L, Berkley KJ, Fillingim RB, Gold MS, Holdcroft A, Lautenbacher S, Mayer EA, Mogil JS, Murphy AZ, Traub RJ; Consensus Working Group of the Sex, Gender, and Pain SIG of the IASP.** Studying sex and gender differences in pain and analgesia: a consensus report. *Pain* 132, *Suppl* 1: S26–S45, 2007. doi:10.1016/j.pain.2007.10.014.
22. **Hargreaves KM.** Orofacial pain. *Pain* 152, *Suppl*: S25–S32, 2011. doi:10.1016/j.pain.2010.12.024.
23. **Hayashi K, Saruta T, Goto Y, Ishii M; JATOS Study Group.** Impact of renal function on cardiovascular events in elderly hypertensive patients treated with efonidipine. *Hypertens Res* 33: 1211–1220, 2010. doi:10.1038/hr.2010.162.
24. **Horst OV, Cunha-Cruz J, Zhou L, Manning W, Mancl L, DeRouen TA.** Prevalence of pain in the orofacial regions in patients visiting general dentists in the Northwest Practice-based REsearch Collaborative in Evidence-based DENTistry research network. *J Am Dent Assoc* 146: 721–728.e3, 2015. [Erratum in: *J Am Dent Assoc* 146: 874, 2015.] doi:10.1016/j.adaj.2015.04.001.
25. **Ito K, Hirooka Y, Kimura Y, Sagara Y, Sunagawa K.** Ovariectomy augments hypertension through rho-kinase activation in the brain stem in female spontaneously hypertensive rats. *Hypertension* 48: 651–657, 2006. doi:10.1161/01.HYP.0000238125.21656.9e.
26. **Ji Y, Murphy AZ, Traub RJ.** Sex differences in morphine-induced analgesia of visceral pain are supraspinally and peripherally mediated. *Am J Physiol Regul Integr Comp Physiol* 291: R307–R314, 2006. doi:10.1152/ajpregu.00824.2005.
28. **Julius D, Basbaum AI.** Molecular mechanisms of nociception. *Nature* 413: 203–210, 2001. doi:10.1038/35093019.
29. **Kannel WB, Dannenberg AL, Abbott RD.** Unrecognized myocardial infarction and hypertension: the Framingham Study. *Am Heart J* 109: 581–585, 1985. doi:10.1016/0002-8703(85)90566-6.
30. **Komisaruk BR, Whipple B.** Vaginal stimulation-produced analgesia in rats and women. *Ann NY Acad Sci* 467, *1 Stress-Induce*: 30–39, 1986. doi:10.1111/j.1749-6632.1986.tb14616.x.
31. **Kuba T, Wu H-BK, Nazarian A, Festa ED, Barr GA, Jenab S, Inturrisi CE, Quinones-Jenab V.** Estradiol and progesterone differentially regulate formalin-induced nociception in ovariectomized female rats. *Horm Behav* 49: 441–449, 2006. doi:10.1016/j.yhbeh.2005.09.007.
32. **Li L-H, Wang Z-C, Yu J, Zhang Y-Q.** Ovariectomy results in variable changes in nociception, mood and depression in adult female rats. *PLoS One* 9: e94312, 2014. doi:10.1371/journal.pone.0094312.
33. **Lopes DM, Denk F, McMahon SB.** The molecular fingerprint of dorsal root and trigeminal ganglion neurons. *Front Mol Neurosci* 10: 304, 2017. doi:10.3389/fnmol.2017.00304.
34. **Maixner W, Touw KB, Brody MJ, Gebhart GF, Long JP.** Factors influencing the altered pain perception in the spontaneously hypertensive rat. *Brain Res* 237: 137–145, 1982. doi:10.1016/0006-8993(82)90562-5.
35. **Mansour A, Watson SJ.** *Anatomical Distribution of Opioid Receptors in Mammalians: An Overview*. Berlin, Heidelberg: Springer, 1993, p. 79–105.
36. **McCubbin JA, Bruehl S.** Do endogenous opioids mediate the relationship between blood pressure and pain sensitivity in normotensives? *Pain* 57: 63–67, 1994. doi:10.1016/0304-3959(94)90108-2.
37. **Mogil JS.** Sex differences in pain and pain inhibition: multiple explanations of a controversial phenomenon. *Nat Rev Neurosci* 13: 859–866, 2012. doi:10.1038/nrn3360.
38. **Mogil JS, Wilson SG, Bon K, Lee SE, Chung K, Raber P, Pieper JO, Hain HS, Belknap JK, Hubert L, Elmer GI, Chung JM, Devor M.** Heritability of nociception II. 'Types' of nociception revealed by genetic correlation analysis. *Pain* 80: 83–93, 1999. doi:10.1016/S0304-3959(98)00196-1.
39. **do Nascimento GC, Leite-Panissi CRA.** Time-dependent analysis of nociception and anxiety-like behavior in rats submitted to persistent inflammation of the temporomandibular joint. *Physiol Behav* 125: 1–7, 2014. doi:10.1016/j.physbeh.2013.11.009.
40. **Qu C-L, Dang Y-H, Tang J-S.** Administration of somatostatin analog octreotide in the ventrolateral orbital cortex produces sex-related antinociceptive effects on acute and formalin-induced nociceptive behavior in rats. *Neurochem Int* 87: 77–84, 2015. doi:10.1016/j.neuint.2015.06.002.
41. **Reckelhoff JF, Zhang H, Srivastava K, Granger JP.** Gender differences in hypertension in spontaneously hypertensive rats: role of androgens and androgen receptor. *Hypertension* 34: 920–923, 1999. doi:10.1161/01.HYP.34.4.920.
42. **Riley JL III, Robinson ME, Wise EA, Myers CD, Fillingim RB.** Sex differences in the perception of noxious experimental stimuli: a meta-analysis. *Pain* 74: 181–187, 1998. doi:10.1016/S0304-3959(97)00199-1.
43. **Ring C, France CR, al'Absi M, Edwards L, McIntyre D, Carroll D, Martin U.** Effects of naltrexone on electrocutaneous pain in patients with hypertension compared to normotensive individuals. *Biol Psychol* 77: 191–196, 2008. doi:10.1016/j.biopsycho.2007.10.006.
44. **Romanowska K, Grotkiewicz M, Rewekant M, Makulska-Nowak HE.** Sex dependent antinociceptive activity and blood pressure changes in SHR, WKY and WAG rat strains after diclofenac treatment. *Acta Pol Pharm* 65: 723–729, 2008.
45. **Saccò M, Meschi M, Regolisti G, Detrenis S, Bianchi L, Bertorelli M, Pioli S, Magnano A, Spagnoli F, Giuri PG, Fiaccadori E, Caiazza A.** The relationship between blood pressure and pain. *J Clin Hypertens (Greenwich)* 15: 600–605, 2013. doi:10.1111/jch.12145.
46. **Sanoja R, Cervero F.** Estrogen modulation of ovariectomy-induced hyperalgesia in adult mice. *Eur J Pain* 12: 573–581, 2008. doi:10.1016/j.ejpain.2007.09.003.
47. **Sheps DS, Bragdon EE, Gray TF III, Ballenger M, Usedom JE, Maixner W.** Relation between systemic hypertension and pain perception. *Am J Cardiol* 70: F3–F5, 1992. doi:10.1016/0002-9149(92)90181-W.
48. **Taylor BK, Peterson MA, Basbaum AI.** Exaggerated cardiovascular and behavioral nociceptive responses to subcutaneous formalin in the spontaneously hypertensive rat. *Neurosci Lett* 201: 9–12, 1995. doi:10.1016/0304-3940(95)12157-Y.
49. **Taylor BK, Roderick RE, St Lezin E, Basbaum AI.** Hypoalgesia and hyperalgesia with inherited hypertension in the rat. *Am J Physiol Regul Integr Comp Physiol* 280: R345–R354, 2001. doi:10.1152/ajpregu.2001.280.2.R345.
50. **Zamir N, Simantov R, Segal M.** Pain sensitivity and opioid activity in genetically and experimentally hypertensive rats. *Brain Res* 184: 299–310, 1980. doi:10.1016/0006-8993(80)90800-8.
51. **Zimlichman R, Gefel D, Eliahou H, Matas Z, Rosen B, Gass S, Ela C, Eilam Y, Vogel Z, Barg J.** Expression of opioid receptors during heart ontogeny in normotensive and hypertensive rats. *Circulation* 93: 1020–1025, 1996. doi:10.1161/01.CIR.93.5.1020.

Artigo publicado na Physiology & Behavior

Physiology & Behavior 188 (2018) 128–133

Contents lists available at ScienceDirect

Physiology & Behavior

journal homepage: www.elsevier.com/locate/physbeh

The therapeutic potential of cystathionine gamma-lyase in temporomandibular inflammation-induced orofacial hypernociception

Bruna M. Santos[a,1], Emanuela G. Garattini[b,1], Luiz G.S. Branco[b], Christie R.A. Leite-Panissi[b,*], Glauce C. Nascimento[b,*]

[a] Department of Physiology, Medical School of Ribeirão Preto, University of São Paulo, Ribeirão Preto, SP, Brazil
[b] Department of Morphology, Physiology and Basic Pathology, Ribeirão Preto Dentistry Faculty, University of São Paulo, Ribeirão Preto, SP, Brazil

ARTICLE INFO

Keywords:
Temporomandibular joint inflammation
Pain
Hydrogen sulfide
Cystathionine gamma-lyase

ABSTRACT

Hydrogen sulfide (H_2S) is an endogenous neuromodulator produced mainly by the enzyme cystathionine gamma-lyase (CSE) in peripheral tissues. A pronociceptive role of endogenously produced H_2S has been previously reported by our group in a model of orofacial inflammatory pain. Using the established persistent orofacial pain rat model induced by complete Freund's adjuvant (CFA) injection into temporomandibular joint (TMJ), we have now investigated the putative role of endogenous H_2S modulating hypernociceptive responses. Additionally, plasmatic extravasation on TMJ was measured following different treatments by Evans blue dye quantification. Thus, rats were submitted to Von Frey and Formalin tests in orofacial region before and after pharmacological inhibition of the CSE-H_2S system combined or not with CFA-induced TMJ inflammation. Pretreatment with CSE inhibitor, propargylglycine (PAG; 88.4 µmol/kg) reduced temporomandibular inflammatory pain when injected locally as well as systemically. In particular, local PAG injection seems to be more effective for hypernociceptive responses in orofacial persistent inflammation since its action is evidenced in the majority analyzed periods of the inflammatory process compared to its systemic use. Moreover, local injection seems to act on temporomandibular vascular permeability, evidenced by decreased plasmatic extravasation induced by local PAG administration. Our data are consistent with the notion that the endogenous synthetized gas H_2S modulates persistent orofacial pain responses revealing the pharmacological importance of the CSE inhibitor as a possible therapeutic target for their control.

1. Introduction

Hydrogen sulfide (H_2S) is endogenously synthesized by the cystathionine-γ-lyase (CSE) and cystathionine-β-synthetase (CBS), and it is increasingly recognized as a biologically important signaling molecule in various tissues related to physiological as well as in pathological processes including neurodegenerative diseases, heart failure, atherosclerosis, diabetes, pain and inflammation [1–4]. Whereas CBS is predominant in the brain, CSE has been found to be the most prevailing H_2S releasing enzyme in peripheral tissues [5]. Additionally, various studies using CSE inhibitors in different pain models indicate a role of this enzyme in chronic pain development [6,7].

Regarding H_2S modulation in pain both pro- and anti-nociceptive effects have been described so far [8]. In this sense, while evidences indicate that the injection of carrageenan into hind paws of rats induces H_2S production [9] and the administration of H_2S donors favors the hyperalgesia responses [7]; other studies report the efficacy of H_2S donors in attenuating leukocyte adhesion as well as edema formation in inflammatory models [10].

Chronic pain from orofacial structures is a condition of difficult treatment due to its multifactorial etiology and lack of elucidation of its molecular mechanisms [11]. The differences between trigeminal system and the sensory neurons of mostly rest of the body are not only anatomical, but has cellular and molecular differences as well [12]. Particularly, temporomandibular joint (TMJ) pain is the most frequent condition among non-dental pain in the orofacial region [13]. One of the possible mechanism that has been related to temporomandibular pain is H_2S modulation. It is well established that the TMJ inflammation-induced hyperalgesia promotes an upregulated intraarticular CBS gene expression [14]. These authors also found that stimulation of H_2S signaling increases neuronal excitability by the decrease of potassium currents of trigeminal neurons. In this sense, recent studies have

* Corresponding authors at: Department of Morphology, Physiology and Basic Pathology, Dental School of Ribeirão Preto, University of São Paulo, 14040-904 Ribeirão Preto, SP, Brazil.
E-mail addresses: christie@forp.usp.br (C.R.A. Leite-Panissi), glauce.nascimento@usp.br (G.C. Nascimento).
[1] The authors contributed equally for the work.

https://doi.org/10.1016/j.physbeh.2018.02.007
Received 2 November 2017; Received in revised form 30 January 2018; Accepted 3 February 2018
Available online 06 February 2018

investigated the involvement of H_2S on orofacial pain [6,15,16].

To perform molecular and/or behavioral analyzes related to temporomandibular muscle and joint pain, several studies use experimental animal models of intra-articular inflammatory process. The development of this methodology with the complete Freund's adjuvant (CFA) has become reliable and effective as it represents a model of persistent and lasting inflammation [17], resulting in inflammatory edema and hyperalgesia associated with peripheral nociceptor activation and local release of inflammatory mediators [18]. We hypothesized that TMJ inflammation-induced hyperalgesia and allodynia responses are mediated by endogenous H_2S. To test this hypothesis, we examined hyperalgesia and allodynia reactions to TMJ inflammation in different times of this process (1, 3, 7 and 10 days) after pharmacological inhibition of the CSE-H_2S system by locally or systemic administration of propargylglycine (PAG), as a useful therapeutic strategy against this type of orofacial pain. Additionally, we measured plasmatic extravasation on inflamed TMJs during both administration ways of CSE inhibitor.

2. Methods

2.1. Animals

Experiments were performed on adult male Wistar rats (250 g). Care and handling of these animals were approved by the Animal Care and Use Committee of the University of São Paulo—Brazil at the Ribeirão Preto campus (Protocol number 2016.1.415.58.5) and are in accordance with the guidelines of the Conselho Nacional de Controle de Experimentação Animal (CONCEA – Ministério da Ciência e Tecnologia - Brazil) as well as International Association for the Study of Pain. Animals were maintained in a temperature-controlled room (24 ± 1 °C) on a 12-h light/dark cycle (lights on at 06:00 h) and food and water ad libitum.

2.2. Drugs

The drugs used in this study - Complete Adjuvant of Freund (CFA, temporomandibular inflammation inducer) and Propargylglycine (PAG, inhibitor of CSE) were purchased from Sigma-Aldrich (St. Louis, MO) were dissolved in sterile saline (vehicle; 0.9%).

2.3. Experimental groups (in vivo approach)

To address the involvement of endogenous H_2S in the genesis of hypernociception due a persistent inflammatory state on temporomandibular joints, we induced the inflammatory process by injected CFA bilaterally in a volume of 50 µl for each TMJ. Thus, we performed the nociceptive tests on days 1, 3, 7 and 10 after this injection. We analyzed the effect of PAG locally or systemically (88.4 µmol/kg) 30 min before the start of the tests. The local administration refers to PAG injection bilaterally in the TMJ regions and in the systemically administration, it was injection PAG intraperitoneally. On each TMJ it was injected 50 µl of PAG, while the systemic injection was 10 mg/ml per kg of animal.

Experimental animals for von Frey and formalin tests, as well as for each period of inflammation and for each region injected by PAG are part of independent experimental groups (n = 192 rats in total). After nociceptive behavior tests, we performed a quantification of plasma extravasation on TMJs, since the exudate produced during an inflammatory process contains more plasma proteins than in physiological conditions because of the inflammation-induced vascular permeability enhancement.

2.4. CFA administration

Rats were anesthetized with i.p. injection of ketamine 10% (75 mg/kg) and xylazine 4% (10 mg/kg) for CFA intraarticular administration (ia). With a 26 G ½ needle attached to a 1 ml plastic syringe, it was injected 50 µg of CFA (Mycobacterium tuberculosis, Sigma, USA) suspended in a 50 µl of saline solution bilaterally in temporomandibular joints. The dosage was based on previous reports [19,20]. Control animals received 0.9% saline solution. To find TMJ localization, we palpated the zygomatic arch and the condyle and the needle was inserted immediately below the posteroinferior border of the zygomatic arch and advanced anteriorly to contact the edge of the posterolateral condyle [21]. We established four different periods for inflammation analyses (1, 3, 7 and 10 days), according to previous studies.

2.5. Von Frey - mechanical threshold for escape behavior

Progressive forces from the filament of an electronic Von Frey anesthesiometer (Insight Instruments, Brazil) were applied to the TMJ region to assess orofacial mechanical sensitivity. It was performed before (control period – Supplementary data) and 1, 3, 5, 7 and 10 days after the bilateral administration of CFA or saline solution 0.9% into the TMJ. We evaluated the head withdrawal reflex during the application of the mechanical stimuli. To measure the head withdrawal reflex, rats were placed in the testing chamber for 30 min adaptation period at least and hence, it was observed the withdrawal threshold head of rats. The withdrawal threshold head of each rat was calculated as the mean ± SEM based on three values obtained in each session. All experiments were carried out in a quiet room during the morning to minimize variations.

2.6. Formalin test – hyperalgesia response

To evaluate a tonic chemogenic pain response of rats in the orofacial region, we performed an orofacial formalin test. For the administration of saline or formalin solutions, the rats were allowed to adapt to a testing chamber for 20 min. The experimental room had little human activity and a controlled temperature of 25 ± 1 °C. The animals were removed from the box and a volume of 50 µl of 2% formalin or 0.9% saline solution (control group) was injected subcutaneously into the orofacial region between the nose and the upper lip (vibrissa area). A 30 G 1/2″ needle attached to a plastic syringe of 1 ml was used for the injections. Injections were performed as quickly as possible to avoid prolonged handling that could interfere with the results of this study. Immediately after the injection, rats were returned to the testing chamber, and the number of seconds they spent rubbing the ipsilateral face was recorded. According to Grabow and Dougherty [22], the orofacial formalin test can be characterized by two phases. Phase 1 is the first interval of vibrissal rubbing (0 to 3 min) and phase 2 is defined as the period of vibrissal rubbing from min 15 to 45 of the test period. In general, the peak of the vibrissal rubbing in phase 2 was observed during interval 7 (min 21 to 24) and diminished before interval 15 (min 43 to 45).

2.7. Quantification of Evans blue extravasation

Extravasated Evans blue dye in the temporomandibular joint tissue was quantitatively measured by spectrophotometry. The rats received i.v. injections of Evans blue dye (25 mg/kg) dissolved in saline 30 min before euthanasia at 1, 3, 7 or 10 days following the onset of the experiments. After transcardiac perfusion with PBS solution, the periarticular tissue was dissected, weighed and inserted in 2 ml of formaldehyde overnight. The supernatant (100 µl) was extracted, and it was read by an absorbance at 630 nm in a spectrophotometer. Dye concentrations were determined by comparison with a standard curve of known amounts of Evans blue dye. It was calculated the quantity of Evans blue dye (µg) per ml of rat tissue exudate [17].

Table 1
Basal mechanical sensitivity (Von frey test) and Basal chemical sensitivity (formaline test) in Systemic/local treatment.

	Von Frey (g)		Formaline (s)	
	Systemic	Local	Systemic	Local
Saline + Sal	63 ± 3.0	79 ± 2.7	10 ± 1.2	10 ± 2.7
Saline + PAG	68 ± 2.5	78 ± 4.7	8 ± 2.7	12 ± 4.2
CFA + Sal	75 ± 3.8	75 ± 5.1	11 ± 1.8	9 ± 4.1
CFA + PAG	72 ± 3.1	69 ± 2.6	12 ± 3.6	8 ± 2.3

Results are show as mean ± SEM. N = 8.

2.8. Euthanasia

All efforts were made to minimize animal suffering during all experiments performed. At the end of each experimental test the rats were euthanized by an anesthesia overdose with ketamine (300 mg/kg) and xylazine (30 mg/kg).

2.9. Data expression and statistics

All data are expressed as the mean the standard error of the mean (SEM). Significant differences were determined by a two-way analysis of variance with repeated measures (ANOVA) followed by Newman-Keuls post-test. A P-value < 0.05 was considered significant. For formalin test results, bar graphs represent the averages of the different two phases, first phase at 0–3 min (Supplementary data – Table 1) and 15–45 min for the second phase (Fig. 2).

3. Results

3.1. CSE inhibitor PAG attenuates inflammatory orofacial allodynia

The systemic pretreatment with PAG at a dose of 88.4 nmol/kg produced a significant increase on mechanical withdrawal threshold in 10 days after CFA-induced inflammation (Fig. 1, lower left) compared to group under inflammatory process with saline treatment (79.5 ± 3.1 g vs. 23 ± 2.3 g, respectively). Alternatively, the local CSE inhibitor injection decreased allodynia response after 3 (74 ± 5.4 g), 7 (81 ± 2.8 g) and 10 (83 ± 3.0 g) days of temporomandibular inflammation (Fig. 1, lower right) compared to saline treatment (day 3: 18 ± 2.6 g; day 7: 24 ± 2.2 g; day 10: 26 ± 2.1 g). The results from basal mechanical sensitivity are demonstrated on Supplementary data (Table 1).

Table 2
First phase of formaline test under Systemic/local treatment.

	Face rubbing time (seconds)	
	Systemic	Local
Saline + Sal	2 ± 3.0	7 ± 1.8
Saline + PAG	6 ± 2.5	8 ± 2.7
CFA + Sal	5 ± 3.2	5 ± 3.1
CFA + PAG	7 ± 3.4	6 ± 3.1

Results are show as mean ± SEM. N = 8.

3.2. CSE inhibitor PAG attenuates inflammatory orofacial hyperalgesia

Under CFA-induced temporomandibular inflammation, CSE inhibition, systemically applied, promoted a significant decrease in the formalin-induced face rubbing nociceptive behavior at the second phase (23.5 ± 1.1 s) compared to the respective CFA group without treatment (222 ± 6.5 s), but did not differ at the first phase (48.57 ± 5.2 vs. 52.27 ± 11.3 s, respectively - Supplementary data – Table 2) after 10 days after temporomandibular inflammation (Fig. 2, lower right). By the way, local injection induced face rubbing reduction in almost all inflammation periods analyzed compared to animals which received it vehicle (day 3: 22.1 ± 1.4 vs. 231 ± 7.7 s; day 7: 22.1 ± 2.3 vs.

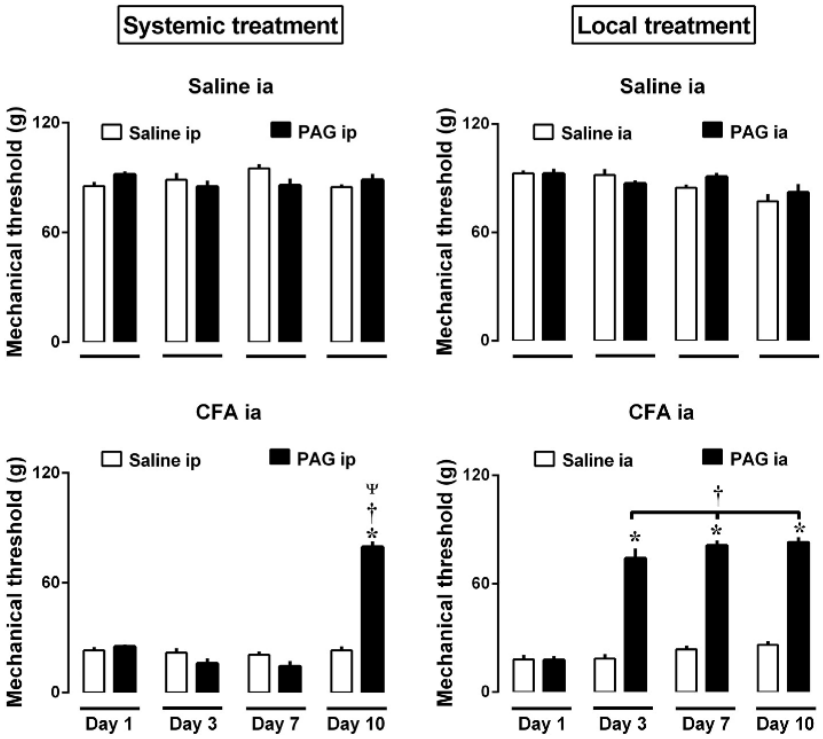

Fig. 1. Inflammatory orofacial allodynia and CSE inhibition treatment. Mechanical threshold in grams after CFA or its vehicle intraarticular injection (disclosed above each graph) with (black columns) or without PAG treatment (white columns). The CSE inhibitor treatment was divided in systemic (upper and lower right graphs) or local (upper and lower left graphs). *vs. control, same day. †vs. day 1, both groups. Ψvs. day 3 and 7, both groups. N = 8.

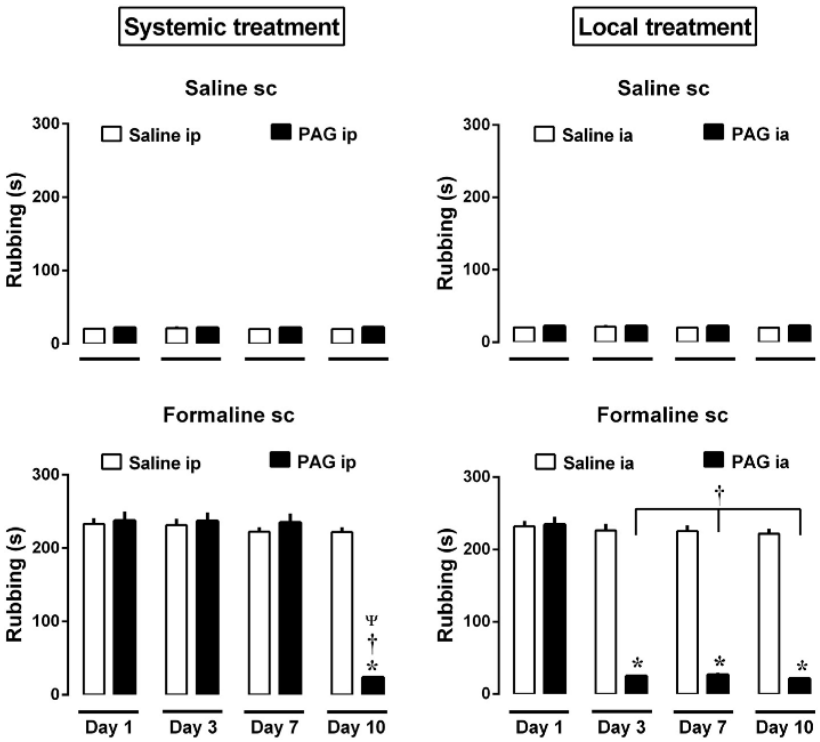

Fig. 2. Inflammatory orofacial hyperalgesia and CSE inhibition treatment. Time spent rubbing it face after orofacial formalin or its vehicle injection subcutaneously (disclosed above each graph) with (black columns) or without PAG treatment. (white columns). The CSE inhibitor treatment was divided in systemic (upper and lower right graphs) or local (upper and lower left graphs). *vs. control, same day. †vs. day 1, both groups. Ψvs. day 3 and 7, both groups. N = 8.

226.4 ± 9.0 s; day 10: 22.5 ± 221.9 ± 6.5 s, respectively - Fig. 2, lower left). The results from basal chemical sensitivity are demonstrated on Supplementary data (Table 2).

3.3. Local injection of CSE inhibitor PAG decreases plasmatic extravasation on TMJ during inflammation

The administration of CFA bilaterally in the TMJ regions promoted greater plasma extravasation in this area compared with groups without inflammation in all periods analyzed (Fig. 3). Under systemic treatment with PAG, there is no alteration on plasmatic proteins synthetized during TMJ inflammation development compared with it control (11 ± 1.8 vs. 12 ± 1.7 μg/g - Fig. 3, lower right). Interestingly, the local treatment was able to decrease plasmatic proteins concentration in periarticular tissue and in the same periods of inflammation affected on hypernociception tests (day 3: 4.4 ± 0.9 μg/g; day 7: 6.1 ± 1.2 μg/g and day 10: 7.9 ± 1.2 μg/g - Fig. 3, lower left) which was attenuated only in day 10 compared with day 1 and 3, same group (Fig. 3, lower left).

4. Discussion

The present study was designed to determine the effects of H_2S using a CSE inhibitor (PAG) on nociceptive processing in orofacial region of rats during inflammation of the TMJ. We first examined the effects of systemically administrated PAG on allodynic and hyperalgesic responses, which was effective in reducing these reactions during the 10 day period (Fig. 1–2). Then, it was determined if a local treatment on TMJ would be efficient on the same allodynic and hyperalgesic responses. We observed that the reduced escape threshold as well as the increased face rubbing produced by CFA injection on TMJ was antagonized by PAG, confirming that these effects are mediated by CSE/H_2S signaling. Interestingly, this effect was observed after 3, 7 and 10 days of temporomandibular inflammation, suggesting a greater contribution of local H_2S in the CFA-induced inflammatory hypernociception in rats. Also, the onset of action of H_2S inhibitor, in regarding of its analgesic effect, was delayed for systemical administration compared to local inhibition. This remarkable difference between the onset of action can be consequence of its route of administration or a possible different analgesic pathway target.

Previous results from our laboratory provide evidence that endogenous H_2S plays a pronociceptive role in the formalin-induced nociception, via T-type Ca^{2+} channels [15]. Now, we used the formalin, as well as, von Frey tests to verify the hyperalgesia and allodynia responses, respectively, during persistent inflammation on TMJ in rats under pretreatment with a CSE inhibitor. This study was conducted due the need for the elucidation of molecular mechanisms related to chronic orofacial pain symptomatology to facilitate the understanding of the etiology as well as proposals for new therapeutic targets for these conditions [25].

Curiously, we have shown an inhibition of temporomandibular plasma extravasation, by Evans blue dye, induced by local PAG use, but not by systemic administration. In this sense, it is proven that H_2S mediates local inflammation through, for example, neutrophil migration and edema formation [23]. Acute pancreatitis and CLP-induced sepsis are models of acute inflammation which H_2S has a pro-inflammatory role [24,25]. Following this line, Cunha et al. [26] have demonstrated a closely association between pro-nociceptive role of H_2S and up-regulation of neutrophil migration to the inflammatory site. A pronociceptive activity of H_2S in peripheral nociceptive processing has also evidenced by Kawabata et al. [7]. Additionally, Lee et al. [27] suggested again a nociceptive-intensity-dependent role for peripheral H_2S in nociception. Employing the same inhibitor of H_2S production in a model of cecal ligation puncture (CLP)-induced sepsis, PAG treatment decreased leukocyte rolling and adherence in mesenteric venules. Moreover, it was observed a decrease in mRNA and protein levels of ICAM-1, P-selectin, and E-selectin in lung and liver [28], indicating a possible pathway for the analgesic effect of PAG in inflammatory

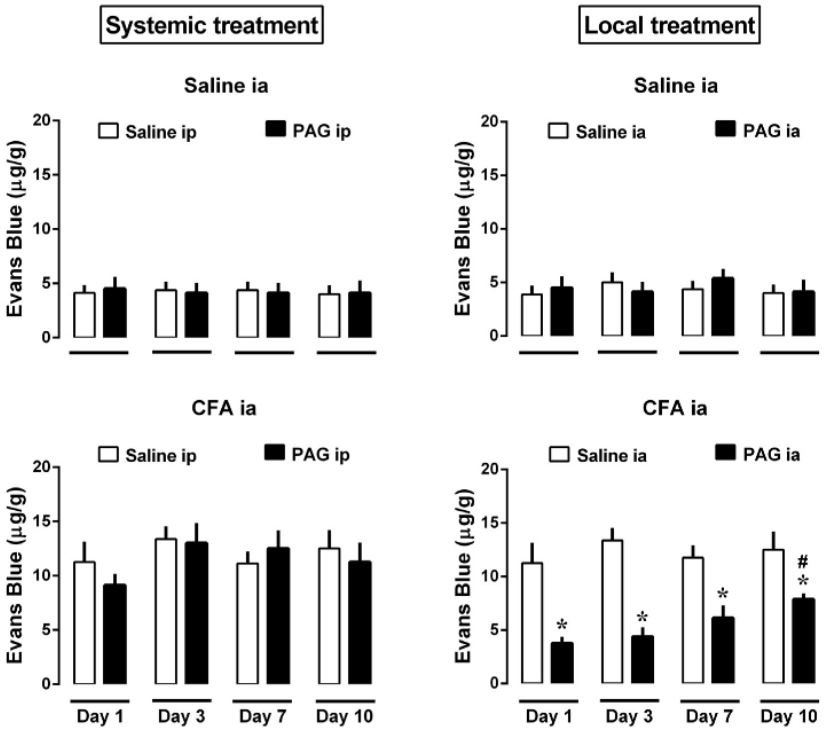

Fig. 3. Evans blue extravasation and CSE inhibition treatment.
Quantitatively measurement of Evans Blue extravasation after CFA or its vehicle intraarticular injection (disclosed above each graph) with (black columns) or without PAG treatment (white columns). The CSE inhibitor treatment was divided in systemic (upper and lower right graphs) or local (upper and lower left graphs). *vs. control, same day. †vs. day 1, both groups. #vs. day 1, same group. N = 8.

process.

Importantly, inflammatory process causes changes in blood flow, vessel size and vascular permeability and the exudate produced when there is a change in vascular permeability contains more plasma proteins than in normal conditions. In this context, Evans blue combines with plasma albumin to form a dye-albumin complex that passes through the injured endothelial barrier [29]. Our data is in accordance with the results about pro-nociceptive action of H_2S on peripheric tissues and proposes CSE-induced modulation through vascular permeability as a possible mechanism responsible for this association.

Despite the systemic administration of PAG attenuating hypernociception by temporomandibular inflammation only in the 10-day period in this study, this pathway may be promising as a new treatment perspective for temporomandibular disorders (TMDs) with inflammatory component. In this sense, the positive effect of this drug is highlighted in more advanced phases of the inflammatory process, but not in the initial states. Also, TMJ plasmatic exudate did not change after this PAG injection, excluding vascular permeability as a mechanism proposed for it functions at 10th day of inflammation. The establishment of inflammatory hypernociception due sensitization of the primary sensory neurons, may be characterized into two phases. The first one involves the non-neuronal events through a vast number of hypernociceptive inflammatory mediators including pro-nociceptive cytokines, leukotrienes, nerve growth factor, endothelins and kinins produced by resident and migratory immune cells [30].

The second state comprises neuronal events related to activation of the receptors on primary nociceptive neurons by direct-acting mediators, such as substance P and Calcitonin Gene Related Protein (CGRP). These molecules activates its receptors and stimulates an intracellular signaling pathways dependent on cyclic AMP, protein kinase A and protein kinase C [31,32], which enhances neuronal excitability and causes pain sensitization by neurogenic inflammation. Substance P, CGRP and neurokinins (NK) are molecules expressed in the trigeminal ganglia recognized by its role in neurogenic inflammation and, as consequence, they have a key role in the persistence of inflammatory pain [33–35]. Furthermore, other studies revealed a putative upregulation of substance P induced by hydrogen sulfide. The treatment with an H_2S donor (NaHS) increased substance P production in a dose dependent manner. Also, the H_2S donor treatment was effective in inducing lung inflammation in mice while it was absent in knockout mice for substance P [36].

Additionally, hydrogen sulfide interacts with TRPV1 channels located in the primary nociceptive nerves and this interaction mediates neurogenic inflammation in CLP-induced sepsis [9]. Assuming all this data, it is possible that the action of systemic PAG used in this work was efficient to interrupts the upregulation of substance P or/and enhances the NK1 receptor activity induced by hydrogen sulfide as well as act on TRPV1-mediated neurogenic inflammation, excluding the role of peripheral inflammatory mediators synthetized on injury local in this treatment.

In accordance with our results, Miao et al. have shown a partial reversion of allodynia induced by CFA on TMJs by injection of O-(Carboxymethyl) hydroxylamine hemihydrochloride (AOAA), an inhibitor for CBS, in a dose-dependent manner. The authors also demonstrated that the administration of AOAA in TMJ area reduced the production of H_2S in trigeminal ganglion and suggest as mechanism the enhanced neural hyperexcitability and increase of the potassium currents of the respective neurons [14].

In conclusion, CSE seems to exert a pro-nociceptive role a long of a persistent orofacial inflammation, with a new mechanism proposed being a local vascular permeability alteration. Relevantly, the region of injection of PAG inhibitor has become important as it interfere the effectiveness of the treatment addressed. This is the first finding about H_2S system modulating a persistent nociception on temporomandibular region in rats and provides expressive evidence for new therapeutic targets for persistent/chronic pain conditions from orofacial structures.

References

[1] U. Shefa, S.G. Yeo, M.S. Kim, I.O. Song, J. Jung, N.Y. Jeong, Y. Huh, Role of

gasotransmitters in oxidative stresses, neuroinflammation, and neuronal repair, Biomed. Res. Int. 2017 (2017) 1–15.
[2] A.S.P. John, S. Kundu, S. Pushpakumar, M. Fordham, G. Weber, M. Mukhopadhyay, U. Sen, GYY4137, a hydrogen sulfide donor modulates miR194-dependent collagen realignment in diabetic kidney, Sci. Rep. 7 (2017) 10924.
[3] K.M. Holwerda, S.A. Karumanchi, A.T. Lely, Hydrogen sulfide, Curr. Opin. Nephrol. Hypertens. 24 (2015) 170–176.
[4] P. Wang, G. Zhang, T. Wondimu, B. Ross, R. Wang, Hydrogen sulfide and asthma, Exp. Physiol. 96 (2011) 847–852.
[5] J.F. Wang, Y. Li, J.N. Song, H.G. Pang, Role of hydrogen sulfide in secondary neuronal injury, Neurochem. Int. 64 (2014) 37–47.
[6] X. Feng, Y.L. Zhou, X. Meng, F.H. Qi, W. Chen, X. Jiang, G.Y. Xu, Hydrogen sulfide increases excitability through suppression of sustained potassium channel currents of rat trigeminal ganglion neurons, Mol. Pain 9 (2013) 1744-8069-9–4.
[7] A. Kawabata, T. Ishiki, K. Nagasawa, S. Yoshida, Y. Maeda, T. Takahashi, F. Sekiguchi, T. Wada, S. Ichida, H. Nishikawa, Hydrogen sulfide as a novel nociceptive messenger, Pain 132 (2007) 74–81.
[8] H.S. Smith, Hydrogen sulfide's involvement in modulating nociception, Pain Physician 12 (2009) 901–910.
[9] M. Bhatia, J. Sidhapuriwala, S.M. Moochhala, P.K. Moore, Hydrogen sulphide is a mediator of carrageenan-induced hindpaw oedema in the rat, Br. J. Pharmacol. 145 (2005) 141–144.
[10] B. Andruski, D.M. McCafferty, T. Ignacy, B. Millen, J.J. McDougall, Leukocyte trafficking and pain behavioral responses to a hydrogen sulfide donor in acute monoarthritis, Am. J. Phys. Regul. Integr. Comp. Phys. 295 (2008) 814–820.
[11] B. Häggman-Henrikson, P. Alstergren, T. Davidson, E.D. Högestätt, P. Östlund, S. Tranaeus, S. Vitols, T. List, Pharmacological treatment of oro-facial pain - health technology assessment including a systematic review with network meta-analysis, J. Oral Rehabil. 44 (2017) 800–826.
[12] D.M. Lopes, F. Denk, S.B. McMahon, The molecular fingerprint of dorsal root and trigeminal ganglion neurons, Front. Mol. Neurosci. 10 (2017) 304.
[13] S. Rajapakse, N. Ahmed, A.J. Sidebottom, Current thinking about the management of dysfunction of the temporomandibular joint: a review, Br. J. Oral Maxillofac. Surg. 55 (2017) 351–356.
[14] X. Miao, X. Meng, G. Wu, Z. Ju, H.-H. Zhang, S. Hu, G.Y. Xu, Upregulation of cystathionine-β-synthetase expression contributes to inflammatory pain in rat temporomandibular joint, Mol. Pain 10 (2014) 9.
[15] A.F. Donatti, R.M. Araujo, R.N. Soriano, L.U. Azevedo, C.A. Leite-Panissi, L.G.S. Branco, Role of hydrogen sulfide in the formalin-induced orofacial pain in rats, Eur. J. Pharmacol. 738 (2014) 49–56.
[16] K. Koroleva, A. Mustafina, A. Yakovlev, A. Hermann, R. Giniatullin, G. Sitdikova, Receptor mechanisms mediating the pro-nociceptive action of hydrogen sulfide in rat trigeminal neurons and meningeal afferents, Front. Cell. Neurosci. 11 (2017) 226.
[17] G.C. do Nascimento, C.R.A. Leite-Panissi, Time-dependent analysis of nociception and anxiety-like behavior in rats submitted to persistent inflammation of the temporomandibular joint, Physiol. Behav. 125 (2014) 1–7.
[18] F.O. de Lima, F.R. Nonato, R.D. Couto, J.M. Barbosa Filho, X.P. Nunes, R. Ribeiro dos Santos, M.B.P. Soares, C.F. Villarreal, Mechanisms involved in the antinociceptive effects of 7-hydroxycoumarin, J. Nat. Prod. 74 (2011) 596–602.
[19] R. Spears, L.A. Dees, M. Sapozhnikov, L.L. Bellinger, B. Hutchins, Temporal changes in inflammatory mediator concentrations in an adjuvant model of temporomandibular joint inflammation, J. Orofac. Pain 19 (2005) 34–40.
[20] R.P. Harper, C.A. Kerins, J.E. McIntosh, R. Spears, L.L. Bellinger, Modulation of the inflammatory response in the rat TMJ with increasing doses of complete Freund's adjuvant, Osteoarthr. Cartil. 9 (2001) 619–624.
[21] Q. Zhou, H. Imbe, R. Dubner, K. Ren, Persistent Fos protein expression after orofacial deep or cutaneous tissue inflammation in rats: implications for persistent orofacial pain, J. Comp. Neurol. 412 (1999) 276–291.
[22] T.S. Grabow, P.M. Dougherty, Cervicomedullary intrathecal injection of morphine produces antinociception in the orofacial formalin test in the rat, Anesthesiology 95 (2001) 1427–1434.
[23] M. Bhatia, Hydrogen sulfide as a vasodilator, IUBMB Life 57 (2005) 603–606.
[24] T. Barichello, M.R. Martins, A. Reinke, L.S. Constantino, R.A. Machado, S.S. Valvassori, J.C.F. Moreira, J. Quevedo, F. Dal-Pizzol, Behavioral deficits in sepsis-surviving rats induced by cecal ligation and perforation, Braz. J. Med. Biol. Res. 40 (2007) 831–837.
[25] A.D. Ang, J. Rivers-Auty, A. Hegde, I. Ishii, M. Bhatia, The effect of CSE gene deletion in caerulein-induced acute pancreatitis in the mouse, AJP Gastrointest. Liver Physiol. 305 (2013) 712–721.
[26] T.M. Cunha, D. Dal-Secco, W.A. Verri, A.T. Guerrero, G.R. Souza, S.M. Vieira, C.M. Lotufo, A.F. Neto, S.H. Ferreira, F.Q. Cunha, Dual role of hydrogen sulfide in mechanical inflammatory hypernociception, Eur. J. Pharmacol. 590 (2008) 127–135.
[27] A.T.H. Lee, J. Jitendrakumar Shah, L. Li, Y. Cheng, P.K. Moore, S. Khanna, A nociceptive-intensity-dependent role for hydrogen sulphide in the formalin model of persistent inflammatory pain, Neuroscience 152 (2008) 89–96.
[28] H. Zhang, L. Zhi, S.M. Moochhala, P.K. Moore, M. Bhatia, Endogenous hydrogen sulfide regulates leukocyte trafficking in cecal ligation and puncture-induced sepsis, J. Leukoc. Biol. 82 (2007) 894–905.
[29] R.H. Steele, D.L. Wilhelm, The inflammatory reaction in chemical injury. I. Increased vascular permeability and erythema induced by various chemicals, Br. J. Exp. Pathol. 47 (1966) 612–623.
[30] W.A. Verri, T.M. Cunha, C.A. Parada, X. Wei, S.H. Ferreira, F.Y. Liew, F.Q. Cunha, IL-15 mediates immune inflammatory hypernociception by triggering a sequential release of IFN, endothelin, and prostaglandin, Proc. Natl. Acad. Sci. 103 (2006) 9721–9725.
[31] K.O. Aley, J.D. Levine, Role of protein kinase A in the maintenance of inflammatory pain, J. Neurosci. 19 (1999) 2181–2186.
[32] R.R. Ji, Z.Z. Xu, Y.J. Gao, Emerging targets in neuroinflammation-driven chronic pain, Nat. Rev. Drug Discov. 13 (2014) 533–548.
[33] A.F. Russo, Calcitonin gene-related peptide (CGRP): a new target for migraine, Annu. Rev. Pharmacol. Toxicol. 55 (2015) 533–552.
[34] K.A. Kristiansen, L. Edvinsson, Neurogenic inflammation: a study of rat trigeminal ganglion, J. Headache Pain 11 (2010) 485–495.
[35] M. Takeda, M. Takahashi, S. Matsumoto, Suppression of neurokinin-1 receptor in trigeminal ganglia attenuates central sensitization following inflammation, J. Peripher. Nerv. Syst. 17 (2012) 169–181.
[36] M. Bhatia, L. Zhi, H. Zhang, S.W. Ng, P.K. Moore, Role of substance P in hydrogen sulfide-induced pulmonary inflammation in mice, Am. J. Phys. Lung Cell. Mol. Phys. 291 (2006) 896–904.

Artigo publicado na Nitric Oxide

Nitric Oxide 93 (2019) 90–101

Contents lists available at ScienceDirect

Nitric Oxide

journal homepage: www.elsevier.com/locate/yniox

Propargylglycine decreases neuro-immune interaction inducing pain response in temporomandibular joint inflammation model

Emanuela G. Garattini[a], Bruna M. Santos[b], Daniele P Ferrari[a], Camila P Capel[a], Heloísa D.C. Francescato[b], Terezila M. Coimbra[b], Christie R.A. Leite-Panissi[c], Luiz G.S. Branco[a,b,**], Glauce C. Nascimento[a,b,*]

[a] Department of Basic and Oral Biology, Dental School of Ribeirão Preto, University of São Paulo, Ribeirão Preto, SP, Brazil
[b] Department of Physiology, Medical School of Ribeirão Preto, University of São Paulo, Ribeirão Preto, SP, Brazil
[c] Psychobiology Graduate Program, School of Philosophy, Science and Literature of Ribeirão Preto, University of São Paulo, Ribeirão Preto, SP, Brazil

ARTICLE INFO

Keywords:
Hydrogen sulfide
Inflammation
Orofacial nociception
Cytokines
Glia

ABSTRACT

The mechanisms underlying temporomandibular disorders following orofacial pain remain unclear. Hydrogen sulfide (H_2S), a newly identified gasotransmitter, has been reported to modulate inflammation. Cystathionine γ-lyase (CSE) is responsible for the systemical production of H_2S, which exerts both pro- and antinociceptive effects through inflammation. In the current study, we investigated whether the endogenous H_2S production pathway contributes to arousal and maintenance of orofacial inflammatory pain, through the investigation of the effects of a CSE inhibitor, propargyglycine (PAG), in a rat CFA (Complete Freund Adjuvant)-induced temporomandibular inflammation model to mimic persistent pain in the orofacial region. For this, rats received either CFA or saline in the temporomandibular joints (TMJs), and after 3 or 14 days, they received a single injection of PAG or saline and were evaluated for nociception with the von Frey and formalin test. Also, pro-inflammatory cytokines, tumor necrosis factor-α (TNF-α), and interleukin-1β (IL-1β) were analyzed in TMJs and trigeminal ganglion (TG). In this last one, glial cells reactivity was also verified. Endogenous H_2S production rate were measured in both, TMJ and TG. Our results indicated decreased allodynia and hyperalgesic responses in rats submitted to CFA after injection of PAG. Moreover, PAG inhibited leucocyte migration to temporomandibular synovial fluid after 3 and 14 days of inflammation. PAG was able to reduce levels of CBS, CSE, TNF-α, and IL-1β in the TMJ and TG, after 13 days of CFA injection. The observed increased activation of glial cells in the trigeminal ganglia on the 14th day of inflammation can be prevented by the highest dose of PAG. Finally, CBS and CSE expression, and endogenous H_2S production rate in the TMJ and TG was found higher in rats with persistent temporomandibular inflammation compared to rats injected with saline and PAG was able to prevent this elevation. Our results elucidated the molecular mechanisms by which H_2S exerts its pro-inflammatory and pro-nociceptive role in the orofacial region by alterations in both local tissue and TG.

1. Introduction

Chronic orofacial pain is a challenging clinical condition due to its multifactorial etiology and, therefore, difficult diagnosis and complex treatment. Likewise, its undefined molecular mechanisms also contribute to the complexity of chronic orofacial pain [1]. Temporomandibular dysfunctions (TMDs) associated or not with muscular symptoms comprise the major cause of chronic states of pain in orofacial structures [2,3]. Besides their high incidence, the pathophysiology of temporomandibular joint (TMJ) pain remains unclear even with the notable evolution already made towards the clarification of their pathogenesis [4]. Classical animal models of inflammatory pain allow us to examine these disorders and their potential therapeutics having remarkable relevance to translational science. In fact, CFA (Complete Freund Adjuvant)-rat is a reliable model that promotes acute and chronic states of inflammatory pain. Numerous studies have been

* Corresponding author. Department of Morphology, Physiology and Basic Pathology, Dental School of Ribeirão Preto, University of São Paulo, Ribeirão Preto, SP, 14040-904, Brazil.
** Corresponding author. Department of Morphology, Physiology and Basic Pathology, Dental School of Ribeirão Preto, University of São Paulo, Ribeirão Preto, SP, 14040-904, Brazil.
E-mail addresses: branco@forp.usp.br (L.G.S. Branco), glauce.nascimento@usp.br (G.C. Nascimento).

https://doi.org/10.1016/j.niox.2019.10.001
Received 28 February 2019; Received in revised form 22 September 2019; Accepted 2 October 2019
Available online 08 October 2019
1089-8603/ Published by Elsevier Inc.

using this model to analyze systemic [5,6] and orofacial pain [7–9].

The closely mutual neuro-immune interaction contributes to the pain response [10]. The release of cytokines [such as tumor necrosis factor-α (TNF-α) and interleukin-1β (IL-1β)] within inflamed joints by many types of cells [11,12] induces pain by the direct activation of their receptors in the terminal nerve or indirectly by increasing the expression and production of others pain-related mediators [10]. TNF-α and IL-1β are strongly expressed in the joints affected by TMJ disorders [11,13]. Many studies have shown substantial levels of both in the synovial fluid of patients suffering from this condition [14]. In chronic pain conditions, there is also an increase in the release of cytokines by the nociceptors neurons activating satellite glial cells and concomitantly facilitating central pain sensitization [15]. Accordingly, TG also has an increase in microglial activation [16] and an increase in TNF-α production [17] in CFA-model.

Hydrogen sulfide (H_2S) is an endogenous gaseous element synthesized from the metabolism of L-cysteine by the handling of cystathionine γ-lyase (CSE – mainly expressed in peripheral tissues) or cystathionine β-synthase (CBS – mainly expressed in the brain) [18]. Numerous efforts have been made to clarify the pathophysiology of this gas since its discovery [19,20]. About pain states, it has been shown that H_2S exerts pro- and antinociceptive effects [21–23] which appear to result from various interrelated mechanisms dependent upon the distinct molecular targets. Among them, H_2S mediates local inflammation-induced pain through mechanisms involving neutrophil migration, cytokine production and edema formation [24,25]. Moreover, a potential therapeutic role of H_2S in systemic and orofacial inflammatory pathologies has been proposed [26–29].

It is a well-acknowledged fact, particularly about orofacial pain, that the TMJ inflammation-induced hyperalgesia produces an upregulated intraarticular CBS gene expression [8]. Additionally, a recent finding from our research group pointed out the anti-nociceptive effect of CSE inhibition on temporomandibular inflammatory pain. This study reveals the acute and persistent anti-nociceptive effect of local H_2S inhibition, while the systemic injection caused only a persistent anti-nociceptive effect [29]. It has also been demonstrated that stimulation of H_2S signaling increases neuronal excitability of trigeminal neurons [30]. The trigeminal system has been plentifully studied in mammals and birds being responsible for motor coordination, sensory and cognitive oral functions [31–33]. The main feature of this system is the presence of two distinct primary afferent neuronal groups: trigeminal ganglion (TG) and mesencephalic trigeminal nucleus (MTN). Cell bodies of these primary afferent neurons are present in TG [34], and a few are located in the MTN. MTN is involved mainly in proprioception [35,36]. Regarding the TG, the dorsomedial part is involved in nociception, thermoreception, and proprioception while its ventrolateral part is involved in mechanoreception [33]. Signals from the trigeminal system are transmitted by second order neurons into the brainstem and ascend to different regions of central nervous system (CNS) [34].

Considering TG is an essential relaying station firstly activated in the processing of painful orofacial information, the study of the role of H_2S in this region may be a promising therapeutic strategy by decreasing neuro-immune interactions inducing pain response. Notably, the doses chosen to our study are described to do not change body core temperature [37] or systolic blood pressure [38] under basal or health conditions, indicating that PAG might be a possible therapeutic target for persistent orofacial pain without side effects. This question is relevant in the context of the necessity to develop novel analgesics since some patients do not respond to analgesics such as opioids and non-steroidal anti-inflammatory drugs and others patients might suffer from their major adverse effects.

Hence, the present study investigated the unexplored anti-nociceptive and anti-inflammatory effects of a CSE inhibitor, propargylglycine (PAG) in different doses on the CFA-induced inflammatory hypernociception (acute and persistent states) in the TMJ of rats by evaluating the leucocytes infiltrate in synovial fluid of the joint and IL-1β and TNF-α levels, CBS and CSE expression in TMJ tissue and trigeminal ganglia. Moreover, the activation of satellite glial cells on ganglion was also investigated, since glial plasticity is part of modifications in the peripheral nervous system during the development of chronic states of pain and inflammation, and it was measured H_2S production rate in both structures. This pioneering investigation was undertaken to test the hypothesis that the modulatory effect of PAG on the orofacial nociception is regulated by H_2S in the TMJ and TG and it may provide insights into chemical events that initiate and maintain chronic inflammatory pain in TMJ.

2. Methods

2.1. Animals

Male Wistar rats (n = 6 per group; 160–220 g) were housed in standard plastic cages, they had access to food and water ad libitum and were maintained in a temperature-controlled room (23 ± 2 °C) with a 12/12-h light-dark cycle. This study was conducted in accordance with the local Institutional Animal Care and with the approval of the local ethical committee (2016.1.415.58.5) and we designed it to reduce animal suffering and the number of animals.

2.2. Drugs

The drugs used in this study - Complete Adjuvant of Freund (CFA, temporomandibular inflammation inducer) and Propargylglycine (PAG, an inhibitor of CSE) - were purchased from Sigma-Aldrich and dissolved in sterile saline (vehicle; 0.9%). The doses of PAG were based according to reports in the literature [39].

2.3. CFA-induced inflammatory hypernociception on temporomandibular region

Initially, rats were anesthetized with an intramuscular injection of ketamine 10% (75 mg/kg) and xylazine 4% (10 mg/kg) followed by bilateral intraarticular administration with 50 μg of CFA (*Mycobacterium tuberculosis*) suspended in a 50 μL paraffin oil (Sigma Aldrich) or 0.9% saline solution (SAL). This dose was based on previous reports [40]. A 26 G ½ needle attached to a 1 mL plastic syringe was used for the injection. To locate the TMJ for the injection, we palpated the zygomatic arch and the condyle. The needle was inserted immediately below the posteroinferior border of the zygomatic arch and advanced anteriorly to contact the edge of the posterolateral condyle [41].

2.4. Experimental protocols

On Fig. 1, it is possible to see an experimental design evidencing the experimental protocols of this work. After 3 and 14 days of CFA injection inducing acute or persistent inflammation, respectively, in the temporomandibular joints, concomitantly or not with local PAG treatment, behavioral tests (orofacial mechanical and chemical nociception), euthanasia and sample collection (synovial fluid, tissue joint, and trigeminal ganglion) and inflammatory analysis (cell counting and ELISA) were all performed.

2.5. Evaluation of orofacial hypernociception

2.5.1. Mechanical threshold evaluation – Von Frey test

Inflammatory hypernociception in the TMJ was evaluated by measuring the threshold of force needed to be applied to the TMJ region until the head withdrawal occurred. The measurements were performed by a blinded examiner who used a digital device (Insight, Brazil) that consisted of a rigid filament linked to an electronic device – automatic Von Frey anesthesiometer, which in turn measures the response

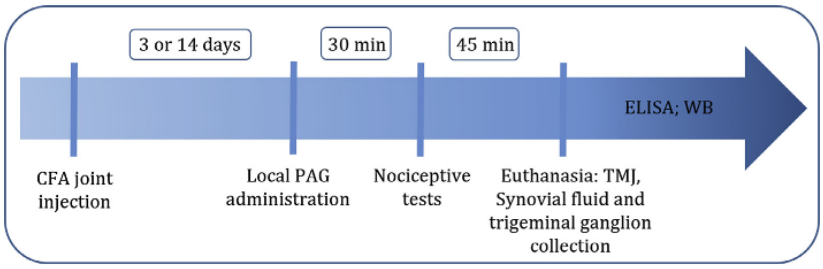

Fig. 1. Experimental line.

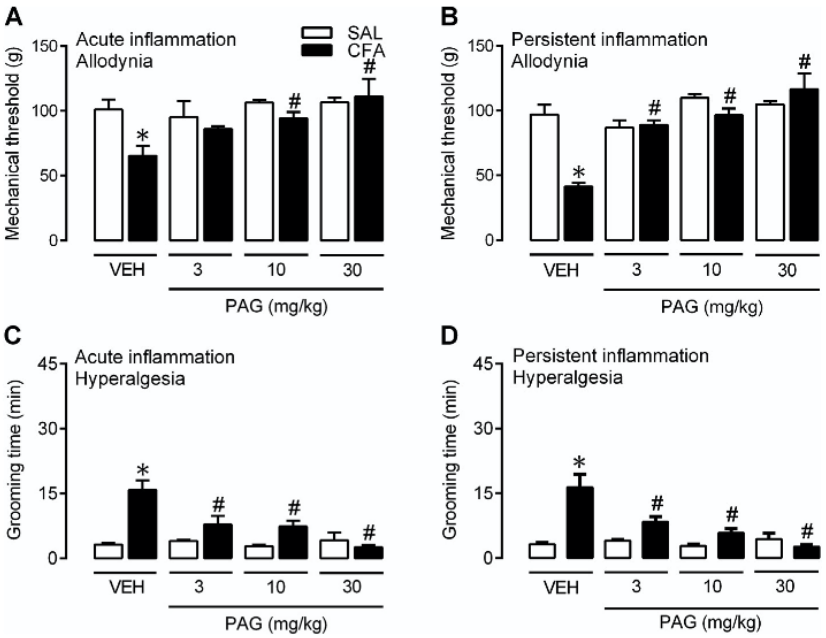

Fig. 2. PAG prevents mechanical alodinia and orofacial hyperalgesia induced by CFA in ATMs. **A:** Mechanical nociception threshold (in grams) of the rats submitted to 3 days of temporomandibular inflammation by CFA or injected with Saline. **B:** Mechanical nociception threshold (in grams) of rats submitted to 14 days of temporomandibular inflammation by CFA or injected with saline (SAL). **C:** Orofacial grooming time after formalin injection (1.5%) in the region of vibrissae of rats submitted to 3 days of temporomandibular inflammation by CFA or injected with saline (SAL). **D:** Orofacial grooming time after formalin injection (1.5%) in the region of vibrissae of rats submitted to persistent temporomandibular inflammation by CFA or injected with Saline. Data are expressed as mean ± standard error of the mean. *P < 0.05, vs. control group (SAL) at the same dose of PAG. #P < 0.05, vs. CFA treated with vehicle of PAG group. The pharmacological treatment consisted of PAG injected locally into the joint at different doses (3, 10, 30 mg/kg) or its vehicle (VEH; saline injection).

Table 1
Quantification of leucocytes on synovial fluid of TMJs from rats submitted to acute (3 days after CFA injection) or persistent (14 days after CFA injection) temporomandibular inflammation or 3 or 14 days after saline injection (SAL). Data are expressed as mean ± standard error of the mean. *P < 0.05, compared to SAL and #P < 0.001, compared to CFA inducing acute temporomandibular inflammation. The pharmacological treatment consisted of PAG injected locally into the joint at different doses (3, 10, 30 mg/kg) or its vehicle (VEH; saline injection).

Leucocytes count in synovial fluid (x 10^3/ul)				
	Saline 3 days	Saline 14 days	CFA 3 days	CFA 14 days
Vehicle	50.3 ± 1	50.2 ± 2.1	115.3 ± 1.3*	210 ± 1.6*#
PAG 3 mg	48.8 ± 0.3	52.3 ± 1.4	106 ± 1.6*+	93.2 ± 0.9*#
PAG 10 mg	52.8 ± 1.3	52.2 ± 1.8	92.8 ± 0.7*+	82.8 ± 0.7*#
PAG 30 mg	53.3 ± 2	49.2 ± 0.4	53.2 ± 1.6+	64.8 ± 1.3*#

threshold in grams (g) when the filament is applied to the surface of the tested region [29]. The facial areas to be tested around the TMJ were shaved before the experimental procedure, and the animals were placed in individual plastic cages 45 min before the tests. The animals underwent conditioning sessions in the testing room for 4 consecutive days. On day five, the basal force threshold value was recorded three times, and the average of these values was calculated.

2.5.2. Formalin test

To evaluate a tonic chemogenic pain response of rats in the orofacial region, we performed an orofacial formalin test. For the administration of saline or formalin solutions, the rats were allowed to adapt to a testing chamber for 20 min. The experimental room had little human activity, and a controlled temperature of 25 ± 1 °C. The animals were removed from the box and a volume of 50 µL of 2% formalin or 0.9% saline solution (control group) was injected subcutaneously into the orofacial region between the nose and the upper lip (vibrissae area). A 30 G 1/2" needle attached to a plastic syringe of 1 mL was used for the injections. Injections were performed as quickly as possible to avoid prolonged handling that could interfere with the results of this study. Immediately after the injection, rats were returned to the testing chamber, and the number of seconds they spent rubbing the ipsilateral face was recorded. According to Grabow and Dougherty [42], the orofacial formalin test can be characterized by two phases. Phase 1 is the first interval of vibrissal rubbing (0–3 min), and phase 2 is defined as the period of vibrissal rubbing from min 15 to 45 of the test period. In general, the peak of the vibrissal rubbing in phase 2 was observed during interval 7 (min 21 to 24) and diminished before interval 15 (min 43 to 45).

2.6. Euthanasia

Rats were deeply anesthetized with urethane (1.5 g/kg, Sigma

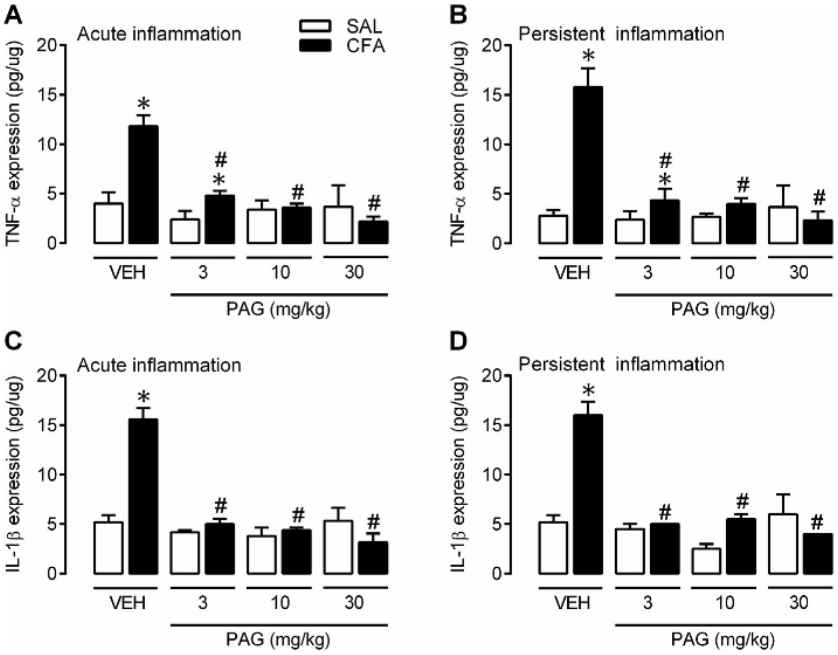

Fig. 3. PAG reduces proinflammatory cytokines in TMJ after 3 (acute inflammation) and 14 days (persistent inflammation) of CFA-induced temporomandibular inflammation. **A:** Quantification of TNF-α from rats submitted to acute temporomandibular inflammation by CFA or injected with Saline. **B:** Quantification of TNF-α from rats submitted to persistent temporomandibular inflammation by CFA or injected with Saline. **C:** Quantification of IL-1β from rats submitted to acute temporomandibular inflammation by CFA or injected with Saline. **D:** Quantification of IL-1β from rats submitted to persistent temporomandibular inflammation by CFA or injected with saline (SAL). Data are expressed as mean ± standard error of the mean. *P < 0.05, vs. control group (SAL) at the same dose of PAG. #P < 0.05, vs. CFA treated with vehicle of PAG group. The pharmacological treatment consisted of PAG injected locally into the joint at different doses (3, 10, 30 mg/kg) or its vehicle (VEH; saline injection).

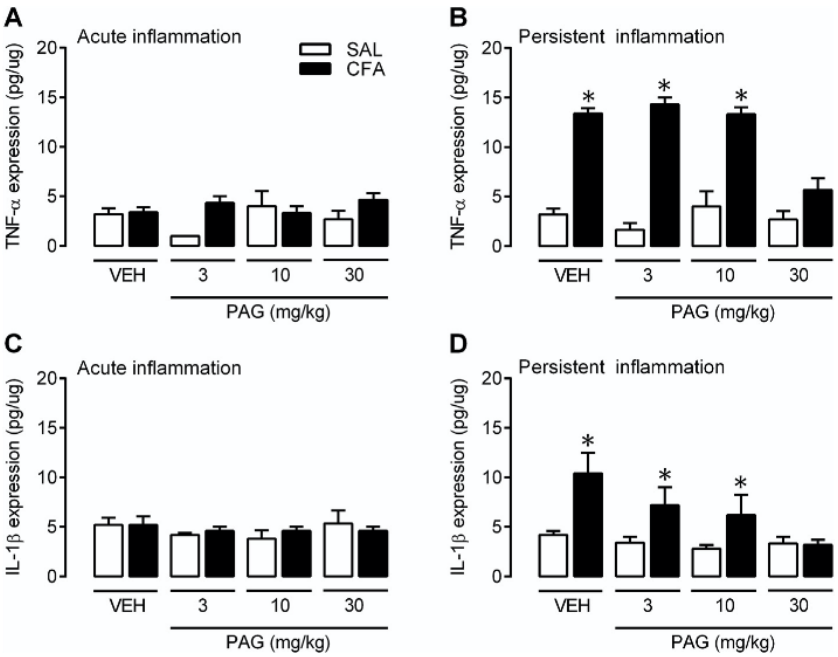

Fig. 4. The major dose of PAG (30 mg/kg) reduces pro-inflammatory cytokines in the trigeminal ganglia after 14 days of CFA-induced persistent temporomandibular inflammation. **A:** Quantification of TNF-α from rats submitted to acute temporomandibular inflammation by using CFA or saline (SAL). **B:** Quantification of TNF-α from rats submitted to persistent temporomandibular inflammation by CFA or injected with saline (SAL). **C:** Quantification of IL-1β from rats submitted to acute temporomandibular inflammation by CFA or injected with saline (SAL). **D:** Quantification of IL-1β from rats submitted to 14 days of temporomandibular inflammation by CFA or injected with saline (SAL). Data are expressed as mean ± standard error of the mean. *P < 0.05, vs. control group (SAL) at the same dose of PAG. #P < 0.05, vs. CFA treated with vehicle of PAG group. The pharmacological treatment consisted of PAG injected locally into the joint at different doses (3, 10, 30 mg/kg) or its vehicle (VEH; saline injection).

Aldrich) and were rapidly euthanized by means of decapitation. To relieve any suffering, decapitation was performed by an experienced person in the area and in a quiet environment. The remaining animals were kept in a separate environment to avoid any influence of the odor of blood. In addition, after each decapitation, the materials were washed and cleaned with 70% alcohol. Brains were immediately removed for TMJ and TG dissection.

2.7. Sample collection

2.7.1. Synovial fluid

The superficial tissues were dissected, and the TMJ cavity was washed two times to collect the synovial fluid by the pumping and aspiration technique using 0.05 mL of EDTA (1.77 mg EDTA/mL PBS). These samples were used for leucocyte count.

2.7.2. Joint tissue and trigeminal ganglion

Temporomandibular joint and trigeminal ganglion were dissected with the help of a magnifying lens (Leica Zoom 2000) and removed

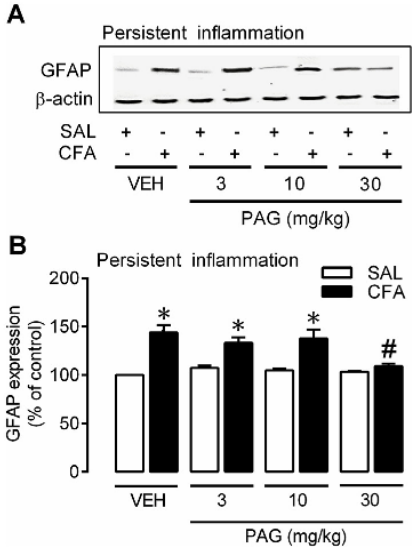

Fig. 5. The persistent state of CFA-induced temporomandibular inflammation (14 days) produced an increased expression of reactive SGCs in trigeminal ganglia and PAG (30 mg/kg) was able to reverse this change. **A:** Representative gel from WB technique indicating expression of GFAP protein in TG from rats submitted to 14 days of temporomandibular inflammation by CFA or injected with Saline and β-actin expression as a control. B: Percentage of GFAP expression in TG from rats submitted to persistent temporomandibular inflammation by CFA or injected with saline (SAL). Data are expressed as mean ± standard error of the mean. *P < 0.05, vs. control group (SAL) at the same dose of PAG. #P < 0.05, vs. CFA treated with vehicle of PAG group. The pharmacological treatment consisted of PAG injected locally into the joint at different doses (3, 10, 30 mg/kg) or its vehicle (VEH; saline injection).

according to Ref. [9]. All joints were weighted and stored in a freezer at −80 °C. These samples were used for ELISA and WB techniques.

2.8. Synovial lavage collection and cell counting

3 or 14 days after CFA injections inducing acute or persistent inflammation, in the temporomandibular joints, respectively, the rats were sacrificed under anesthesia and the synovial fluid from TMJs was collected. The present protocol was based in previously described studies [43]. For the determination of the total number of white cells in the synovial lavage, a total leucocyte count was performed in a Neubauer chamber using 20 µl of articular lavage solution diluted in 380 µl Turk (1:20 dilution).

2.9. TNF-α and IL-1β ELISA assays

The TMJ tissue and the trigeminal ganglion were excised 3 or 14 days after the CFA-injection inducing acute or persistent temporomandibular inflammation, respectively, in rats and were homogenized in a solution of RIPA Lysis Buffer System (Santa Cruz Biotechnology). The samples were centrifuged at 10,000 rpm for 15 min at 4 °C. The supernatants were stored at −80 °C for posterior analysis to evaluate the protein levels of TNF-α and IL-1β in the TMJ tissue and the trigeminal ganglion. The following kits quantified the cytokine levels: TNF-α–Rat TNF-alpha/TNFSF1A Quantikine ELISA Kit (R&D Systems, catalog number RTA00); and IL-1β–Rat IL-1 beta/IL-1F2 Quantikine ELISA Kit (R&D Systems, catalog number DY501). The absorbance was measured at 450 nm. IL-1β and TNF-α concentrations were expressed as pg/µg.

2.10. Western blot (WB) analysis

Trigeminal ganglion (TG) samples were stored at −80 °C until use. The sample was homogenized on ice in 200 µL of tissue in sterile saline using a Polytron® PT 1200 handheld homogenizer (Kinematica Inc). The homogenate was used for WB measurement. For the immunoblot analysis, the protein was isolated from the TGs of both controls and experimental rats. Samples were treated with boiling lysis buffer (1% sodium dodecyl sulfate, 1.0 mM sodium orthovanadate, 10 mM Tris, pH 7.4). Equal amounts (30 µg) of total protein were separated by sodium dodecyl sulfate-polyacrylamide gel electrophoresis (10%) and transferred to polyvinylidene difluoride membranes. Immunostaining of the blots was performed using four primary antibodies, rabbit polyclonal antibody to GFAP, CBS (1:1.000; Millipore and Cell Signaling, respectively) and mouse monoclonal antibody to CSE and anti-β-actin (1:1,000 and 1:10,000; Sigma-Aldrich and Abnova Corporation, respectively). Membranes were then incubated with peroxidase-coupled secondary antibodies (1:2,000; Millipore) for 1 h at room temperature. Blots were developed using the Amersham ECL Prime western blotting detection reagent (GE Healthcare). Densitometric analysis was performed using the Eagle Eye TMII Still Video System (Stratagene).

2.11. Measurements of H_2S production rate in the TMJ and TG

To test our hypothesis that H_2S production is altered in TMJ and TG, we measured H_2S production rate in homogenates of these tissues of animals with or without temporomandibular inflammation. TMJs and TGs samples were homogenized in potassium phosphate buffer (100 mM; pH 7.4) using a microprocessor (VirTis, Gardiner). Each sample (50% w/v; 100 µl) contained L-cysteine (10 mM; 20 µl), pyridoxal 5′-phosphate (2 mM; 20 µl) and PBS (30 µl). The reaction was performed in eppendorf tubes sealed with parafilm, and started by transferring the tubes from ice to bath at 37 °C. After 2 h incubation, zinc acetate (1% w/v; 100 µl) was included to trap evolved H_2S followed by tricloroacetic acid (10% w/v; 100 µl) to precipitate proteins and thus finalize the reaction. After centrifugation, *N*,*N*-dimethyl-p-phenylenediamine sulfate (20 mM; 50 µl) in HCl 7.2 M followed by $FeCl_3$ (30 mM; 50 µl) in HCl 1.2 M was then added to 50 µl of the supernatant, and optical density was measured at 670 nm. The H_2S concentration of each sample was calculated against a calibration curve of absorbance of Na_2S solutions (0.1–100 µg/mL). To quantified the protein content of the samples, the pellets were diluted in 4 mL of sodium hydroxide (0.1 N) and the solution was then assayed by using a protein dye reagent (Bio-Rad Laboratories; code number: 500–0006). NaSH (0–250 µM). The results were expressed as nmol/mg proteins per 1 h.

2.12. Statistical analysis

The data are presented as the mean ± SEM when appropriate. Differences between means were compared using two-way ANOVA followed by the Student-Newman-Keuls post-test. A value of $p < 0.05$ indicated significant differences.

3. Results

3.1. Endogenous H_2S mediates mechanical orofacial acute and persistent inflammatory hypernociception

Recent studies have shown a dual role of H_2S in inflammatory hypernociception. Pro- and anti-nociceptive functions have been recognized for this endogenous gas until now [39]. Notably, on the orofacial region, evidence has indicated H_2S exerting a pro-nociceptive effect [28,29,44]. The present study evaluated the effect of the pretreatment of rats with PAG (3–30 mg/kg) on the nociceptive mechanical threshold (Fig. 2A and B), as well as chemical nociception (Fig. 2C and D) in the orofacial region. These data show decreased hyperalgesia

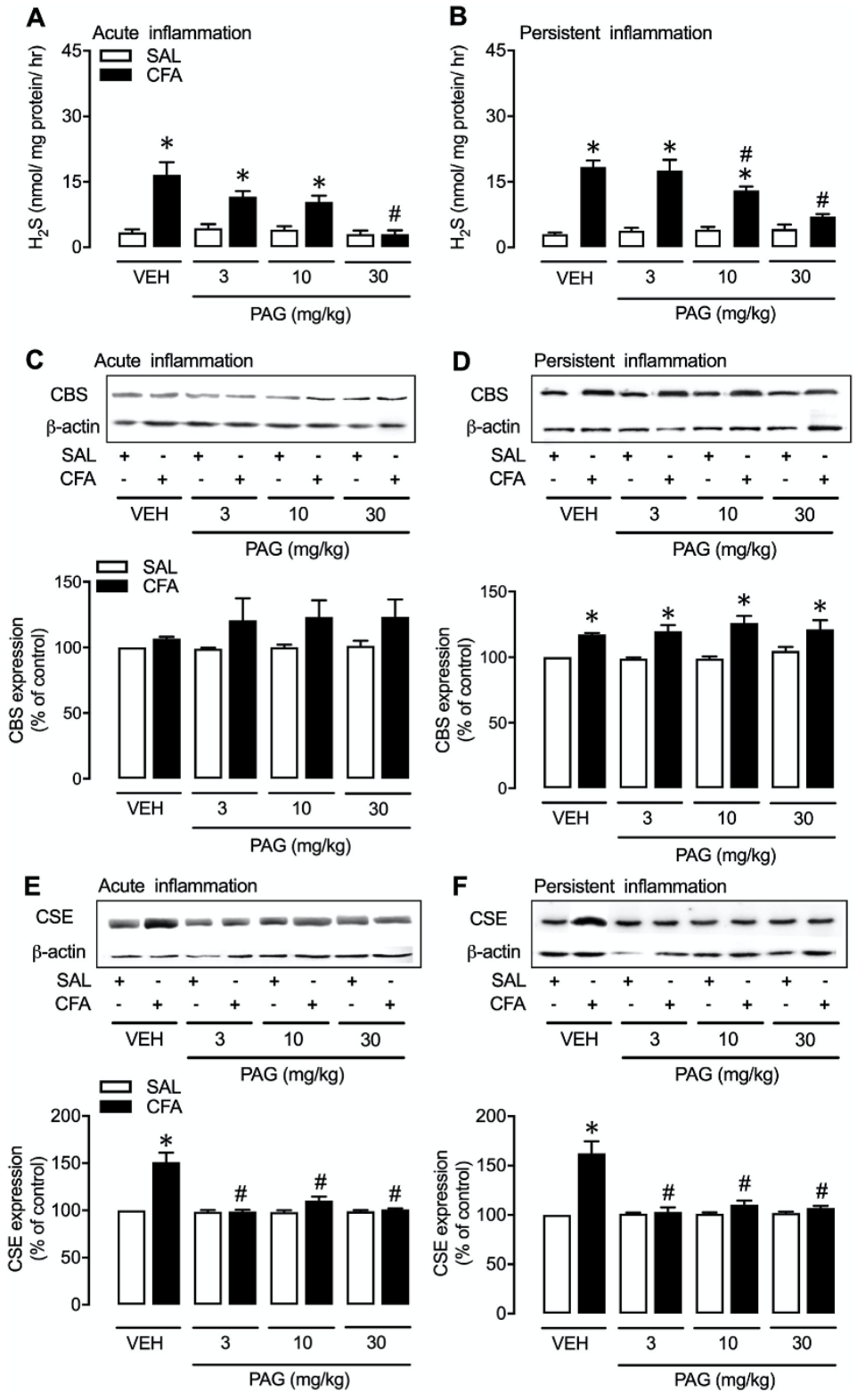

(caption on next page)

Fig. 6. Acute and persistent state of CFA-induced temporomandibular inflammation (3 and 14 days) and the H_2S production rate (A, B), CBS (C, D) and CSE (E, F) expression in the TMJ. Data are expressed as mean ± standard error of the mean. Representative gel from WB technique indicating expression of each protein in the TMJ is shown at the top of its respective graph. β-actin expression was used as a control.*$P < 0.05$, vs. control group (SAL) at the same dose of PAG. #$P < 0.05$, vs. CFA treated with vehicle of PAG. The pharmacological treatment consisted of PAG injected locally into the joint at different doses (3, 10, 30 mg/kg) or its vehicle (VEH; saline injection).

and allodynia in CFA-induced acute or persistent temporomandibular inflammation rats treated with PAG. The only exception was on the mechanical threshold of animals that received 3 mg/kg of PAG acutely, since there was no difference between its control (SAL) at same dose of PAG.

3.2. Leucocyte migration seems to be involved in the pro-nociceptive role of endogenous H_2S

Research groups have shown that neutrophils and leucocytes [39,45–47] play an important role in the genesis of inflammatory hypernociception. Since endogenous H_2S production has been shown to be involved in the recruitment of inflammatory cells [27,48] during the inflammatory disease, we tested the hypothesis that leucocyte recruitment mediates the inflammatory hypernociception also in orofacial processes. Our data consistently show that PAG (3–30 mg/kg) pretreatment inhibited CFA-induced leucocyte migration to temporomandibular synovial fluid (Table 1). This effect was observed in the acute and persistent phase of the inflammation.

3.3. Endogenous H_2S inhibition reduce joint tissue TNF-α and IL-1β in both, acute and persistent phases of temporomandibular pain

Based on the TMJ-leucocyte role in the effect of H_2S inhibition as an anti-nociceptive mechanism and considering also previous results about plasmatic extravasation on TMJ mediating this reaction [29], we now investigate the role of the main inflammatory cytokines related to inflammatory hypernociception on pro-nociceptive H_2S function. The data evidenced on TNF-α and IL-1β on temporomandibular tissue from CFA-induced inflamed rats after treatment with PAG, in acute and persistent inflammation development in all doses tested (Fig. 3).

3.4. Endogenous H_2S inhibition reduce TNF-α and IL-1β in trigeminal ganglion in persistent phase of temporomandibular pain

Considering that H_2S exerts an effect on the periphery and also on the nervous system [39], it is important to evaluate if, in our temporomandibular inflammation model, there is some indication of neural plasticity. The first structure on the nervous system related to the processing of orofacial nociceptive information is the trigeminal ganglion, which contains the bodies of the primary neurons participating in this modulation. There are significant findings of H_2S effects on neuron excitability [30,49], receptors [44] and enzymes (CBS and CSE [8]) on trigeminal ganglion. However, the present study is the pioneer in analyzing inflammatory cytokines in this structure after H_2S inhibition (Fig. 4). Our data support the idea that PAG is able to reduce the production of TNF-α and IL-1β on trigeminal ganglion in a persistent temporomandibular inflammation in a dose of 30 mg/kg. The other doses had no significant effect. Remarkably, the highest dose of PAG was able to block the CFA-induced IL-1β increase at 14 days of inflammation, since it was not observed statistical difference between its control (SAL) at the same dose of PAG (Fig. 4D).

3.5. The reduction of TNF-α and IL-1β in the TG in the persistent phase of temporomandibular pain is accompanied by reduction activation of satellite glial cells (SGCs) in trigeminal ganglion induced by endogenous H_2S inhibition

Following an abnormally intense pain elicited by noxious stimuli, increased levels of Anti-Glial Fibrillary Acidic Protein (GFAP), a marker of activated glial cells, can be detected [50]. This effect occurs in the CNS as well as in the peripheral nervous system on nervous ganglia, as TG [51]. This glial activation leads to pro-inflammatory cytokines like TNF-α and IL-1β [52]. Fig. 5B precisely shows increased activation of SGCs in TG on the 14th day of temporomandibular inflammation. Interestingly, the highest dose of PAG (30 mg/kg) was able to prevent this stimulation, since, after the therapy; the levels of GFAP protein expression on TG are in basal conditions, found by Western blotting analysis (Fig. 5).

3.6. Endogenous H_2S inhibition reduces TMJ and TG H2S production rate in both, acute and persistent phases of temporomandibular pain

The production rate of H_2S was measured in TMJ and TG samples of Wistar rats at 3 and 10 days of inflammation treated or not with PAG (Fig. 6A and B; 7A, B, respectively). Fig. 6A and B precisely show increased H_2S production rate in the TMJs after 3 and 14 days of CFA induced inflammation and specific doses of PAG inhibiting this H2S elevation in both acute inflammation (PAG – 30 mg/kg) and persistent process (PAG – 10 and 30 mg/kg). In the same manner, Fig. 7A and B presents an increased H_2S production rate in the TG after 3 and 14 days of CFA-induced inflammation and all doses of PAG inhibiting this H_2S elevation in both acute inflammation and persistent process.

3.7. CSE (but not CBS) expression is increased in the TMJ in the acute phase of temporomandibular pain

CSE and CBS expression were measured in TMJ samples of Wistar rats at 3 and 10 days (acute and persistent inflammation, respectively) of inflammation treated or not with PAG (Fig. 6). It was observed that the inflammatory response and consequently the acute pain observed at the initial days of this model is only related to an increase in the expression of CSE in the TMJ and this response was abolished using PAG (Fig. 6C, E).

3.8. CSE and CBS expression are increased in the TMJ in the persistent phase of temporomandibular pain

Interestingly, CSE expression was maintained increased (Fig. 6F), but an increase in CBS expression in the TMJ was observed at the persistent phase of inflammation (Fig. 6D). This result indicates that CBS overexpression in the TMJ is a consequence of the neuro-immune interaction at the persistent phase of this inflammation model. Unfortunately, PAG was not capable of decrease the expression of CBS in the TMJ of rats with persistent inflammation.

3.9. TG CSE and CBS expression are increased in both, acute and persistent phases of TMJ pain and PAG treatment caused a decrease in the expression of CBS and CSE in the TG

As expected [8], the overexpression of CBS in the TG was observed at the acute and persistent phase of inflammation induced in the TMJ area (Fig. 7C and D). Likewise, CSE expression was also increased in the TG of Wistar rats in both phases of inflammation indicating its role in orofacial inflammatory response (Fig. 7E and F). The peripheral treatment with PAG caused a decrease not only in the expression of CSE in the TMJ (Fig. 6E and F) but also in the TG, indicating its action centrally. Also, the highest dose of PAG used here caused a decrease in CBS

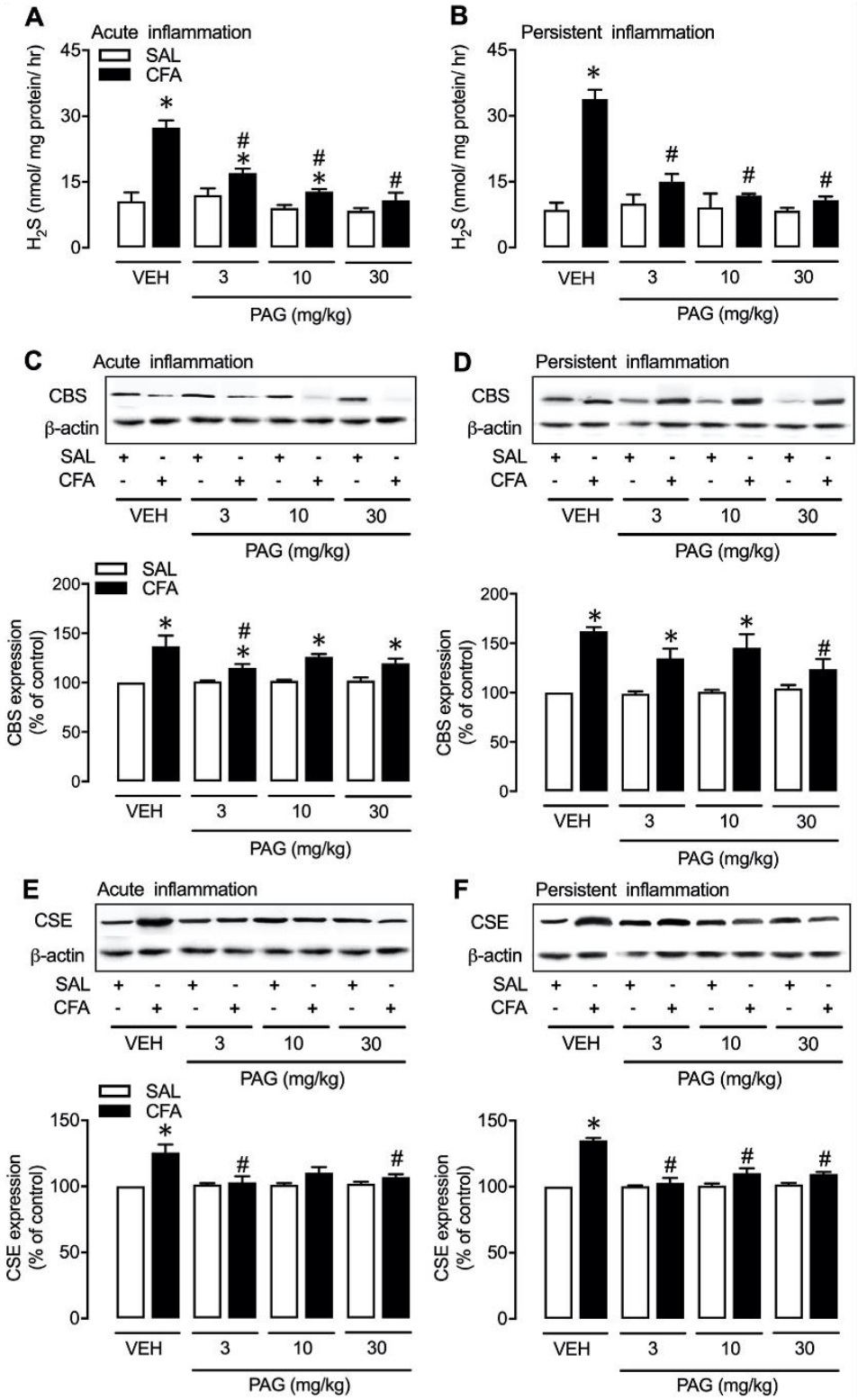

(caption on next page)

Fig. 7. Acute and persistent state of CFA-induced temporomandibular inflammation (3 and 14 days) and the H_2S production rate (A, B), CBS (C, D) and CSE (E, F) expression in the TG. Data are expressed as mean ± standard error of the mean. Representative gel from WB technique indicating expression of each protein in the TMJ is shown at the top of its respective graph. β-actin expression was used as a control.*P < 0.05, vs. control group (SAL) at the same dose of PAG. #P < 0.05, vs. CFA treated with vehicle of PAG. The pharmacological treatment consisted of PAG injected locally into the joint at different doses (3, 10, 30 mg/kg) or its vehicle (VEH; saline injection).

expression in the TMJ (Fig. 7D), highlighting the importance of CBS in the TMJ inflammatory-induced pain.

4. Discussion

We recently reported that a CSE inhibitor was able to produce an anti-nociceptive effect induced by temporomandibular inflammation which was accompanied by the decrease in joint region-plasmatic extravasation [29]. Since local injection has shown consistent results in this nociception model, PAG was injected on TMJs in distinct doses. We demonstrate here that the endogenous H_2S could upregulate cytokine production in both, TMJ and TG tissue, contributing to TMJ inflammatory hypernociception. These results are based on the PAG effect in local tissue (TMJ) and trigeminal ganglion (TG). Moreover, this study is pioneer in detecting molecularly H_2S production rate in TMJ and TG of rats with CFA-induced temporomandibular inflammation treated with PAG at distinct doses, as well as, in two phases of orofacial pain (acute and persistent).

The periods of 3 and 14 days after CFA injection used for analysis were established based on previous evidences with CFA-induced inflammation [53]. The two periods chosen for the analysis of this study show a peak of the acute phase of the CFA effect as an inflammatory agent and an established chronic inflammatory phase of the painful state, respectively. According to reports in the literature, CFA as an inflammatory inducing agent may be active within 42 days of experimentation [54], and this model is one of the major types to show long-lasting chronic pain [55]. In general, the CFA model stability starts to represent severe hypersensitivity to mechanical and thermal stimulation from one to three days [53]. Importantly, this model also presents an advantage to produce neuroplasticity in diverse parts from the central and the peripheral nervous system [56]. In fact, besides cellular alterations [57], synaptic transmission is altered in critical cortical areas for nociceptive and chronic pain processing after a CFA-induced peripheral inflammation [53].

Our results show an acute and persistent nociceptive profile in rats injected with CFA in the temporomandibular joints. These results are consistent with previous studies showing the greater effectiveness of CFA compared to other irritants inducing articular inflammation in various periods of time [58,59]. Evidently, PAG was able to reduce the nociceptive behavior, in both phases of pain, suggesting an acute and chronic pro-nociceptive role of H_2S in orofacial inflammatory pain.

Physiological gaseous mediators have been proposed to induce, inhibit and regulate the inflammatory process [60]. We believe that the antinociceptive effect of inhibition of H_2S synthesis is directly related to its anti-inflammatory action. The number of leucocytes and proinflammatory cytokines on TMJ of CFA-inflamed rats were reduced by PAG injection. Accordingly, Andruski [61] used an acutely inflamed knee joints model to show an H_2S effect on leucocyte-endothelium interactions. The authors reveal that H_2S has the propensity to interfere in the generation of mediators necessary for leucocyte recruitment. Again, the absence of leucocyte trafficking was attributed to an alteration in the expression of adhesion molecules and their associated ligands in the synovial microvasculature. Considering our results about leucocytes count on synovial fluid and an inflamed joint model used for us, it is possible that PAG effects on leucocytes are related to these impairments on the infiltration of leukocytes into the temporomandibular joint.

Leucocyte growth and differentiation are stimulated by cytokines in an inflammatory process [62]. The proinflammatory cytokines tumor necrosis factor (TNF) α, and interleukin (IL) 1β have been strongly implicated in the pathogenesis of chronic pain [63]. In addition, TNF-α and IL-1β are mediators associated with structural changes found in osteoarthritis or other arthritic conditions of the TMJ [64,65]. In agreement, these cytokines reduce the expression of type II collagen and aggrecan by the increased secretion of matrix metalloproteinases by chondrocytes, favoring joint destruction [66]. We observed increased levels of TNF-α and IL-1β in TMJ tissue on the 3rd and 14th days after inflammation induction. Consistent with our results, other studies showed statistically higher concentrations of these proinflammatory mediators upon induction of articular inflammation in acute [40], intermediate [67] and chronic phases [58,68]. The inhibition of H_2S synthesis caused a reduction of these levels in both phases of pain and the three doses of PAG were effective. In agreement, the literature shows this ability of PAG in decreasing these cytokines during inflammatory states [27,69]. In the data, nothing was known in relation to the temporomandibular joint or orofacial structures, which reinforces the novelty of the present study.

Moreover, we observed a reduction in TNF-α and IL-1β in the trigeminal ganglion (TG) after PAG treatment in rats from 14 days of CFA-induced temporomandibular inflammation. This effect was found when 30 mg/kg of PAG was administered. In the trigeminal ganglia, TNF- α is mostly produced by the satellite reactive glial cells which increases BDNF expression suggesting its role in neuroplasticity [70]. Reconciling the neuroplastic effect of TNF- α with our data, we suggest that there is a process of neuroplasticity installed in the structure. This process includes morphological, physiological and neurochemical modifications of the cells that make up the neural tissue, including both neurons and glial ones [71]. Satellite glial cells (SGCs) are the main type of glia in sensory ganglia, such as TG, and SGCs can proliferate under pathological conditions [72], upregulating glial fibrillary acidic protein (GFAP) and interleukin-1β, augmenting intercellular coupling to increase gap junctions [73] as evidenced by upregulation of gap junction connexin 43 [73], and altering electrophysiological properties [74]. Such changes suggest that glial cell activation in peripheral ganglia participates in nociception [75,76]. Furthermore, TNF-α expression increases in dorsal root ganglion which has been immunoreactively detected in SGCs and neuronal bodies after neuropathic hyperalgesia [77,78]. In fact, according to the literature, glial cells are able to produce pro-inflammatory substances in the face of insults, such as a nociceptive state [79,80]. They become reactive through proliferation, conformational change, and production of these pro-inflammatory agents. These events participate in the neuroplasticity process and normally occur in chronic conditions of injury with the goal of adjusting the tissue to the ongoing condition and ensure the system is sensitized [81].

The pro-inflammatory changes observed in our work in TG occurred after 14 days of inflammation that is indicative of the neuroplasticity installed in this structure. PAG was effective in controlling the inflammation and pain evoked by CFA on TMJs, not only blocking local alterations, but also modulating the information transmitted by peripheral sensory nerve endings. This proposal is further supported by the data found in the analysis of GFAP expression in TG. Our results evidenced that the increase of pro-inflammatory cytokines in this region induced by the inflammatory state in the TMJs at 14 days. This response was accompanied by an increase in activated SCGs. Similarly; the robust reduction in pro-inflammatory response caused by PAG locally was also reproduced for glial cells. In fact, elegant studies have suggested that SGCs are also involved in the peripheral mechanisms of pain facilitation. Morphologically, the cell bodies of TG neurons are completely surrounded by several SGCs, forming distinct functional

units [82]. Following an abnormally intense pain elicited by noxious stimuli, increased levels of GFAP, a marker of activated glia cells, can be detected [50]. The activated SGCs may directly influence neuronal activity by releasing inflammatory mediators such as IL-1β and TNF-α, contributing to the development and maintenance of allodynia and hyperalgesia responses [15]. Our suggestion is that the local H_2S acts on neuro-immune interactions inducing painful states from orofacial regions since its action was not restricted to local effects, but it also increases central pain sensitization by increasing the production of IL-1β and TNF-α in the TG and facilitating glial activation. This suggestion is sustained not only by the increase overproduction rate of H_2S, by also by the overexpression of CSE and CBS in both tissues.

Miao [8] observed that CBS overexpression in the trigeminal ganglia contributes to inflammatory pain in the TMJ. Here, we add the importance of TMJ CBS/H_2S pathway in the induction of persistent TMJ pain. It is also described in the literature that H_2S production is increased after inflammatory stimuli and thus, stimulates TRPV1 receptors which are intrinsically involved in central pain sensitization [15,83]. Our hypothesis is that CFA induces inflammation and, consequently, can increase H_2S production in the TMJ. This increase in H_2S levels activate TRPV1 receptors in the nerve sensory endings facilitating central pain sensitization leading to CBS and CSE overexpression in the trigeminal ganglia.

The analysis of H_2S production rate, CBS and CSE expression in both tissues, TMJ and TG are firstly described by the present data. Our evidences indicate an increased H_2S production rate in both structures after the temporomandibular inflammation stimulation and interestingly, PAG treatment prevented this elevation, strongly suggesting a modulation of H_2S as one of the mechanisms for temporomandibular nociception and indicating H_2S as a proinflammatory and pro-nociceptive endogenous gas for orofacial conditions.

5. Conclusion

For the first time, we elucidated one of the molecular mechanisms, acting in the nervous system, both locally and peripherally (TG), by which H_2S plays a role as a pro-inflammatory and pro-nociceptive endogenous gas for orofacial conditions. The pathophysiologic relevance of our findings is consistent in deepening the search for new therapeutic targets for TMDs.

Funding

This work was supported by the FAPESP [grant numbers #15/03053-3; #16/17681-9; #17/03645-3 and #16/09364-3, São Paulo Research Foundation]; CNPq and Capes.

Declaration of competing interest

We have no conflict of interest to declare.

Acknowledgements

We are grateful for Grant Thomas Harris' English writing support.

Appendix A. Supplementary data

Supplementary data to this article can be found online at https://doi.org/10.1016/j.niox.2019.10.001.

References

[1] L.N. Melek, M. Devine, T. Renton, The psychosocial impact of orofacial pain in trigeminal neuralgia patients: a systematic review, Int. J. Oral Maxillofac. Surg. 47 (2018) 869–878, https://doi.org/10.1016/j.ijom.2018.02.006.

[2] M.J. Racich, Occlusion, temporomandibular disorders, and orofacial pain: an evidence-based overview and update with recommendations, J. Prosthet. Dent. 120 (2018) 678–685, https://doi.org/10.1016/j.prosdent.2018.01.033.

[3] O.C. Eller-Smith, A.L. Nicol, J.A. Christianson, Potential mechanisms underlying centralized pain and emerging therapeutic interventions, Front. Cell. Neurosci. 12 (2018) 35, https://doi.org/10.3389/fncel.2018.00035.

[4] M.M. Sperry, M.E. Ita, S. Kartha, S. Zhang, Y.-H. Yu, B. Winkelstein, The interface of mechanics and nociception in joint pathophysiology: insights from the facet and temporomandibular joints, J. Biomech. Eng. 139 (2017), https://doi.org/10.1115/1.4035647.

[5] M. V Hamity, R.Y. Walder, D.L. Hammond, Increased neuronal expression of neurokinin-1 receptor and stimulus-evoked internalization of the receptor in the rostral ventromedial medulla of the rat after peripheral inflammatory injury, J. Comp. Neurol. 522 (2014) 3037–3051, https://doi.org/10.1002/cne.23564.

[6] M. Llorián-Salvador, S. González-Rodríguez, A. Lastra, M.T. Fernández-García, A. Hidalgo, L. Menéndez, A. Baamonde, Involvement of CC chemokine receptor 1 and CCL3 in acute and chronic inflammatory pain in mice, Basic Clin. Pharmacol. Toxicol. 119 (2016) 32–40, https://doi.org/10.1111/bcpt.12543.

[7] H. Imbe, K. Iwata, Q.Q. Zhou, S. Zou, R. Dubner, K. Ren, Orofacial deep and cutaneous tissue inflammation and trigeminal neuronal activation. Implications for persistent temporomandibular pain, Cells Tissues Organs 169 (2001) 238–247, https://doi.org/10.1159/000047887.

[8] X. Miao, X. Meng, G. Wu, Z. Ju, H.-H. Zhang, S. Hu, G.-Y. Xu, Upregulation of cystathionine-β-synthetase expression contributes to inflammatory pain in rat temporomandibular joint, Mol. Pain 10 (2014) 9, https://doi.org/10.1186/1744-8069-10-9.

[9] G.C. do Nascimento, C.R.A. Leite-Panissi, Time-dependent analysis of nociception and anxiety-like behavior in rats submitted to persistent inflammation of the temporomandibular joint, Physiol. Behav. 125 (2014) 1–7, https://doi.org/10.1016/j.physbeh.2013.11.009.

[10] A.D. Cook, A.D. Christensen, D. Tewari, S.B. McMahon, J.A. Hamilton, Immune cytokines and their receptors in inflammatory pain, Trends Immunol. 39 (2018) 240–255, https://doi.org/10.1016/j.it.2017.12.003.

[11] S.F. Ahmad, M.A. Ansari, K.M.A. Zoheir, S.A. Bakheet, H.M. Korashy, A. Nadeem, A.E. Ashour, S.M. Attia, Regulation of TNF-α and NF-κB activation through the JAK/STAT signaling pathway downstream of histamine 4 receptor in a rat model of LPS-induced joint inflammation, Immunobiology 220 (2015) 889–898, https://doi.org/10.1016/j.imbio.2015.01.008.

[12] N. Yeremenko, K. Zwerina, G. Rigter, D. Pots, J.E. Fonseca, J. Zwerina, G. Schett, D. Baeten, Brief report: tumor necrosis factor and interleukin-6 differentially regulate dkk-1 in the inflamed arthritic joint, Arthritis Rheum. 67 (2015) 2071–2075, https://doi.org/10.1002/art.39183.

[13] S.V. Kellesarian, A.A. Al-Kheraif, F. Vohra, A. Ghanem, H. Malmstrom, G.E. Romanos, F. Javed, Cytokine profile in the synovial fluid of patients with temporomandibular joint disorders: a systematic review, Cytokine 77 (2016) 98–106, https://doi.org/10.1016/j.cyto.2015.11.005.

[14] J.W. Park, J.W. Chung, Inflammatory cytokines and sleep disturbance in patients with temporomandibular disorders, J. Oral Facial Pain Headache 30 (2016) 27–33, https://doi.org/10.11607/ofph.1367.

[15] F.A. Pinho-Ribeiro, W.A. Verri, I.M. Chiu, Nociceptor sensory neuron–immune interactions in pain and inflammation, Trends Immunol. 38 (2017) 5–19, https://doi.org/10.1016/j.it.2016.10.001.

[16] G. Villa, S. Ceruti, M. Zanardelli, G. Magni, L. Jasmin, P.T. Ohara, M.P. Abbracchio, Temporomandibular joint inflammation activates glial and immune cells in both the trigeminal ganglia and in the spinal trigeminal nucleus, Mol. Pain 6 (2010) 89, https://doi.org/10.1186/1744-8069-6-89.

[17] Q. Bai, S. Liu, H. Shu, Y. Tang, S. George, T. Dong, B.L. Schmidt, F. Tao, TNFα in the trigeminal nociceptive system is critical for temporomandibular joint pain, Mol. Neurobiol. 56 (2019) 278–291, https://doi.org/10.1007/s12035-018-1076-y.

[18] G.K. Kolluru, X. Shen, S.C. Bir, C.G. Kevil, Hydrogen sulfide chemical biology: pathophysiological roles and detection, Nitric Oxide Biol. Chem. 35 (2013) 5–20, https://doi.org/10.1016/j.niox.2013.07.002.

[19] L. Li, M. Bhatia, Y.Z. Zhu, Y.C. Zhu, R.D. Ramnath, Z.J. Wang, F.B.M. Anuar, M. Whiteman, M. Salto-Tellez, P.K. Moore, Hydrogen sulfide is a novel mediator of lipopolysaccharide-induced inflammation in the mouse, FASEB J. 19 (2005) 1196–1198, https://doi.org/10.1096/fj.04-3583fje.

[20] C. Szabó, Hydrogen sulphide and its therapeutic potential, Nat. Rev. Drug Discov. 6 (2007) 917–935, https://doi.org/10.1038/nrd2425.

[21] S. Fiorucci, S. Orlandi, A. Mencarelli, G. Caliendo, V. Santagada, E. Distrutti, L. Santucci, G. Cirino, J.L. Wallace, Enhanced activity of a hydrogen sulphide-releasing derivative of mesalamine (ATB-429) in a mouse model of colitis, Br. J. Pharmacol. 150 (2007) 996–1002, https://doi.org/10.1038/sj.bjp.0707193.

[22] M. Matsunami, T. Tarui, K. Mitani, K. Nagasawa, O. Fukushima, K. Okubo, S. Yoshida, M. Takemura, A. Kawabata, Luminal hydrogen sulfide plays a pronociceptive role in mouse colon, Gut 58 (2009) 751–761, https://doi.org/10.1136/gut.2007.144543.

[23] J.L. Wallace, J.G.P. Ferraz, M.N. Muscara, Hydrogen sulfide: an endogenous mediator of resolution of inflammation and injury, Antioxidants Redox Signal. 17 (2012) 58–67, https://doi.org/10.1089/ars.2011.4351.

[24] M. Bhatia, J. Sidhapuriwala, S.M. Moochhala, P.K. Moore, Hydrogen sulphide is a mediator of carrageenan-induced hindpaw oedema in the rat, Br. J. Pharmacol. 145 (2005) 141–144, https://doi.org/10.1038/sj.bjp.0706186.

[25] T.M. Cunha, W.A. Verri, Hydrogen sulfide, is it a promise analgesic drug or another inflammatory pain mediator? Pain 130 (2007) 300–302, https://doi.org/10.1016/j.pain.2007.04.036.

[26] G. Yang, L. Wu, B. Jiang, W. Yang, J. Qi, K. Cao, Q. Meng, A.K. Mustafa, W. Mu, S. Zhang, S.H. Snyder, R. Wang, H2S as a physiologic vasorelaxant: hypertension in

mice with deletion of cystathionine gamma-lyase, Science 322 (2008) 587–590, https://doi.org/10.1126/science.1162667.
[27] H. Zhang, L. Zhi, S.M. Moochhala, P.K. Moore, M. Bhatia, Endogenous hydrogen sulfide regulates leukocyte trafficking in cecal ligation and puncture-induced sepsis, J. Leukoc. Biol. 82 (2007) 894–905, https://doi.org/10.1189/jlb.0407237.
[28] A.F. Donatti, R.M. Araujo, R.N. Soriano, L.U. Azevedo, C.A. Leite-Panissi, L.G.S. Branco, Role of hydrogen sulfide in the formalin-induced orofacial pain in rats, Eur. J. Pharmacol. 738 (2014) 49–56, https://doi.org/10.1016/j.ejphar.2014.05.023.
[29] B.M. Santos, E.G. Garattini, L.G.S. Branco, C.R.A. Leite-Panissi, G.C. Nascimento, The therapeutic potential of cystathionine gamma-lyase in temporomandibular inflammation-induced orofacial hypernociception, Physiol. Behav. 188 (2018) 128–133, https://doi.org/10.1016/j.physbeh.2018.02.007.
[30] X. Feng, Y.-L. Zhou, X. Meng, F.-H. Qi, W. Chen, X. Jiang, G.-Y. Xu, Hydrogen sulfide increases excitability through suppression of sustained potassium channel currents of rat trigeminal ganglion neurons, Mol. Pain 9 (2013) 4, https://doi.org/10.1186/1744-8069-9-4.
[31] K.G. Usunoff, E. Marani, J.H. Schoen, The trigeminal system in man, Adv. Anat. Embryol. Cell Biol. 136 (I–X) (1997) 1–126.
[32] E. Marani, K.G. Usunoff, The trigeminal motonucleus in man, Arch. Physiol. Biochem. 106 (1998) 346–354, https://doi.org/10.1076/apab.106.5.346.4364.
[33] N.E. Lazarov, The mesencephalic trigeminal nucleus in the cat, Adv. Anat. Embryol. Cell Biol. 153 (2000) 1–103 iii–xiv.
[34] N.E. Lazarov, Comparative analysis of the chemical neuroanatomy of the mammalian trigeminal ganglion and mesencephalic trigeminal nucleus, Prog. Neurobiol. 66 (2002) 19–59 http://www.ncbi.nlm.nih.gov/pubmed/11897404 , Accessed date: 17 September 2019.
[35] N.F. Copra, K.V. Anderson, R.C. Atkinson, Localization and morphometric analysis of masticatory muscle afferent neurons in the nucleus of the mesencephalic root of the trigeminal nerve in the cat, Cells Tissues Organs 122 (1985) 115–125, https://doi.org/10.1159/000145992.
[36] Y. Shigenaga, M. Sera, T. Nishimori, S. Suemune, M. Nishimura, A. Yoshida, K. Tsuru, The central projection of masticatory afferent fibers to the trigeminal sensory nuclear complex and upper cervical spinal cord, J. Comp. Neurol. 268 (1988) 489–507, https://doi.org/10.1002/cne.902680403.
[37] R.N. Soriano, S.P. Braga, J.S.C. Breder, M.E. Batalhao, G.R. Oliveira-Pelegrin, L.F.R. Ferreira, M.J.A. Rocha, E.C. Carnio, L.G.S. Branco, Endogenous peripheral hydrogen sulfide is propyretic: its permissive role in brown adipose tissue thermogenesis in rats, Exp. Physiol. 103 (2018) 397–407, https://doi.org/10.1113/EP086775.
[38] X. Zhou, S. Tang, K. Hu, Z. Zhang, P. Liu, Y. Luo, J. Kang, L. Xu, dl-Propargylglycine protects against myocardial injury induced by chronic intermittent hypoxia through inhibition of endoplasmic reticulum stress, Sleep Breath. 22 (2018) 853–863, https://doi.org/10.1007/s11325-018-1656-0.
[39] T.M. Cunha, D. Dal-Secco, W.A. Verri, A.T. Guerrero, G.R. Souza, S.M. Vieira, C.M. Lotufo, A.F. Neto, S.H. Ferreira, F.Q. Cunha, Dual role of hydrogen sulfide in mechanical inflammatory hypernociception, Eur. J. Pharmacol. 590 (2008) 127–135, https://doi.org/10.1016/j.ejphar.2008.05.048.
[40] R.P. Harper, C.A. Kerins, J.E. McIntosh, R. Spears, L.L. Bellinger, Modulation of the inflammatory response in the rat TMJ with increasing doses of complete Freund's adjuvant, Osteoarthr. Cartil. 9 (2001) 619–624, https://doi.org/10.1053/joca.2001.0461.
[41] Q. Zhou, H. Imbe, R. Dubner, K. Ren, Persistent Fos protein expression after orofacial deep or cutaneous tissue inflammation in rats: implications for persistent orofacial pain, J. Comp. Neurol. 412 (1999) 276–291, https://doi.org/10.1002/(sici)1096-9861(19990920)412:2<276::aid-cne7>3.0.co;2-9.
[42] T.S. Grabow, P.M. Dougherty, Gabapentin produces dose-dependent antinociception in the orofacial formalin test in the rat., Reg. Anesth. Pain Med. 27 (n.d.) 277-283. http://www.ncbi.nlm.nih.gov/pubmed/12016601 (accessed September 18, 2019).
[43] F.F.B. de Oliveira, J.C.B. de Araújo, A.F. Pereira, G.A.C. Brito, D.V. Gondim, R. de A. Ribeiro, I.R.A. de Menezes, M.L. Vale, Antinociceptive and anti-inflammatory effects of Caryocar coriaceum Wittm fruit pulp fixed ethyl acetate extract on zymosan-induced arthritis in rats, J. Ethnopharmacol. 174 (2015) 452–463, https://doi.org/10.1016/j.jep.2015.08.017.
[44] K. Koroleva, A. Mustafina, A. Yakovlev, A. Hermann, R. Giniatullin, G. Sitdikova, Receptor mechanisms mediating the pro-nociceptive action of hydrogen sulfide in rat trigeminal neurons and meningeal afferents, Front. Cell. Neurosci. 11 (2017), https://doi.org/10.3389/fncel.2017.00226.
[45] A.T.G. Guerrero, W.A. Verri, T.M. Cunha, T.A. Silva, I.R.S. Schivo, D. Dal-Secco, C. Canetti, F.A.C. Rocha, C.A. Parada, F.Q. Cunha, S.H. Ferreira, Involvement of LTB_4 in zymosan-induced joint nociception in mice: participation of neutrophils and PGE_2, J. Leukoc. Biol. 83 (2008) 122–130, https://doi.org/10.1189/jlb.0207123.
[46] J.D. Levine, J. Gooding, P. Donatoni, L. Borden, E.J. Goetzl, The role of the polymorphonuclear leukocyte in hyperalgesia, J. Neurosci. 5 (1985) 3025–3029 http://www.ncbi.nlm.nih.gov/pubmed/2997412 , Accessed date: 17 September 2019.
[47] T.M. Cunha, W.A. Verri, I.R. Schivo, M.H. Napimoga, C.A. Parada, S. Poole, M.M. Teixeira, S.H. Ferreira, F.Q. Cunha, Crucial role of neutrophils in the development of mechanical inflammatory hypernociception, J. Leukoc. Biol. 83 (2008) 824–832, https://doi.org/10.1189/jlb.0907654.
[48] M. Bhatia, Hydrogen sulfide as a vasodilator, IUBMB Life 57 (2005) 603–606, https://doi.org/10.1080/15216540500217875.
[49] V. Wild, K. Messlinger, M.J.M. Fischer, Hydrogen sulfide determines HNO-induced stimulation of trigeminal afferents, Neurosci. Lett. 602 (2015) 104–109, https://doi.org/10.1016/j.neulet.2015.06.056.
[50] S. Matsuura, K. Shimizu, M. Shinoda, K. Ohara, B. Ogiso, K. Honda, A. Katagiri, B.J. Sessle, K. Urata, K. Iwata, Mechanisms underlying ectopic persistent tooth-pulp pain following pulpal inflammation, PLoS One 8 (2013), https://doi.org/10.1371/journal.pone.0052840.
[51] R. Ito, M. Shinoda, K. Honda, K. Urata, J. Lee, M. Maruno, K. Soma, S. Okada, N. Gionhaku, K. Iwata, Tumor necrosis factor Alpha signaling in trigeminal ganglion contributes to mechanical hypersensitivity in masseter muscle during temporomandibular joint inflammation., J. Oral Facial Pain Headache. 32 (n.d.) 75–83. doi:10.11607/ofph.1854.
[52] H. Zhang, L. Zhi, S.M. Moochhala, P.K. Moore, M. Bhatia, Endogenous hydrogen sulfide regulates leukocyte trafficking in cecal ligation and puncture-induced sepsis, J. Leukoc. Biol. 82 (2007) 894–905, https://doi.org/10.1189/jlb.0407237.
[53] K. Koga, S. Shimoyama, A. Yamada, T. Furukawa, Y. Nikaido, H. Furue, K. Nakamura, S. Ueno, Chronic inflammatory pain induced GABAergic synaptic plasticity in the adult mouse anterior cingulate cortex, Mol. Pain 14 (2018), https://doi.org/10.1177/1744806918783478.
[54] U. Snekhalatha, M. Anburajan, B. Venkatraman, M. Menaka, Evaluation of complete Freund's adjuvant-induced arthritis in a Wistar rat model, Z. Rheumatol. 72 (2013) 375–382, https://doi.org/10.1007/s00393-012-1083-8.
[55] S.B, Stephen B. McMahon, Wall and Melzack's Textbook of Pain, Elsevier/Saunders, 2013.
[56] A.C. Desiderá, G.C. Nascimento, R.F. Gerlach, C.R.A. Leite-Panissi, Laser therapy reduces gelatinolytic activity in the rat trigeminal ganglion during temporomandibular joint inflammation, Oral Dis. 21 (2015) 652–658, https://doi.org/10.1111/odi.12330.
[57] J.R. Ghilardi, K.T. Freeman, J.M. Jimenez-Andrade, K.A. Coughlin, M.J. Kaczmarska, G. Castaneda-Corral, A.P. Bloom, M.A. Kuskowski, P.W. Mantyh, Neuroplasticity of sensory and sympathetic nerve fibers in a mouse model of a painful arthritic joint, Arthritis Rheum. 64 (2012) 2223–2232, https://doi.org/10.1002/art.34385.
[58] P.R. Kramer, C.A. Kerins, E. Schneiderman, L.L. Bellinger, Measuring persistent temporomandibular joint nociception in rats and two mice strains, Physiol. Behav. 99 (2010) 669–678, https://doi.org/10.1016/j.physbeh.2010.01.037.
[59] G.A. Lemos, R. Rissi, I.L. de Souza Pires, L.P. de Oliveira, A.A. de Aro, E.R. Pimentel, E.T. Palomari, Low-level laser therapy stimulates tissue repair and reduces the extracellular matrix degradation in rats with induced arthritis in the temporomandibular joint, Lasers Med. Sci. 31 (2016) 1051–1059, https://doi.org/10.1007/s10103-016-1946-3.
[60] A.E. Dief, D.K. Mostafa, G.M. Sharara, T.H. Zeitoun, Hydrogen sulfide releasing naproxen offers better anti-inflammatory and chondroprotective effect relative to naproxen in a rat model of zymosan induced arthritis, Eur. Rev. Med. Pharmacol. Sci. 19 (2015) 1537–1546 http://www.ncbi.nlm.nih.gov/pubmed/25967731 , Accessed date: 17 September 2019.
[61] B. Andruski, D.M. McCafferty, T. Ignacy, B. Millen, J.J. McDougall, Leukocyte trafficking and pain behavioral responses to a hydrogen sulfide donor in acute monoarthritis, Am. J. Physiol. Regul. Integr. Comp. Physiol. 295 (2008), https://doi.org/10.1152/ajpregu.90524.2008.
[62] P.G. Winyard, D.A. Willoughby, Inflammation Protocols, Humana Press, 2003, https://doi.org/10.1385/1592593747.
[63] Y.-J. Gao, L. Zhang, O.A. Samad, M.R. Suter, K. Yasuhiko, Z.-Z. Xu, J.-Y. Park, A.-L. Lind, Q. Ma, R.-R. Ji, JNK-induced MCP-1 production in spinal cord astrocytes contributes to central sensitization and neuropathic pain, J. Neurosci. 29 (2009) 4096–4108, https://doi.org/10.1523/JNEUROSCI.3623-08.2009.
[64] P.C. Cordeiro, J.P. Guimaraes, V.A. de Souza, I.M. Dias, J.N. Silva, K.L. Devito, L.L. Bonato, Temporomandibular joint involvement in rheumatoid arthritis patients: association between clinical and tomographic data, Acta Odontol. Latinoam. 29 (2016) 123–129.
[65] R. de Leeuw, Internal derangements of the temporomandibular joint, Oral Maxillofac. Surg. Clin. N. Am. 20 (2008) 159–168, https://doi.org/10.1016/j.coms.2007.12.004.
[66] M. Kobayashi, G.R. Squires, A. Mousa, M. Tanzer, D.J. Zukor, J. Antoniou, U. Feige, A.R. Poole, Role of interleukin-1 and tumor necrosis factor alpha in matrix degradation of human osteoarthritic cartilage, Arthritis Rheum. 52 (2005) 128–135, https://doi.org/10.1002/art.20776.
[67] D.-H. Wang, M.-C. Yang, W.-E. Hsu, M.-L. Hsu, L.-M. Yu, Response of the temporomandibular joint tissue of rats to rheumatoid arthritis induction methods, J. Dent. Sci. 12 (2017) 83–90, https://doi.org/10.1016/J.JDS.2016.12.001.
[68] R. Spears, L.A. Dees, M. Sapozhnikov, L.L. Bellinger, B. Hutchins, Temporal changes in inflammatory mediator concentrations in an adjuvant model of temporomandibular joint inflammation, J. Orofac. Pain 19 (2005) 34–40 http://www.ncbi.nlm.nih.gov/pubmed/15779537 , Accessed date: 17 September 2019.
[69] H.D.C. Francescato, J.R.A. Cherice, E.C.S. Marin, F.Q. Cunha, R.S. Costa, C.G.A. Silva, T.M. Coimbra, Effect of endogenous hydrogen sulfide inhibition on structural and functional renal disturbances induced by gentamicin, Braz. J. Med. Biol. Res. Rev. Bras. Pesqui. Med. Biol. 45 (2012) 244–249, https://doi.org/10.1590/s0100-879x2012007500016.
[70] E. Bałkowiec-Iskra, A. Vermehren-Schmaedick, A. Balkowiec, Tumor necrosis factor-α increases brain-derived neurotrophic factor expression in trigeminal ganglion neurons in an activity-dependent manner, Neuroscience 180 (2011) 322–333, https://doi.org/10.1016/j.neuroscience.2011.02.028.
[71] M. Kandasamy, L. Aigner, Neuroplasticity, limbic neuroblastosis and neuro-regenerative disorders, Neural Regen. Res. 13 (2018) 1322–1326, https://doi.org/10.4103/1673-5374.235214.
[72] R.R. Ji, T. Berta, M. Nedergaard, Glia and pain: is chronic pain a gliopathy? Pain, Elsevier B.V., 2013, , https://doi.org/10.1016/j.pain.2013.06.022.
[73] P.T. Ohara, J.-P. Vit, A. Bhargava, L. Jasmin, Evidence for a role of connexin 43 in trigeminal pain using RNA interference in vivo, J. Neurophysiol. 100 (2008)